Saga
Petroleum a.s.

Benin Basin
Evaluation Report

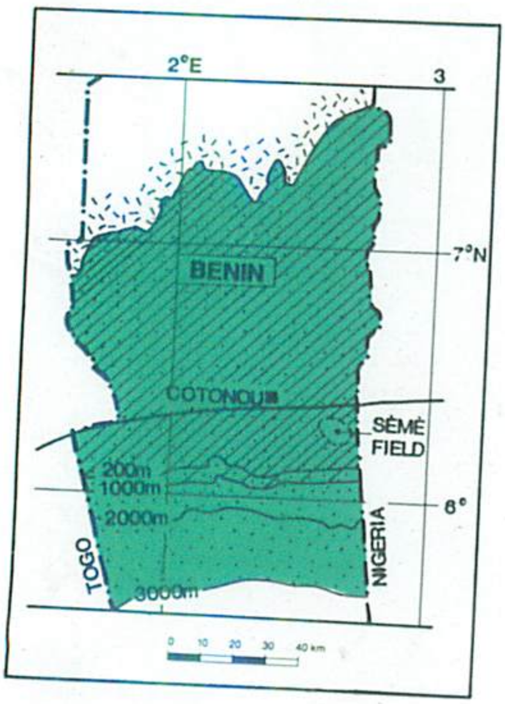

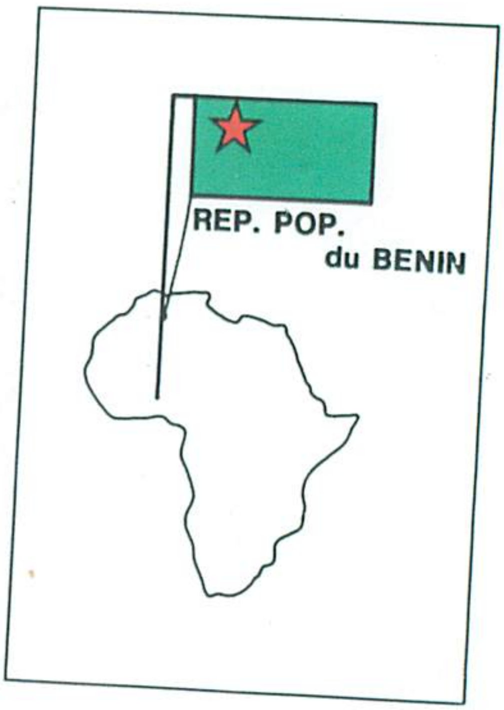

December 1984

VOLUME II

BENIN BASIN EVALUATION

VOLUME I: HYDROCARBON PROSPECT EVALUATION OF BENIN

BENIN BASIN EVALUATION

VOLUME II

LIST OF CONTENTS:

LIST OF ENCLOSURES:

VOL VI

DO-D1

Borehole compensated sonic log,	1:200	Interval:	700'-2821'
	"	"	2797'-5546'
	1:1000	Interval:	200'-5500'
	"	"	2797'-5546'
	"	"	(700'-2821')
Gamma Ray log	1:1000		700'-5546'
Composite Well log	1:1000	Interval:	(TD) 2151.28 m

DO-D2

Borehole compensated sonic log	1:200	Interval:	3153'-3771'
	"	"	795'-3196'
	1:1000	Interval:	800'-3700'
	"	"	795'-3196'
	"	"	3153'-3771'

DO-D3

Induction log	1:1000		825'-3019'
Induction log-gamma ray	1:200	Interval:	825'-3019'
	"	"	3016'-6659'
	1:1000	Interval:	3016'-6659'
Borehole compensated sonic log	1:200	Interval:	625'-3000'
	1:1000	"	3016'-6648'
	1:200	Interval:	3016'-6648'
	1:1000	Interval:	925'-2008'
Composite Well log	1:X	Interval:	-(TD) 2037 mRKB

DO-A3

Induction-Electrical log	1:200 Interval: 3042'-9225'
	1:1000 Interval: 3042'-9224'
Laterolog-gamma ray-neutron log	1:200 Interval: 3042'-9220'
	1:1000 Interval: 3042'-9220'
Borehole compensated sonic log	1:1000 Interval: 3042'-9210'
	" " 530'-3037'
	1:200 Interval: 475'-3030
Composite Well log	1:1000 Interval -(TD) 2812 mRKB
	1:200 (TD) 2812 mRKB

DO-A4

Inductian log-gamma ray	1:200 Interval: 2700'-6875'
	1:1000 Interval: 2700'-6875'
Borehole compensated sonic log	1:200 Interval: 2994'-6873'
	" " 746'-2750'
	1:1000 Interval: 2994'-6873'
	" " 746'-2750'
Composite Well log	1:1000 Interval: (TD) 2188

DO-F1

Induction log	1:200 Interval: 815'-2987'
	1:1000 : 1000'-2987'
Induction log-gamma ray	1:200 Interval: 2983'-7200'
	" " 7000'-7400'
	1:1000 Interval: 2983'-7200'
	1:1000 : 7000'.7400'

Borehole compensated sonic log	1:200 Interval: 815'-2976'
	" " 2983'-6196'
	1:1000 Interval: 2983'-6196'
	1:1000 : 815'-2976'
Composite Well log	1:1000 Interval: -(TD) 2261 mRKB

DO-2A

Microlaterolog	1:200 Interval:	5997'-6600'
	" "	5997'-6600'
	" "	8000'-9070'
	1:1000 :	5997'-6600'
	"	8000'-9070'
Induction-Electrical log	1:200 Interval:	7000'-9069'
	" "	5308'-8020'
	1:1000 Interval:	7000'-9069'
	" "	5308'-8020'
Laterolog-gamma ray-neutronlog	1:200 Interval:	80'-5312'
	1:1000 Interval:	80'-5312'
Laterolog-gamma ray	1:200 Interval:	5308'-8022'
Gamma ray	1:200 Interval:	6000'-8942'
Borehole compensated sonic log	1:200 Interval:	576'-5100'
	" "	5308'-9060'
	1:1000 Interval:	576'-9060'
Composite Well log	1:1000 Interval:	-(TD) 2774 m RKB
Continous dipmeter	1:200 Interval:	8000'-9065'
	" "	6000'-6600'
	1:1000 Interval:	8000'-9065'
	" "	6000'-6600'

DO-C1

Induction-Electrical log	1:200 Interval: 2813'-7366'
	1:1000 Interval: 2813'-7366'
Laterolog-gammaray-neutron log	1:200 Interval: 2813'-7366'
	1:1000 Interval: 2813'-7311'
Borehole compensated sonic log	1:200 Interval: 640'-2844'
	" " 2813'-7366'
	1:1000 Interval: 2813'-7538'
	" " 640'-2844'
	" " 2813'-7350'
Borehole compensated sonic log	1:1000 Interval: 640'-7350'
Composite Well log	1:1000 Interval: - (TD) 2245 mRKB,

DO1

Microlaterolog	1:200 Interval: 3963'-8021'
	" " 8021'-9610'
	" " 9510'-10072'
	1:1000 Interval: 3963'-8121'
Induction-Electrical log	1:200 Interval: 8014'-9605'
	1:200 Interval: 9504'-10085'
	" " 3963'-8114'
	1:1000 Interval 598'-3975'
Laterolog-gamma ray	1:200 Interval: 3963'-9607'
	1:1000 Interval: 3963'-9607'
Electrical log	1:200 Interval: 598'-4008'

Gamma ray-neutron log	1:200	Interval:	3720'-8114'
	"	"	8014'-9604'
	"	"	6000'-9105'
	1:1000	Interval:	6000'-9105'
	"	"	200'-3973'
	1:X	Interval:	(1:2000) 200'-3973'
Borehole compensated sonic log	1:200	Interval:	8010'-10085'
	"	"	3963'-8110'
	"	"	598'-3968'
	1:1000	Interval:	598'-3968'
Composite Well log	1:1000	Interval:	- (TD) 3081.5 mRKB
Continous dipmeter	1:200	Interval:	3963'-10090'
	1:1000	Interval:	3963'-10090'
Compensated formation density log	1:200	Interval:	3963'-9610'
	"	"	9510'-10070'
	1:1000	Interval:	3963'-9610'
Sample log with gamma ray-neutron-composite	1:1000	Interval:	-(TD) 10100'

DO-D2A

Induction-Electrical log	1:200 Interval:	6350'-10194'
	" "	5300'-6740'
	" "	10050'-10726'
	1:1000 Interval:	5300'-6740'
Gamma ray-neutron log	1:200 Interval:	3000'-10731'
	1:1000 Interval:	3000'-10731'
Gamma ray	1:200 Interval:	6300'-10171
	1:1000 Interval:	6300'-10171'
Borehole compensated sonic log	1:200 Interval:	3000'-6237'
	" "	10050'-10722'
	" "	6350'-10190'
	" "	6000'-6736'
	1:1000 Interval:	6000'-10190
	" "	6000'-6736'
	" "	2988'-6237'
	" "	2988'-6237'
	" "	10100'-10722'
Composite Well log	1:X Interval:	- (TD) 3268 mRKB
Continous dipmeter	1:200 Interval:	2725'-8000'
Compensated formation density log	1:200 Interval:	6800'-10550'
Formation density log	1:1000 Interval:	6800'-10500'

CHAPTER 1 22.6.84

INTRODUCTION

1.1 Geological Province

1.2 Exploration Status Dahomey Embayment

1.1 Geological Province

The coastal basin of Benin belongs, speaking in geological terms, to the Dahomey Embayment (fig. 1.1), an elongated depression that stretches from the Volta Delta in eastern Ghana through Togo and Benin and into western Nigeria. The basin is situated on the continental margin of the northern Gulf of Guinea, with the larger area exposed onshore but with a substantially thicker succession of sediments present offshore.

It is of crucial importance to note that the Dahomey Embayment is an aerially restricted geologic province with its own unique characteristics. Although similarities can be found in the evolutionary history and the stratigraphy of the various coastal basins in the northern Gulf of Guinea, each of these basins exhibits their own hydrocarbon habitats that may show no resemblance whatsoever. Exploration philosophy offshore Benin must for this reason for the larger part rely on ideas that have not been the clue to success neither in the Niger Delta nor in the Ivory Coast Basin. Relevant experience must primarily be sought from exploration efforts in other parts of the Dahomey Embayment, and its counterpart on the equatorial margin of Brazil.

1.2 Exploration Status Dahomey Embayment

Explorationwise, the Dahomey Embayment is considered partially unexplored on a worldwide scale (Halbouty 1982). This is opposed to the neighbouring Niger Delta which by the same author is classified as intensely explored. This difference in exploration status reflects a difference in prospectivity between the two provinces as well as a difference in exploration history.

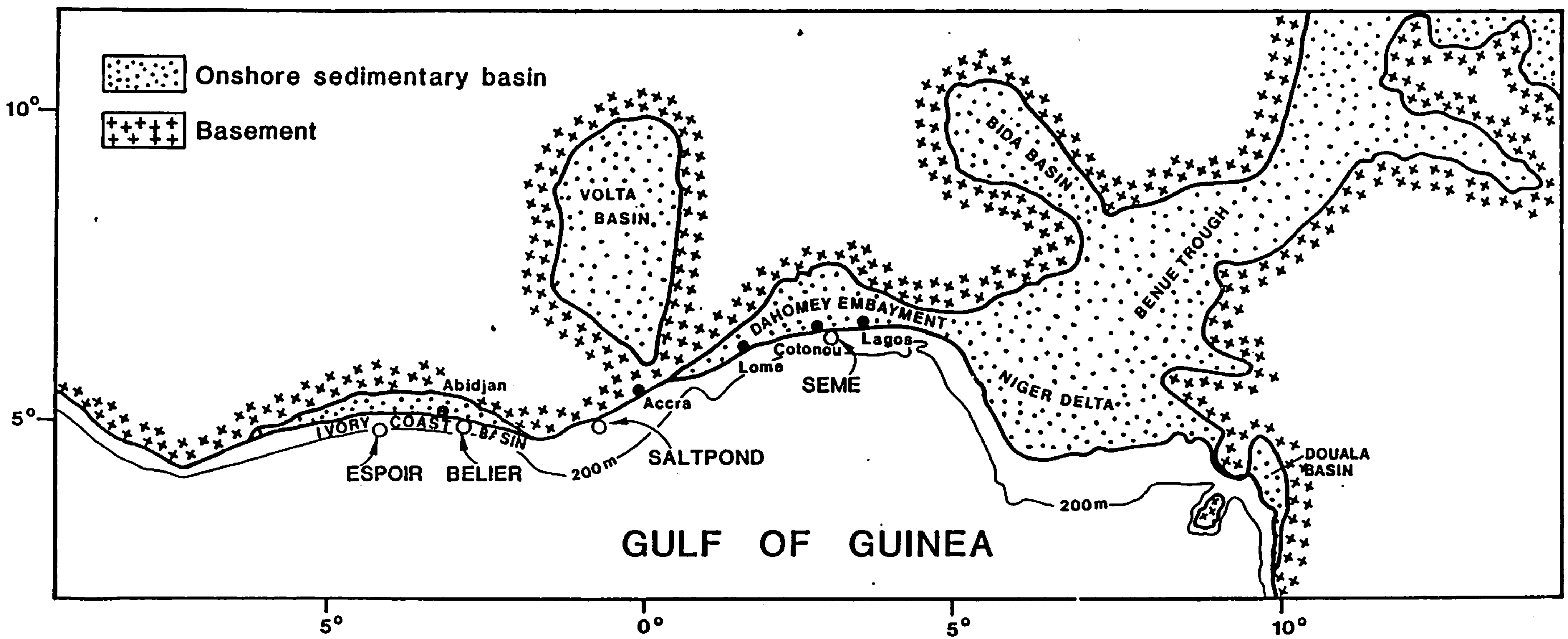

Fig. 1.1: The northern Gulf of Guinea geological province.

Sèmè Oil Field offshore Benin, with production from Cretaceous sandstones, (Ræstad et al 1983) is the only field on stream in the Dahomey Embayment to date (ref. Appendix A.3). Low gravity oil impregnated sands in western Nigeria have, however, proven reserves in the order of 1 x 10^9 bbls, but are as yet not economical to develop (Adegoke and Ibe 1982). Hydrocarbon shows have been reported in several wells along the basin, but none of these appear at present to represent any significant accumulations.

In the Keta Basin of eastern Ghana (the westernmost extension of the Dahomey Embayment) a very modest exploration program has been carried out (Akpati 1978). Drilling is limited to three deep holes. Two (Atiavi, TD 1560 m and Anloga, TD 2135 m) were drilled by a Romanian company in the sixties based on gravity surveys. Mesa Petroleum drilled a third well in 1973 after having shot a seismic survey the same year. Dzita-1 (TD 4100 m) tested small quantities of oil and salt water from a Devonian sandstone. Texas Pacific was awarded a concession on the onshore Keta Basin in 1979, and is currently trying to get partners in and drill two wells.

In Togo exploration drilling consists of two offshore wells operated by Union Carbide in 1971, Lome 1 (TD 2333 m) and Lome 2 (TD 2929 m). They both had multiple shows of oil in the Lower Cretaceous and in the Devonian series. Late 1982 Getty Oil was awarded a production sharing contract covering the entire offshore area. GSI shot an exclusive seismic survey early 1983. A trade agreement was signed between Benin and Ashland (rightholders of Lome 1 and Lome 2) March 1983, in which the two Togo wells were traded against DO-1 and DO-2A offshore Benin.

Some few deep wells have also been sunk in western Nigeria without any apparent success neither onshore nor offshore. Oil and tar seeps do, however, occur in Cretaceous outcrops, and a heavy oil deposit is located due south of the Ilesha Spur. The gravity of the oil is 5-15^{o} API (Adegoke and Ibe 1982).

CHAPTER 2 22.6.84

DATA BASE

2.1 Well Data

2.2 Seismic Data

2.3 Well Data Summaries

2.1 Well Data

Well data included in the Basin Evaluation Study can be grouped into three categories:

* Exploratory wells drilled in Benin by Union Oil of California (compare chapter 3.3)

* Development wells Sèmè Field operated by Saga Petroleum Benin a.s. (compare Appendix A.3).

Electric logs, mud logs, geological reports and engineering reports from the first category consitute the main data base for stratigraphic, lithologic and petrophysical information. However, important additional data for all purposes have been obtained from the third category wells. It is emphasized that the Sèmè development well data definitely have improved the understanding of the Benin offshore basin, and hence the value of this report. Also wells outside Benin have given important contributions, in particular in regards to stratigraphic and petrohysical knowledge of stratigraphically deeper strata.

Fig. 2.1 shows the location of all wells, fig. 2.2 to 2.14 and tables 2.1 and 2.2 summarize the well data.

2.2 Seismic Data

The seismic interpretation and mapping is mainly based on the regional survey operated by Saga on behalf of the Beninian Government, conducted by Western Geophysical and processed by Sefel Geophysical in 1982. This survey (fig. 3.15) comprises 1450 km of offshore seismic data.

The survey area covers the entire continental shelf out to a

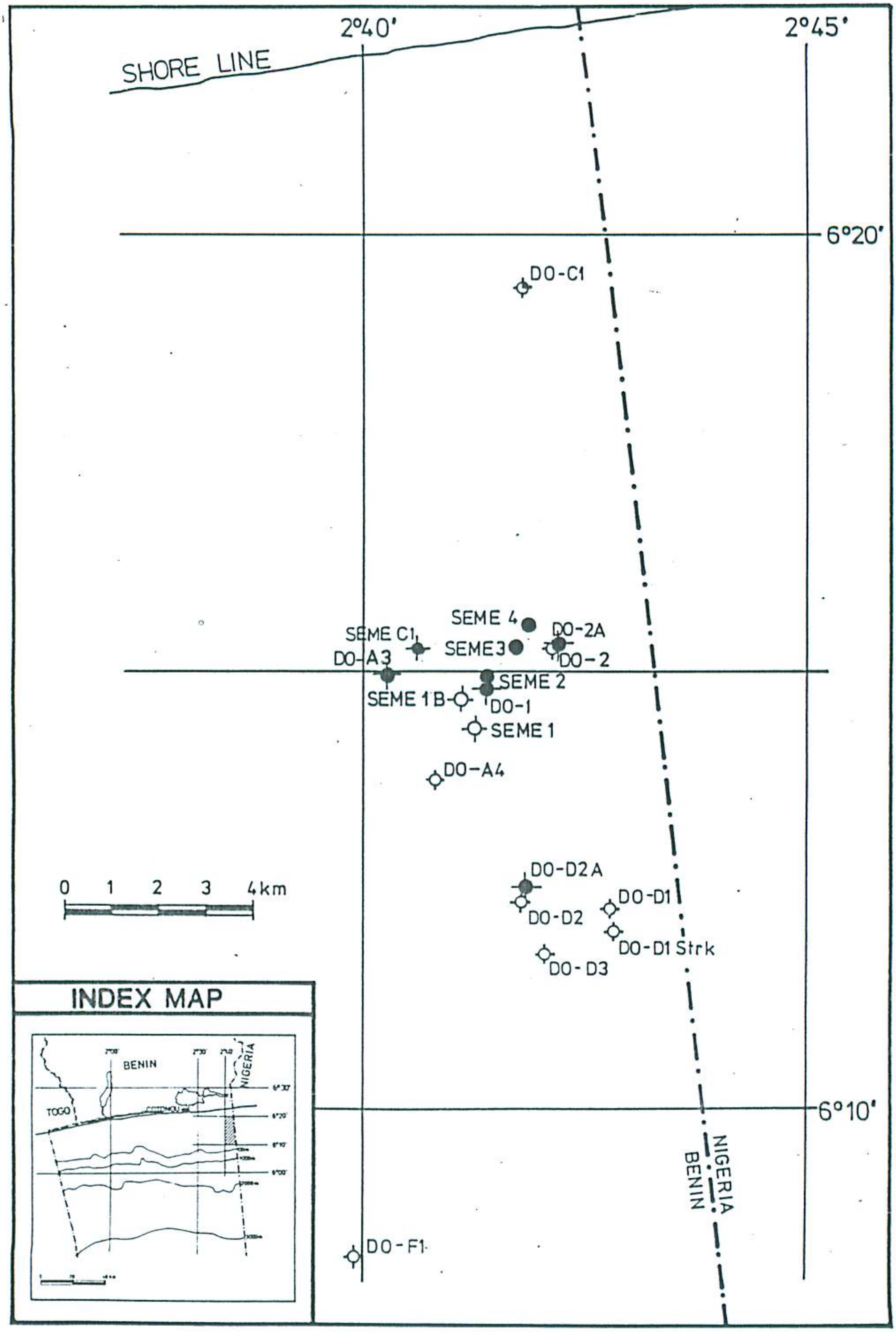

Fig. 2.1: Location of Union Oil exploratory wells offshore Benin and Sèmè development wells.

WELL	Mud-log	IEL	FDC-CNL	ISF-Sonic	MLL	Laterolog	Gamma Ray	CBL	HDT	HDT,Computed	Perforating Depth Control	Perforating Record & CCL
DO-1	200'-10100'	598'- 3975' 3963'- 8114' 8014'- 9604' 9504'-10085'	3961'- 9623' 9504'-10083'	598'- 3975' 3963'- 8114' 8010'-10083'	3963'- 8114' 8014'- 9604' 9504'-10085'	3963'- 9607' 9504'-10085'	200'- 3973' 3963'- 8114' 8014'- 9604' 6000'- 9105'		3963'-10090'*	3963'-10090'		
DO-2A	100'- 9100'	5308'- 8020' 7000'- 9069'		576'- 5100' 5303'- 9060'	5997'- 6600' 8000'- 9070'**	80'- 5312' 5308'- 8020'**	6000'- 8942'	8400'- 8932'**	6000'- 8000' 6600'- 9065'	6000'-8000' 6600'-9065'		
DO-A3	700'- 9300'	3042'- 9210'		530'- 3037' 3042'- 9210'		3042'- 9210'		4260'- 8940'			6000'-8930'**	
DO-A4	800'- 7000'	2700'- 6875'		746'- 2750' 2994'- 6873'								
DO-C1	650'- 7450'	2813'- 7366'		640'- 2844' 2813'- 7366'		2813'- 7366'						
DO-D1	800'- 7300'			700'- 2821' 2797'- 5546'								
DO-D2	800'- 4300'			795'- 3196' 3153'- 3771'								
DO-D2A	400'-10700'	5300'- 6740' 6300'-10171' 10050'-10722'	6800'-10550'	2988'- 6237' 6000'- 6736' 6350'-10190' 10050'-10722'			3000'-10722' 6300'-10171'	500'- 6617' 6520'-10163'	8000'-10725'**	8000'-10725'**		10012'-10082'
DO-D3	800'- 6600'	800'- 3000' 3016'- 6648'		800'- 3000' 3016'- 6648'								
DO-F1	300'- 7900'	815'- 2976'** 2983'- 7200' 7000'- 7400'		815'- 2976'** 2933'- 6196'								

Table 2.1: Well data-logs.

WELL	Well Drilling Program	Daily Drilling Reports	Daily Operations Report	Daily Drilling Mudreport	Weekly Geological Report	Well Completion Program	Evaluation & recommended Testing Program	AFE	Well Prognosis	Monthly Well Report
DO-1	X	X	X	X	X					
DO-2	X		X	X		X				
DO-2A	X	X	X	X	X					
DO-3	X									
DO-A3	X	X			X		X	X		
DO-A4					X					
DO-C1	X	X	X	X	X			X		
DO-D1		X		X						
DO-D2	X	X	X	X	X					
DO-D2A		X								
DO-D3		X		X					X	X
DO-F1		X								

Table 2.2: Information from drilling operations.

water depth of approximately 200 m. The grid density is 4.5 by 5 km with a few additional infill lines especially in the eastern part of the shelf. Almost all of the north-south directed lines continue into the deep water area, and the southernmost strike line straddles the shelf break. The acquisition and processing of these data is thoroughly discussed in Appendix A.1.

In addition to the 1982 Western survey, three Shell operated surveys from 1971, 1972 and 1975 (figs. 3.11, 3.12 and 3.13) were partly used in the seismic interpretation. The three surveys total 3115 km of offshore seismic data; details are given in chapter 3.

The Shell data were, however, not included in the generation of maps due to the regional character of this study and superior quality of the most recent grid. The quality of the 1982 survey is considered very good with high resolution all the way down to and including the basement reflector. Regarding the Shell surveys the data quality varies from fair to good with the 1975 detailed grid as the best one.

Compare chapter 3.2 for additional information as to seismic surveys offshore Benin.

WELL DATA SUMMARY

WELL	: DO-1	LOCATION	: 06°14'51" N
OPERATOR	: UNION		: 02°41'24" E
SPUD DATE	: 7.12.1967	RKB (m)	: 15
COMP DATE	: 15.21968	WD (m)	: 26
STATUS	:	TD (m RKB)	: 3081.5

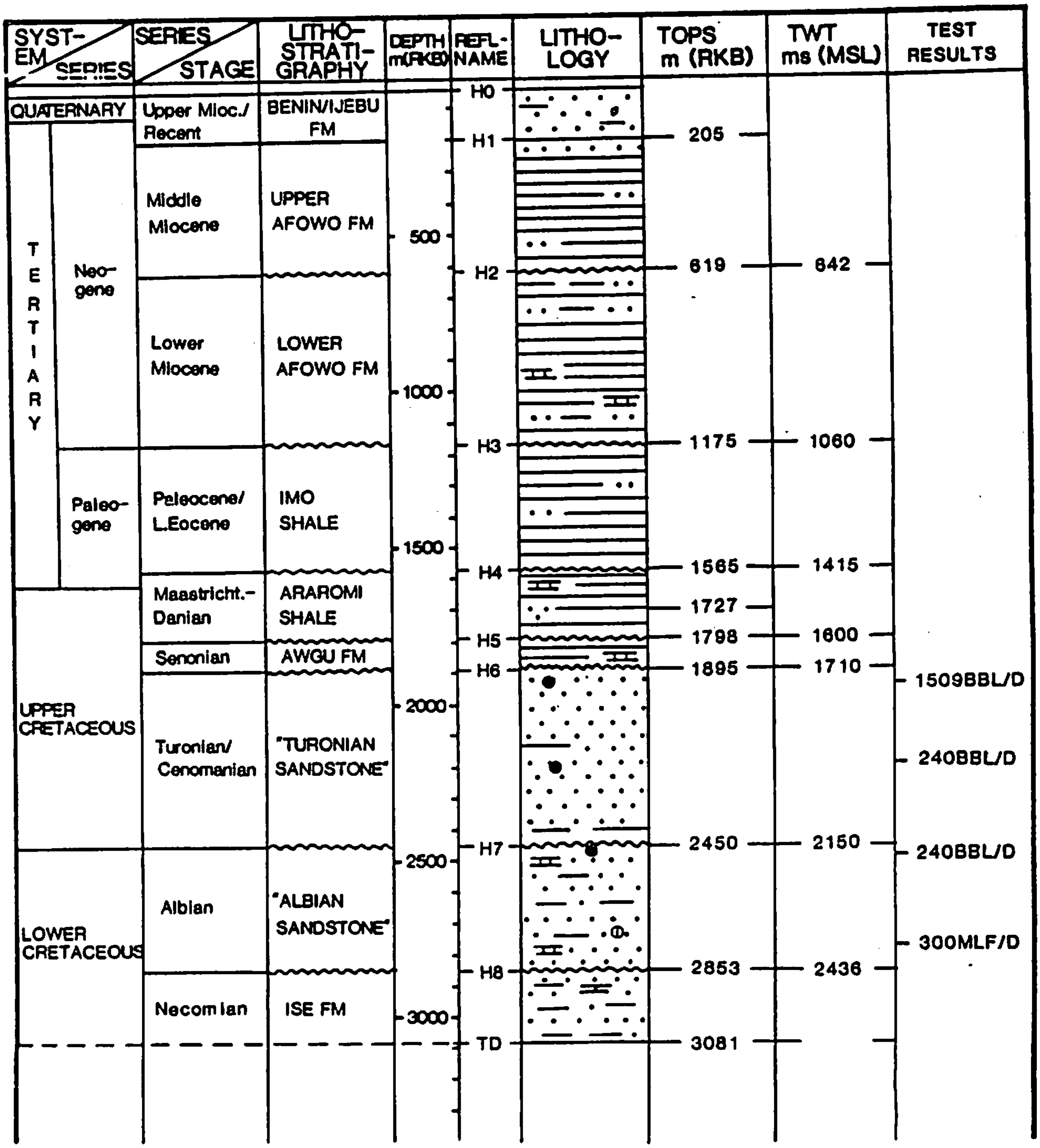

Fig. 2.2

WELL DATA SUMMARY

WELL	: DO-2A	LOCATION	: 06°15'20.2" N
OPERATOR	: UNION		: 02°42'11.4" E
SPUD DATE	: 4.3.1968	RKB (m)	: 21
COMP DATE	: 24.6.1968	WD (m)	: 26
STATUS	:	TD (m RKB)	: 2766.4

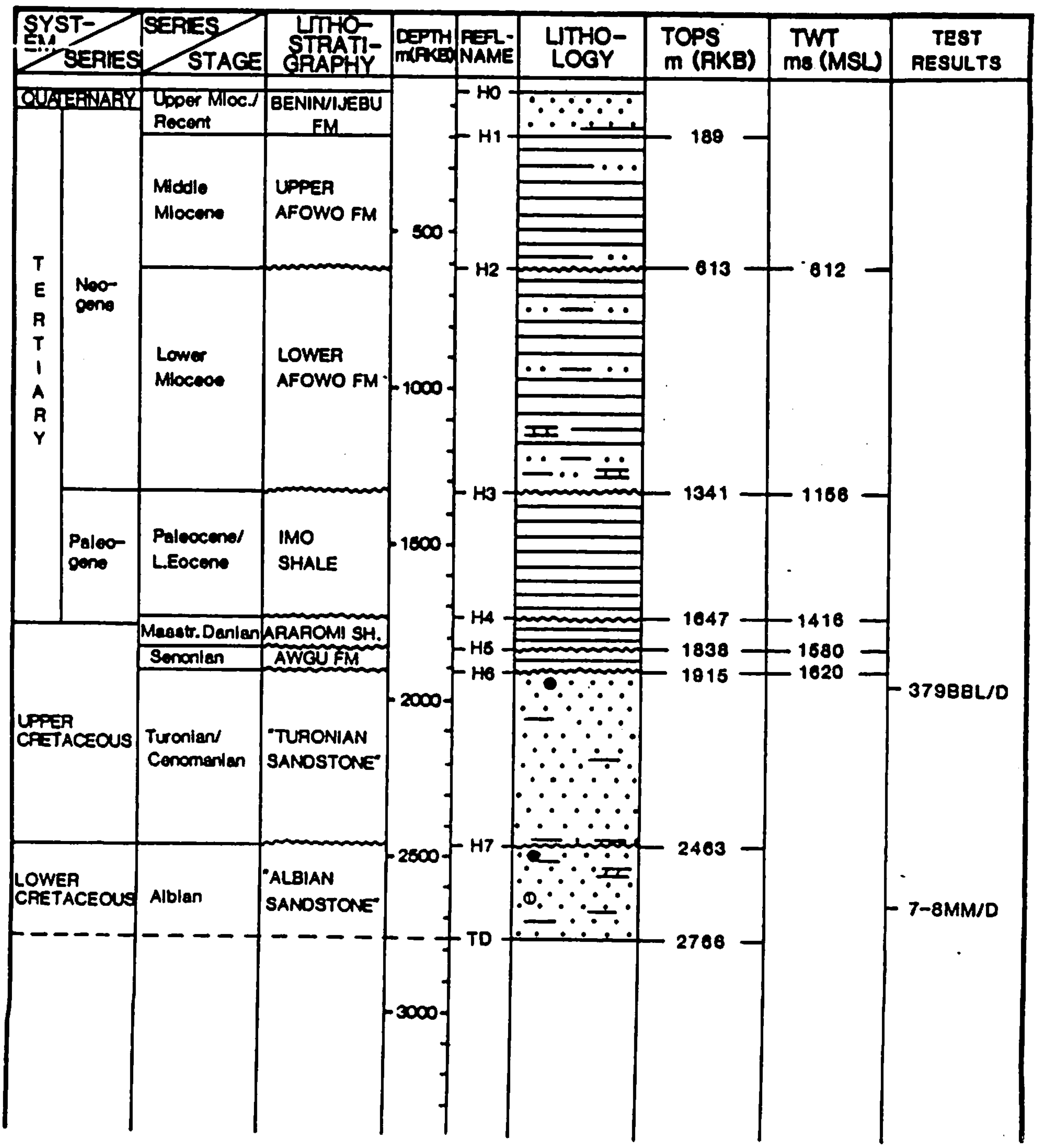

Fig. 2.3

WELL DATA SUMMARY

WELL	: DO-A3	LOCATION	: 06°15'02" N
OPERATOR	: UNION		: 02°40'16" E
SPUD DATE	: 5.9.1969	RKB (m)	: 22
COMP DATE	: 28.10.1969	WD (m)	: 26
STATUS	: ✦	TD (m RKB)	: 2812

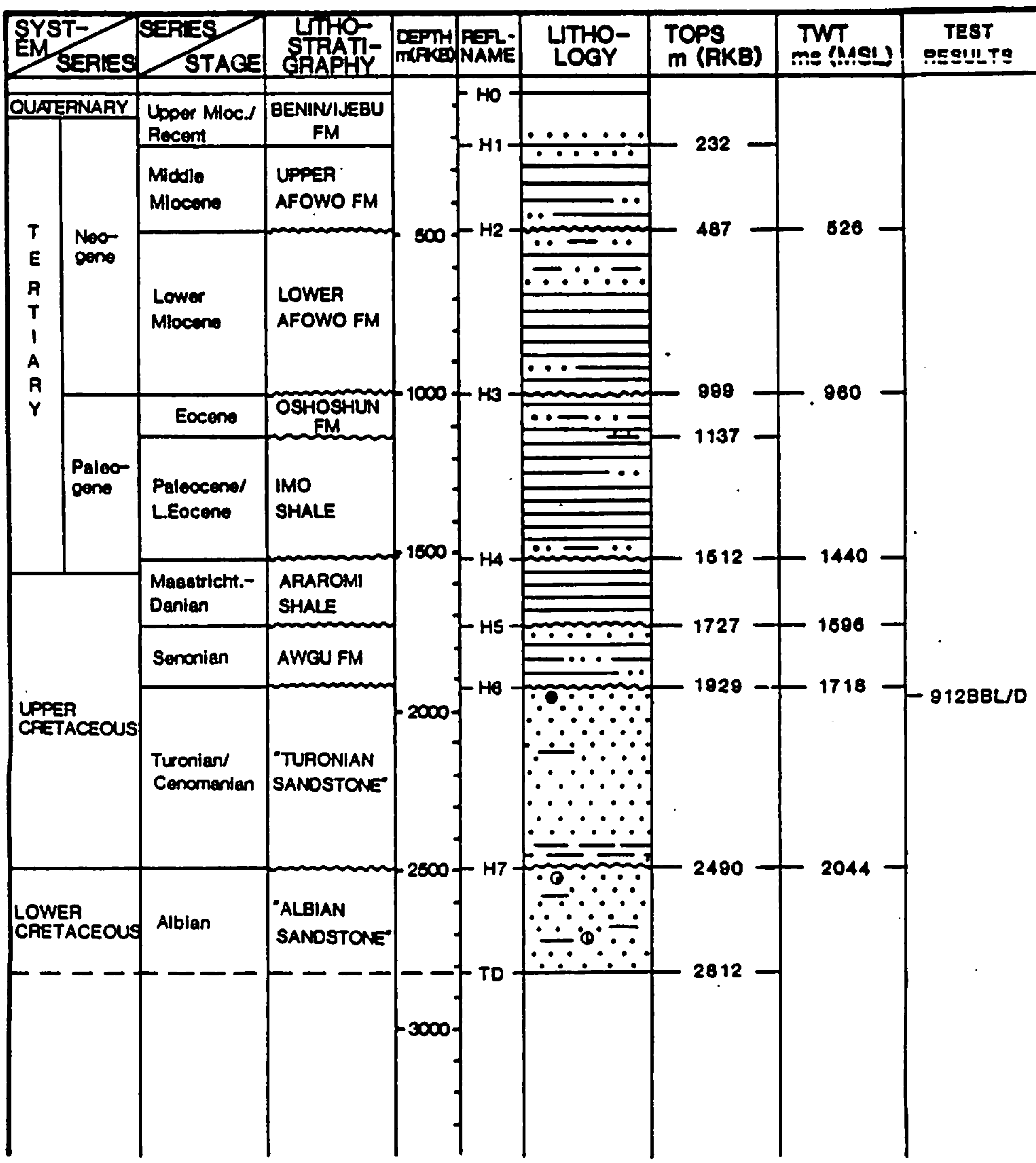

Fig. 2.4

WELL DATA SUMMARY

WELL	: DO-A4	LOCATION	: 06°13'46" N
OPERATOR	: UNION		: 02°40'46" E
SPUD DATE	: 20.11.1970	RKB (m)	: 20
COMP DATE	: 10.12.1970	WD (m)	: 32
STATUS	: ⌖	TD (m RKB)	: 2118

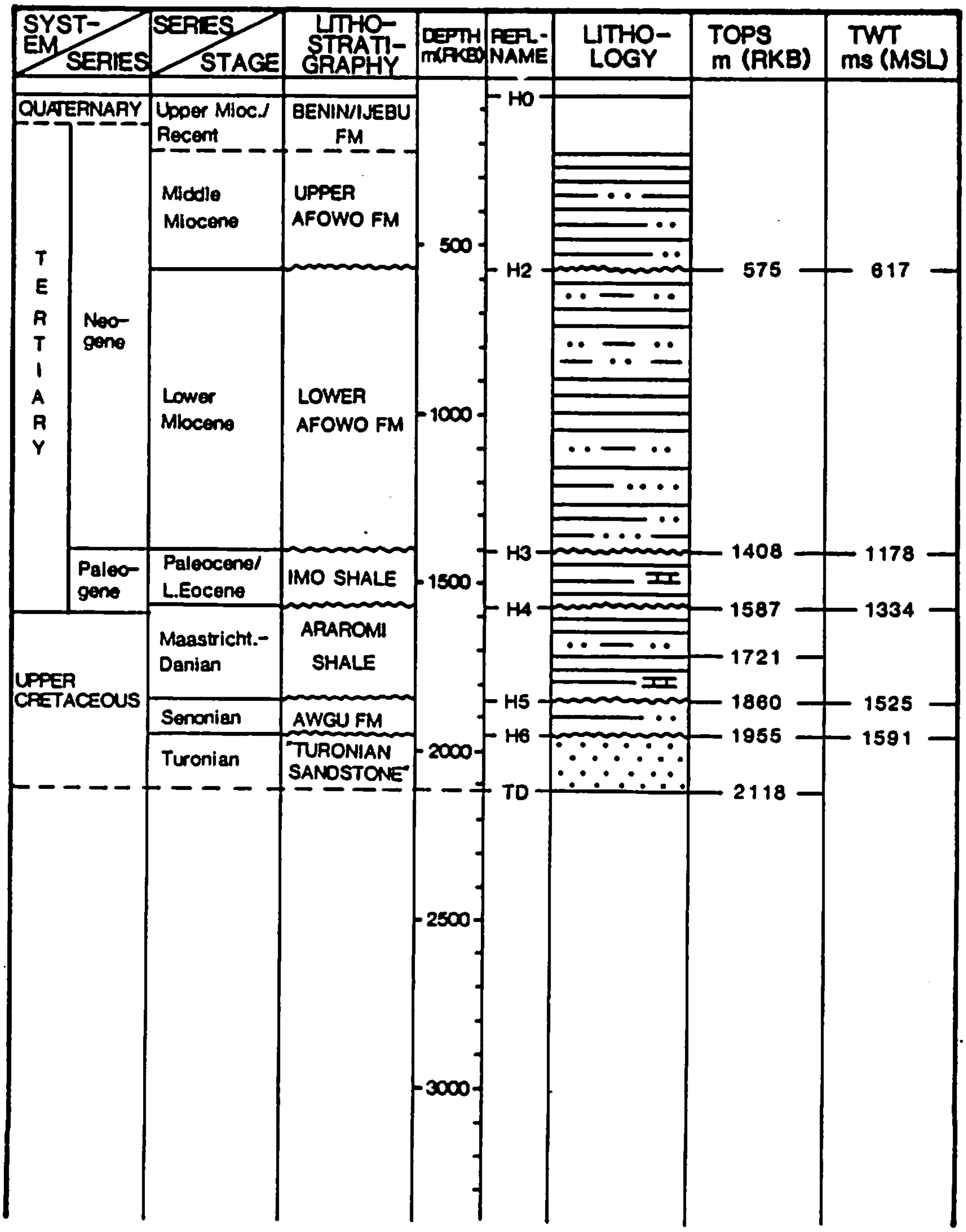

Fig. 2.5

WELL DATA SUMMARY

WELL	: DO-C1	LOCATION	: 06°19'22.03"N
OPERATOR	: UNION		: 02°41'46.28"E
SPUD DATE	: 18.7.1969	RKB (m)	: 24
COMP DATE	: 27.8.1969	WD (m)	: 20
STATUS	: ⌖	TD (m RKB)	: 2245

SYSTEM	SERIES	SERIES / STAGE	LITHO-STRATIGRAPHY	DEPTH m(RKB)	REFL. NAME	TOPS m (RKB)	TWT ms (MSL)
QUATERNARY		Upper Mioc./Recent	BENIN/IJEBU FM		H0		
		M/U Miocene	U.AFOWO FM		H1	250	
TERTIARY	Neogene	Lower Miocene	LOWER AFOWO FM		H2	308	342
	Paleogene	Middle Eocene	OSHOSHUN FM	500	H3	488	494
		Paleocene/L.Eocene	IMO SHALE	1000		723	
UPPER CRETACEOUS		Maastricht.-Danian	ARAROMI SHALE		H4	1103	1136
		Senonian	AWGU FM		H5	1350	1322
		Turonian/Cenomanian	"TURONIAN SANDSTONE"	1500	H6	1440	1376
LOWER CRETACEOUS		Albian	"ALBIAN SANDSTONE"	2000	H7	1979	1666
PROTEROZOIC			BASEMENT		H9	2210	1794
					TD	2245	
				2500			
				3000			

Fig. 2.6

WELL DATA SUMMARY

WELL	: DO-D1	LOCATION	: 06°12'18.93" N
OPERATOR	: UNION		: 02°42'47.09" E
SPUD DATE	: 30.10.1969	RKB (m)	: 19
COMP DATE	: 12.1.1970	WD (m)	: 52
STATUS	: ⌖	TD (m RKB)	: 2151.28

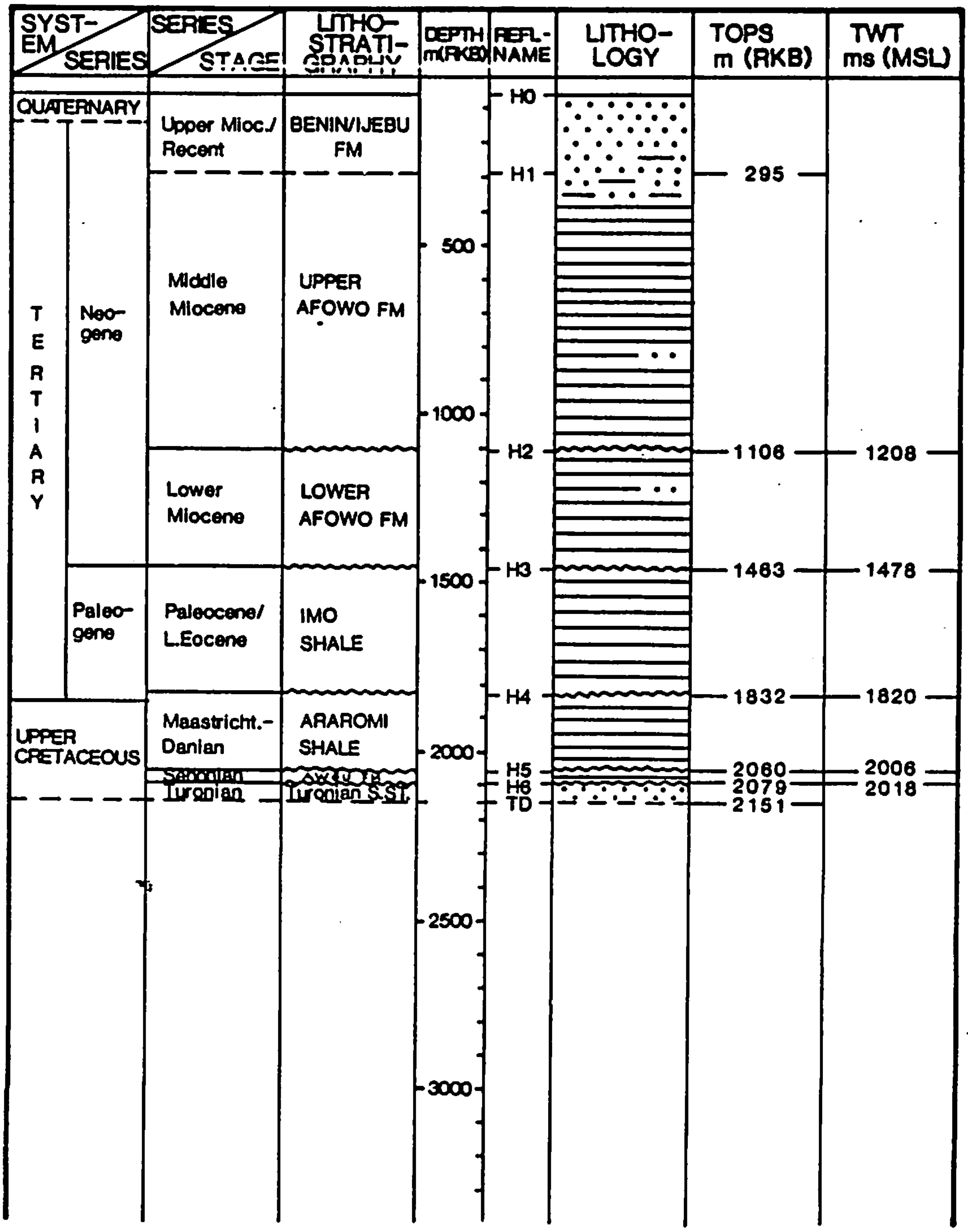

Fig. 2.7

WELL DATA SUMMARY

WELL	: D0-D2A	LOCATION	: 06°12'33.2"N
OPERATOR	: UNION		: 02°41'49,6"E
SPUD DATE	: 16.5.1970	RKB (m)	: 20
COMP DATE	: 14.8.1970	WD (m)	: 46
STATUS	:	TD (m RKB)	: 3268

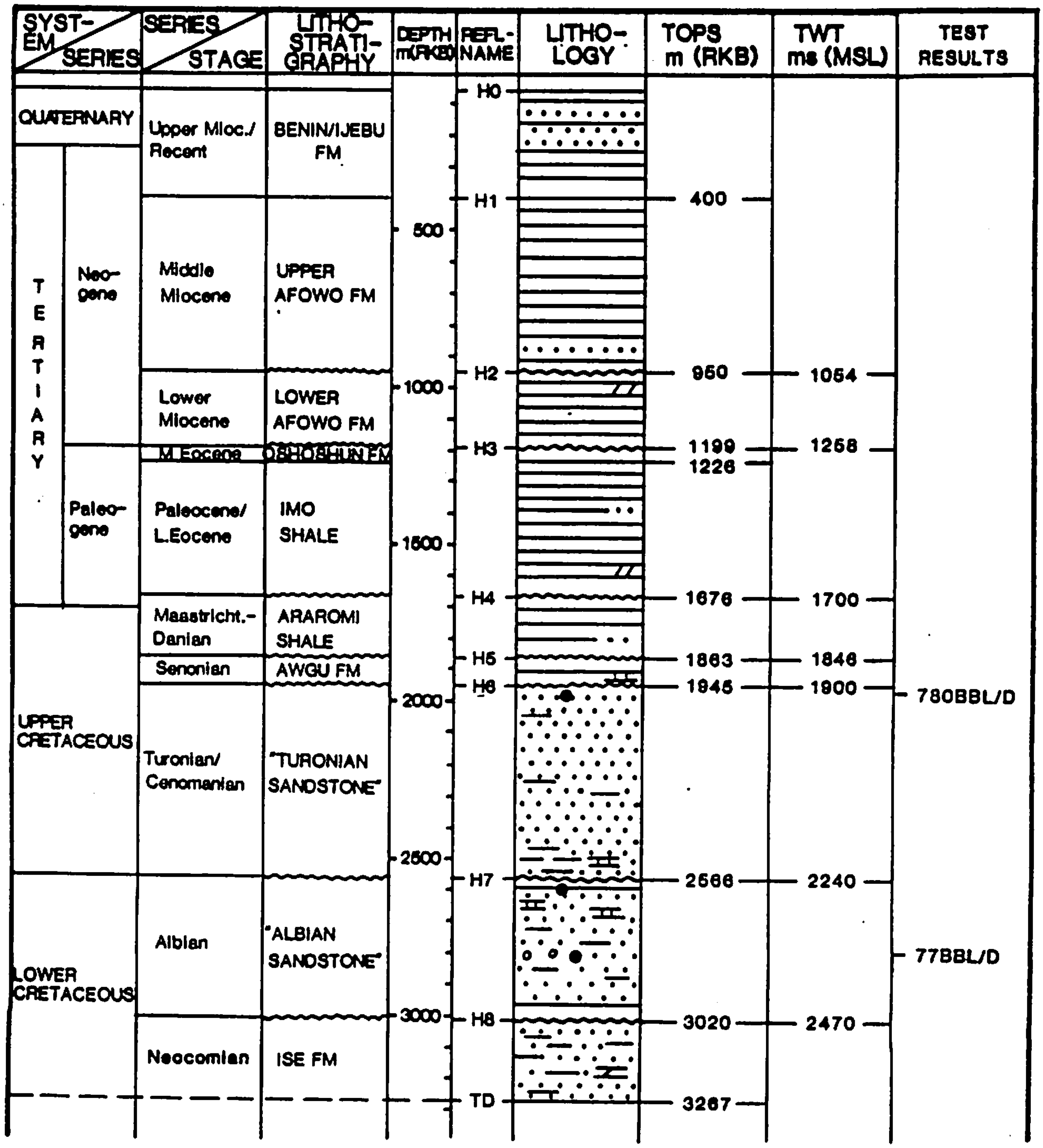

Fig. 2.8

WELL DATA SUMMARY

WELL	: D0-D3	LOCATION	: 06°11'49"N
OPERATOR	: UNION		: 02°42'05"E
SPUD DATE	: 4.12.1973	RKB (m)	: 10
COMP DATE	: 1.5.1974	WD (m)	: 54
STATUS	:	TD (m RKB)	: 2037

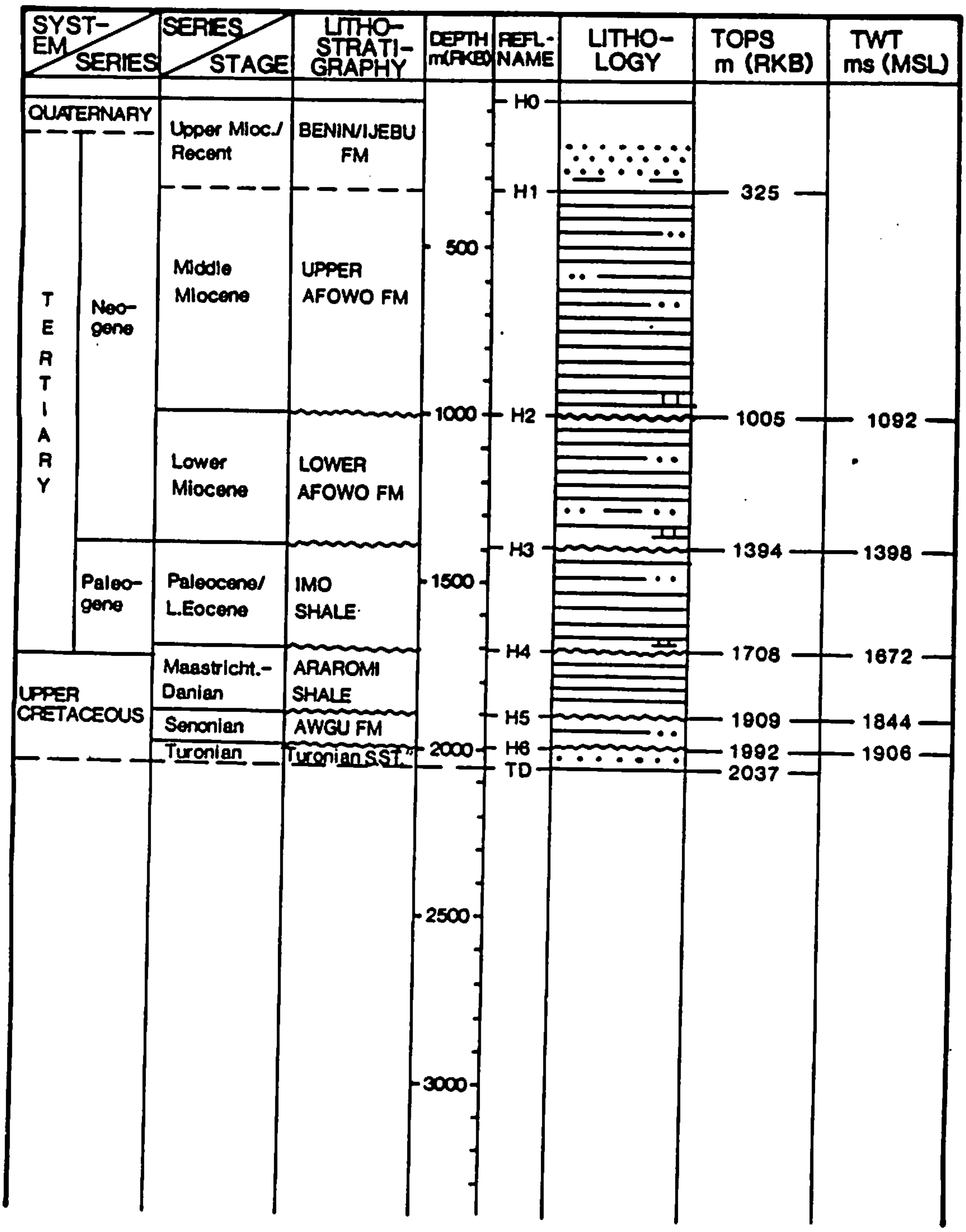

Fig. 2.9

WELL DATA SUMMARY

WELL	: D0-F1	LOCATION	: 06°08'18,5"N
OPERATOR	: UNION		: 02°39'53"E
SPUD DATE	: 11.1.1973	RKB (m)	: 10
COMP DATE	: 2.2.1973	WD (m)	: 87
STATUS	: ⌖	TD (m RKB)	: 2261

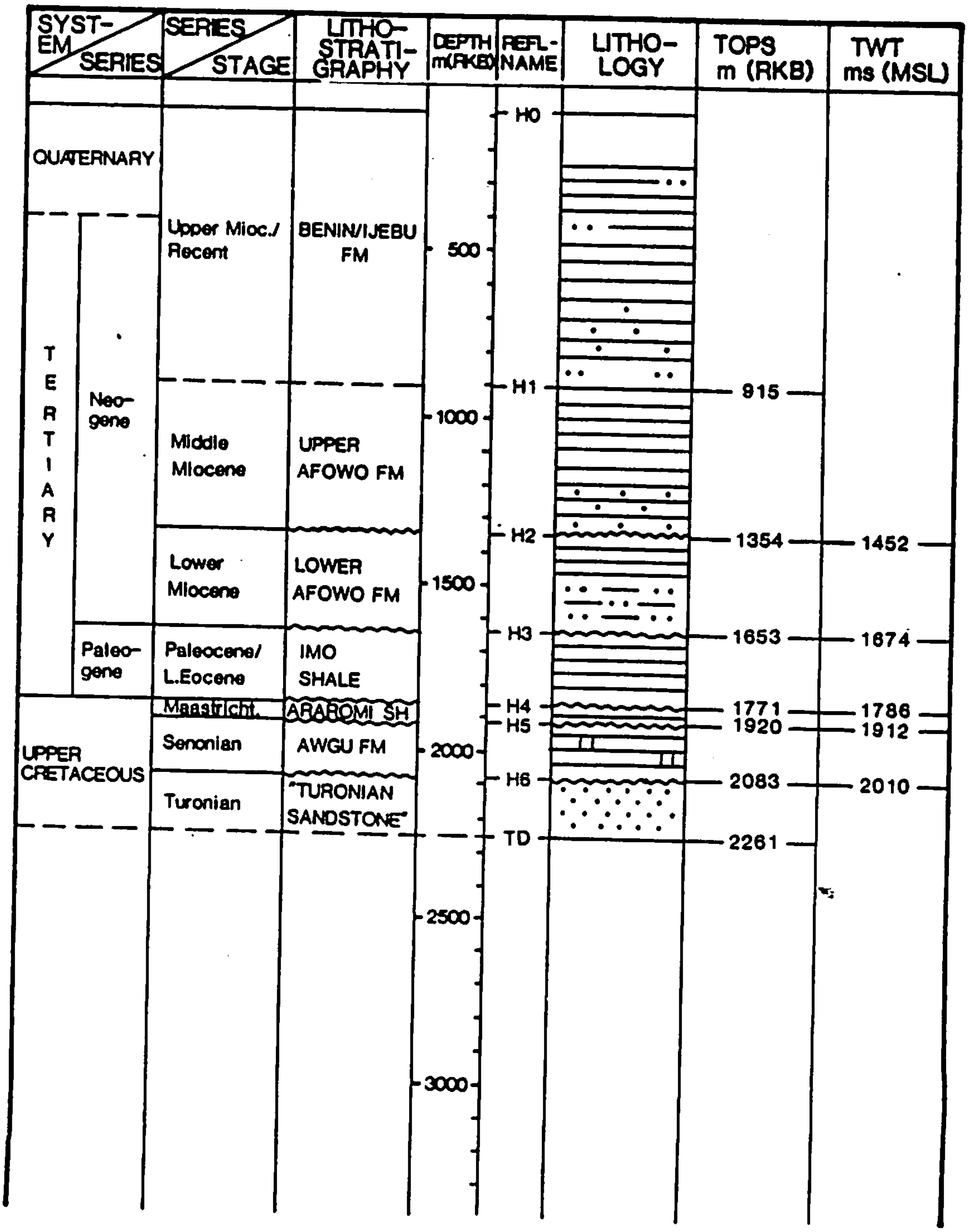

Fig. 2.10

WELL DATA SUMMARY

WELL	: SEME 1 (P1)	LOCATION	: 06°14'20.33"N
OPERATOR	: SAGA		: 02°41'15.24"E
SPUD DATE	: 1.6.1982	RKB (m)	: 26
COMP DATE	: 10.8.1982	WD (m)	: 28
STATUS	: ⌖	TD (m RKB)	: 2120

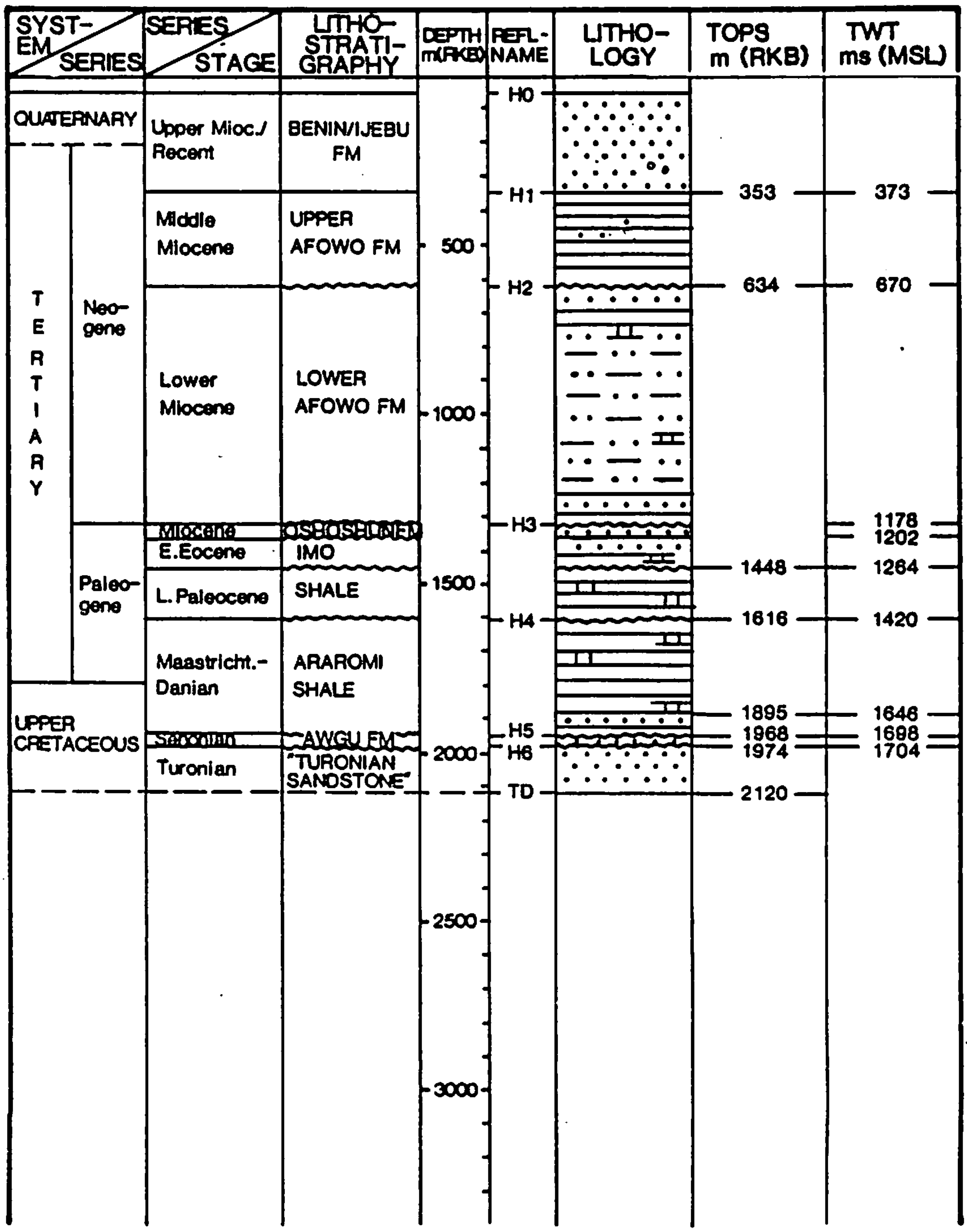

Fig. 2.11

WELL DATA SUMMARY

WELL	: SEME 2 (P1)	LOCATION	: 06°14'20.23"N
OPERATOR	: SAGA		: 02°41'15.24"E
SPUD DATE	: 11.8.1982	RKB (m)	: 26
COMP DATE	: 24.9.1982	WD (m)	: 28
STATUS	: ●	TD (m RKB)	: 1995 (TVD)

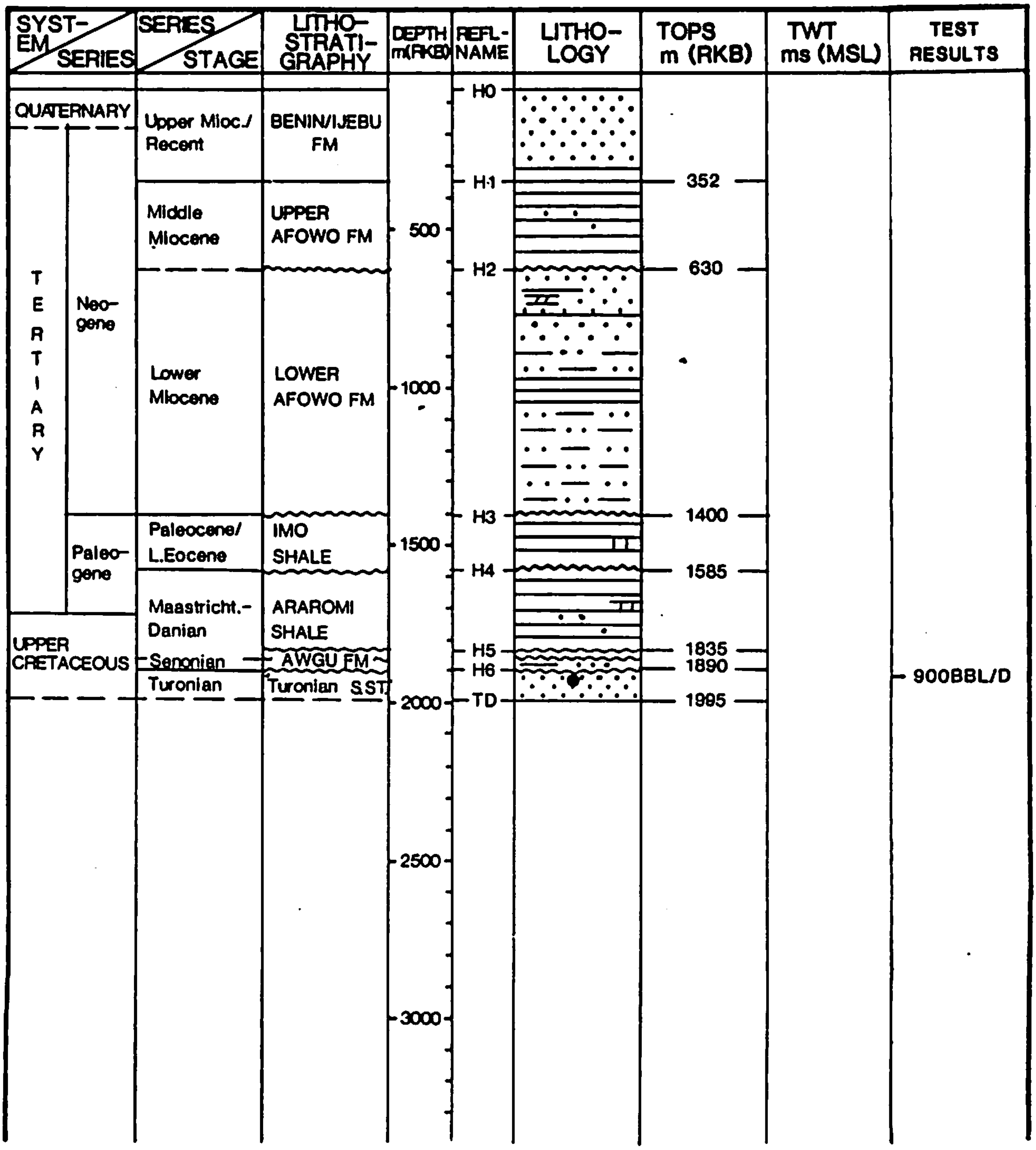

Fig. 2.12

WELL DATA SUMMARY

WELL	: SEME 3(P3)	LOCATION	: 6°15'13.983"N
OPERATOR	: SAGA		: 2°41'44.799"E
SPUD DATE	: 6.12.1982	RKB (m)	: 33
COMP DATE	: 12.1.1983	WD (m)	: 25
STATUS	: ●	TD (m RKB)	: 2015 (TVD)

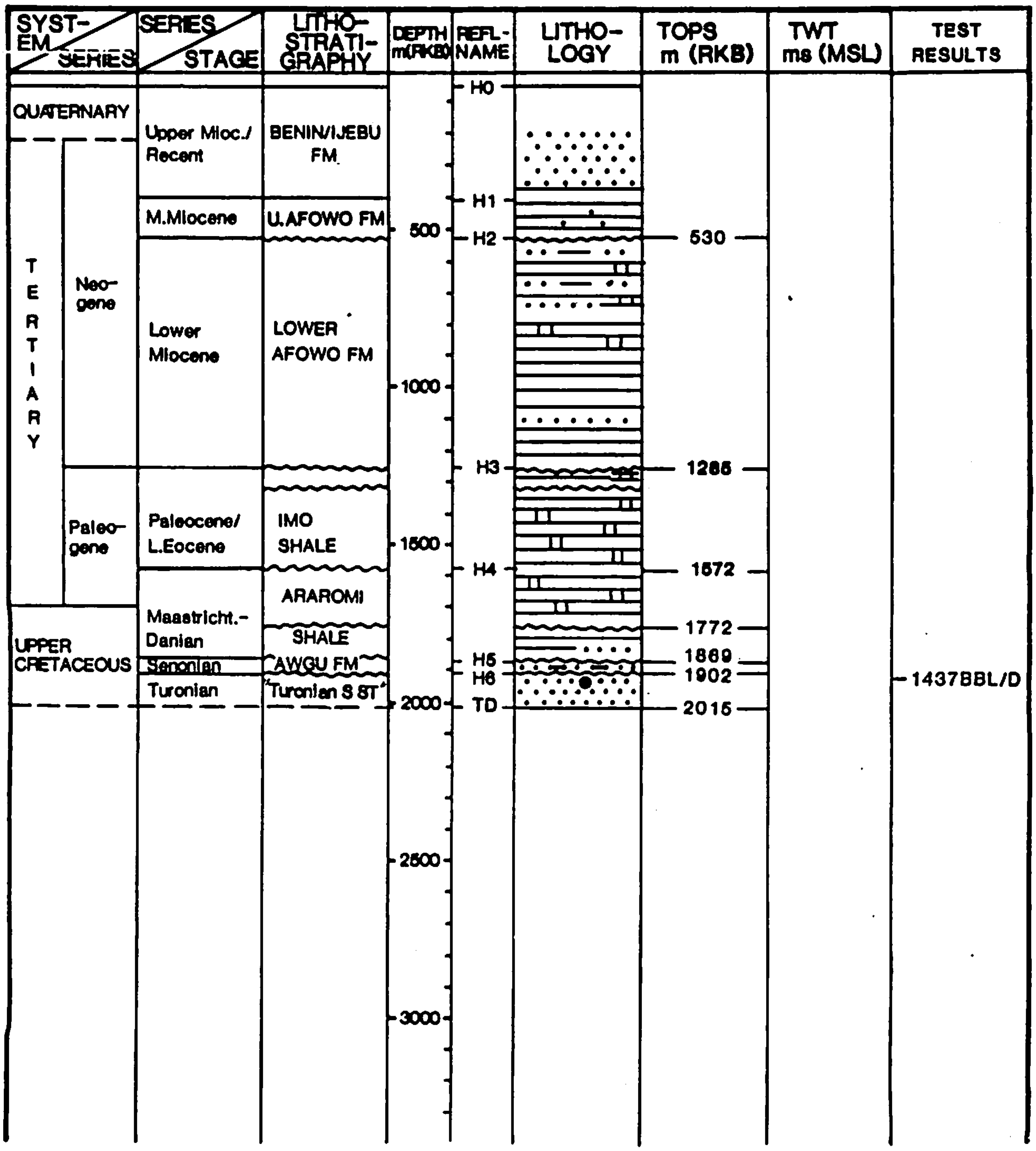

Fig. 2.13

WELL DATA SUMMARY

WELL	: SEME 4(P3)	LOCATION	: 6°15'13.983"N
OPERATOR	: SAGA		: 2°41'44.799"E
SPUD DATE	: 13.1.1983	RKB (m)	: 33
COMP DATE	: 7.3.1983	WD (m)	: 25
STATUS	: ●	TD (m RKB)	: 2720

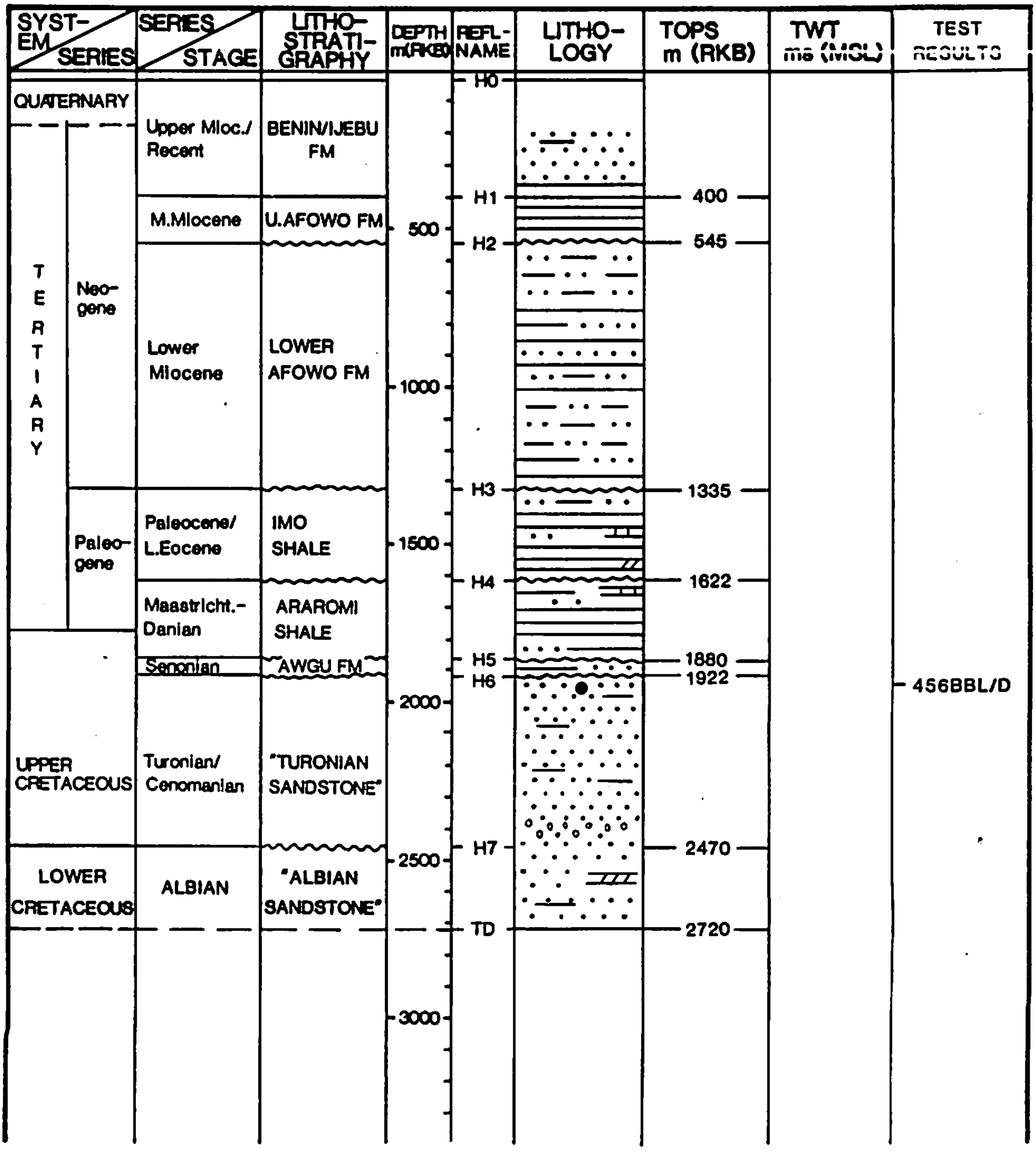

Fig. 2.14

2.3 Well Data Summaries

LEGEND:

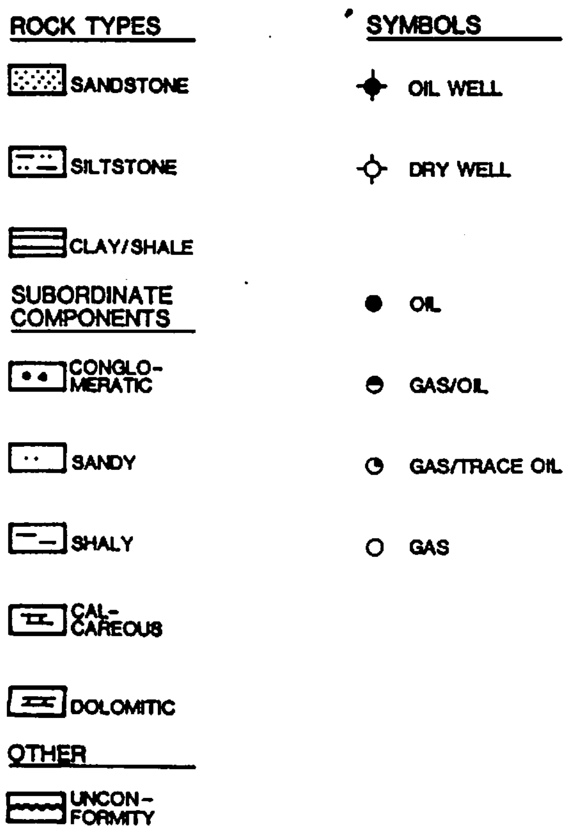

CHAPTER 3 22.6.84

EXPLORATION HISTORY

3.1 General

3.2 Seismic Surveys

3.3 Drilling

3.1 General

The first geological reconaissance of Benin was made in late 1800. With the discovery of phosphate in 1908 detailed surface studies were made up to 1920. Organized geologic mapping did not, however, begin until 1952 with the main objective being to locate sedimentary deposits of phosphates and metallic minerals in crystalline rocks. Ground water studies were initiated in 1950 by the French Government and continued into the late fifties. Their studies were subsequently published (Slansky 1962), and is to our knowledge the only geological publication that deals in detail with the sedimentary rocks onshore Benin. The work of Slansky is the result of field mapping, photogeologic interpretations and subsurface studies (cuttings and cores of stratigraphic tests, fig. 3.1).

Exploration for oil and gas in Benin began in 1964 when Union Oil Company of California and the Government of the Republic of Dahomey signed a convention whereby Union Oil acquired all rights in petroleum exploration and exploitation onshore south of basement outcrop as well as offshore as far out as the shelf break. This area equals approximately 15125 sq.km of which the offshore part constitutes roughly 3500 sq.km (fig. 3.2).

Data acquisition began in 1965 and consisted of geological field work, photogeology and an offshore regional seismic survey. In addition to the shooting of additional detailed and regional seismic data up to 1972, altogether 2616 km, Union Oil also conducted an onshore gravity survey of 4 months in 1969.

Drilling commenced in December 1967 as the offshore well DO-1 was spudded. It was abandoned the next year as an oil well after testing multiple pay zones. In 1968 and the five consecutive years altogether 9 successfull wells were operated by Union, all of them within or in the vicinity of the Sèmè Field close to the Nigerian border.

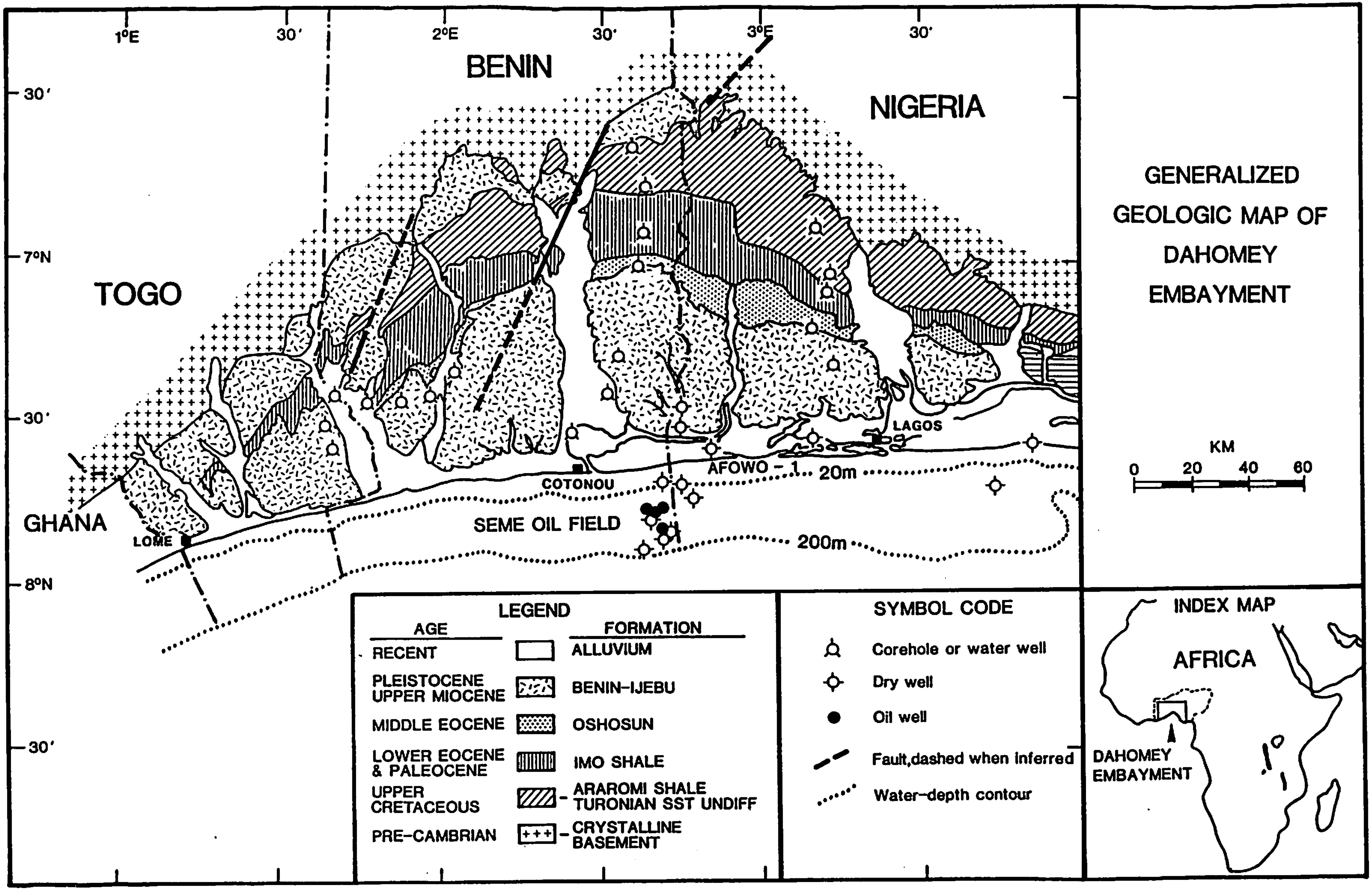

Fig. 3.1: Generalized geologic map of Dahomey Embayment. Based on Slansky (1962) and Jones and Hockey (1964), compiled by Billman (1976).

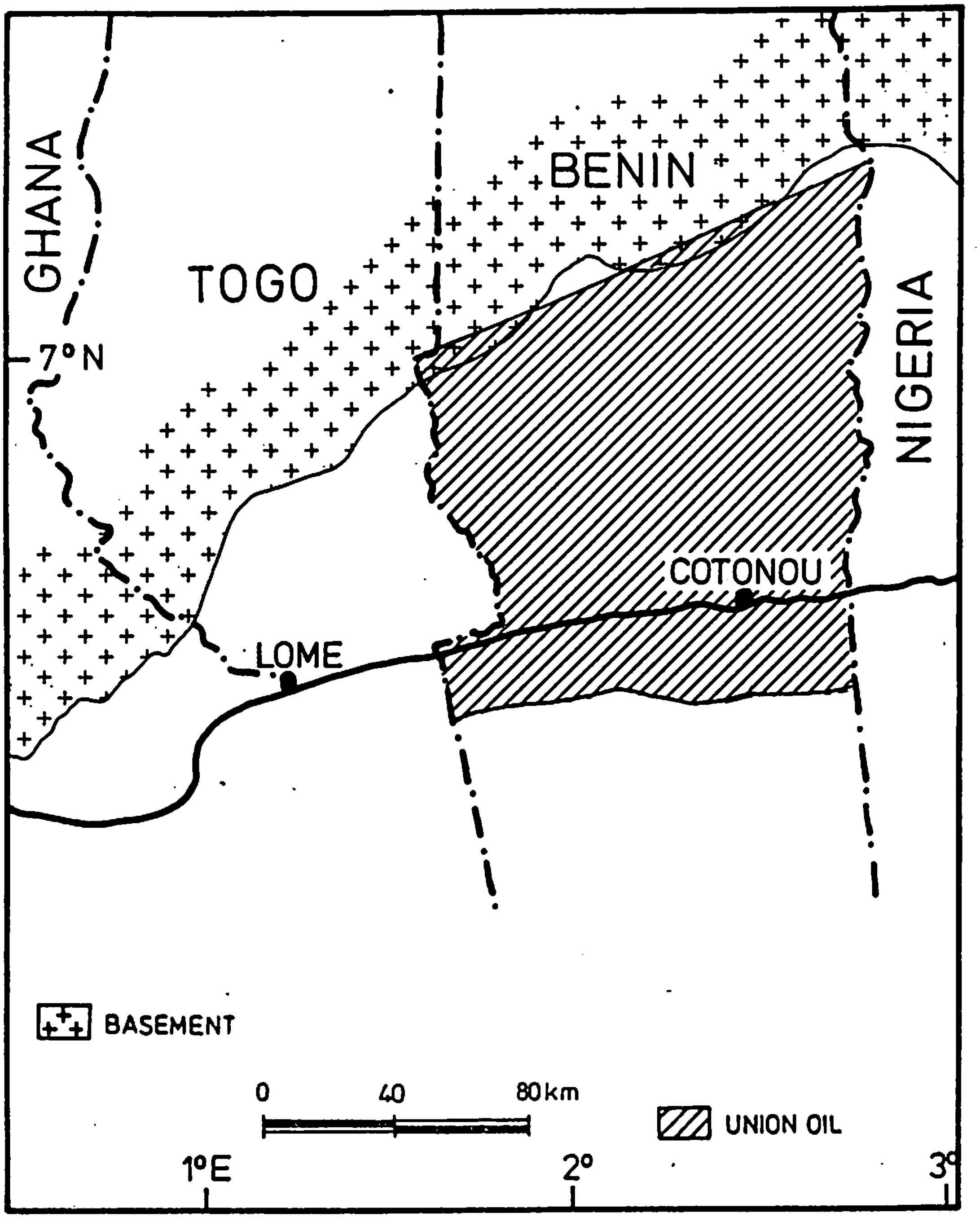

Fig. 3.2: Licenced area acquired by Union Oil in 1964.

In 1970 Union Oil relinquished in excess of 25% (4144 sq.km) of their acreage. This block was in 1971 awarded to Shell Dahorex (later Shell Beninrex), a subsidiary of Shell International, which altogether acquired 12000 sq.km onshore and offshore including 8000 sq.km in water depths greater than 180 m (600 ft) (fig. 3.3).

In 1971 Union Oil made a second relinquishment of 3626 sq.km (thus retaining 7355 sq.km) which was awarded to the American company Pivipoy Int. Co. (fig. 3.4). Their lease was again relinquished in 1973 without any data acquisition or drilling. The remaining Union Oil concession expired in 1975 after which Union Oil withdrew from Benin.

Shell Dahorex kept their acreage acquired in 1971 up to 1975 when the larger part of it was relinquished. This includes the entire onshore and shallow offshore, thus retaining two deep water offshore blocks that proved to contain structural closures. Additionally, Shell got a new block inside of the shelf break in which a detailed seismic survey was shot (fig. 3.5). This shallow water block was relinquished already the next year (1976) while the remaining two blocks were relinqusihed in 1977.

Since 1977 no concessions have been held neither onshore nor offshore Benin.

Union Oil's efforts offshore Benin resulted in the discovery of the Sèmè Oil Field, a sub marginal field at that time which was later considered profitable because of the rapidly increasing oil price in the seventies.

In 1976 negotiations thus began between Benin, Saga Petroleum and Kværner Engineering for a Field Development Feasibility Study. The study included a new seismic survey and was paid in full by the Benin Government. In 1977 it was decided that the

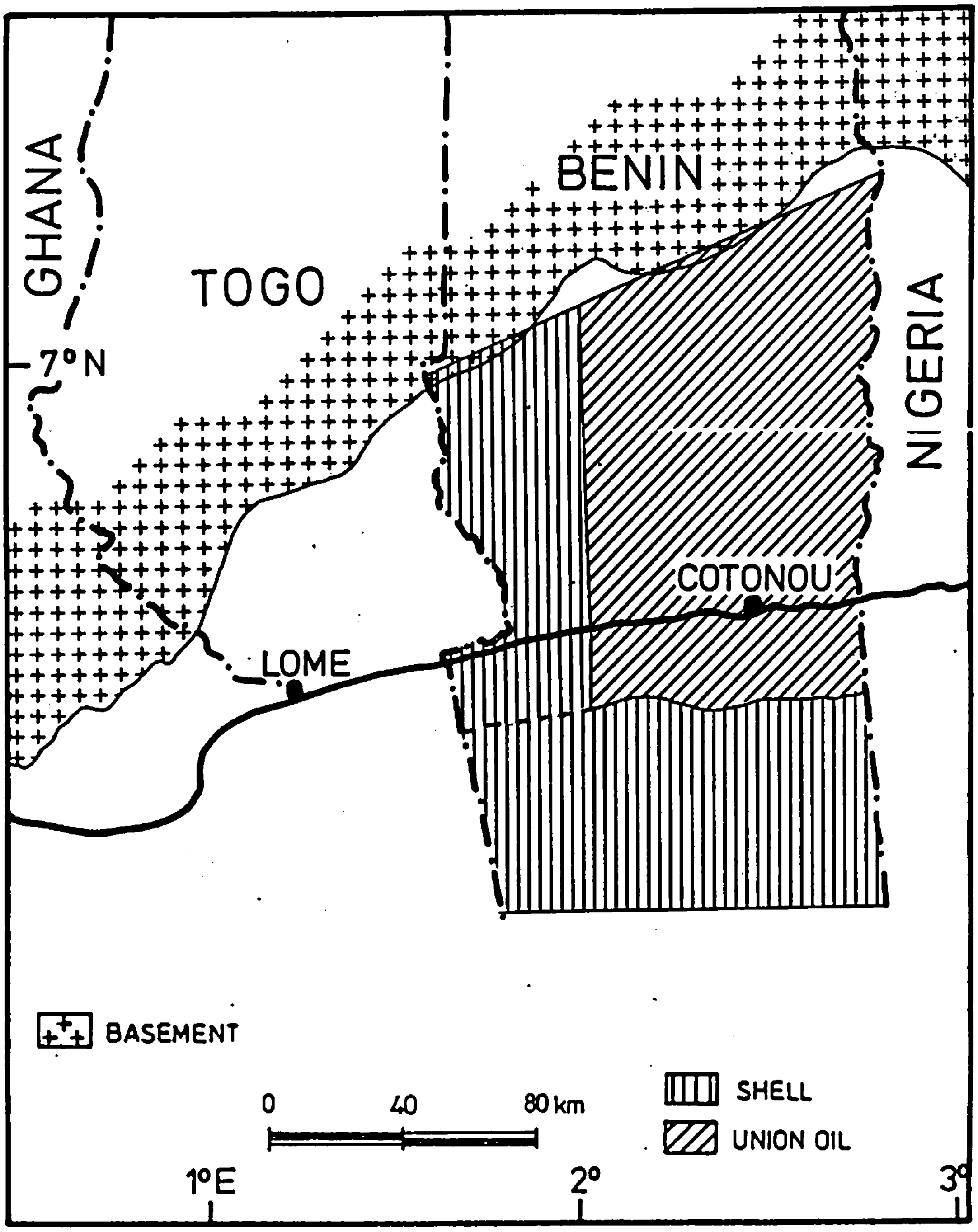

Fig. 3.3: Acreage held by Union Oil and Shell Dahorex following the 1970 relinquishment and the 1971 allocation.

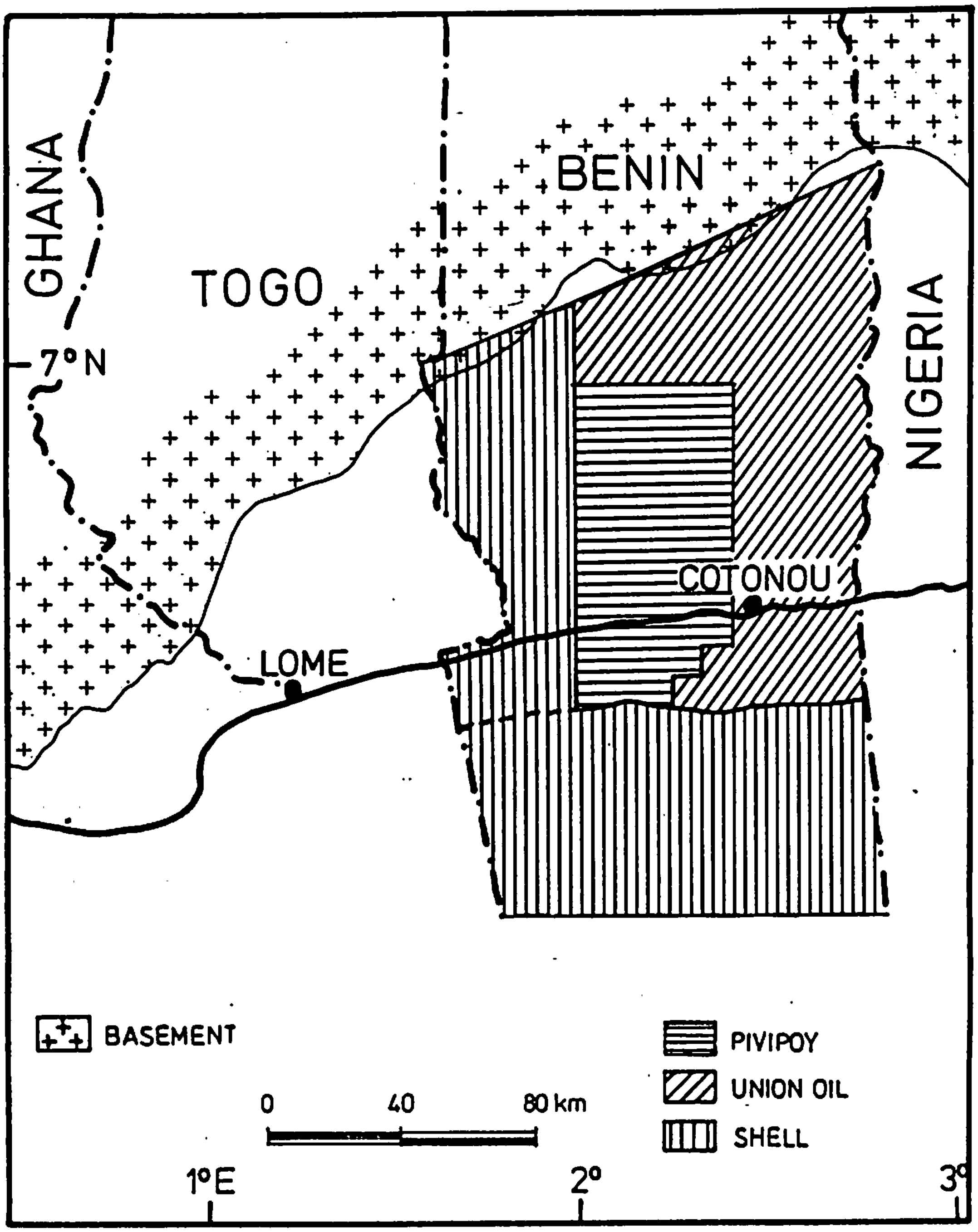

Fig. 3.4: Licence situation 1971 - 1973.

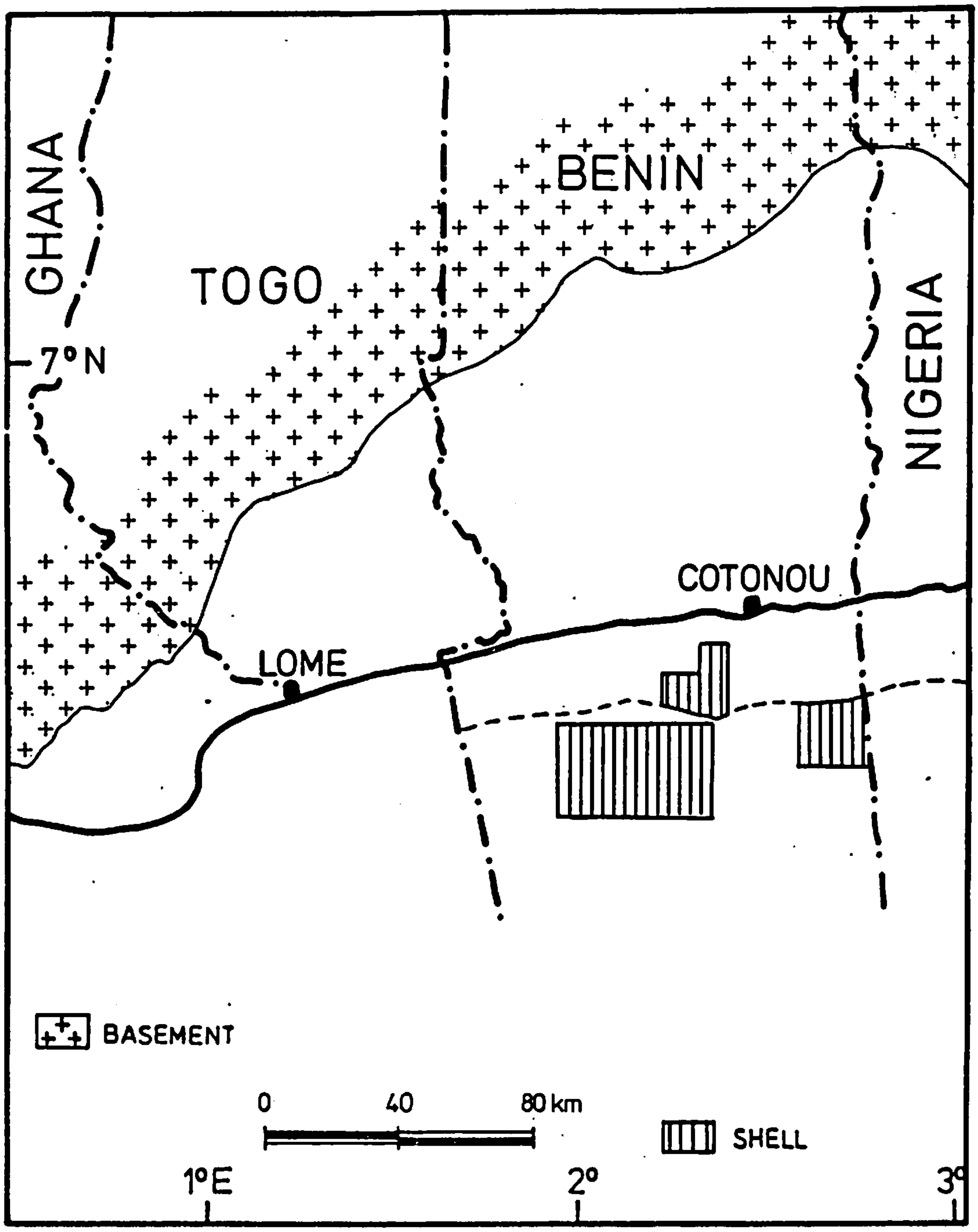

Fig. 3.5: Licence situation 1975.

oil field could be developed via a service contract. Such a contract was signed in 1979 by Saga Petroleum Benin a.s., a wholly owned subsidiary of Saga Petroleum a.s., and the Republic of Benin (Glenne 1981). The project then was officially started in 1980, and production began October 1, 1982. As of December, 1983, the daily production averaged about 8000 barrels of oil from 3 wells.

3.2 Seismic Surveys (table 3.1, figs. 3.6 - 3.15)

The very first industry seismic survey offshore Benin was shot in 1965 for Union Oil. This was a regional grid of 1363 km covering the entire shelf. The next survey shot in 1966 focused on the Sèmè structure and totalled only 212 km. The following three surveys (1968, 1970 and 1972) did also focus on the Sèmè Field in the progressive evaluation by Union Oil of the structure which was found oil bearing. All programs were rather small; 370, 170 and 501 km respectively.

Shell became active offshore Benin in 1971 when a triple survey program was initiated (1971, 1972 and 1975). The 1971 regional survey (1500 km) covered the western part of the shelf as well as the continental slope. The 1972 regional survey of 900 km was also mainly shot beyond the shelf break, but excluded the slope west of longitude 2° E. The 1975 survey had a detailed program of 715 km in shallow water mainly southwest of Cotonou and thus west of the Sèmè Field.

Except for two test lines shot by Saga in 1980, the last program up to the 1982 regional survey was operated by Saga on behalf of the Beninian Government in 1977. It totalled 428 km over the Sèmè Field as part of the Sèmè Feasibility Study (ref. chapter 3.1).

OPER-ATOR	CONTR-ACTOR(s)	YEAR OF	NOS. OF KMS	SOURCE	FOLD COVER-AGE	PROCESSED VERSIONS			AREA OF SURVEY	DATA QUALITY
						Filt. stack	Migr.	Rel. Amp.		
Union	Western	1965	1363	Explosives	600				Regional	Useless
Union	GSI	966	212	Explosives	600	X			Sèmè	Useless
Union	GSI	1968	370	Airgun	600	X			Mainly Sèmè	Fair
Union	GSI	1970	170	Airgun	1200	X			Sèmè and west of Sèmè	Fair
Union	CGG	1972	501	Vaporchoc	4800	X			Sèmè and south of Cotonou	Good
Shell	GSI	1971	1500	Airgun	2400	X			Deep water south of Cotonou and westwards	Fair to good
Shell	Mandrel	1972	900	Airgun	2400	X			Middle of the shelf	Fair to good
Shell	GSI	1975	715	Airgun	2400	X			South of Cotonou	Good
Saga	Geco	1977	428	Airgun	2400	X	X		Sèmè	Good
Saga	Horizon	1981	40	Airgun	2400	X	X		Sèmè	Good
Saga	Western/ Sefel	1982	1450	High pressure airgun	4800	X	X	X	Regional mainly within shelf break	Very good

Table 3.1: Seismic offshore Benin.

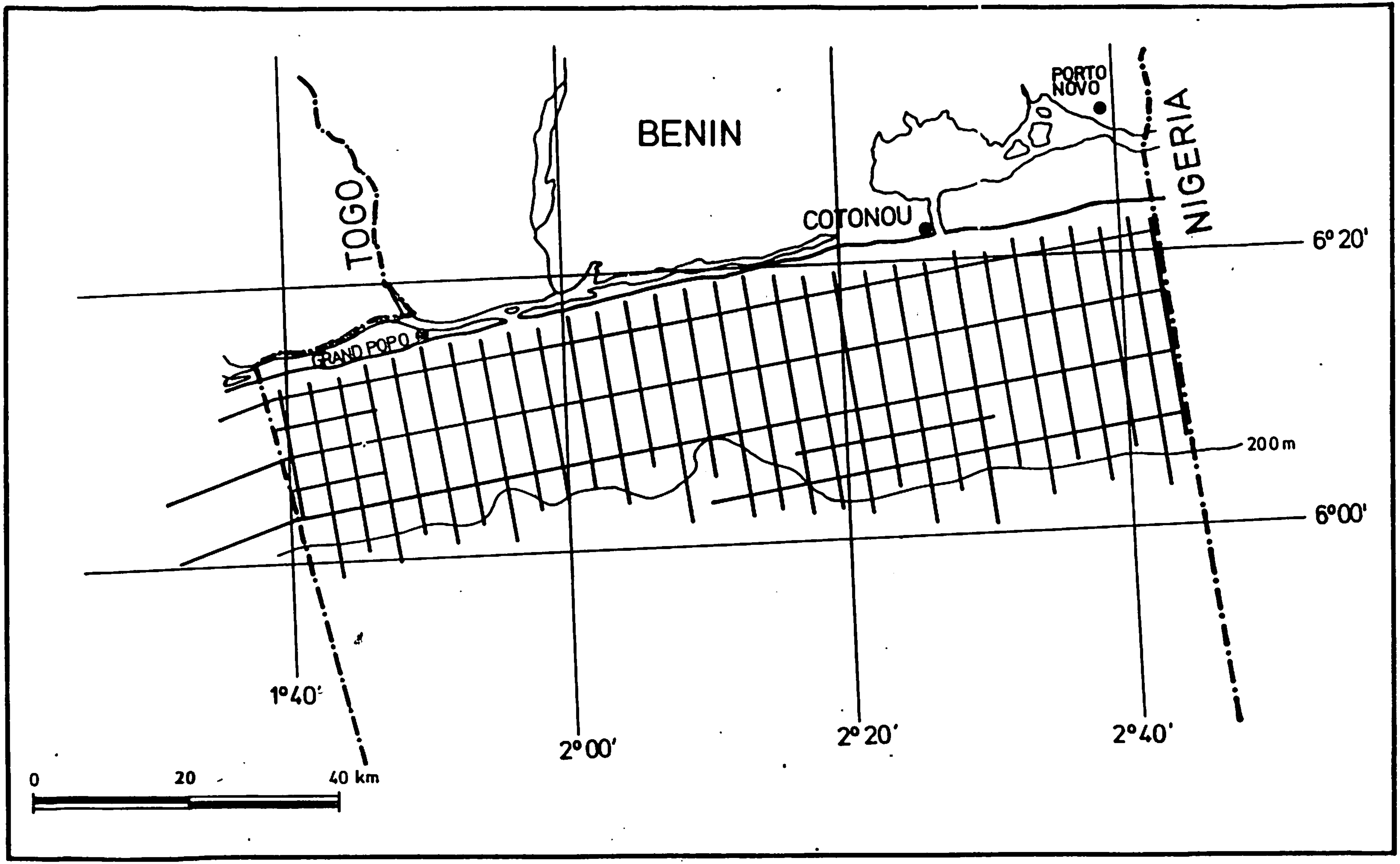

Fig. 3.6: Seismic grid operated by Union Oil in 1965 (1363 km).

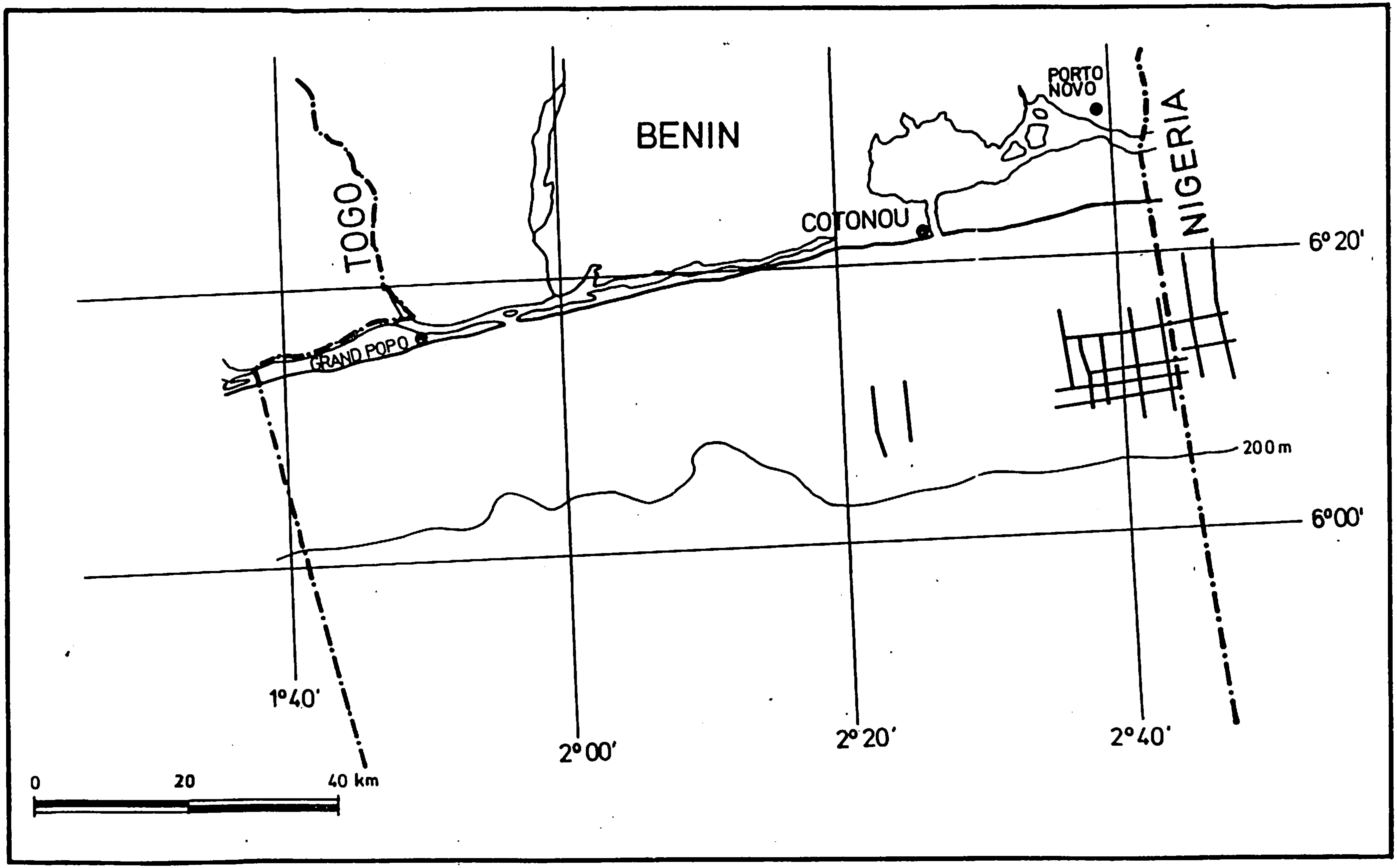

Fig. 3.7: Seismic grid operated by Union Oil in 1966 (212 km).

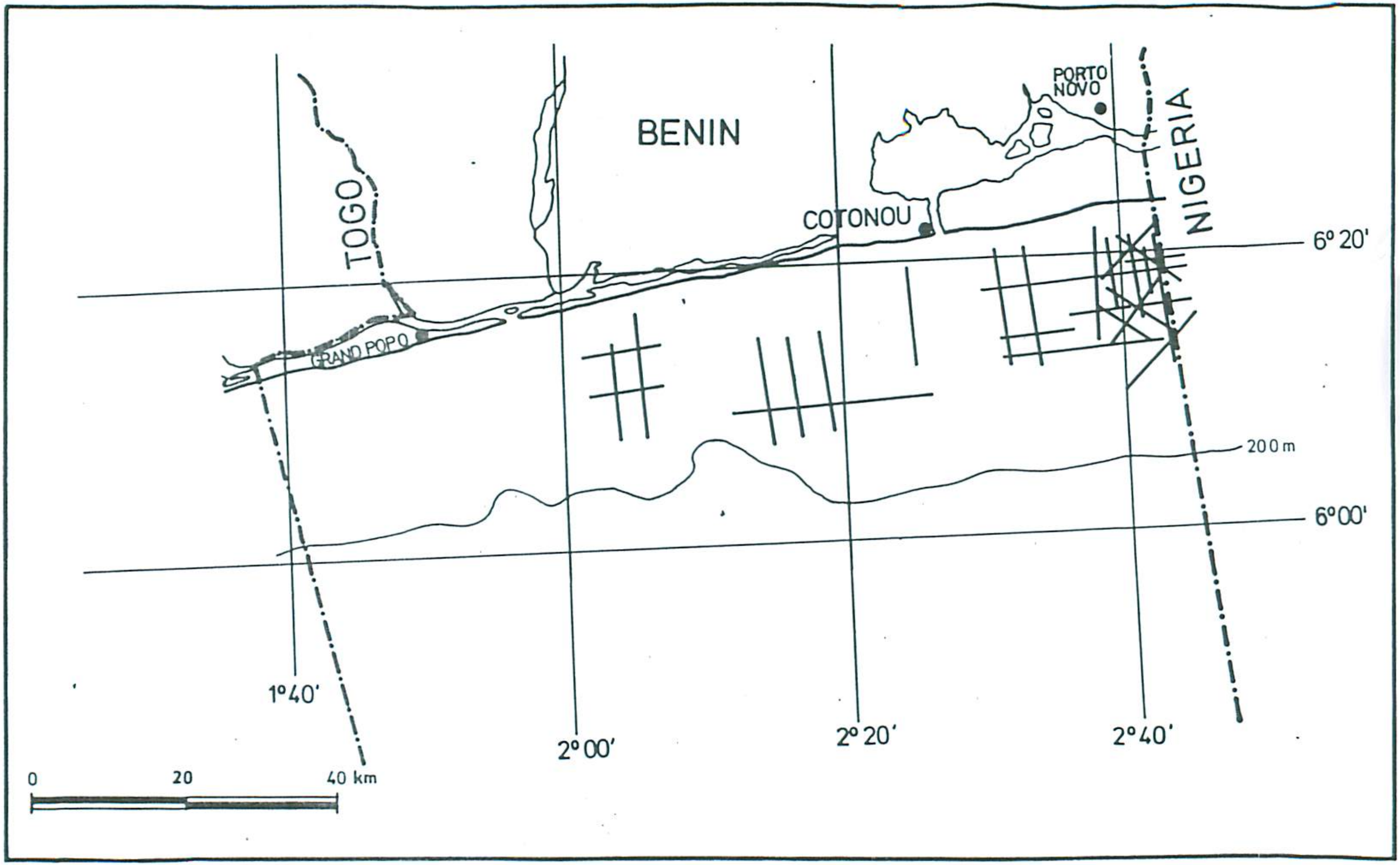

Fig. 3.8: Seismic grid operated by Union Oil in 1968 (370 km).

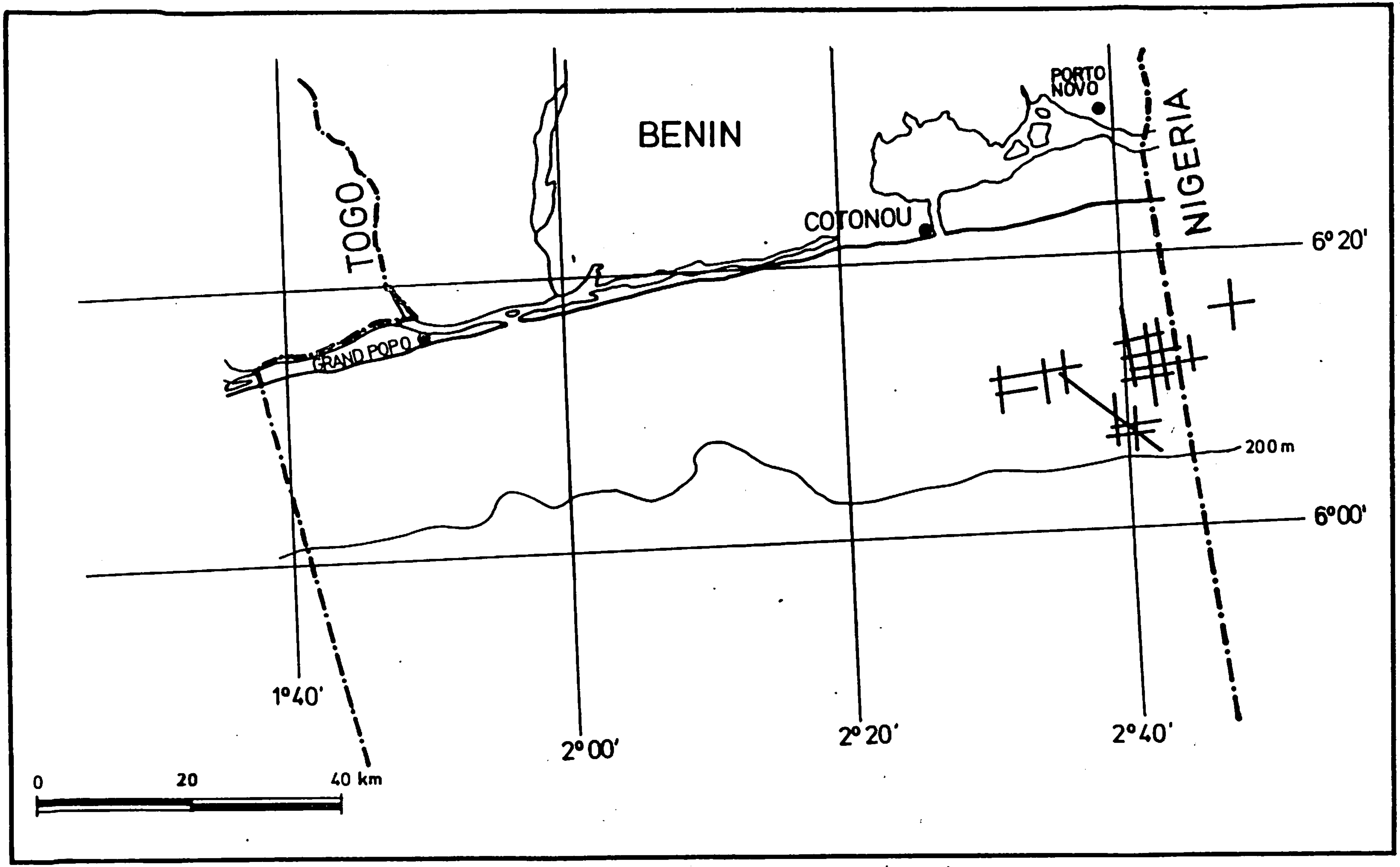

Fig. 3.9: Seismic grid operated by Union Oil in 1970 (170 km).

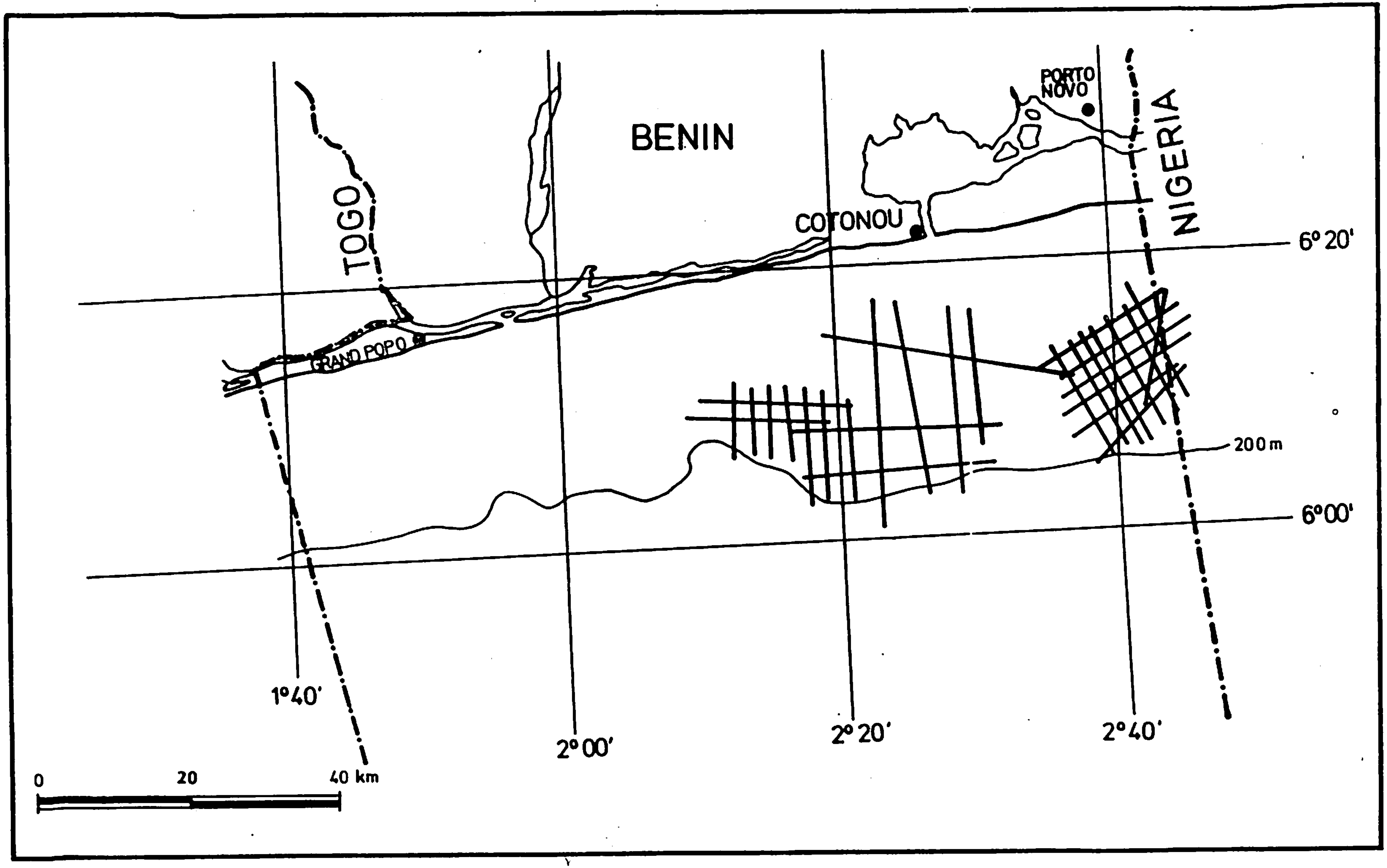

Fig. 3.10: Seismic grid operated by Union Oil in 1972 (501 km).

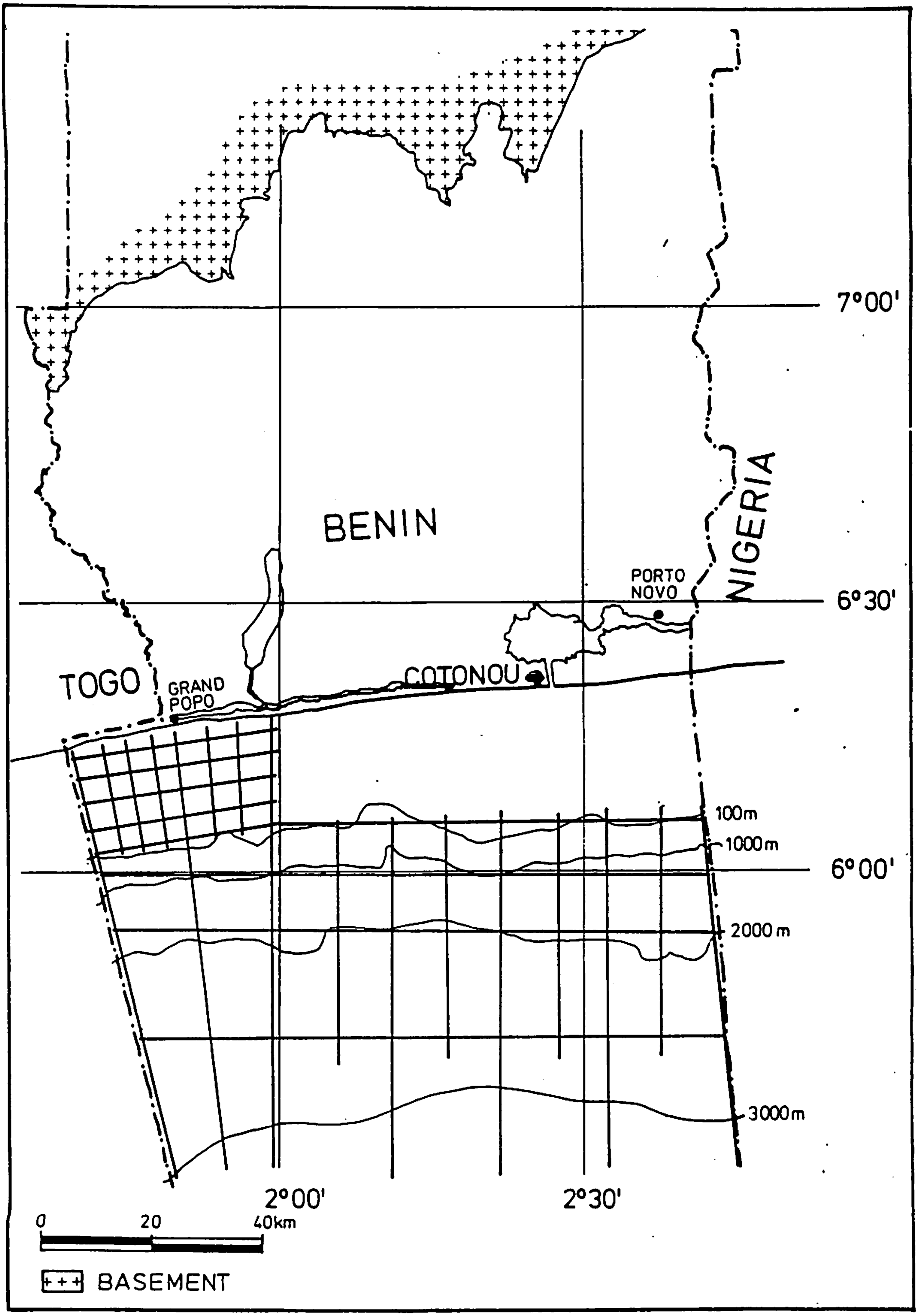

Fig. 3.11: Seismic grid operated by Shell in 1971 (1500 km).

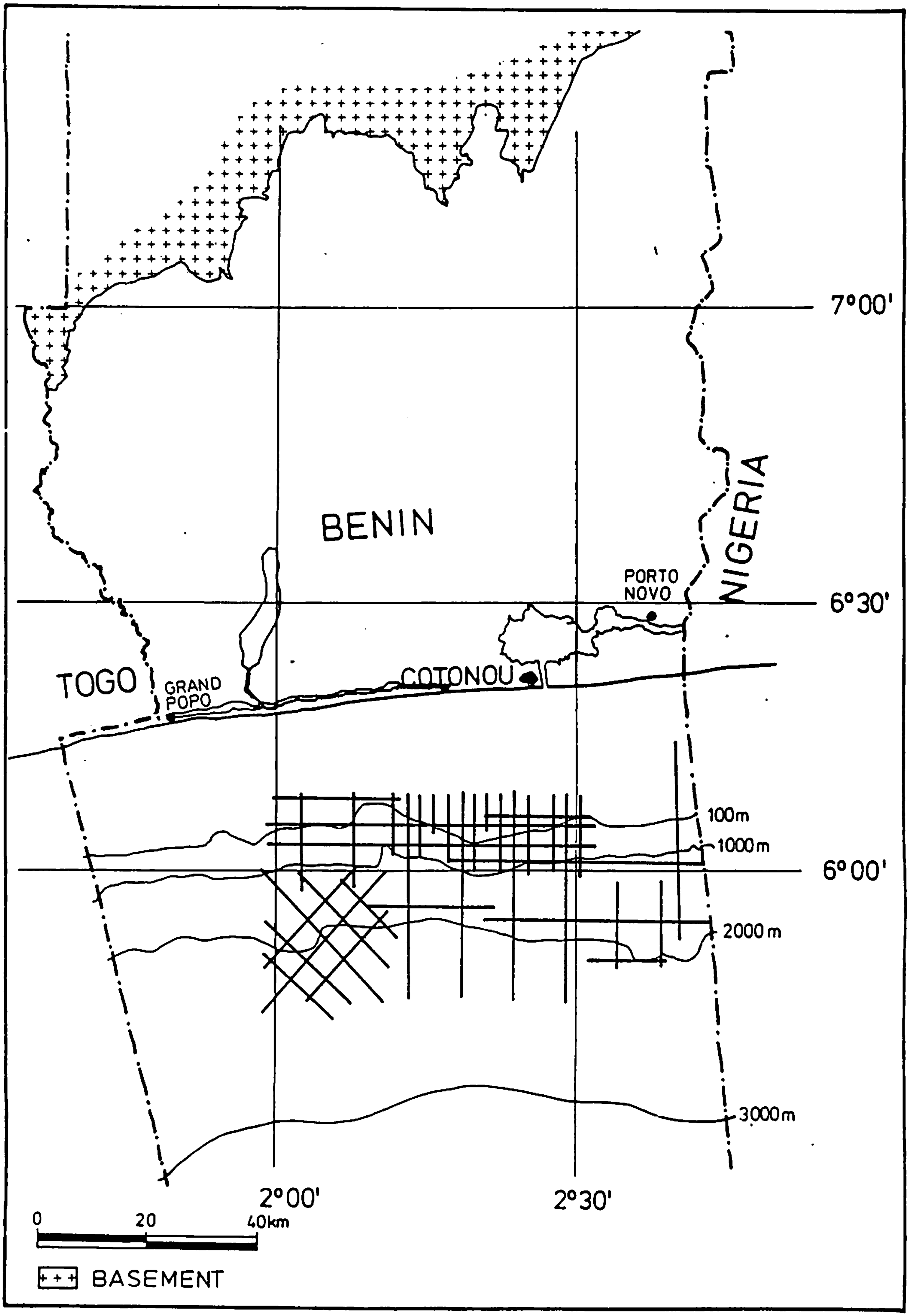

Fig. 3.12: Seismic grid operated by Shell in 1972 (900 km).

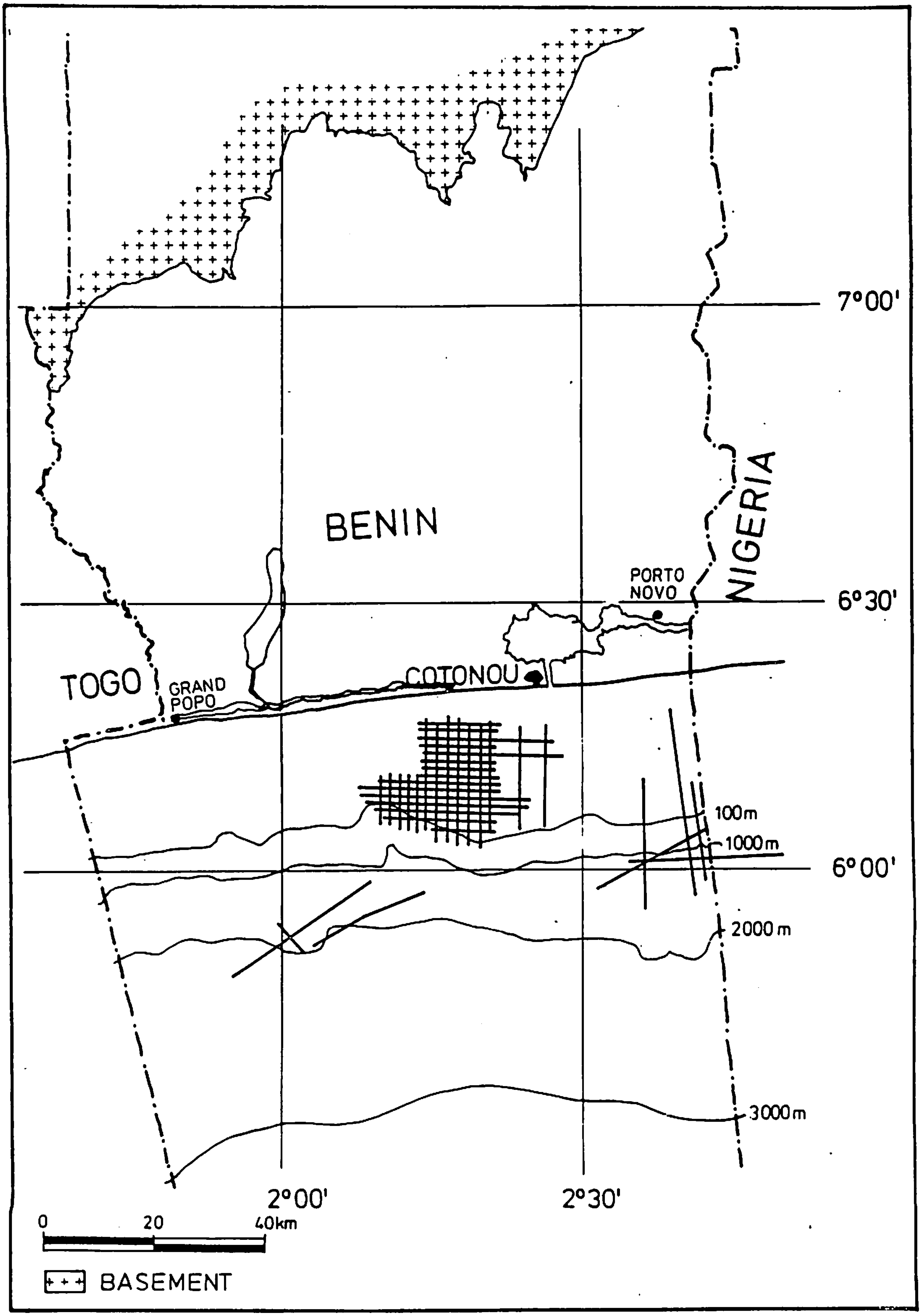

Fig. 3.13: Seismic grid operated by Shell in 1975 (715 km).

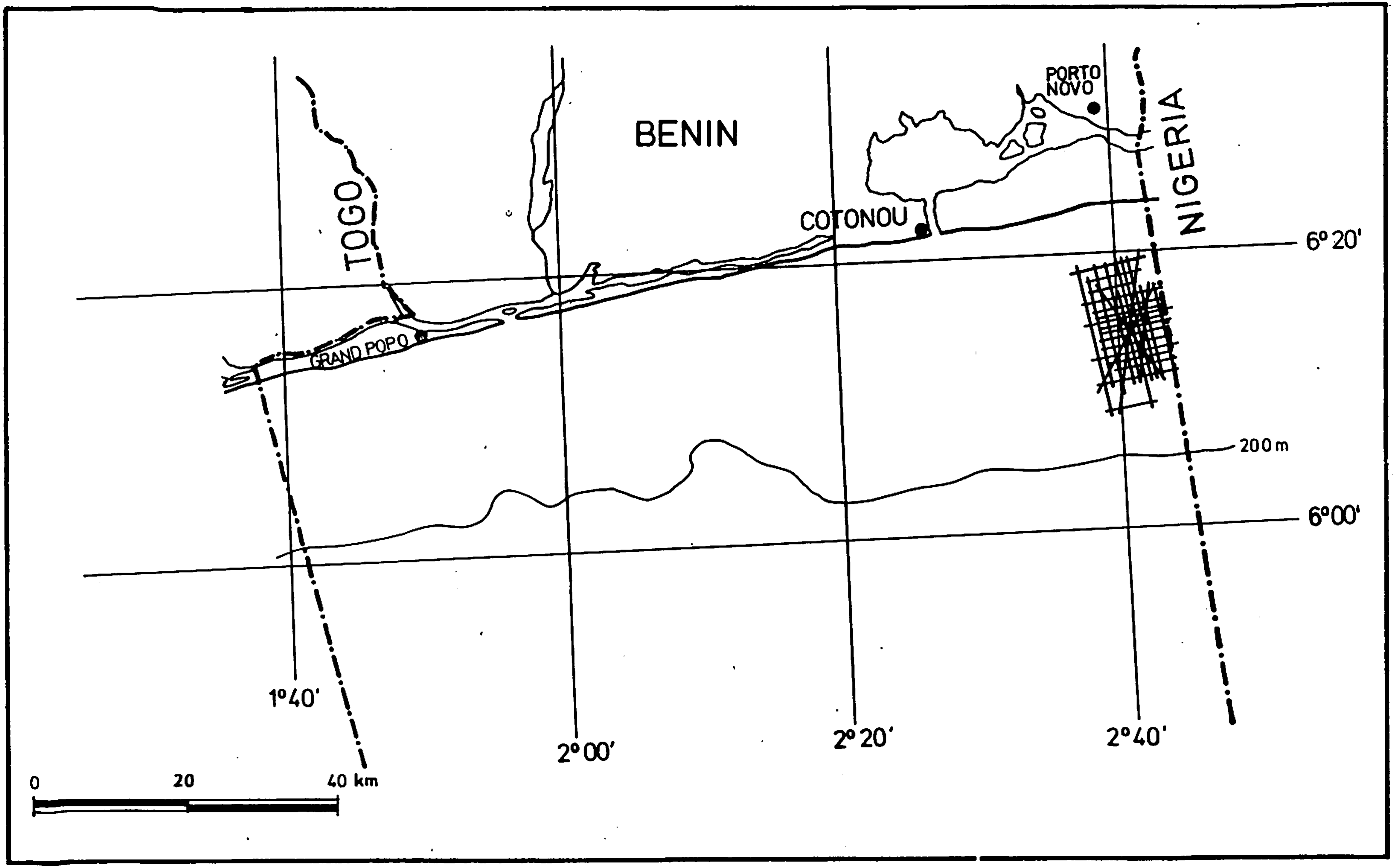

Fig. 3.14: Seismic grid operated by Saga Petroleum on behalf of the Beninian Government in 1977 (428 km).

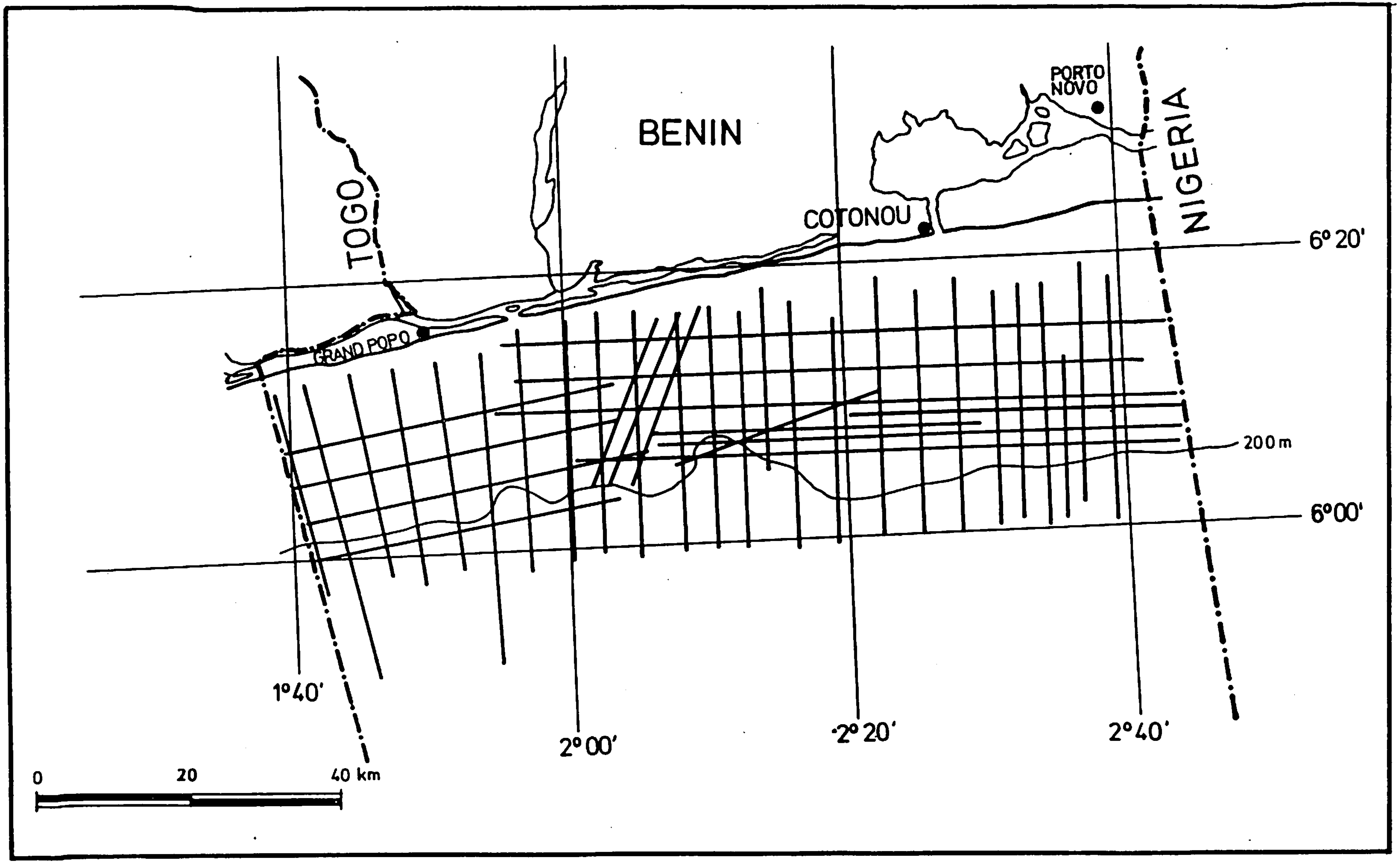

Fig. 3.15: Seismic grid operated by Saga Petroleum on behalf of the Beninian Government in 1982 (1450 km).

3.3 Drilling, (table 3.2, fig. 3.16)

Following two years of data acquisition, including two seismic surveys, the first well was spudded by Union Oil late 1967 on a structural high close to the Nigerian border. DO-1 came in as a discovery with four pay zones, three of them testing oil and one gas. The best zone (Zone 1 in the "Turonian Sandstone") produced close to 1500 BOPD of low gravity oil (22° API), while the deeper oil zone (Zone 3 in the "Albian Sandstone") reached a production rate of 240 BOPD. The deepest zone (Zone 4 in the "Albian Sandstone") tested 0.3 - 1.6 MMCFGPD, and represents a gas cap overlying a fourth oil zone. A probable second potential gas zone underlies the oil in Zone 4, only separated by a thin water bearing interval.

The encouraging results obtained in the first well led to the drilling of another well on the same structural high which appeared to be an E-W trending closure as mapped by Union Oil. DO-2A (DO-2 was abandoned) seemed to confirm the presence of multiple pay zones, and drill stem testing gave a flow rate of 780 BOPD (Zone 1) and an estimated flow rate of 8 MMSCFGPD (Zone 4). Union Oil had consequently by mid 1968 established the presence of a small oil field offshore Benin in water depths of about 25 m. Certain hopes were particularly entertained of the "Turonian Sandstone" (Zone 1) as a producing interval as this had far better porosities than the "Albian Sandstone" (Zones 3 and 4).

Union Oil now moved northwards to test another closed structural high close to the Nigerian border and 6-7 km offshore. The main objectives of DO-C1 which was spudded in July 1969, was to evaluate the same zones which had oil and gas shows in DO-1 and DO-2A and get a complete evaluation of the section down to basement. Both the "Turonian Sandstone" and the "Albian Sandstone" were present in this well which bottomed in crystalline rocks. Only minor oil and gas shows were

WELL	SPUD DATE	COMPL. DATE	TD	STATUS
DO-1	07.12.67	15.02.68	3081.5	Oil
DO-2A	04.03.68	24.06.68	2766.4	Oil
DO-A3	05.09.69	28.10.69	2812	Oil
DO-A4	20.11.70	10.12.70	2118	Dry
DO-C1	18.07.69	27.08.69	2245	Dry
DO-D1	30.10.69	12.01.70	2151.28	Dry
DO-D2A	16.05.70	14.08.70	3268	Oil
DO-D3	04.12.73	01.05.74	2037	Dry
DO-F1	11.01.73	02.02.73	2261	Dry
Sèmè 1 (P1)	01.06.82	10.08.82	2120	Dry
Sèmè 2 (P1)	11.08.82	24.09.82	1995	Oil
Sèmè 3 (P3)	06.12.82	12.01.83	2015	Oil
Sèmè 4 (P3)	13.01.83	21.03.83	2720	Oil
Sèmè 1A/B (P1)	15.04.83	09.06.83	2370	Dry
Sèmè SC (1)	20.07.83	23.08.83	2771	Oil
Sèmè 5 (P2)	15.11.83	End December		Oil

Table 3.2: Summary of drilling offshore Benin up to December 1983.

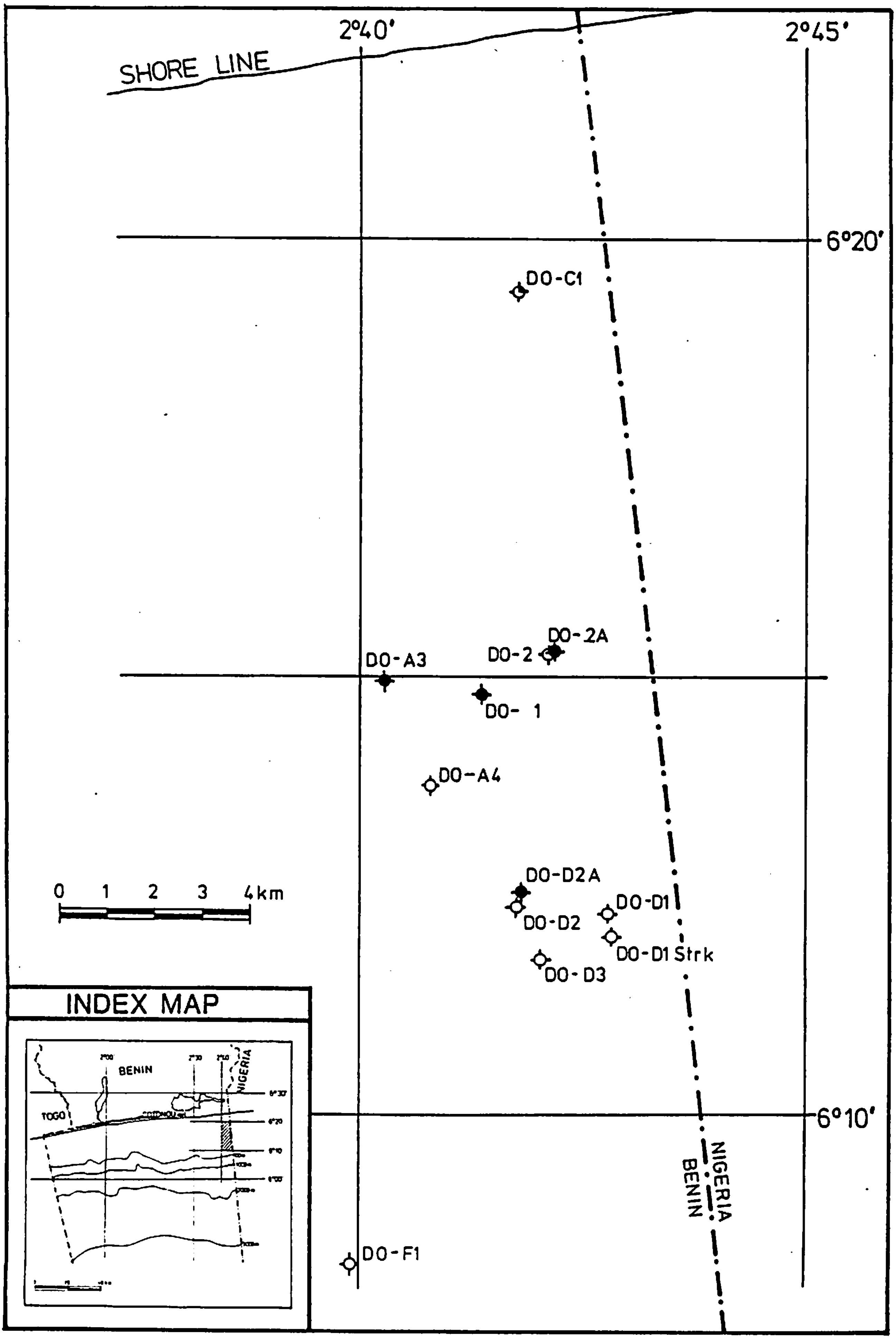

Fig. 3.16: Location of exploratory wells in Benin drilled by Union Oil.

reported from the "Albian Sandstone", but none of these were production tested as e-logs indicated water saturation ranging from 70 to 100%. The second anticlinal structure evaluated by Union Oil thus proved to be dry.

Infill seismic was shot by Union in 1968, and the next well was located as a delineation well on the western flank of the same high as DO-1 and DO-2A were drilled. DO-A3 was spudded in September 1969 and could also be classified as a successfull oil well. The "Turonian Sandstone" was again oil bearing, and a production test gave 912 BOPD. Zone 3 was in this well apparently encountered below the OWC and Zone 4 below the GOC but above the OWC. Testing of Zone 4 which primarily is a gas zone did not yield flow in this well.

Still in 1969, Union Oil moved further south to another anticline with closure at Cretaceous levels. DO-D1 was spudded in October, but encountered mechanical problems and never got any e-logs over the "Turonian Sandstone". Minor oil shows were reported by mud logging, but the well was classified as dry. It did not reach the "Albian Sandstone".

Encouraging oil and gas shows and an uncomplete evaluation of the D-structure by the drilling of DO-D1 resulted in a new exploratory well updip on the same high. DO-D2 had to be abandoned due to severe hole problems, but DO-D2A successfully penetrated all prospective formations as defined in the well program: the "Turonian Sandstone", the "Albian Sandstone" and the "Folded Cretaceous" (in this report: "Ise Formation"). Oil and gas shows occurred in the top of part of the "Turonian Sandstone" and throughout the "Albian Sandstone" as well as the Ise Formation all the way down to TD. Mostly these shows appeared to be of residual tarry oil. The Ise Formation was tested in a 10 m interval which had particularly good hydrocarbon indications. No oil, gas or formation fluid was produced, however, due to low permeability. From a drill stem test in the "Albian Sandstone" (Zone 4) 10 barrels of low gravity oil (18-20^{o} API) was recovered. The "Turonian Sandstone" again proved to have the best reservoir properties as Zone 1 flowed 1150 bbls/d of 22^{o} API oil and 0.1 MMCFGPD. By mid 1970 Union Oil had thus proved the presence of two separate oil accumulations offshore Benin.

The next step was now to further delineate the A-structure through a southern step out. DO-A4 was spudded in November 1970. TD was reached in the "Turonian Sandstone" without encountering any significant shows. The top of the reservoir was below the OWC. DO-A4 was consequently not tested.

After a two years' halt in drilling, Union Oil spudded DO-F1 in January 1973. DO-F1 is the southernmost test, and was also located on an appearant high. Minor shows were reported but did not substantiate any production tests. Log calculations showed high water saturation. Only the upper part of the "Turonian Sandstone" (Zone 1) was evaluated.

The last exploration well drilled by Union Oil offshore Benin, late 1973, was a southern step out on the D-structure (DO-D3). It also evaluated Zone 1 in the "Turonian Sandstone", but this proved to be dry.

CHAPTER 4 22.6.84

REGIONAL TECTONIC ANALYSIS AND HISTORY

4.1 General

The entire Atlantic margin of western Africa consists of open sedimentary basins of Mezozoic to Tertiary age, the existance of which is attributed to the separation of the African from the American continent (fig. 4.1). In the terminology of Klemme (1980) most of these basins would be classified as break up basins of passive margins (type V). (Exceptions are deltas (type VIII) which are superimposed on the former type.) The geological history of these basins is therefore closely interrelated and must be discussed with reference to the opening of the Atlantic Ocean.

The northern Gulf of Guinea forms the coastline of Liberia, Ivory Coast, Ghana, Togo, Benin and Cameroon, and includes the following sedimentary basins (fig. 4.2): Sierra Leone, Ivory Coast, Dahomey Embayment, Niger Delta and Douala Basin (northern Cameroon). The marginal basins are limited to the north by the Upper Guinea Arch which stretches for more than 2000 km in a east-west direction from Cameroon to Liberia. In this arch region, which comprises the Birrimian Shield and the Dahomeyan Shield, metamorphic basement is exposed over wide areas.

The Dahomey Embayment is an elongated basin that extends onshore from the Volta Delta (Ghana) in the west through Togo and Benin and as far east as the Okitipupa High in Nigeria (fig. 4.3). Offshore it may extend further west along the continental shelf of Ghana. Considerable thickness of sedimentary rocks is also evident beneath the continental slope. The basin's total length is thus approximately 700 km with a maximum width to the shelf break of close to 180 km along the Benin/Nigeria border. The basin's total area onshore and offshore to the 200 m isobath is on the low side of 50 000 sq.km. The offshore part constitutes more than 10 000 sq.km.

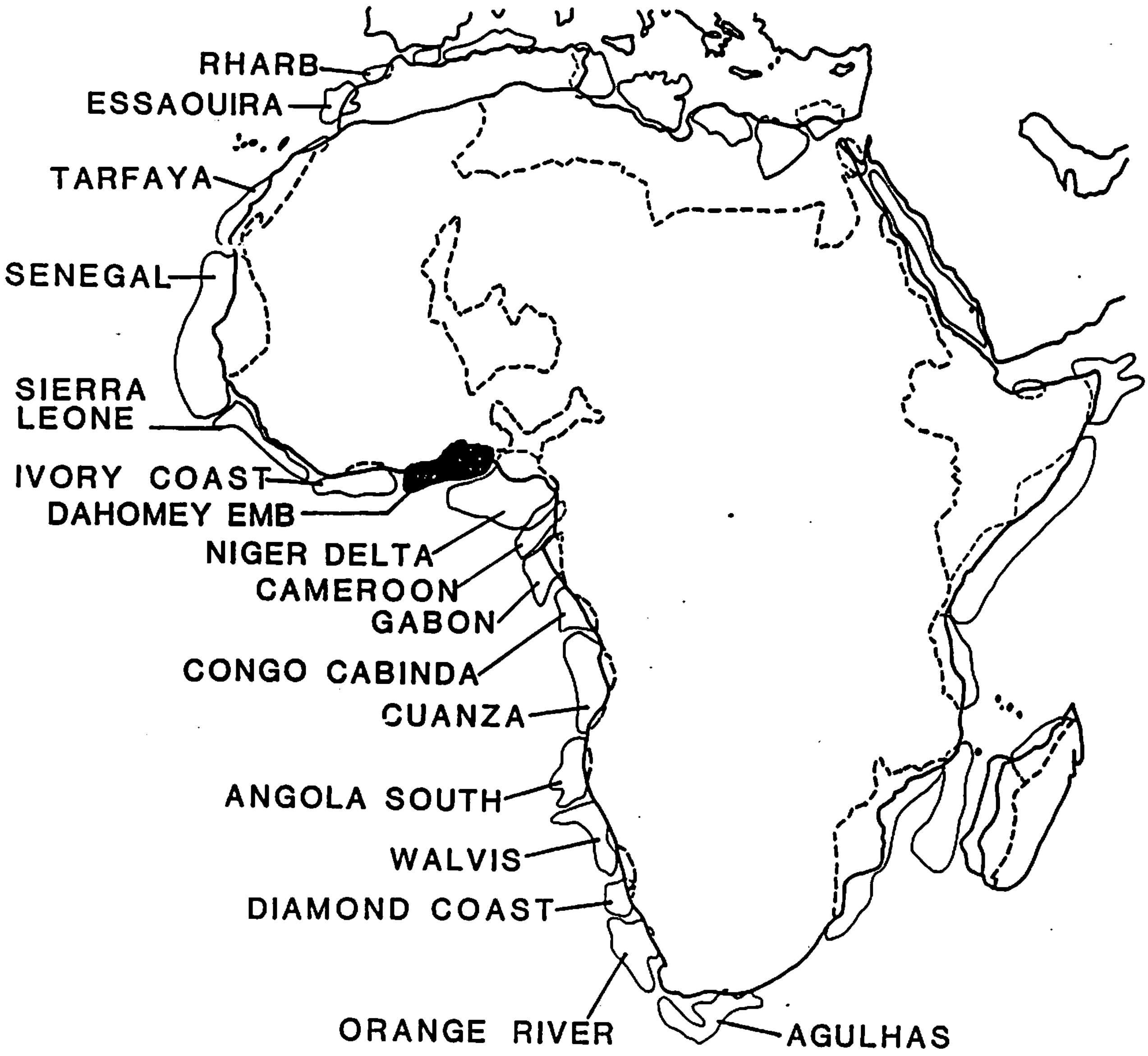

Fig. 4.1: Sedimentary basins off western Africa. Based on St. John (1980).

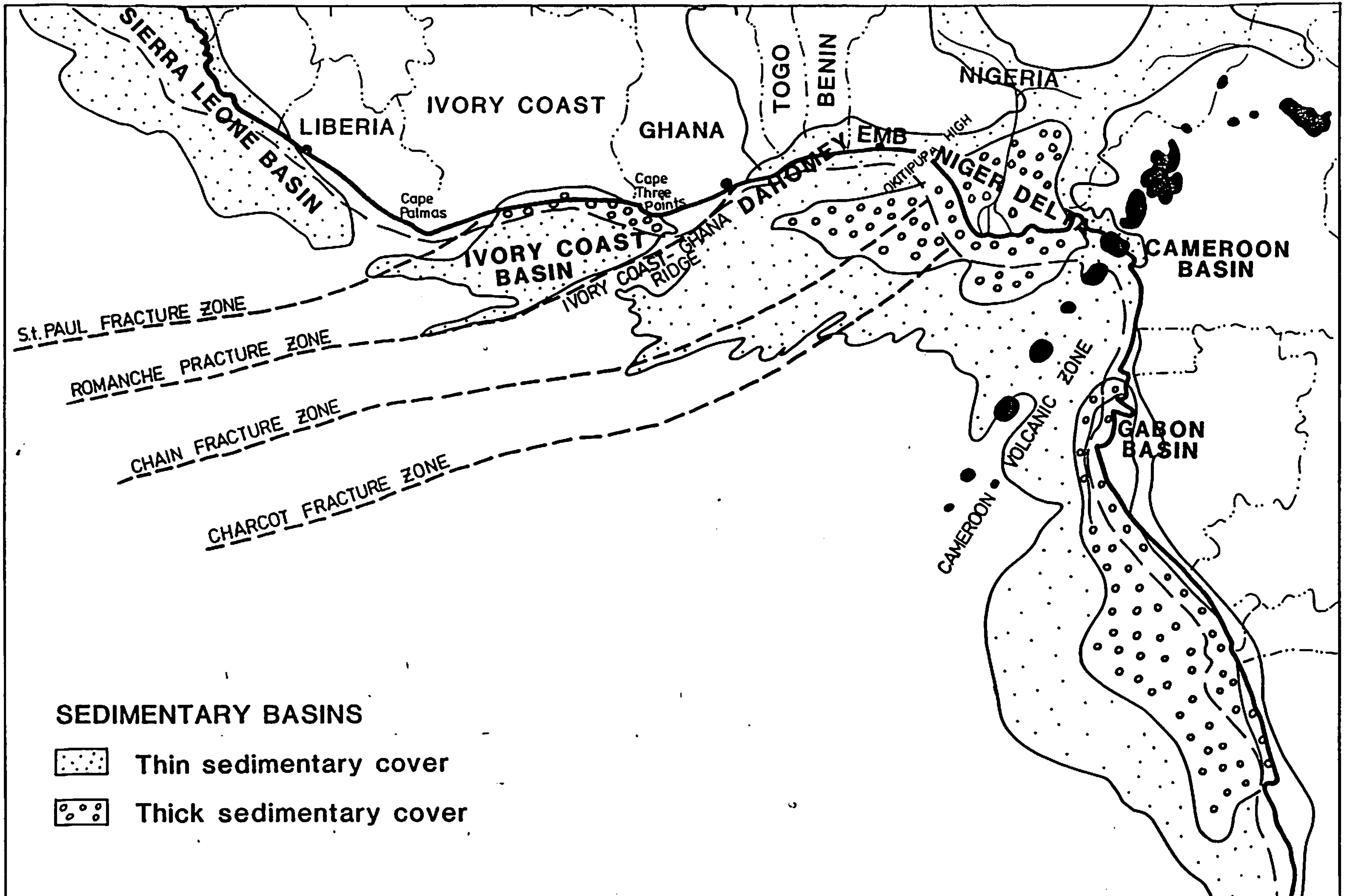

Fig. 4.2: Sedimentary basins, Gulf of Guinea.

The coastal area of Africa between Liberia and Nigeria is influenced by several major transform faults from northwest to southeast: St. Paul Fracture Zone, Romanche Fracture Zone, Chain Fracture Zone and Charcot Fracture Zone (Francheton & Le Pichon 1972). It is not clear to what extent these structures should be matched with lineaments in the onshore part of the area (Whiteman 1982, p. 170), although there seems to be a close correlation between development of sedimentary basins and fracture zones within the continental shelf of Northern Gulf of Guinea (Burke 1969). On the other hand, the structural grain of the basement does not seem to have influenced the tectonic development (Whiteman 1982).

The Romanche and Chain Fracture Zones are the most prominent regional tectonic features in the Northern Gulf of Guinea. These structures were initiated as transform faults in ?Late Jurassic - Early Cretaceous times as a part of a RRR-triple junction. The movements along the transforms were of a right-lateral type (Burke et al 1971, 1972). The fracture zones trend ENE, bending into a somewhat more NE-SW direction close to the Dahomey Embayment (figs. 4.2 and 4.3).

The eastern part of the Romanche Fracture Zone runs into the Ivory Coast - Ghana Ridge, whereas the eastern termination of the Chain Fracture Zone is obscure. Okipitua High is another NE-SW trending structure, bordering the Dahomey Embayment on its eastern flank (fig. 4.3).

4.2 Opening of the South Atlantic

The Central Atlantic between the east coast of North America and the bulge of Africa was the first part of the Atlantic Ocean to open. Triassic - Jurassic grabens with vast amounts of non-marine sediments formed on the continental margins prior to the split-up in Late Jurassic times.

In the Middle Jurassic (about 165 ma) North America, South America, Greenland, Europe and Africa still formed one expanse of land (fig. 4.4) although continental rupture was evident. Oceanic crust now started to develop between North America and Northwest Africa, separating the northern continents from Africa and South America and opening up the infant North Atlantic and Caribbean. At this stage pre-oceanic rifting processes probably was initiated between South America and Africa. A narrow rift valley existed with numerous lakes and volcanoes, and the conditions might have been similar to those in the present East Africa rift zone. As the rifting process continued for some 45 million years, the rift expanded and deepened considerably. It did, however, not yet extend as far as the Gulf of Guinea.

By about 130 ma, at the end of Berriasian, South America began to separate from Africa (fig. 4.5). Simultaneously, the ocean transgressed the former rift valley south of the aseismic ridges Rio Grande Rise and Walvis Ridge, thus forming a linear seaway with marine carbonate-rich sediments being deposited. The rift now extended northwards and contained lacustrine sediments, non-marine red sandstones and thick piles of conglomerates. Rifting also began in the proto-Gulf of Guinea, and this area eventually reached the "East Africa stage" while the South Atlantic was already into the "Red Sea stage".

Physiographically, the ocean floor of the South Atlantic was split into three basins in Early to Late Cretaceous times. The two southern basins were divided by the precursor of the Mid Atlantic Ridge while the northern basin was bounded to the south by the Rio Grande Rise and Walvis Ridge. Now landlocked on three sides evaporation in excess of precipation occurred in the northern basin, resulting in the deposition of massive salt layers (Aptian age). Salt deposition did, however, not reach

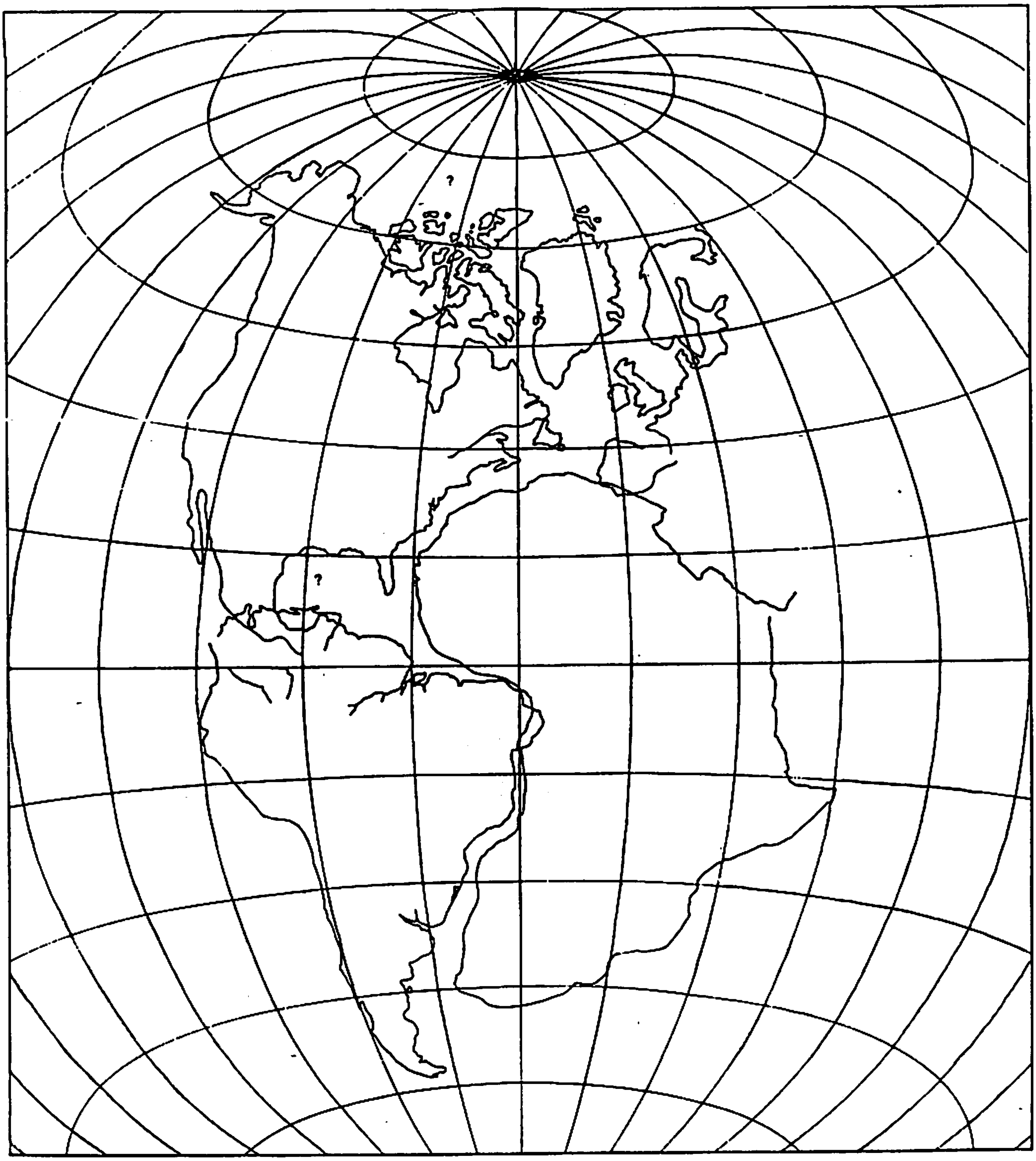

Fig. 4.4: The continents 165 million years ago (Middle Jurassic). (Sclater and Tapscot.)

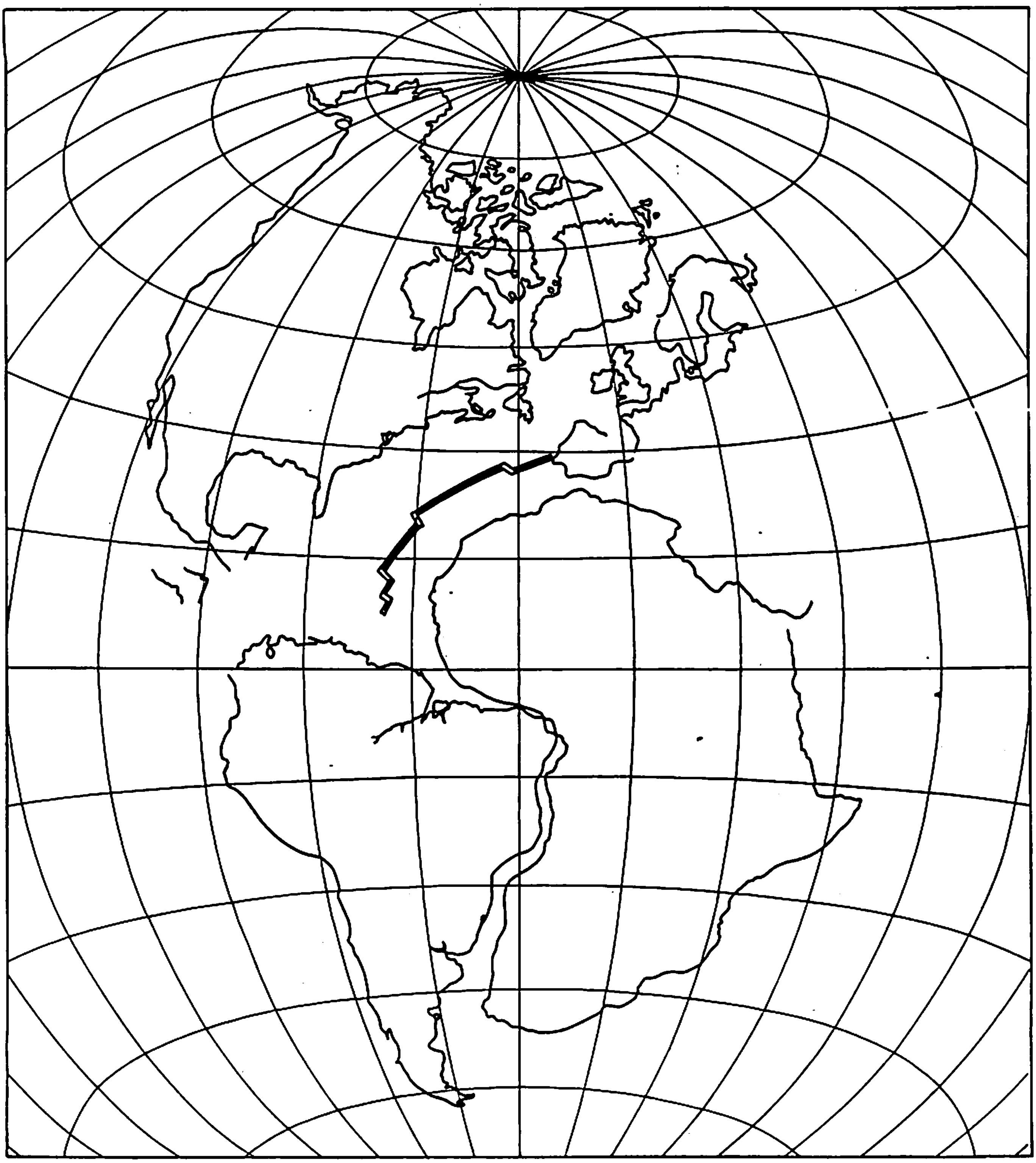

Fig. 4.5: The continents 130 million years ago (Neocomian). (Sclater and Tapscot.)

any further than the Cameroon basin. Neither seismic data nor well data have shown (Aptian) salt to be present in the northern Gulf of Guinea sedimentary basins.

As marine sedimentation continued in the south Atlantic in the Albian and Upper Cretaceous, the rifting process subsequently came to an end in the northern Gulf of Guinea. Continental separation in this area, i.e. detachment of West Africa from northern Brazil, was followed by lateral movements of the two continents against each other. Free water circulation was established at the earliest in Turonian time, and by Coniacian time (85 ma) enlargement of the basin resulted in that ocean/ continent boundaries had been formed along all margins of the South Atlantic - the split was complete (fig. 4.6).

The South Atlantic Ocean was now truly into the sea floor spreading stage, and by Oligocene time most of the major topographical features had formed (fig. 4.7).

The distinctive right angle bends of the South America and Africa coast lines result from three Cretaceous rift systems meeting at the site of the present Niger Delta (fig. 4.8). Two of the arms of this triple junction have continued to spread, taking the continents to their present positions. The third arm, the Benue Trough, was spreading for about 30 million years. The history of the Benue Depression and the Niger Delta are related and falls into three stages: 1) Pre-Santonian phase with continuous sedimentation since Albian, 2) Santonian folding episode and 3) End-Cretaceous and Cenozoic phase of deposition of sediments eroded from the folded Santonian. By Eocene times these sediments had spilled off the continents and onto oceanic crust where they built the Niger Delta. Compressional structures, believed to be associated with strike-slip faulting, have been described in the Benue Trough.

Fig. 4.9 summarizes the main events in the creation of the

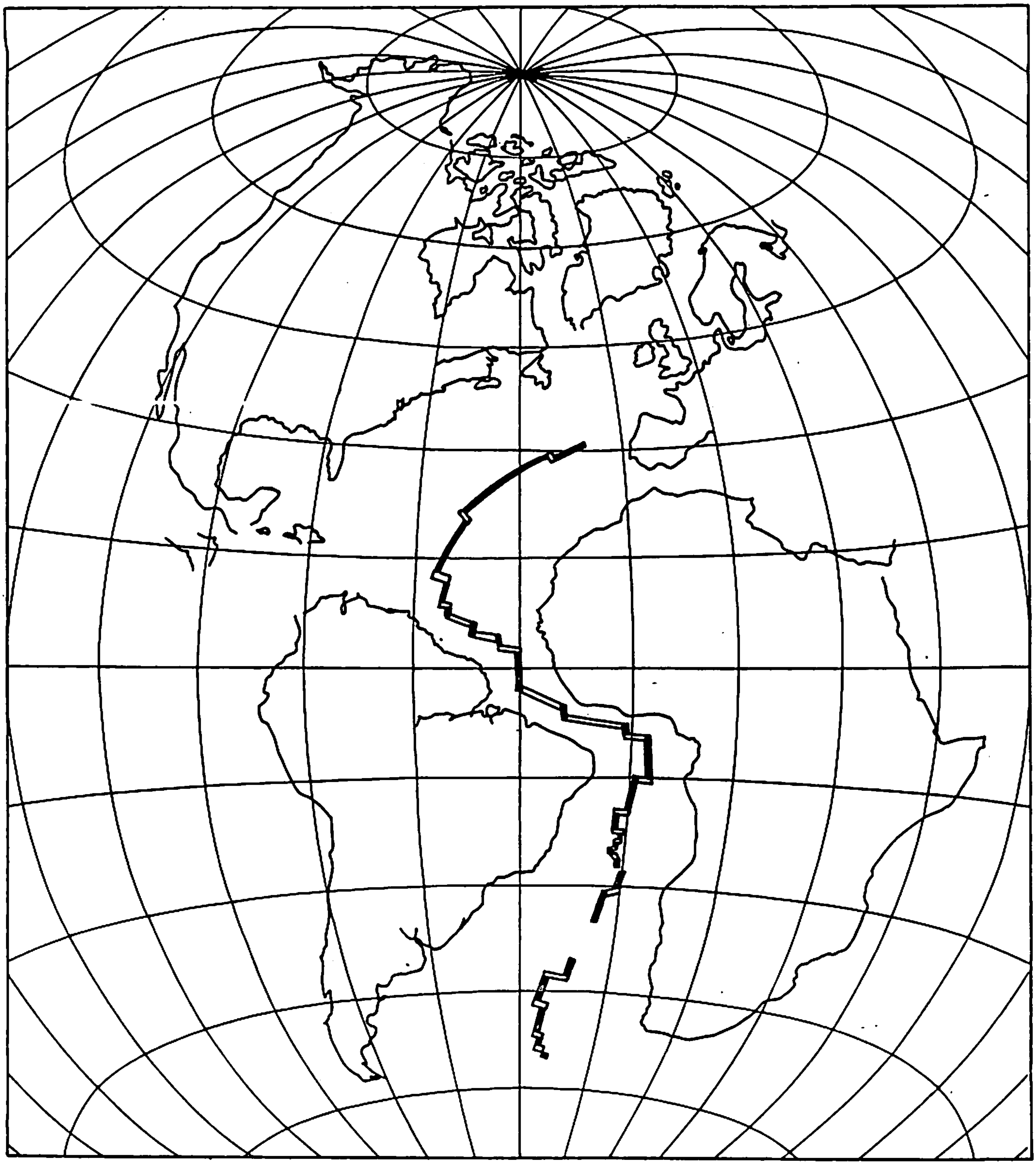

Fig. 4.6: The continents 85 million years ago (Santonian).
(Sclater and Tapscot.)

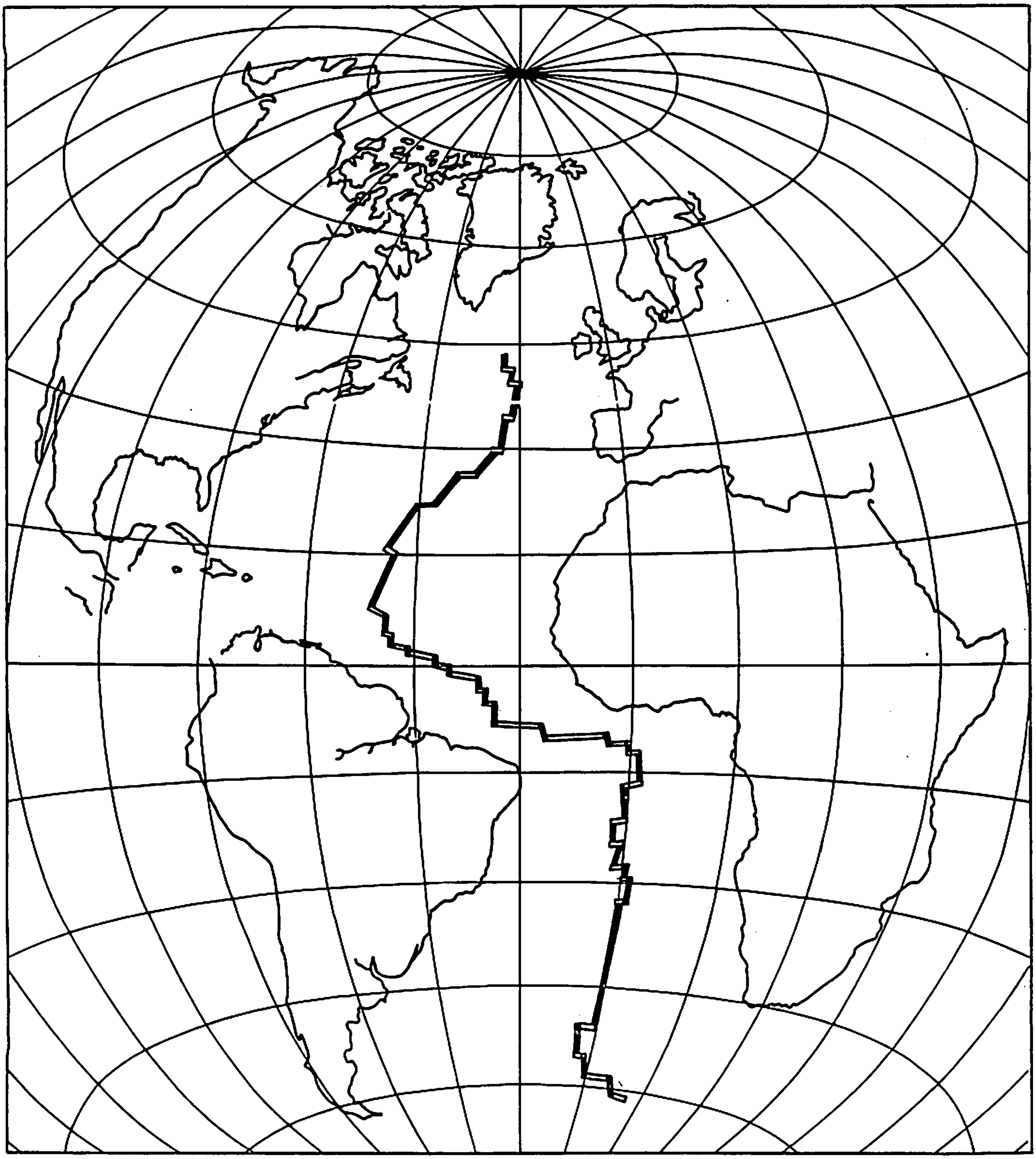

Fig. 4.7: The continents 36 million years ago (Oligocene). (Sclater and Tapscot.)

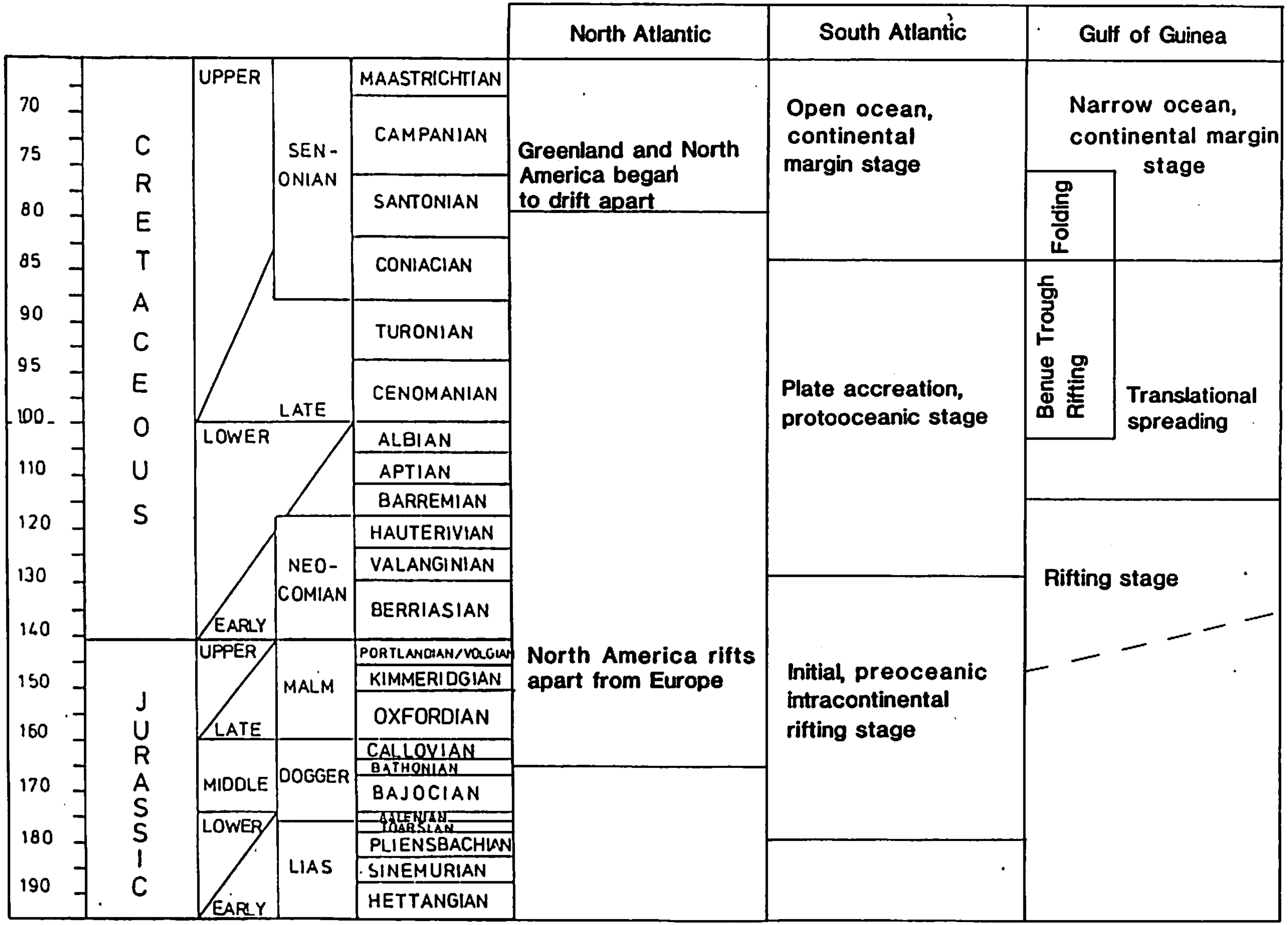

Fig. 4.9: Main events in the opening of the Atlantic Ocean and the Gulf of Guinea.

South Atlantic Ocean. Most important in this context is that while divergent continental margins were forming south of the later Gulf of Guinea, translational movements occurred in the northern Gulf of Guinea until Santonian time.

The counterpart of northern Gulf of Guinea in South America is the equatorial margin of Brazil (fig. 4.10). It is evident that the Ceara - Potiguar Basins were opposite the Dahomey Embayment at the stage of formation while the Barreirinhas Basin was opposite the Ivory Coast Basin. Only Ceara - Potiguar is productive, but have less than 2% of Brazil's total reserves.

4.3 Tectonic Framework of the Dahomey Embayment

Coupling the above outline with available geological data, four stages are recognized in the formation of the Dahomey Embayment (fig. 4.11):

1. A pre-rift arch stage (Late Jurassic - Early Neocomian) in which crustal uplift caused denudation of Precambrian basement and possible Paleozoic intracontinental basin deposits. An incipient rift was formed at the end of this stage as the crest of the dome slowly collapsed.

2. An intracratonic rift valley stage (Early Cretaceous) characterized by the formation of a central graben as well as asymmetric rift valleys and horsts towards the stable craton. The grabens and troughs are arranged in an <u>en echelon</u> fashion and transform off-sets. Non-marine sedimentation took place in elongated basins parallel to the central rift, and clastic deposits (mainly fluvial and deltaic) should be expected as is also shown to be true from scattered well data. Volcanic rocks may also be

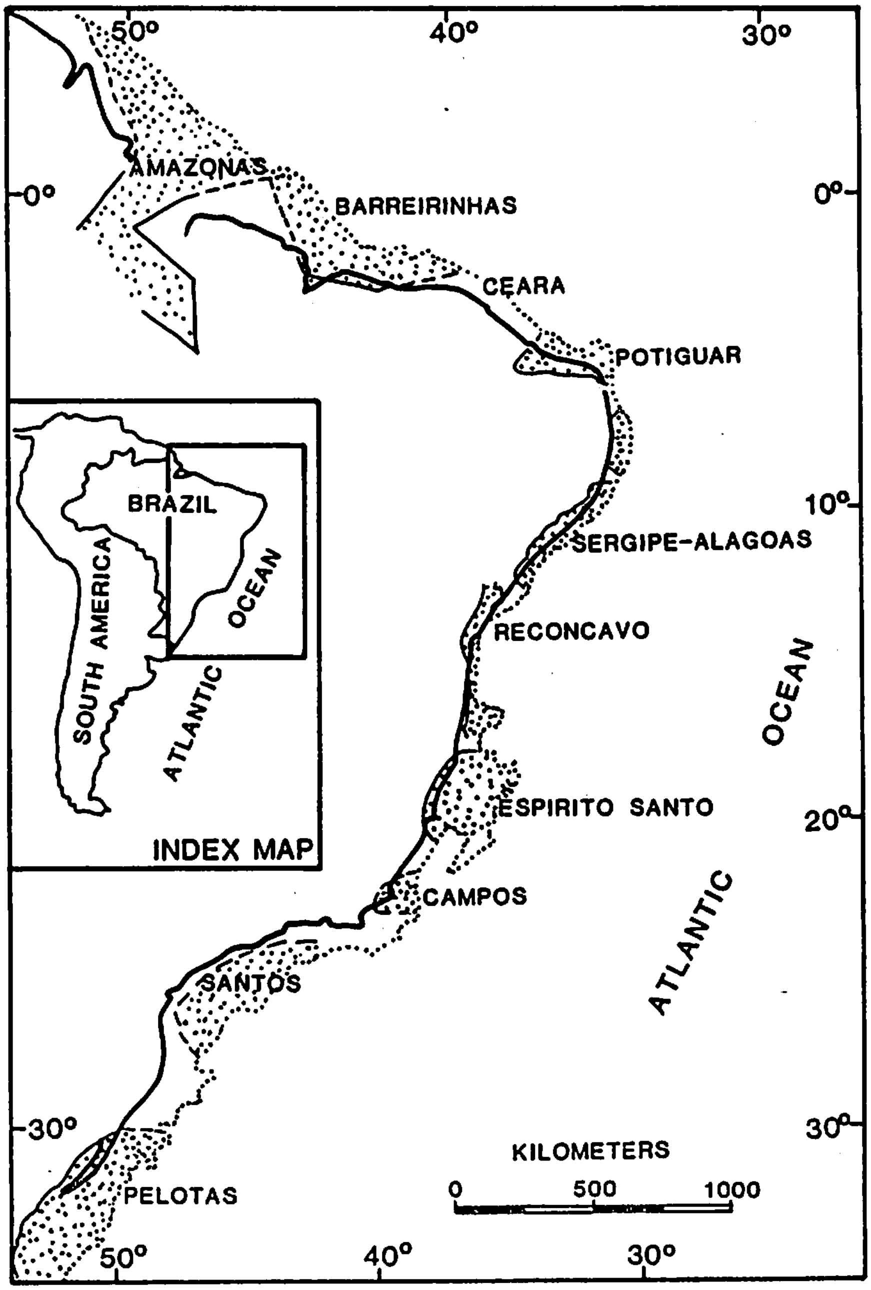

Fig. 4.10: Marginal sedimentary basins of Brazil. (Modified after Asmus and Ponte, 1973.)

N S

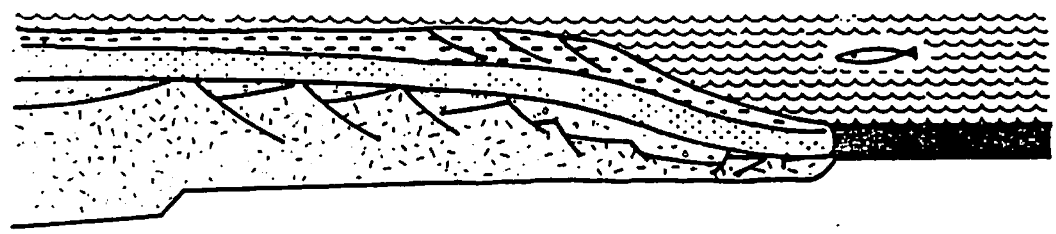

4 CONTINENTAL MARGIN DRIFT STAGE (Thermal subsidence,sediment loading)

N S

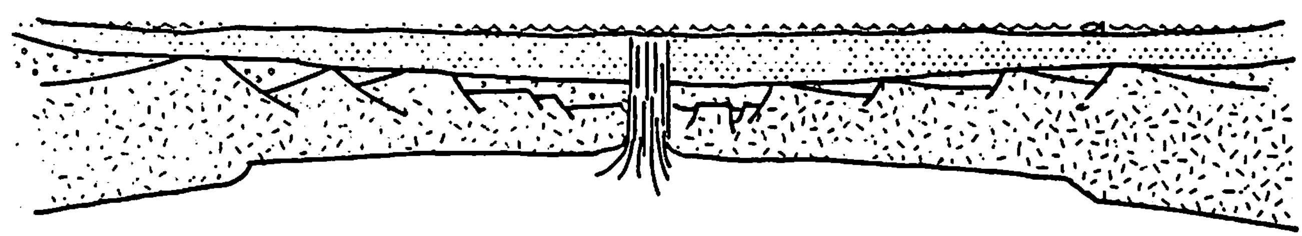

3 INTERMEDIATE PROTO-OCEANIC STAGE (Sediment loading)

N S

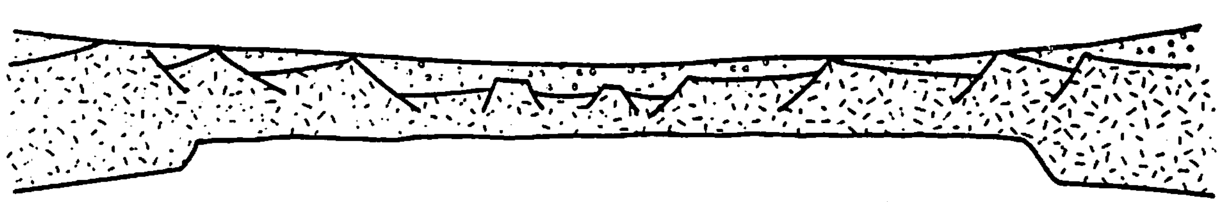

2 RIFT STAGE;EARLY CRETACEOUS (Continued initial subsidence, strike-slip movements,sediment loading)

N S

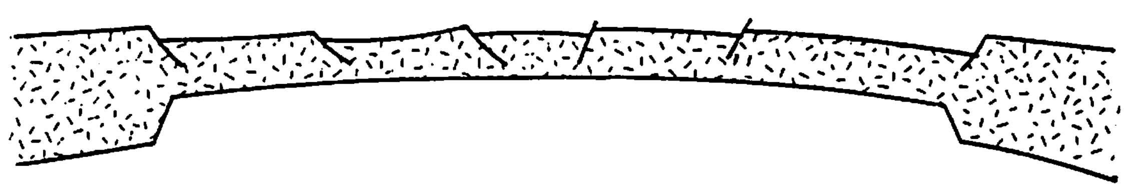

1 PRE-RIFT ARCH STAGE; LATE JURASSIC - EARLY CRETACEOUS (Initial subsidence)

Fig. 4.11 Schematic structural evolution Dahomey Embayment, Benin continental margin present but have as yet not been drilled into. The upper boundary of this rift valley sequence can easily be mapped as it constitutes a major unconformity.

3. An intermediate proto-oceanic stage (Cenomanian - Santonian) in which transform fault related tectonism dominated while the equatorial margin of Brazil slid past the northern Gulf of Guinea continental margin. Marine sedimentation gradually replaced non-marine processes, and towards the end of this stage free water circulation was eventually established. The end of this stage is in part of the study area marked by a prominent unconformity (Senonian Unconformity) and is suggested to be simultaneous with the Santonian Folding episode in the Benue Trough. Several internal unconformities in this intermediate sedimentary sequence may be related to the transform motions.

4. A continental margin drift stage (Santonian - Recent), characterized by only modest diastrophic activity and increased adiastrophic deformation as divergent spreading of South America away from Africa took place through growth of oceanic fracture zones. Two sedimentary megacycles can be recognized in the Dahomey Embayment; an early transgressive (Campanian - Eocene) with mainly clay being deposited, and a later regressive (Miocene - Recent) with progradation and outbuilding.

4.4 Structural Analysis Offshore Benin

4.4.1 Description of Fault Pattern

Mapping offshore Benin has revealed a pronounced E-W trending structural grain on basement level. This is composed of two

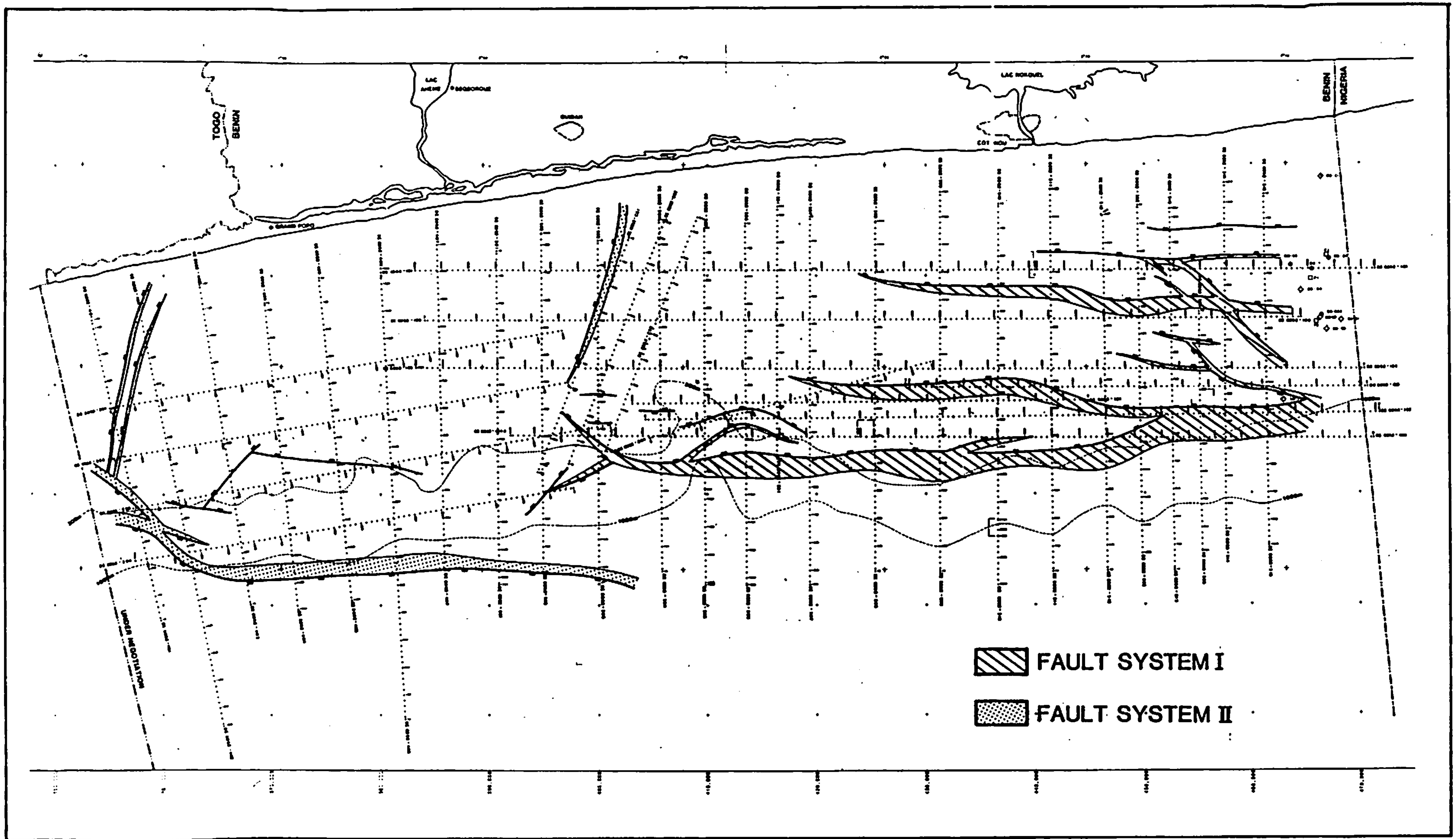

Fig. 4.12: Fault pattern offshore Benin on basement level.
Fault systems I and II as indicated.

types of subparallel E-W trending faults, modified by NW-SE and NNE-SSW trending structures (fig. 4.12). The resulting fracture pattern can be divided into two fault systems, one found in the eastern part of the mapped area (System I), the other in the western part and onshore (System II). Generally, there is a striking correlation between the fault pattern inferred from magnetic maps (depth to magnetic basement) (enclosure 44) and the fault pattern inferred from reflection seismic data (ref. fig. 10.1). For sections through these fault systems, see figs. 4.13, 4.19 and 4.20. Compare fig. 3.1 for onshore faults.

<u>Fault system I</u> which is found in the eastern part is composed of one E-W trending "left-stepping" set of major faults (Set IA) which are arranged in an en echelon pattern, and one NW-SE trending set of shorter, interconnecting faults (Set IB).

The faults of Set IA can be followed for tens of kilometers, and are generally characterized by fault blocks downthrown towards north. Throws in the order of 1 sec (two-way reflection time) are common, and splay faults seem to be associated with this set. The geometry of the fault planes cannot be determined in detail, although several of them must have had steep northerly dips prior to rotation (see below).

The faults of Set IB are frequent in the northeastern part of the mapped area where they interconnect the E-W trending faults and give rise to sediment-filled sub-basins. In general the elements of this set indicates that a considerable subsidence of the northeastern fault blocks relative to the southwestern has taken place during faulting, although faults with southwesterly throw also are found within this fault-set. The geometric relation between faults of Set IA and IB indicates that these are genetically related.

<u>Fault System II</u> is dominating in the southern and western

region of the Benin continental shelf. Even this system is dominated by an E-W trending fault set (Set IIA), which is associated with a NE-SW to NNE-SSN trending set (Set IIB).

Set IIA encompasses only two faults which are characterized by downthrow of the southern (oceanward) fault blocks. The throw is considerable, probably in the range of several seconds two-way travel time. Set IIA faults coincide with a marked hinge line effecting the younger strata in the area.

Fault Set IIB, which is found in the western part of the shelf and possibly onshore (fig. 3.1), has a general NNE-SSW trend. The throws on these faults are minor compared to Fault Set IIA. The time of activation of Fault Set IIB, together with its close spatial association to Fault Set IIA, indicate that these sets are genetically related.

The character of Fault Systems I and II are summarized in fig. 4.14.

4.4.2 Timing of Faulting

The only horizon mapped which is affected by the System I faults is the basement reflector which probably defined a fairly flat surface previous to faulting. The faulting episode resulted in a considerable relief with grabenlike structures which were filled with sediments. This is valid for the situation over fault set IA as well as IB, and fits well with the present geological model of an "initial rift stage" in Neocomian times. The system later developed into a translational spreading situation. After this event no activity is detected in connection with this fault system, except for some gentle sudsidence that may be traced over these Early Cretaceous basinal features as late as Turonian. These late

	FAULT SYSTEM I		FAULT SYSTEM II	
	SET A	SET B	SET A	SET B
DIRECTIONAL TR.	E-W	NW-SE	E-W	NNE-SSW
DIP	LANDWARD	LANDWARD	OCEANWARD	
TYPE	OBLIQUE	NORMAL	NORMAL	NORMAL
GEOMETRY	EN ECHELON	INTERCONNECT.		
AGE	BERRIASIAN-HAUTERIVIAN (INITIAL RIFT STAGE - TRANSLATIONAL SPREADING) TURONIAN REACTIVATION		LATE CRETACEOUS (DIVERGENT SPREADING)	

Fig. 4.14: Characteristics of Fault Systems I and II offshore Benin.

effects may be related to compactional processes or rotation of basement fault blocks as described from the Sèmè Oil Field (Ræstad et al 1983).

In the western part of the area north of the major faults of Fault Set IIA, the sequence (basement included) is generally not faulted, except where transected by elements of Fault Set IIB. However, the entire sequence (including basement) shows a strong tilt towards the major E-W (IIA) fault. Although the detailed correlation across this fault is uncertain, the Ise Formation is down-faulted along the continental slope in the eastern half of the study area. (The prolongation of Fault System II is not shown in fig. 4.12.) This indicates that at least the latest phase of activity along the IIA faults took place in Late Cretaceous, and accordingly after the faulting within Fault System I had terminated. Hence, the faults of Fault System II are related to the Late Cretaceous divergent spreading phase and were active into Early Cenozoic times.

Also faults belonging to the IIB set affects Lower Tertiary strata. This, together with the close relation to the IIA faults in the western part of the mapped region, strengthen the assumption that these fault sets are genetically related.

4.4.3 Rotation of Fault Blocks

As indicated in chapter 4.4.2, the deformation associated with Fault Set IIA involves oceanward rotation of large parts of the shelf. This may suggest that this faulting was connected to subsidence due to cooling of the margin, and that faulting accordingly took place over a considerable time-span.

To evaluate the original geometry of the fault planes of Fault Set IIA, a reconstruction has been made, assuming that basement constituted a flat surface prior to rotation in Late Cretaceous. The reconstruction was carried out on migrated, not depth-converted sections, and the calculated dips accordingly should be regarded as minimum values. Altogether 27 faults or fault segments were treated. The results show that most of the faults originally were characterized by steep dip; 19 of 27 had a calculated original dip of more than 65° N, of which 6 had dips steeper than 76° N. Maximum calculated dip was 86° N. However, no reverse (overturned) faults were detected (fig. 4.15). These anomalously steep dipping fault planes may suggest that a strike-slip mechanism rather than tensional normal faulting should be considered for Fault Set I.

4.4.4 Landsat Analysis

A survey of available Landsat imagery (MSS and RBV, all together 20 frames) from the adjacent onshore area of Dahomey Embayment has been carried out in order to increase the amount of structural data from the area. However, a combination of poor data quality and poor coverage has prevented a comprehensive analysis, and no lineament map has been produced.

The conclusions drawn from this study may be summarized as follows:

1. A certain dominance of ENE and NE trending lineaments may be seen in the Abakali Fold Belt.

2. A swarm of NE to NNE trending lineaments is associated with the Great Accra Fault.

3. Useful remote sensing analysis in the area probably should await new Landsat data, or preferably side-scan aperture radar imagery.

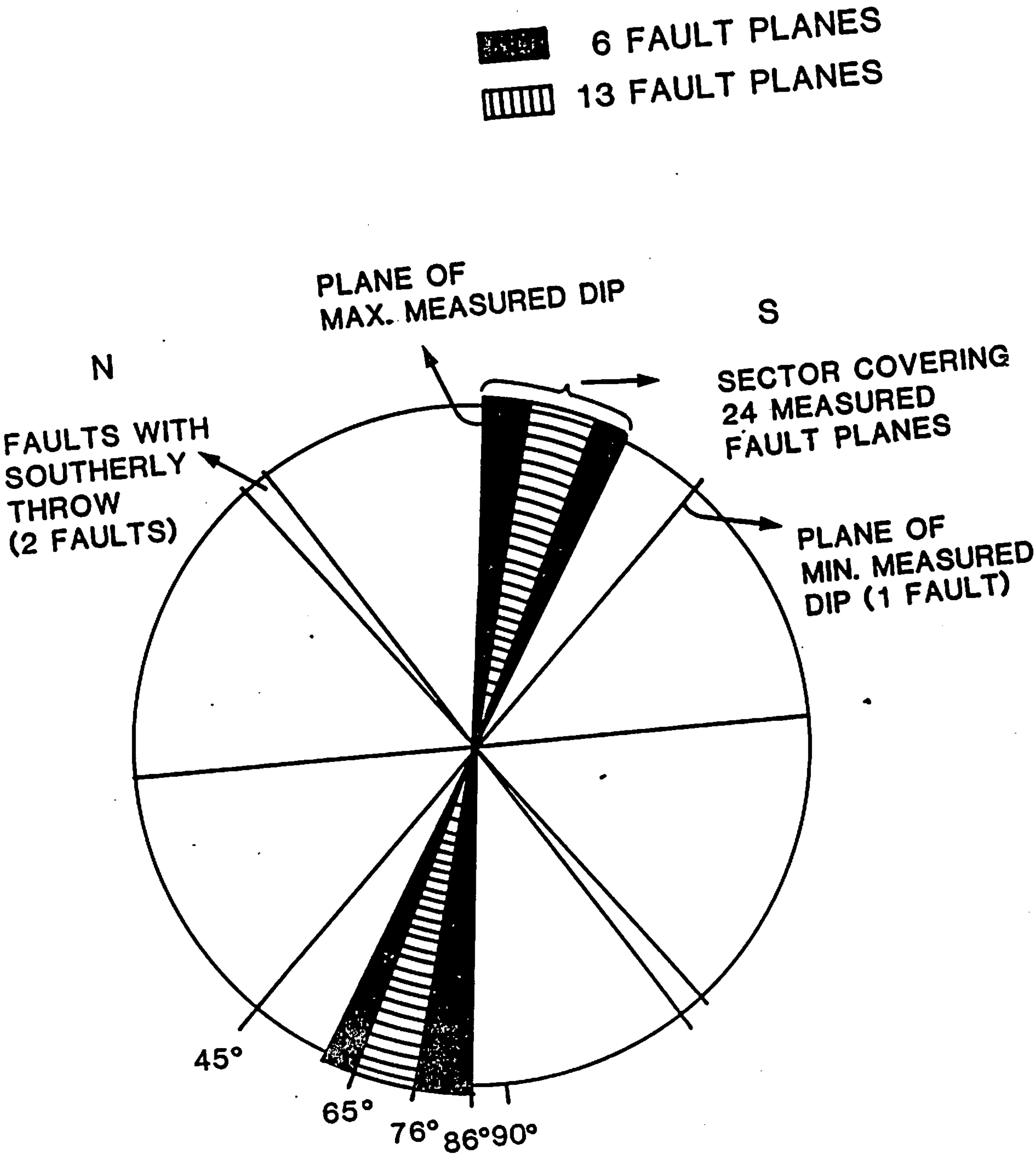

Fig. 4.15: Dip of 27 fault planes of Fault Set IA (E-W striking) after rotation (see text). Measurements are made on migrated time sections, and should be seen as minimum values.
Dips are plotted relative to a horizontal datum line in a N-S section.

4.4.5 Tectonic Model

The available structural data in the Dahomey Embayment call for a three-stage tectonic model (fig. 4.16).

Stage I which initiated Fault Set I took place under an initial rift stage in the northern Gulf of Guinea, developing into a situation ruled by dextral shear. The shear strain ellipsoide (e.g. Hardin 1974, Crowell 1979) of an ENE-WSW oriented dextral shear situation shows that a set of E-W oriented synthetic dextral strike slip faults would be initiated, and rotate towards parallelity with the major movement direction. Also one set of sinistral antitethic NNW-SSE oriented structures would be generated. The latter would tend to die out due to the antithetic movements associated with this set. Also NW-SE trending normal faults would occur (fig. 4.17). The dominating structures of this system would be the E-W oriented synthetic dextral faults (Tchalenko 1971), and the NE-SW trending set of normal faults, which are parallel to the two trends of Fault System I as described in chapter 4.4.1.

Concidering the original steep dips of several of the faults belonging to Fault Set IA (chapter 4.4.3), a transpressional (Harland 1969) origin of these elements might be reasonable, in accordance to what should be expected from the above model. This model also explains the normal faulting associated with Fault Set IB.

The basins associated with Fault System I might accordingly be regarded as pull-apart basins* (Crowell 1974), although no compressional features, as should be expected within a left stepping, dextral shear system (Rodgers 1978), have been mapped as far.

*The term "pull-apart" is here used for a strike-slip basin

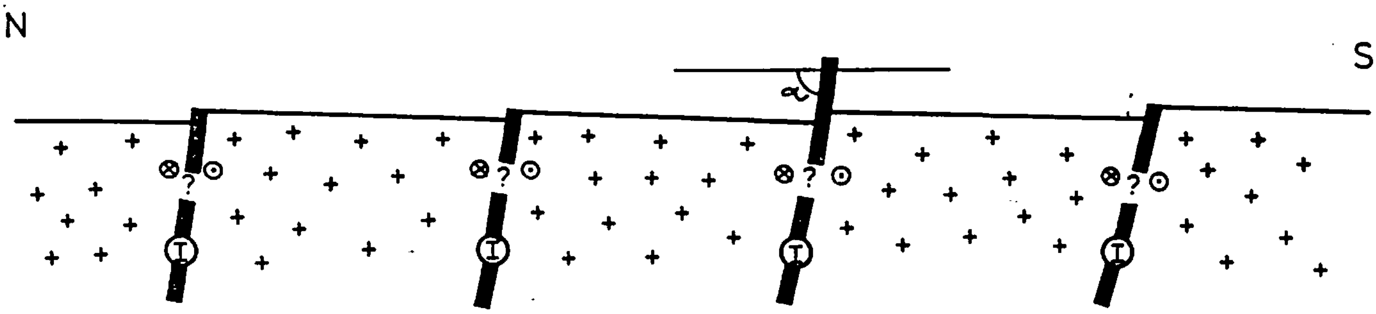

STAGE I : INITIAL RIFTING/DEXTRAL SHEAR. ACTIVATION OF FAULT SYSTEM I.
TRANSPRESSION ?
STEEP-DIPPING FAULT PLANES NECOMANIAN

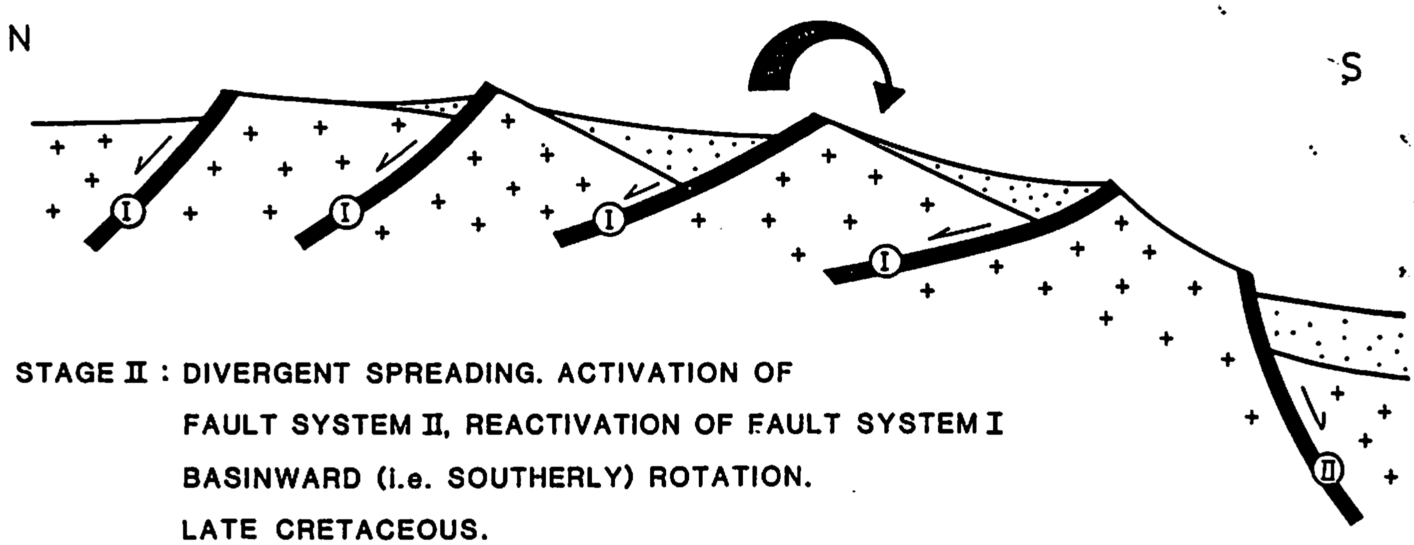

STAGE II : DIVERGENT SPREADING. ACTIVATION OF
FAULT SYSTEM II, REACTIVATION OF FAULT SYSTEM I
BASINWARD (i.e. SOUTHERLY) ROTATION.
LATE CRETACEOUS.

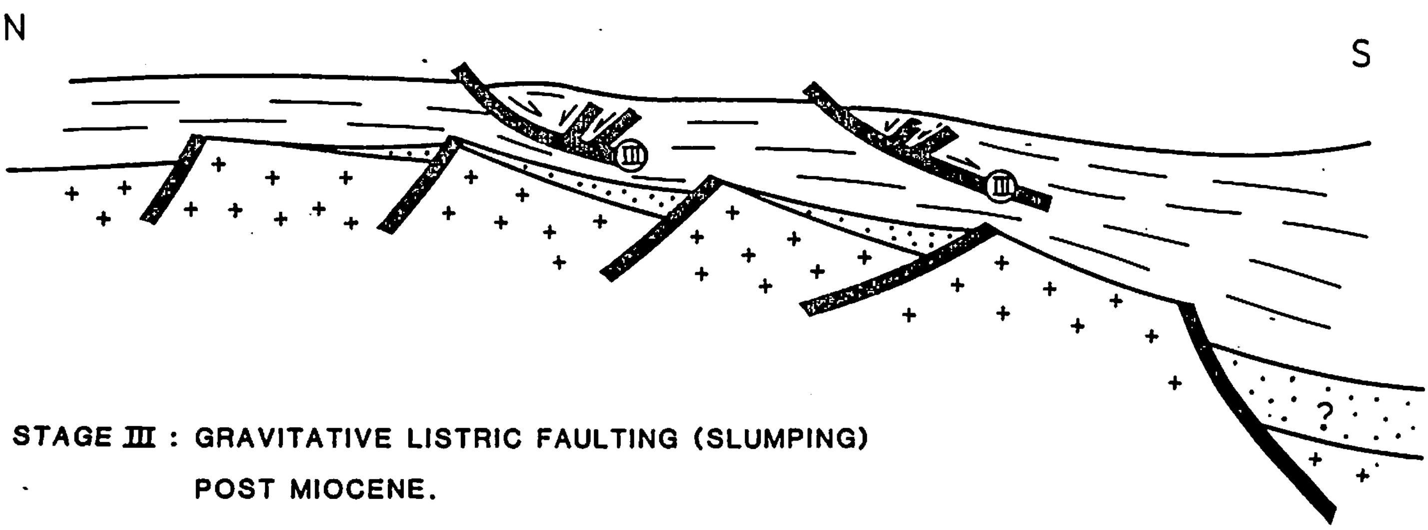

STAGE III : GRAVITATIVE LISTRIC FAULTING (SLUMPING)
POST MIOCENE.

Fig. 4.16: Schematic three-stage model, offshore Benin.

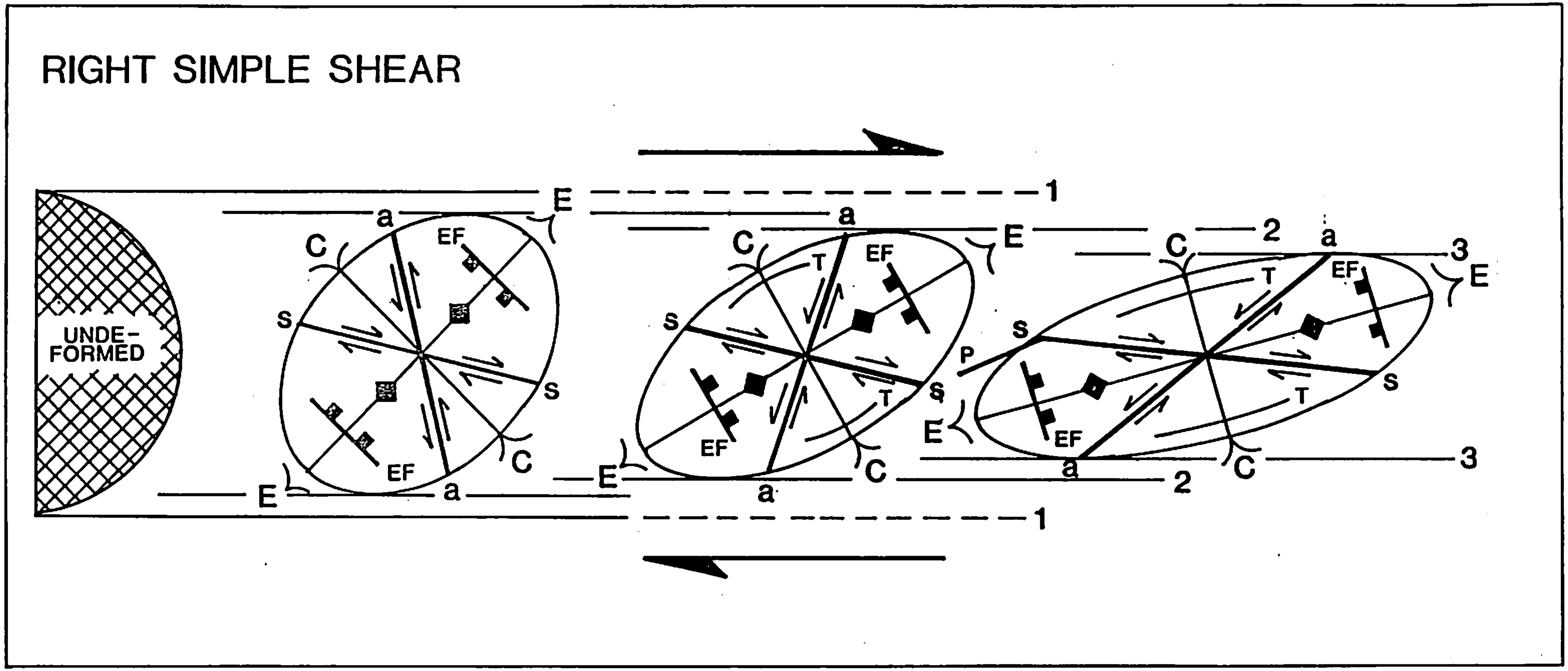

Fig. 4.17: Strain diagram of a right simple shear situation with increasing deformation (stage 1-3). After Crowell 1979.

Stage II which is characterized by strong subsidence south of the faults of Fault Set IIA and activation of Fault Set IIB is correlated to the Late Cretaceous divergent spreading in the northern Gulf of Guinea. The faults of this system have a fault plane geometry characteristic of normal faults, and have influenced even the near Base Tertiary reflector (H4).

The faulting is associated with oceanward rotation, which is common along passive, continental margins. The rotational event has also influenced the area north of the faults in the eastern half of the study area, thus rotating the fault planes of Fault Set IA into their present position.

It is uncertain which part Fault Set IIB has played during this event.

Stage III is associated with gravitative, oceanward slumping in post Miocene times. No detailed mapping within this part of the section has been carried out in the present study.

4.5 Implications to Hydrocarbon Exploration

The Dahomey Embayment fits a continental margin model with four lithotectonic elements (fig. 4.18): A pre-rift intracratonic basin (Type I), only present offshore Togo and onshore as well as offshore Ghana; a rift basin (Type III) which has been located on the eastern half of the Benin continental shelf and also beyond the shelf break in the western half; a transverse breakup basin (Type VB) present all over the shelf and finally a divergent (parallel) drift basin (Type VA) also found along the entire shelf.

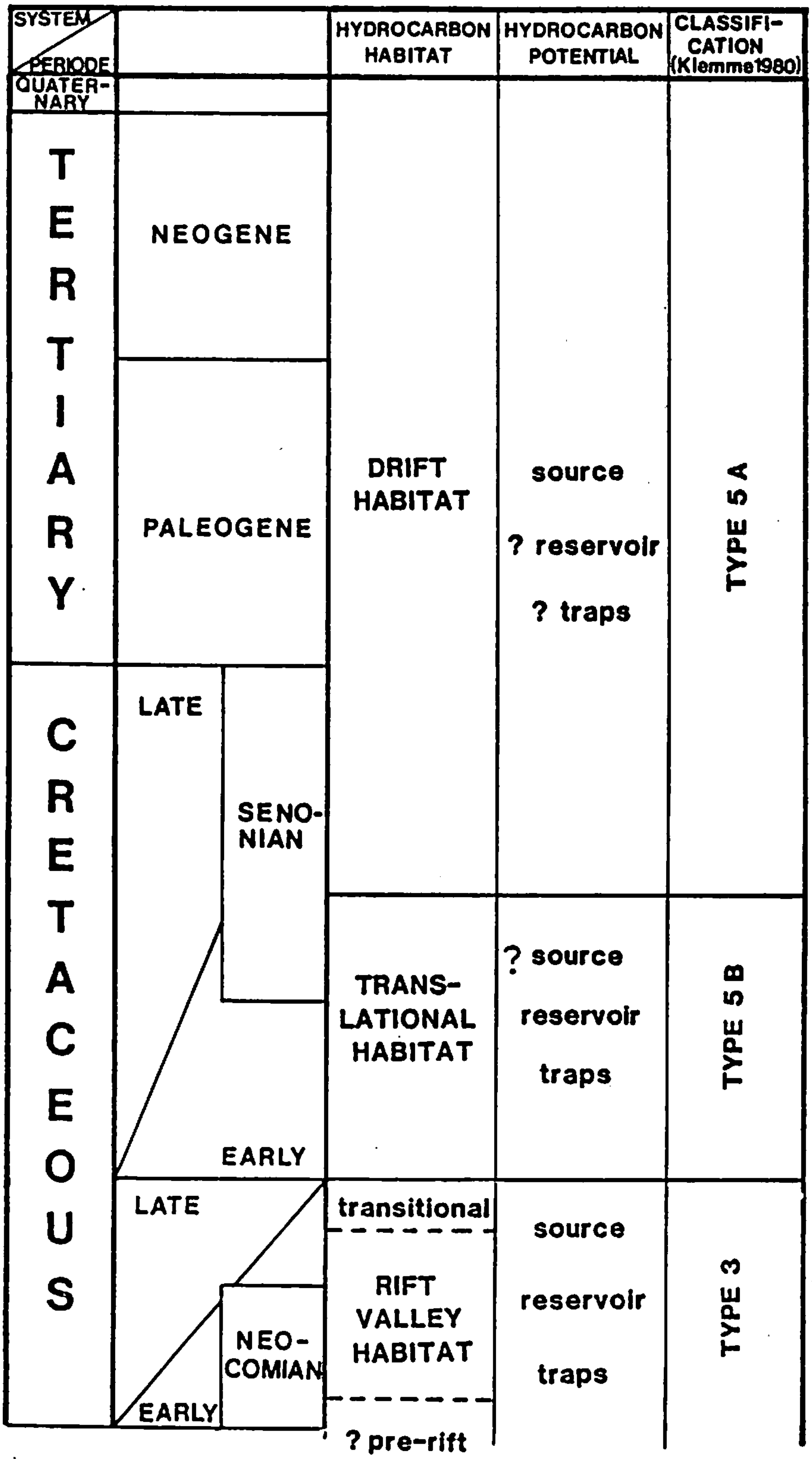

Fig. 4.18: Hydrocarbon habitat offshore Benin related to structural evolution.

Offshore seismic data and onshore geological mapping suggest that Paleozoic intracratonic basins are not present neither onshore nor offshore Benin. We are therefore left with three possible hydrocarbon habitats:

1. Rift Valley Habitat (non marine)
2. Translational Habitat (continental/marine)
3. Drift Habitat (marine)

Only two wells offshore Benin have drilled into the uppermost part of the true Rift Valley Habitat. Oil and gas shows within these, two encouraging wells offshore Togo and correlation with the equatorial margin of Brazil do, however, suggest the possibility of both mature source rocks and reservoir rocks. The seismic data indicates that trapping mos likely will be of the stratigraphic or unconformity type.

The Translational Habitat is fairly well known through Sèmè well data, and this sedimentary succession has several possibl reservoir horizons but also a fair source potential in a seaward direction. Pure structural traps are scarce, but stratigraphic traps are likely to occur.

The Drift Habitat does not appear to have any reservoir rock potential. However, black shales may constitute source rock i the southeasternmost part of the shelf where maturity possibly has been reached.

Figs. 4.19 and 4.20 show two depth converted dip sections, illustrating the presence of all three petroleum habitats on the eastern shelf, while only the two younger habitats are present on the western shelf. The Rift Valley Habitat will only be present in the rift grabens on the shelf and slope, of which the areal outline is discussed elsewhere (chapter 5.2).

Page

APPENDIXES

CHAPTER 5 22.6.84

LITHOSTRATIGRAPHY

5.1 General

This account is an attempt to summarize the present knowledge of the stratigraphy offshore Benin. Detailed descriptions of the onshore stratigraphy is given by Slansky (1962), whose work synthesises outcrop descriptions, photogeology and shallow borehole data. Slansky's approach is mainly biostratigraphic and a lithostratigraphic interpretation is therefore not attempted by him. Based on published studies from the onshore Dahomey Embayment as well as Union Oil's offshore wells, Billman (1976) gave a combined biostratigraphic/lithostratigraphic interpretation of the Sèmè area. Billman's paper appears to be the only one dealing with offshore stratigraphy in the Dahomey Embayment. It is the main reference for the following lithostratigraphic description.

It should be realized that there has never been suggested a unified lithostratigraphic scheme covering both the onshore and the offshore of the Dahomey Embayment. Rather, scattered published papers are quite confusing and partly contradicting. This is due to poor dating, no available electric logs and lack of coordination. This is our reasoning for only presenting a stratigraphic framework for the offshore basin without doing detailed comparisons with the onshore.

Fig. 5.1 summarizes the stratigraphy offshore Benin as it is known in the easternmost part of the shelf; in the vicinity of the Sèmè Field. Some changes have been made from Billman's (1976) suggested terminology:

- The "Folded Cretaceous" is called the Ise Formation in line with its usage in eastern Dahomey Embayment (Nigeria).

- The "Turonian Sandstone" is preferred to Abeokuta Formation to avoid confusion with the Abeokuta type section in Nigeria.

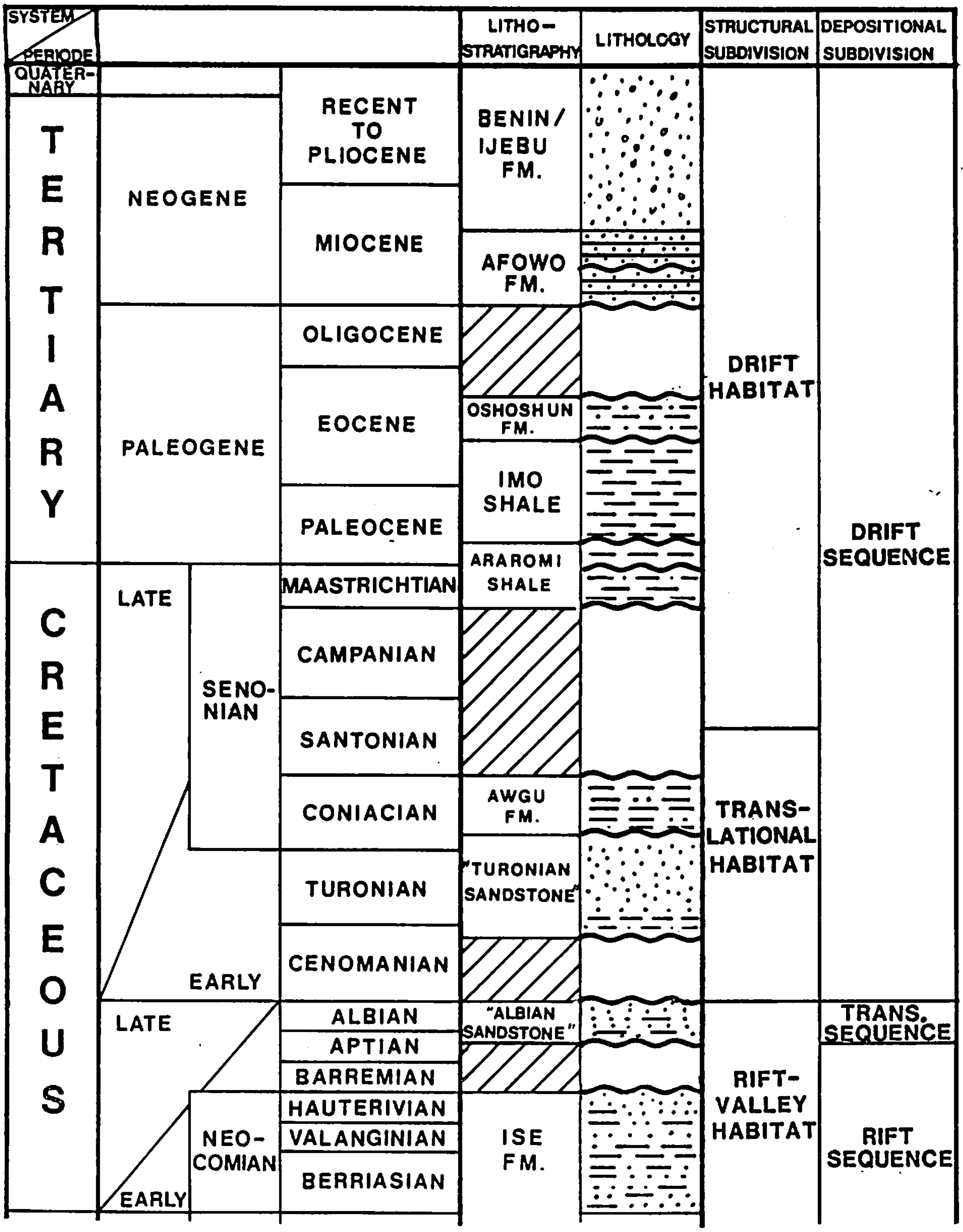

Fig. 5.1: Lithostratigraphy offshore Benin.

- The Nkporo Shale should be referred to as <u>Araromi Shale</u> which is the applied name of this shale sequence in western Nigeria.

In the previous chapter a threefold division of the structural evolution was sketched: A Rift Stage, a Translational Stage and a Drift Stage. From a depositional viewpoint, a slightly different subdivision is preferred: An Early Cretaceous (?Necomian) Rift Sequence, a late Early Cretaceous (?Aptian - Albian) Transitional Sequence and a Late Cretaceous - Cenozoic Drift Sequence (fig. 5.1).

5.2 Lower Cretaceous

5.2.1 Ise Formation

The name Ise Formation is adapted from Adegoke and Ibe (1982) applied to a lithologic unit described in western Nigeria west of the Okitipupa High. The same formation is encountered in two wells offshore Benin and was informally named "Folded Cretaceous" by Union Oil, presumably due to a "folded appearance" on poor quality seismic sections. Few details are disclosed about the Ise Formation in Nigeria. The tentative correlation is based largely on it being interpreted as an Early Cretaceous rift deposit.

In the Ivory Coast and in the coastal region of western Ghana, a rock series of continental origin discordantly overlies the Precambrian basement. It is composed of sandstones, conglomerates and bright-colored shales (therefore known as "série versicolore") and may obtain thickness greater than 2000 m. The age of the series is not exactly known, but may range from Late Jurassic up to the Aptian - Albian (Machens 1964).

Lower Cretaceous rocks with equivalent lithologic characteristics are described also from wells offshore Togo. A threefold division of the Lower Cretaceous offshore Togo has been suggested by Union Carbide (operator): Unit I sandstone and shale, Unit II shale with sandstone beds and Unit III massiv sandstone with shale streaks.

The Ise Formation is not described in outcrops of the Dahomey Embayment. This is due to its presence in fault bounded half grabens only present offshore.

Lithology (fig. 5.2)

The formation as described offshore Benin consists of sandstones and shales interbedded. The sandstones are white to grey, unsorted, conglomeratic, quartzitic and well indurated with abundant mafic minerals and clay aggregates. The shales are grey to brown, fissile and hard.

Boundaries (fig. 5.2)

The top of this formation corresponds to a well defined angular unconformity that can easily be picked from both dipmeter logs and seismic lines. The top also corresponds to a substantial increase in accoustic velocity, due to increased induration.

The base of the formation has not been encountered, but it is supposed to extend down to crystalline basement as is indicated by seismic data.

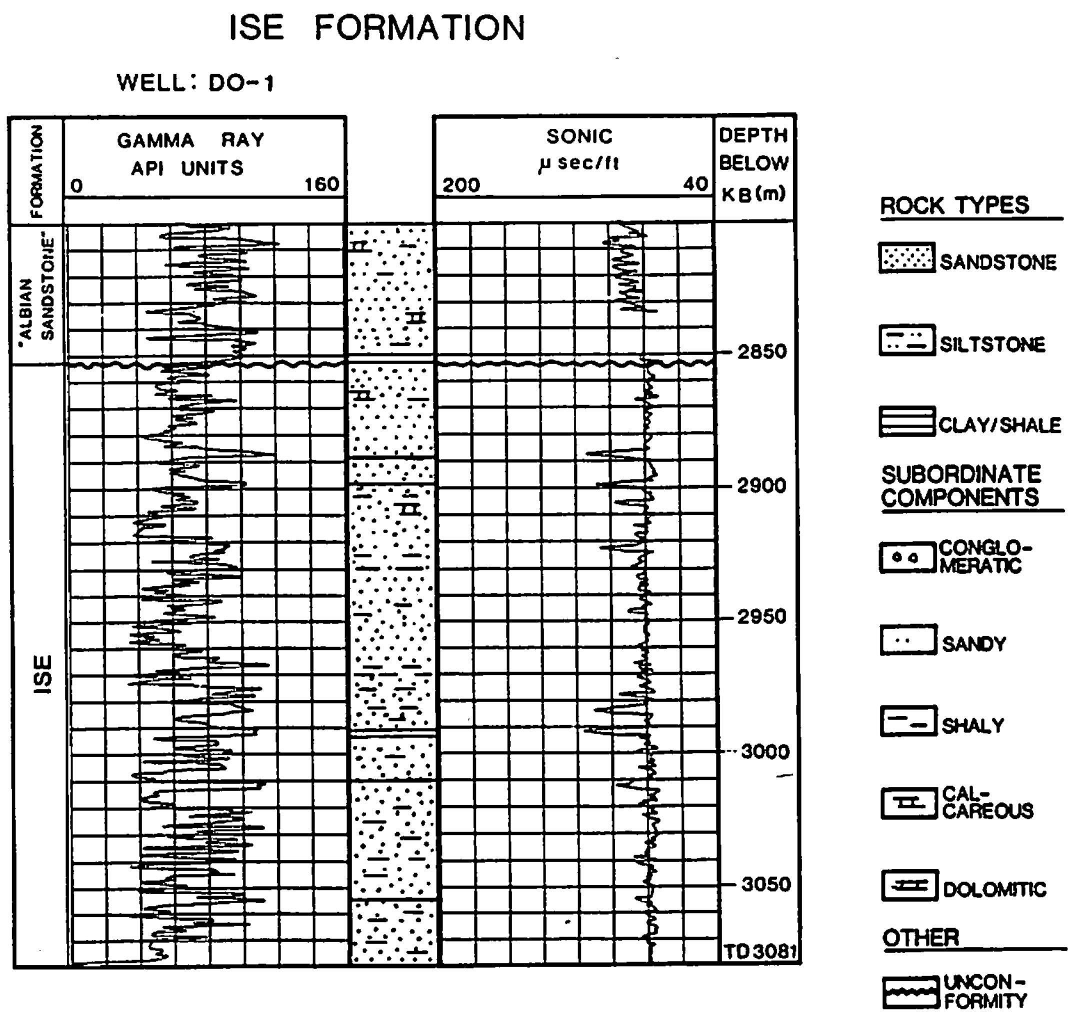

Fig. 5.2: Log character and lithology of the Ise Formation.

Depositional Environment

The formation is interpreted as non marine, an interpretation supported both by its description and also by its presence in half grabens related to the breakup of South America from Africa.

Age

No fossils have been recovered in the two Benin wells, but an Early Cretaceous age seems logical. In western Nigeria the Ise Formation is assigned a Neocomian age (Adegoke and Ibe 1982).

Distribution/Thickness (fig. 5.3)

As much as 248 m of the Ise Formation was penetrated in DO-D2A and 229 m in DO-1. Maximum thickness and lateral extent have been estimated from the seismic interpretation by accepting the crystalline basement as the base of the formation.

The distribution of this lithological unit is outlined in fig. 5.3 showing that it is not present on the entire shelf, and probably not at all onshore. As much as 3000 m is present on the shelf, and an even thicker sequence is found beyond the shelf break.

5.2.2 "Albian Sandstone"

The very informal formation name "Albian Sandstone" has been used by Billman (1976) for a sequence of essentially non marine sandstones penetrated in several wells offshore Benin. In the Sèmè Field terminology the top part of this formation is

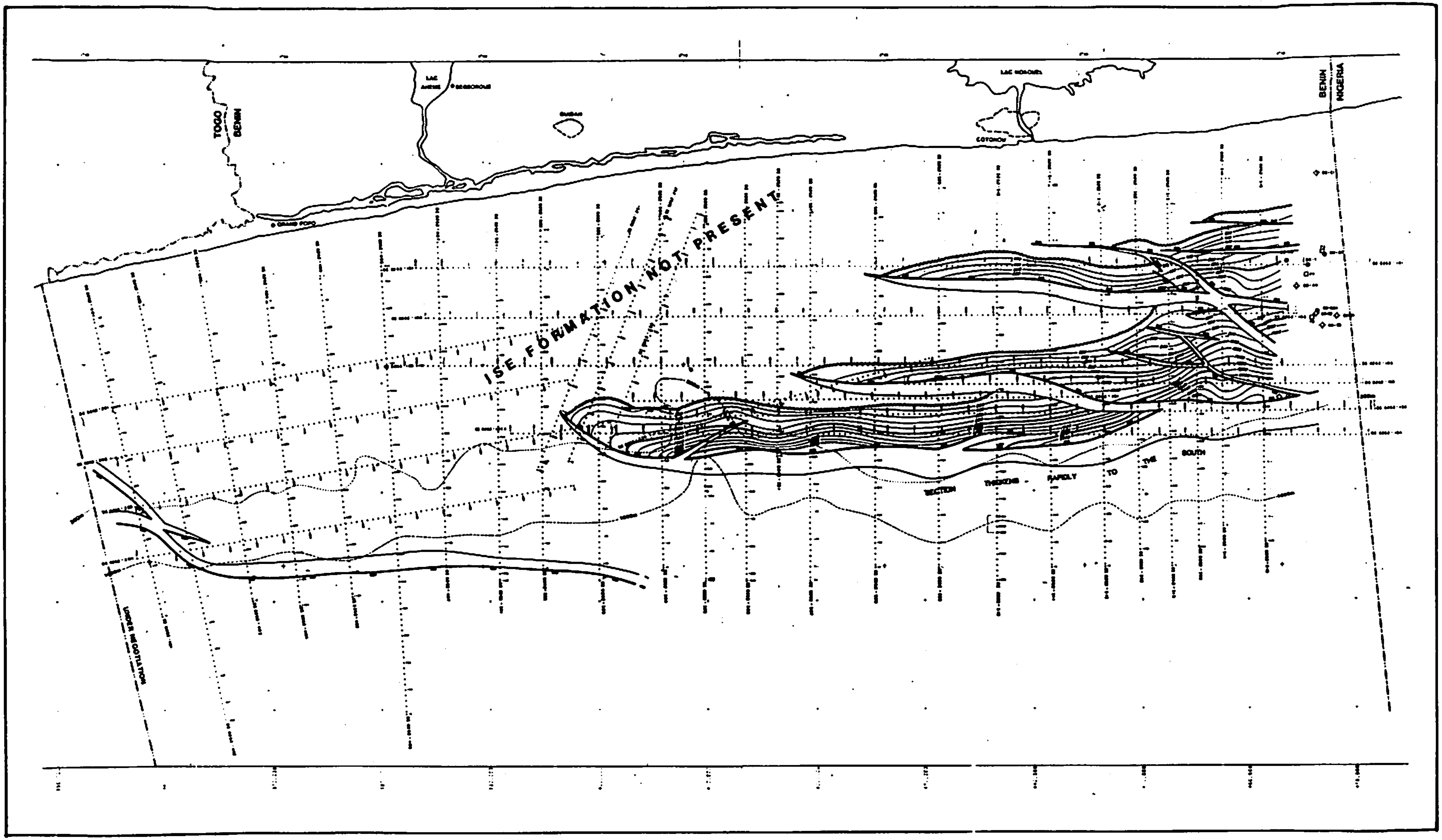

Fig. 5.3: Ise Formation, isopach map.

defined as Zone 3 that tested oil in DO-1. Zone 4, which has proved to be gas and oil bearing, also belongs to this formation. Increased knowledge of the "Albian Sandstone" has resulted from the studies and analyses of cores taken in development well Sèmè 4.

The "Albian Sandstone" is not described onshore in outcrops, this being due to its presence in the fault bounded rift basins that do not appear to extend onshore.

The presence of this formation in the two wells drilled offshore Togo is questionable.

Lithology (fig. 5.4)

The lithology of this unit is predominantly sandstone, but with frequent shaley and dolomitic stringers which distinguishes it from the overlying unit. The sandstones are described in cores as white to grey to dark brown, fine to coarse grained, fair to poor sorting, feldspatic and micaceous (compare chapter 7.2.3).

Boundaries (fig. 5.4)

The "Albian Sandstone" unconformably overlies the Ise Formation, and its lower boundary can easily be picked on logs by a marked decrease in interval transit time. A comparatively thick shale sequence is also present at the base of this unit.

The upper boundary occurs as a transition upwards from sandstone with shale interbeds to a clean sandstone unit with a smooth log character.

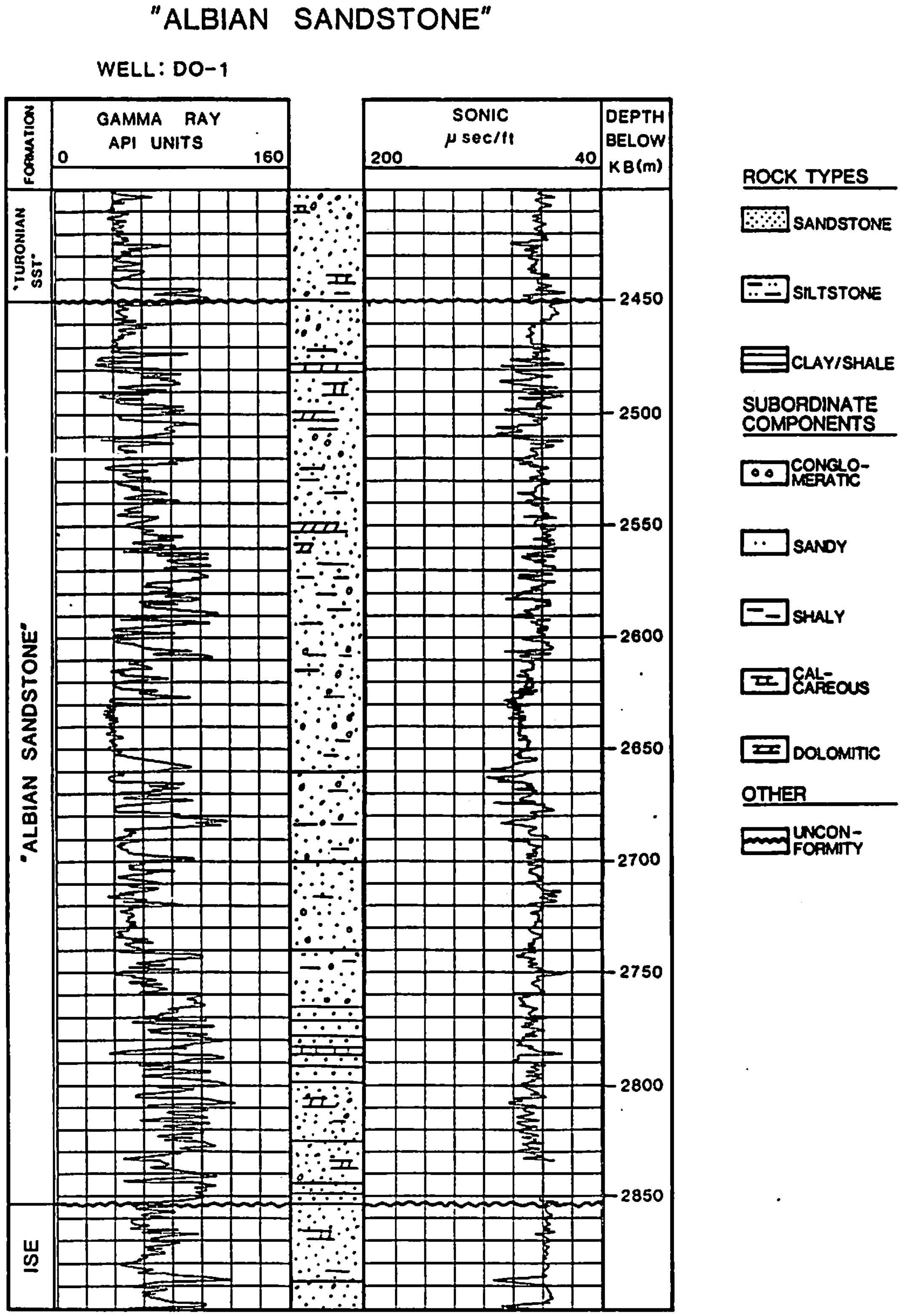

Fig. 5.4: Log character and lithology of the "Albian Sandstone".

Depositional Environment

The "Albian Sandstone" is interpreted as representing a transgressive phase with the sea advancing a tilted and eroded rift basin. The depositional environment ranges from essentially non marine to marine in a seaward direction with a possible transition to marine shales beyond the shelf break.

Age

The palynological assemblages of this unit suggest Albian age.

Distribution/Thickness (fig. 5.5)

A maximum thickness of 455 m was penetrated in well DO-D2A while 403 m was encountered in DO-1. In DO-C1, in which the "Albian Sandstone" rests on crystalline basement, it is 234 m thick. As evident from the isopach map (fig. 5.5) the formation thickens in an oceanward direction, and it is close to 1000 m thick in the southeastern part of the area mapped.

5.3 Upper Cretaceous

5.3.1 "Turonian Sandstone"

The name Abeokuta Formation has been applied to a sequence of claystones and sandstones as seen in bore holes and outcrops of southwestern Nigeria, Benin and Togo (Jones and Hockey 1964). The type locality is in south-western Nigeria and is compiled from three bore holes, totalling 198 m. According to Kogbe (1974), four members can be recognized, a very thin lower conglomeratic member, a sand/clay member, a silty mudstone and

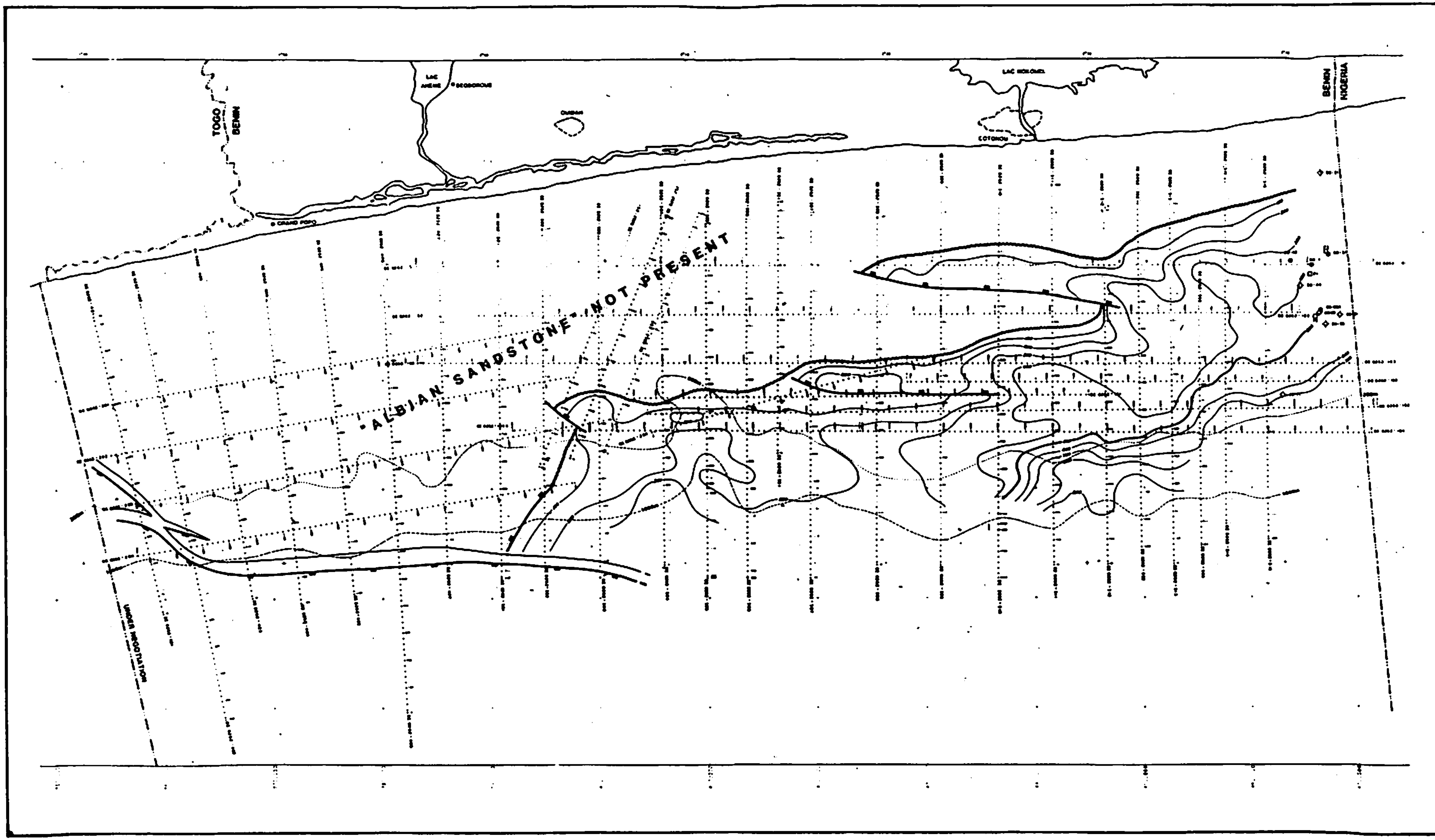

Fig. 5.5: "Albian Sandstone", isopach map.

red sand member and an upper reddish brown sand.

Billman (1976) "very tentatively" (p. 23) correlates the two lowermost members (fig. 5.6) with the offshore sandy section named Abeokuta Formation by Union Oil.

The validity of this correlation is not discussed here, it will only be noted that the type section preferably should be divided into several formations as they appear to constitute different lithological units separated by unconformities. If this is accepted, only the lower 129 feet (39 m) of the type section might be named Abeokuta Formation (in accordance with Billman's work).

To avoid any confusion with the onshore type section the present report favours usage of the name "Turonian Sandstone" for the sandstone series known as "Abeokuta Sandstone" in the reinterpretation of the Sèmè Oil Field (Ræstad et al 1983).

The offshore "Turonian Sandstone" comprises the main pay zone in the Sèmè Field (Zone 1) and also a deeper zone with scattered shows (Zone 2); compare Appendix A.3.

The presence of the "Turonian Sandstone" offshore Togo is questionable. Upper Cretaceous sandstones with shale interbedded are present in both Lome 1 and Lome 2. These rocks are, however, somewhat younger than the supposed equivalent offshore Benin, being dated as Coniacian - Santonian. Log character and lithologic description do, however, have important similarities. The equivalent is about 130 m thick in the two wells, which is in agreement with a thinning westwards of this formation as evident from seismic mapping (compare fig. 5.8).

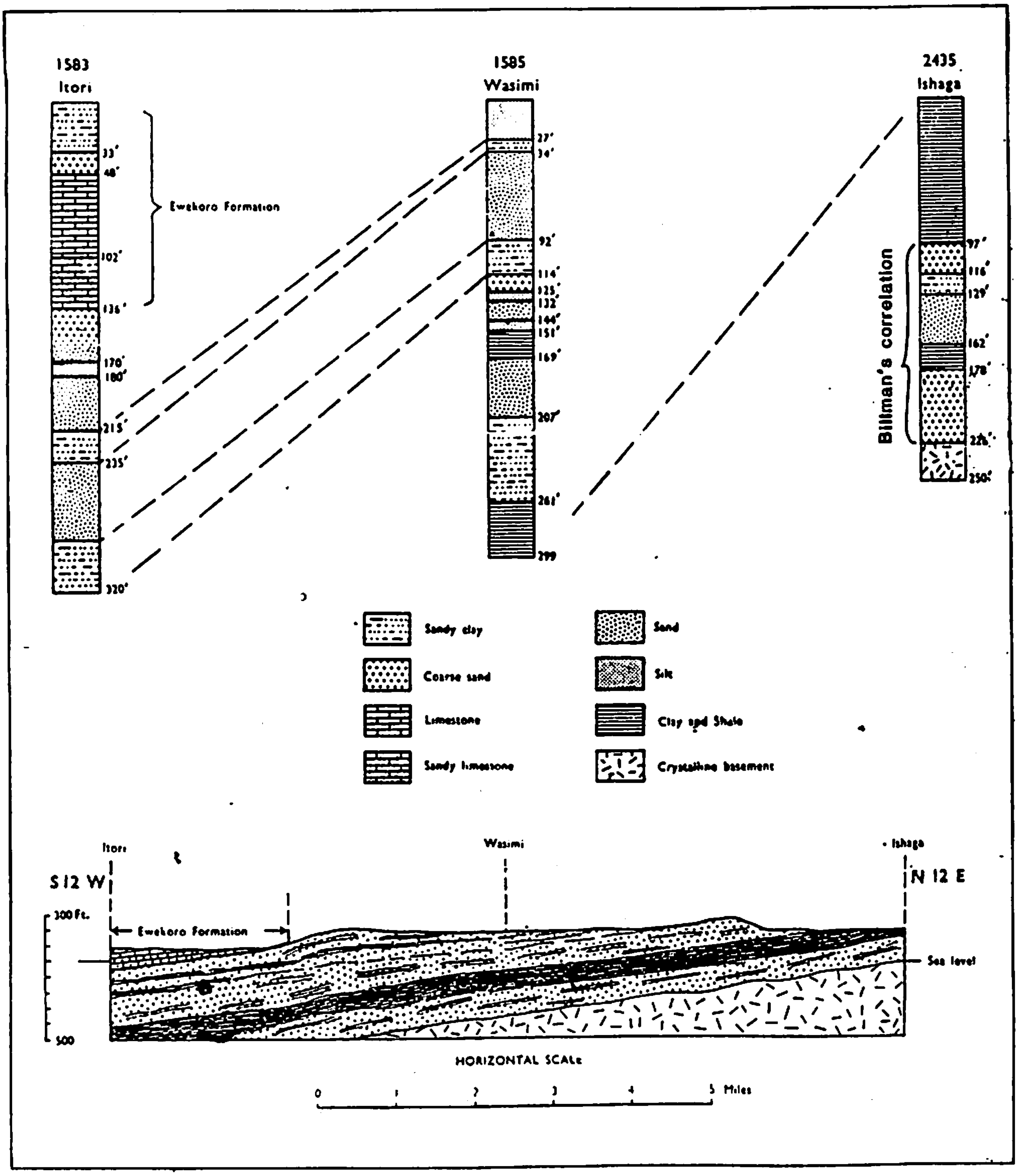

Fig. 5.6: Diagrammatic section of the Abeokuta Formation in the type locality. Also shown is Billman's correlation of the offshore "Turonian Sandstone" (which he named Abeokuta) with the Abeokuta type section (from Jones and Hockey 1964).

Lithology (fig. 5.7)

The "Turonian Sandstone" is a predominantly massive sandstone unit with occasional thin shale stringers. The sandstones are light grey to white, generally coarse grained, poorly sorted, and with abundant pyrite.

Boundaries (fig. 5.7)

The lower boundary is marked by a distinct change in log character associated with a lithological change from a massive sand to a sand with shale beds where the "Albian Sandstone" is present. On the larger part of the shelf area the "Turonian Sandstone" rests on crystalline basement.

The upper boundary to the Awgu Formation is associated with an unconformity and marked by a change from the massive sand to a sandy shale with relatively higher resistivity and lower acoustic velocity. In places, where the Senonian Unconformity cuts into the "Turonian Sandstone", the upper boundary may be with the highly radioactive Araromi Shale.

Depositional Environment

Based on cores cut in development wells Sèmè 1 and Sèmè 2 the depositional environment is interpreted as marginal marine to inner shelf reworked fan deltas. Restricted circulation is indicated.

Age

Due to a lack of diagnostic foraminifera the age assessment has to rely fully upon palynology. The "Turonian Sandstone" is

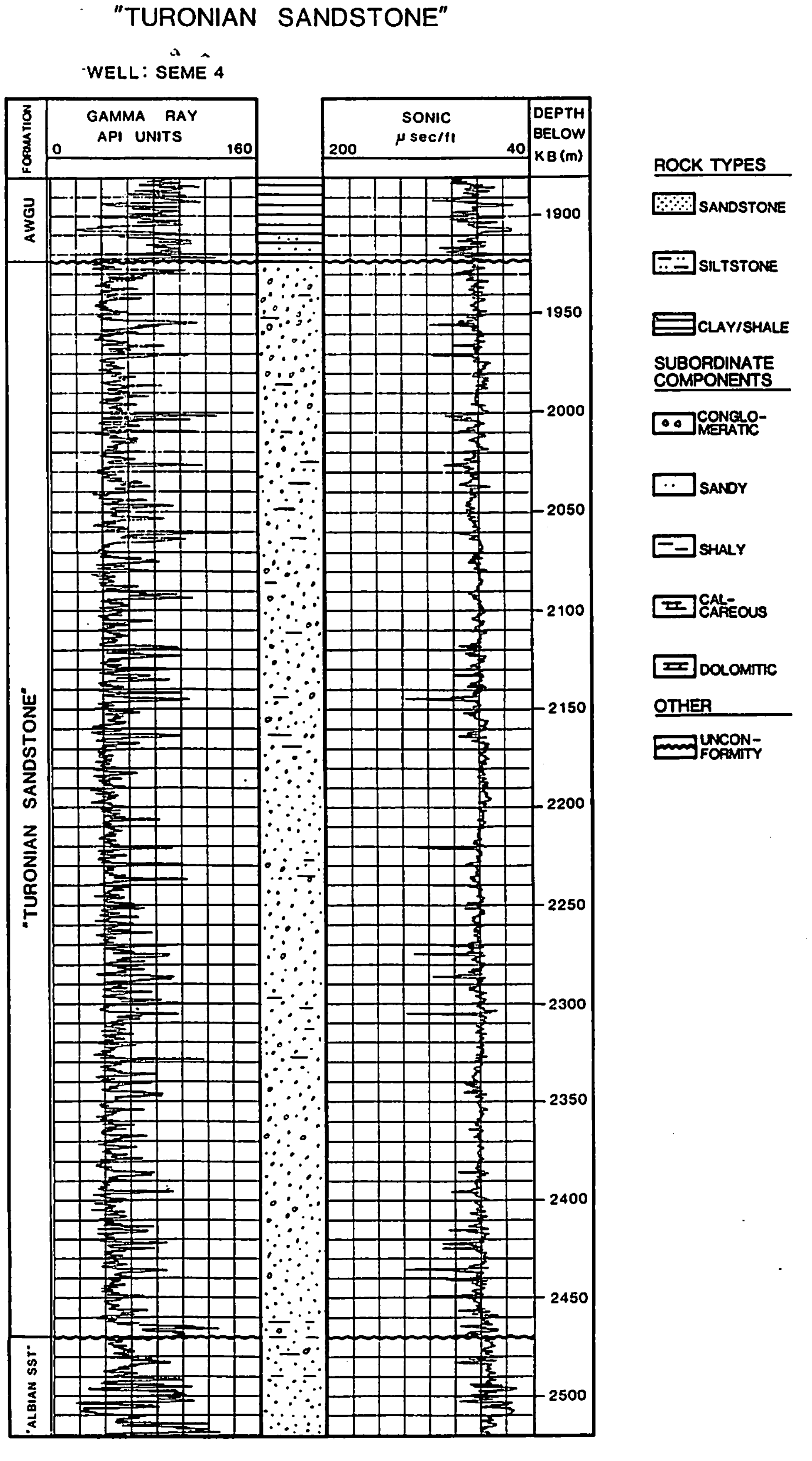

Fig. 5.7: Log character and lithology of the "Turonian Sandstone".

assigned a Turonian to Early Senonian age.

Distribution/Thickness (fig. 5.8)

The "Turonian Sandstone" is present on the entire shelf offshore Benin and partly also on the slope. The depocenter for this unit is located in the eastern part of the shelf where the formation attains a thickness close to 1000 m. The isopach map evidences a westward and northward thinning. Two erosional episodes have influenced the isopach. The Senonian Unconformity cuts into the formation in the easternmost part of the shelf in the vicinity of the Sèmè Field, while the Mid Miocene Unconformity only affects the formation beyond the shelf edge.

The "Turonian Sandstone" is present in all wells drilled by Union as well as all Sèmè development wells.

5.3.2 Awgu Formation

The formation name Awgu is originally used in Nigeria for a sequence of deep water shales of Turonian - Coniacian age. It has been adopted by Billman (1976) for a sandy shale overlying the Abeokuta Formation ("Turonian Sandstone" in this report). Also according to Billman (1976) beds equivalent to the offshore Awgu Formation has been mapped as part of the onshore Abeokuta Formation as discussed in the previous section.

Lithology (fig. 5.9)

The formation consists of dark grey calcareous shale interbedded with light grey calcareous siltstone and fine

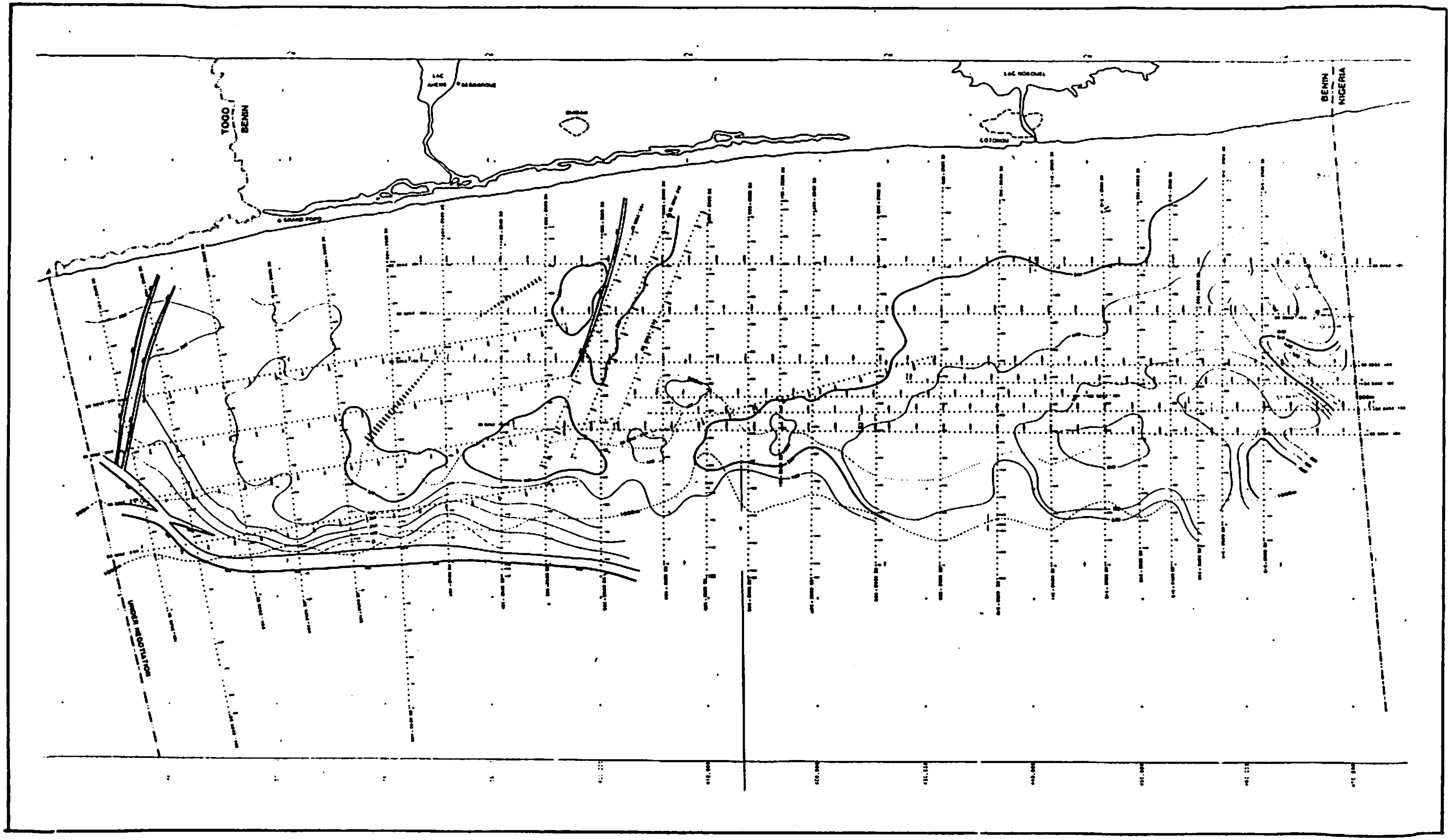

Fig. 5.8: "Turonian Sandstone", isopach map.

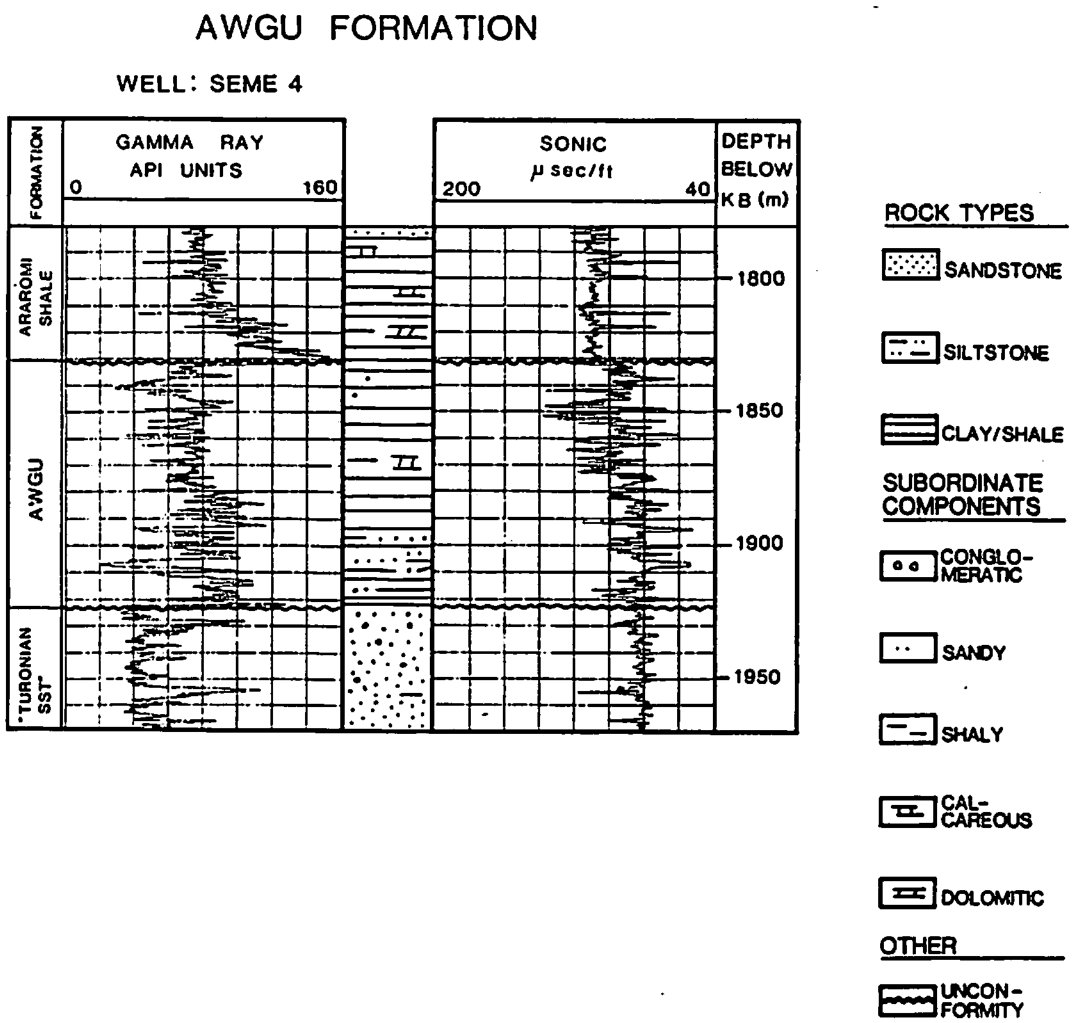

Fig. 5.9: Log character and lithology of the Awgu Formation.

grained sandstone.

Boundaries (fig. 5.9)

The lower boundary to the Abeokuta Formation can easily be picked from e-logs by a downward change from sandy shale to cleaner sand with corresponding decrease in gamma response and interval transit time.

The upper boundary is picked at a marked log break reflecting the downhole income of sandy and calcareous beds. A downward decrease in gamma response and interval transit time is also associated with this boundary.

Depositional Environment

An anaerobic marine environment is suggested for the deposition of this unit.

Age

The Awgu Formation is assigned an Early Senonian/Turonian age by Billman (1976). This dating is, however, very uncertain.

Distribution

The Awgu Formation is present on the entire shelf except for localized areas in the vicinity of the Sèmè Field.

5.3.3 Araromi Shale

The formation name "Nkporo Shale" is originally applied to a dark grey to blue shale unit deposited in the Anambra Basin of Nigeria. It was laid down in a marine environment following the Late Campanian transgression, and may reach a thickness of 1000 m in the type area (Whiteman 1982).

Billman (1976) correlated the offshore unit of dark grey shale with the Nkporo Shale in the Anambra Basin.

Downdip from the Anambra Basin, in the subsurface of the Benin Flank and the Ilesha Spur, marine deposits of Upper Senonian age are referred to as the "Araromi Shale" (Murat 1972, Adegoke and Ibe 1982). The Nkporo Shale offshore Benin, as it is named by Ræstad et al (1983) and Billman (1976), should therefore rather be referred to as the Araromi Shale, as is being done in this report.

The Araromi Shale has not been specifically referred to onshore by neither Slansky (1962) nor Jones and Hockey (1964). The onshore equivalent of the offshore Araromi Shale is therefore probably included in the Abeokuta Formation type section of Jones and Hockey (1964).

Lithology (fig. 5.10)

The formation consists of black to dark grey calcareous and carbonaceous shales in parts with abundant pyrite and pyritized microfauna. Limestone stringers occur frequently.

Boundaries (fig. 5.10)

The Araromi Shale is characterized by a high gamma ray response which ensure that both the lower and upper boundaries are marked by log breaks. Characteristic of the upper sequence of the formation is a gradually increasing velocity with depth, and the lower boundary down into the Awgu Formation can also be associated with an increase in velocity.

The base of the Araromi Shale is in well data identified as the Senonian Unconformity which is clearly defined on seismic data in the eastern part of the Benin offshore basin.

Depositional Environment

The depositional environment has in the offshore wells been interpreted as outer sublittoral to upper bathyal. The organic facies further indicate restricted circulation (Augedal et al 1983).

Age

Maastrichtian to Danian age is assigned to this formation offshore Benin. In the Anambra Basin of Nigeria the Nkporo Shale dates back to Late Campanian while the Araromi Shale is assigned a Campanian to Maastrichtian age (Murat 1972).

The Araromi Shale has been subdivided into an upper and lower member by Ræstad et al (1983). The upper member is of Danian age while the lower member is of Maastrichtian age.

Distribution/Thickness (fig. 5.11)

Over the major part of the Benin offshore basin the Araromi Shale is very thin, less than or approximately 100 m. Exceptions occur in the eastern part on the shelf as well as

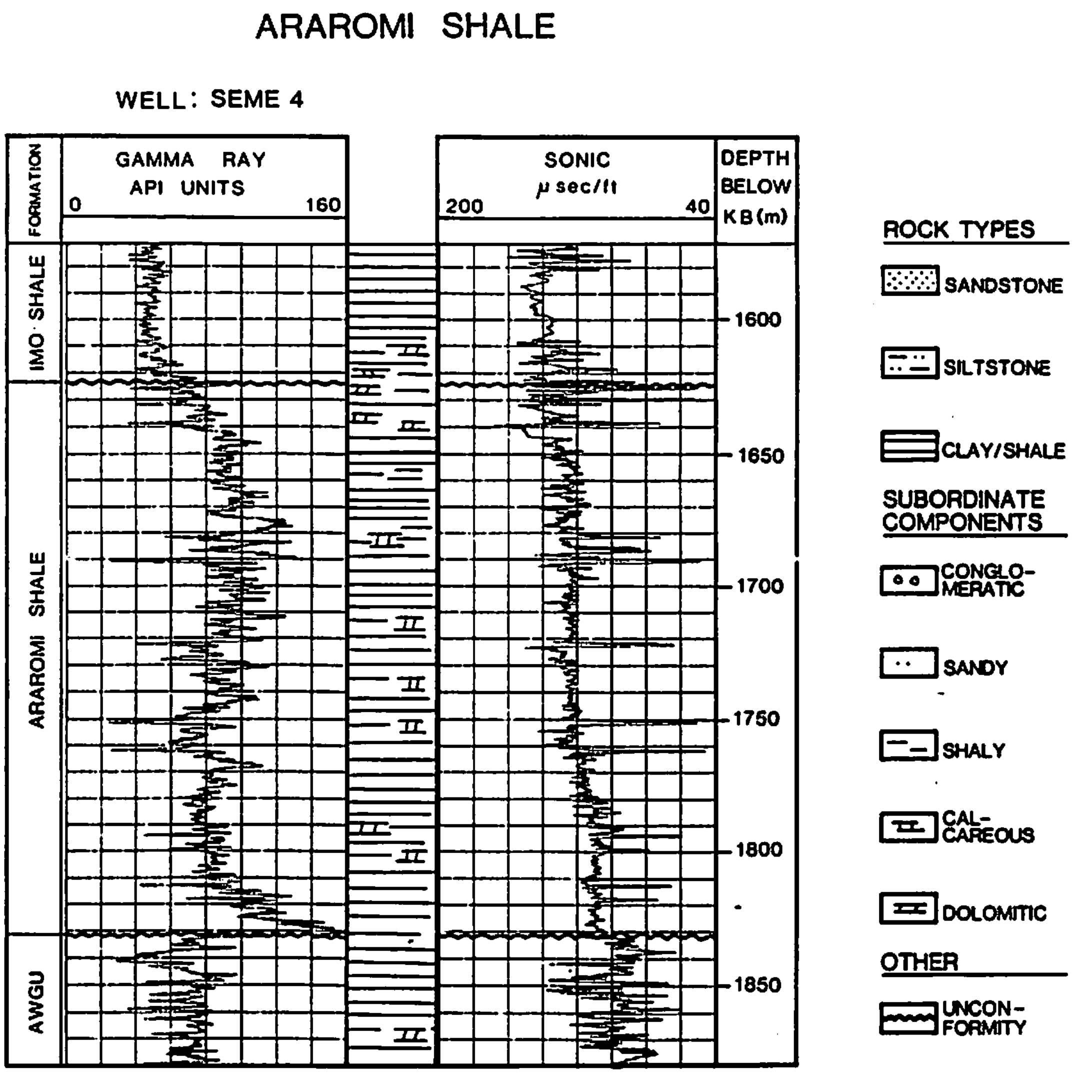

Fig. 5.10: Log character and lithology of the Araromi Shale.

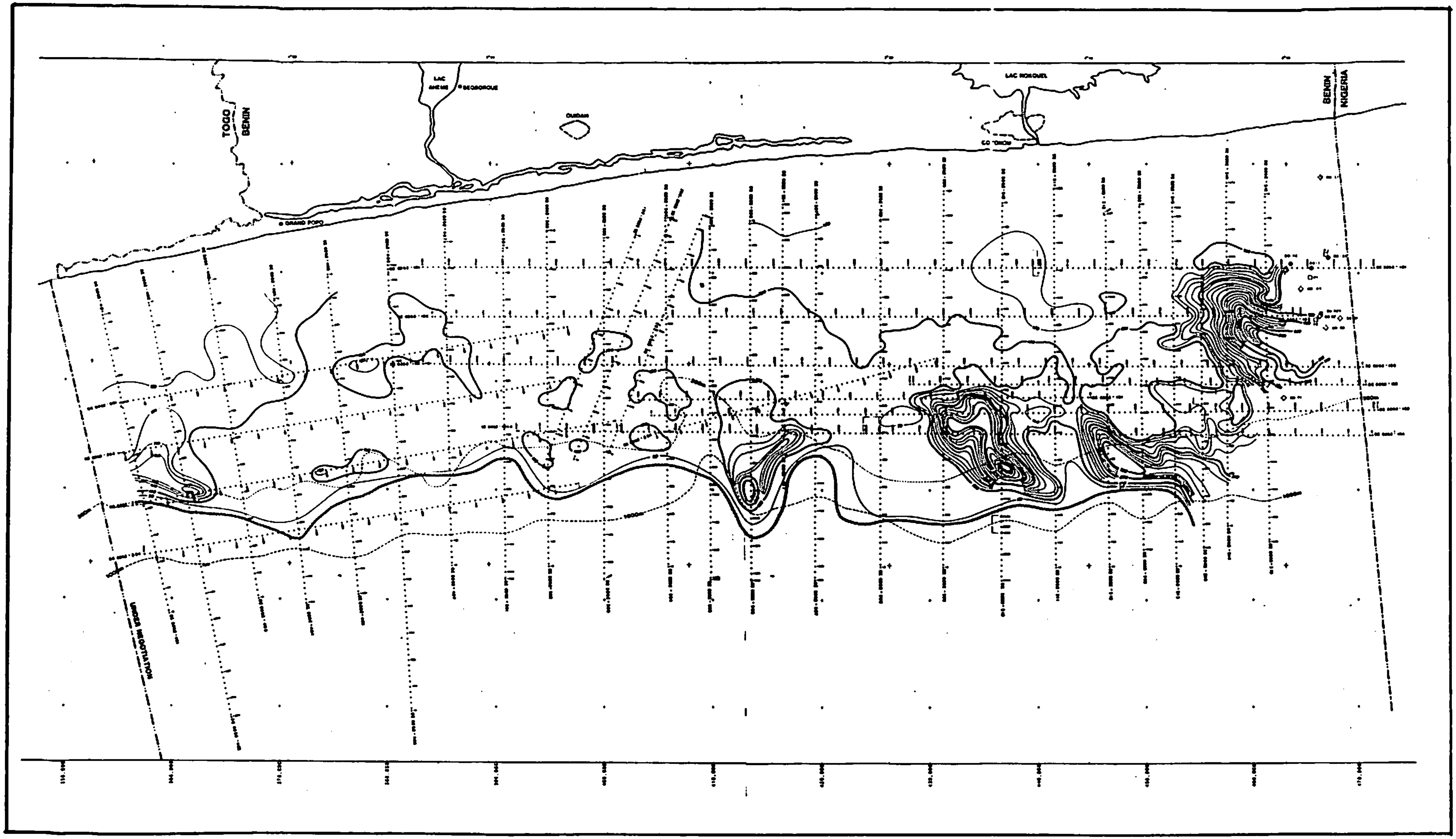

Fig. 5.11: Araromi Shale, isopach map.

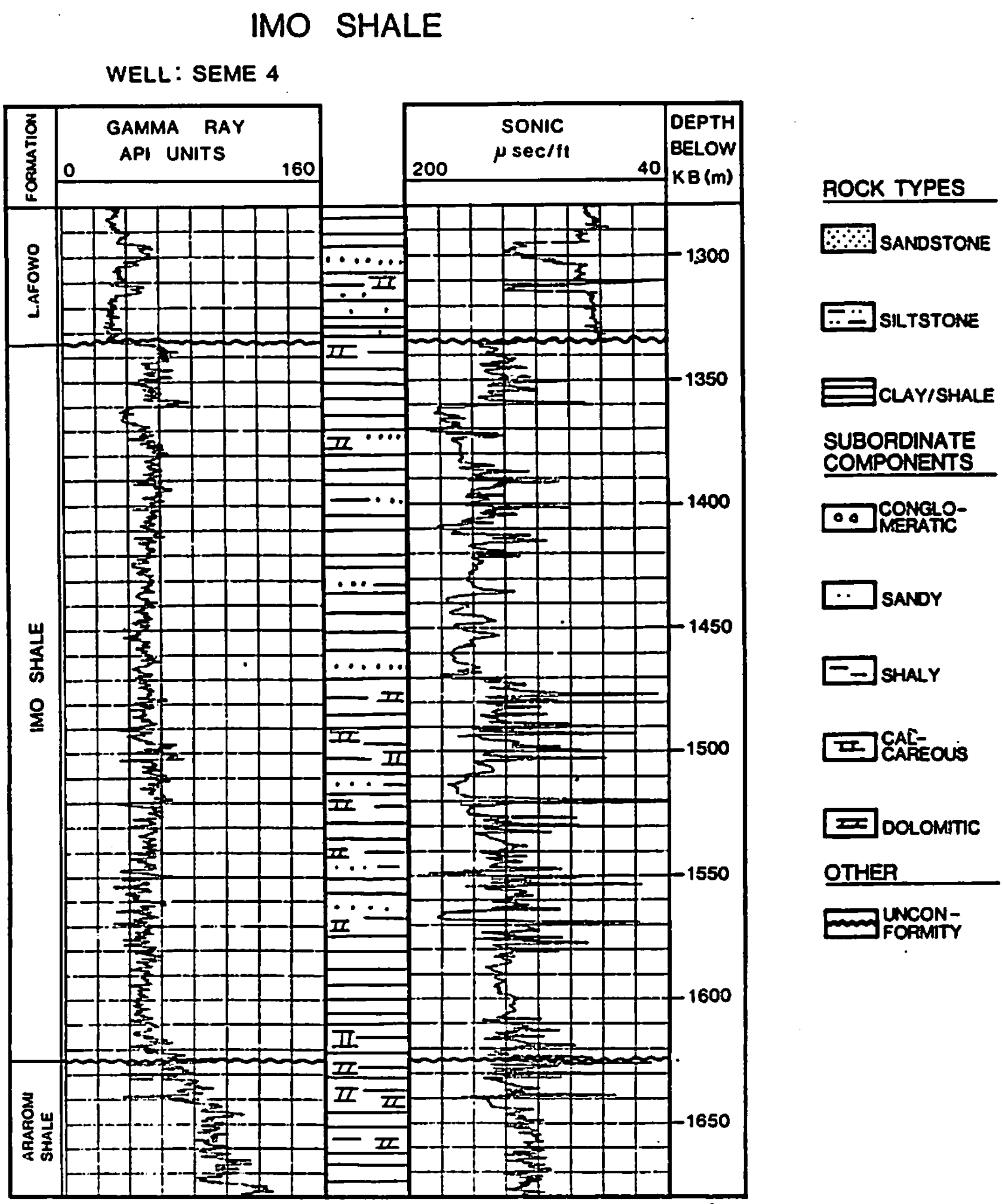

Fig. 5.12: Log character and lithology of the Imo Shale.

increase in both gamma ray response and velocity occur. A change from grey to predominantly black shales is also characteristic of this transition.

The definition of the top is more subtle where the Oshoshun Formation is present. However, an upward change to sandy formations should be diagnostic.

Depositional Environment

The Imo Shale has been deposited in an upper bathyal to outer sublittoral marine, well oxygenated environment. A shallowing seems to occur with time (Augedal et al 1983).

Age

The age of this formation ranges from Middle Paleocene into Early Eocene (Billman 1976, Crittenden et al 1983).

Distribution/Thickness

The Imo Shale is present on the entire shelf offshore Benin and attains a thickness of approximately 400 m in the Sèmè area. The formation has a reduced thickness in a westward direction.

5.4.2 Oshoshun Formation

The name Oshoshun Formation is vaguely defined (Adegoke 1969), but is in the current report assigned to an offshore sequence of marine shales and sandy shales with abundant phosphatic material as suggested by Billman (1976).

The type area of the Oshoshun Formation is in western Nigeria where it consists of sandstones, sandy mudstones and mudstones with phosphate horizons that may be traced over long distances from Nigeria in the east to Togo in the west (Adegooke 1969). The formation is only present in the Dahomey Embayment. According to Whiteman (1982) it does not exceed a thickness of approximately 60 m onshore.

Lithology (fig. 5.13)

The formation consists of sandy, varied coloured claystone grading to siltstone.

Boundaries (fig. 5.13)

The lower boundary to the Imo Shale occurs as a distinct log break from sandy formations to predominantly shale going downhole.

The top of the Oshoshun Formation will be an unconformity in the eastern part of the study area. Lack of well control prohibits a description of the upper boundary in the remaining areas where seismic interpretation indicates it as an unconformity.

Depositional Environment

The depositional environment of the Oshoshun Formation is interpreted as marine, outer sublittoral to bathyal and well oxygenated from offshore Benin well data (Crittenden et al 1983). Onshore data also indicates deposition in fairly deep water (Whiteman 1982) in a coastal position, with a gradual shallowing (possibly grading to continental?) from south to the slope. Three depocenters are mapped with thickness up to more than 600 m.

5.4 Cenozoic

5.4.1 Imo Shale

The formation name Imo Shale is applied to a unit of dark grey to bluish shale that has been deposited in the entire Dahomey Embayment and southern Nigerian basins following a Paleocene transgression. Onshore the lower part is developed in a limestone facies (Ewekoro Limestone, Jones and Hockey 1964).

The type area of the Imo Shale is in eastern Nigeria where it may reach a thickness of 500 m. It is the updip equivalent of the younger subsurface Akata Formation which is the main source rock of the Niger Delta Basin (Adegoke 1969).

The Imo Shale is offshore Benin conformably overlying the Araromi Shale and over the larger shelf area conformably underlies the Oshoshun Formation. The latter may be missing if younger formations have eroded into the Imo Shale.

Lithology (fig. 5.12)

As described in offshore wells the Imo Shale consists of light greenish grey to dark grey, noncalcareous, hard shales with stringers of dark grey, microcrystalline limestone.

Boundaries (fig. 5.12)

The base of the Imo Shale is defined as where a substantial

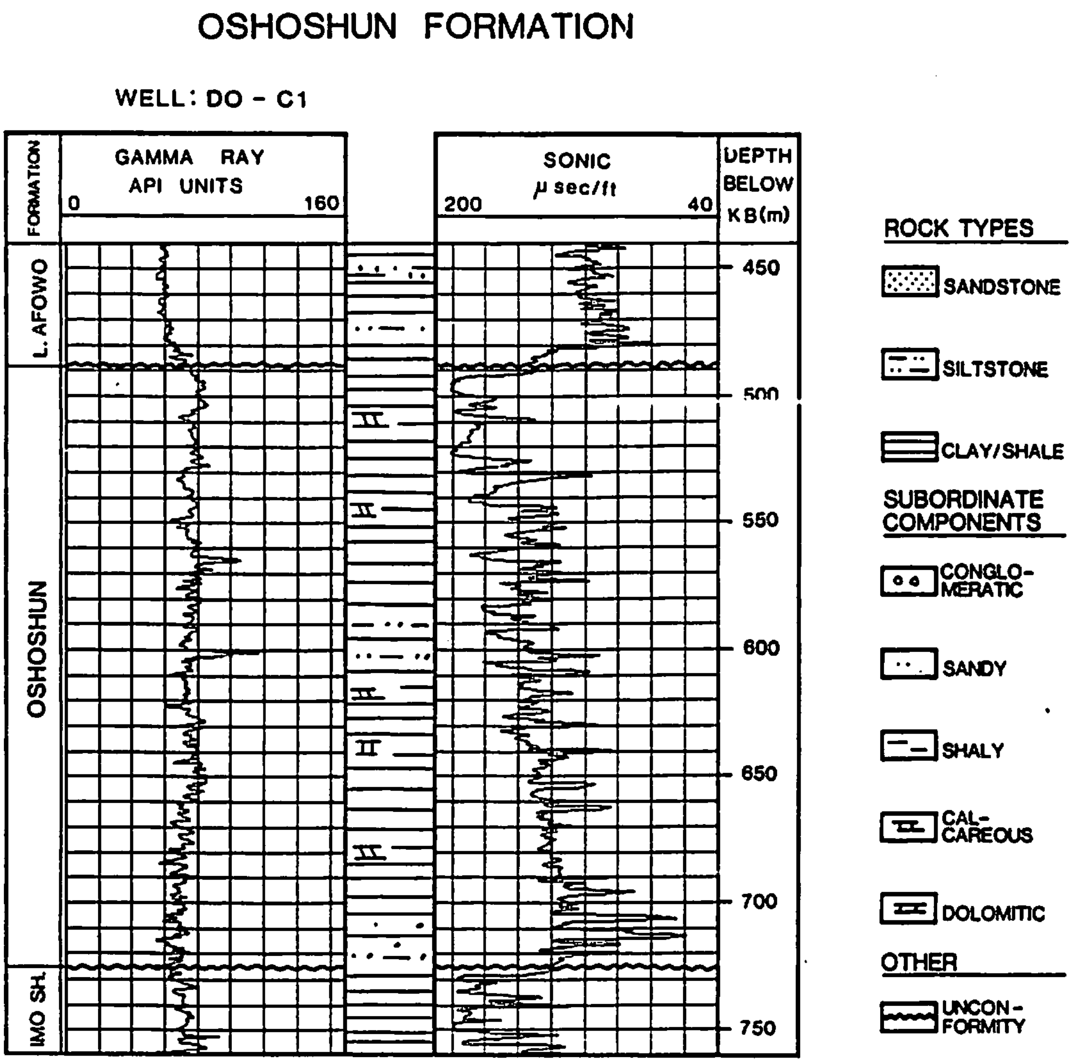

Fig. 5.13: Log character and lithology of the Oshoshun Formation.

north (Jones and Hockey 1964).

Age

Both onshore and offshore data points to a Middle Eocene age.

Distribution/Thickness

The Oshoshun Formation appears to be present all over the shelf area, although eroded close to the shelf break by the Mid Miocene Unconformity and locally in the vicinity of the Sèmè Field.

5.4.3 Afowo Formation

The informal name Afowo Formation has been applied by Billman (1976) for a thick section of marine shale, siltstone and sandstone that do not crop out in the Dahomey Embayment. The name should preferably be avoided as it is also applied to an Upper Cretaceous sandstone sequence in western Nigeria (Adegoke and Ibe 1982). It is nevertheless used here as no alternative name has been suggested.

The type well of the Afowo Formation, as proposed by Billman, is the Afowo 1 drilled by Mobil in the eastern Dahomey Embayment (West Nigeria) in which a sequence of 2700' (820 m) was penetrated.

The Afowo Formation is subdivided into an upper and lower unit being separated by an unconformity named Mid Miocene Unconformity which is easily picked both from seismic data and well logs.

Lithology (fig. 5.14)

The Upper Afowo Formation is a sequence of grey-brown soft, sticky and silty clay interbedded with friable, coarse grained sandstone with glauconite, pyrite and shell debris.

The Lower Afowo Formation is described as a light grey siltstone grading upwards to fine grained sandstone but becoming claystone towards the base. Limestone and dolomitic interbeds are common. Typical of the Lower Afowo is the salt and pepper texture.

Boundaries (fig. 5.14)

The lower boundary is an unconformity which in the larger part of the shelf corresponds to the Base Miocene Unconformity (Horizon 3), but on the outer part of the shelf and in the eastern part is defined by the Base Mid Miocene Unconformity (Horizon 2). A distinct log break marks the boundary, with a downward increase in interval transit time. The upper boundary to the Benin/Ijebu Formation appears to be conformable with an increase in sand content.

Depositional Environment

The depositional environment of the Afowo Formation has by Crittenden et al (1983) been interpreted as marine, outer sublittoral to upper bathyal well oxygenated environment. The interbedded sands have resulted from turbidity currents.

Age

The Afowo Formation is of Early to Middle Miocene age (Billman

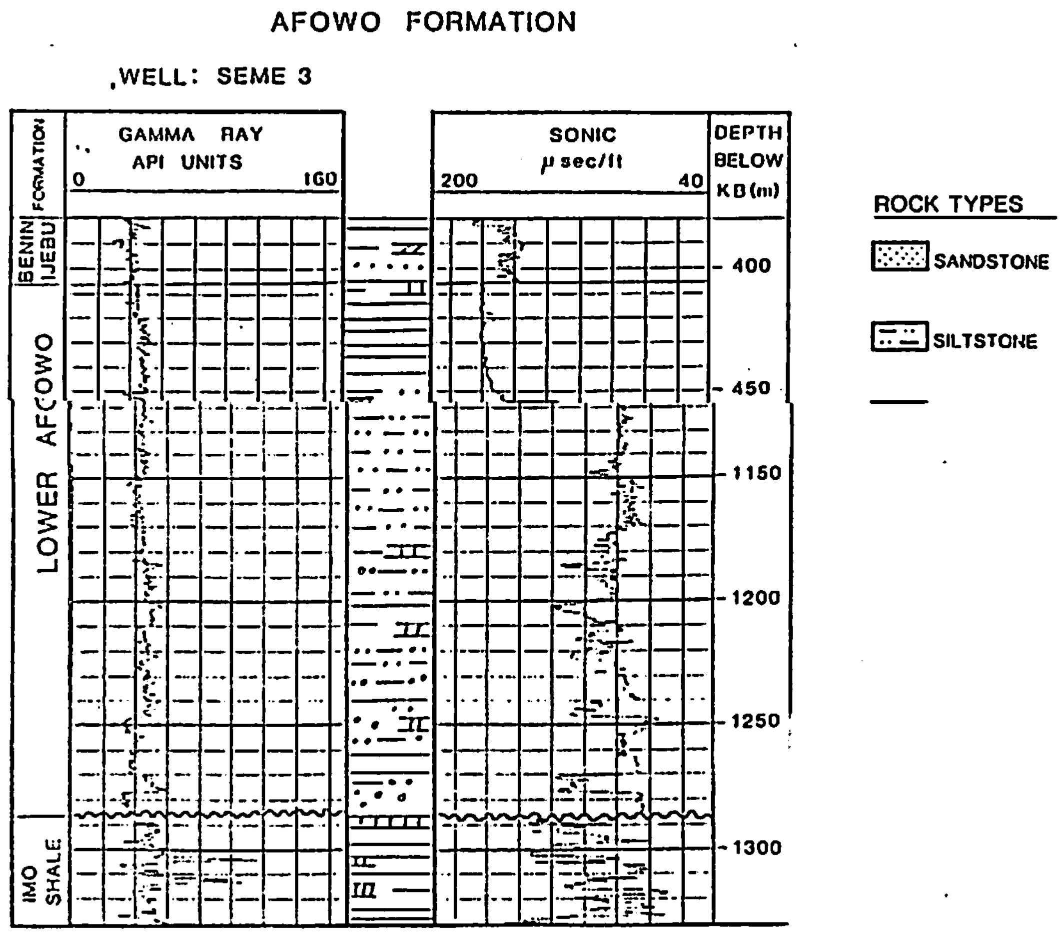

Fig. 5.14: Log character and lithology of the Afowo Formation.

1976, Crittenden et al 1983).

Distribution/Thickness (fig. 5.15)

A composite structural depth map of horizons 2 and 3 is constructed (fig. 5.15). This being the Base Afowo Formation, it illustrates the thickness variations of this unit (Benin/ Ijebu included). On the seaward side of the truncation line, only the Upper Afowo Formation is present.

5.4.4 Benin/Ijebu Formations

The formation names Benin Formation and Ijebu Formation have been applied by Billman (1976) to the uppermost sequence of marine coarse grained sands that overly the Afowo Formation conformably. The sequence range in thickness up to possibly more than 500 m, but is generally in the order of some few hundred meters. The age of the Benin/Ijebu Formations is Late Miocene and younger. The base is not mapped.

In the Niger Delta the Benin Formation is the topmost unit of Miocene - Recent age. It is composed of fluviatile gravels and sands and may be as thick as 2100 m in the central part (Short and Stäuble 1967).

5.5 Depth Converted Cross Sections

Two depth converted seismic lines illustrate the distribution of the offshore sedimentary sequences in the vicinity of the Sèmè area where the Rift, Translational and Drift Sequences are all present (fig. 5.16), and in the western part of the shelf in which the Rift and Translational Sequences both are missing (fig. 5.17).

Enclosure 2 is a stratigraphic cross-section in the eastern part of the shelf through the Sèmè Field.

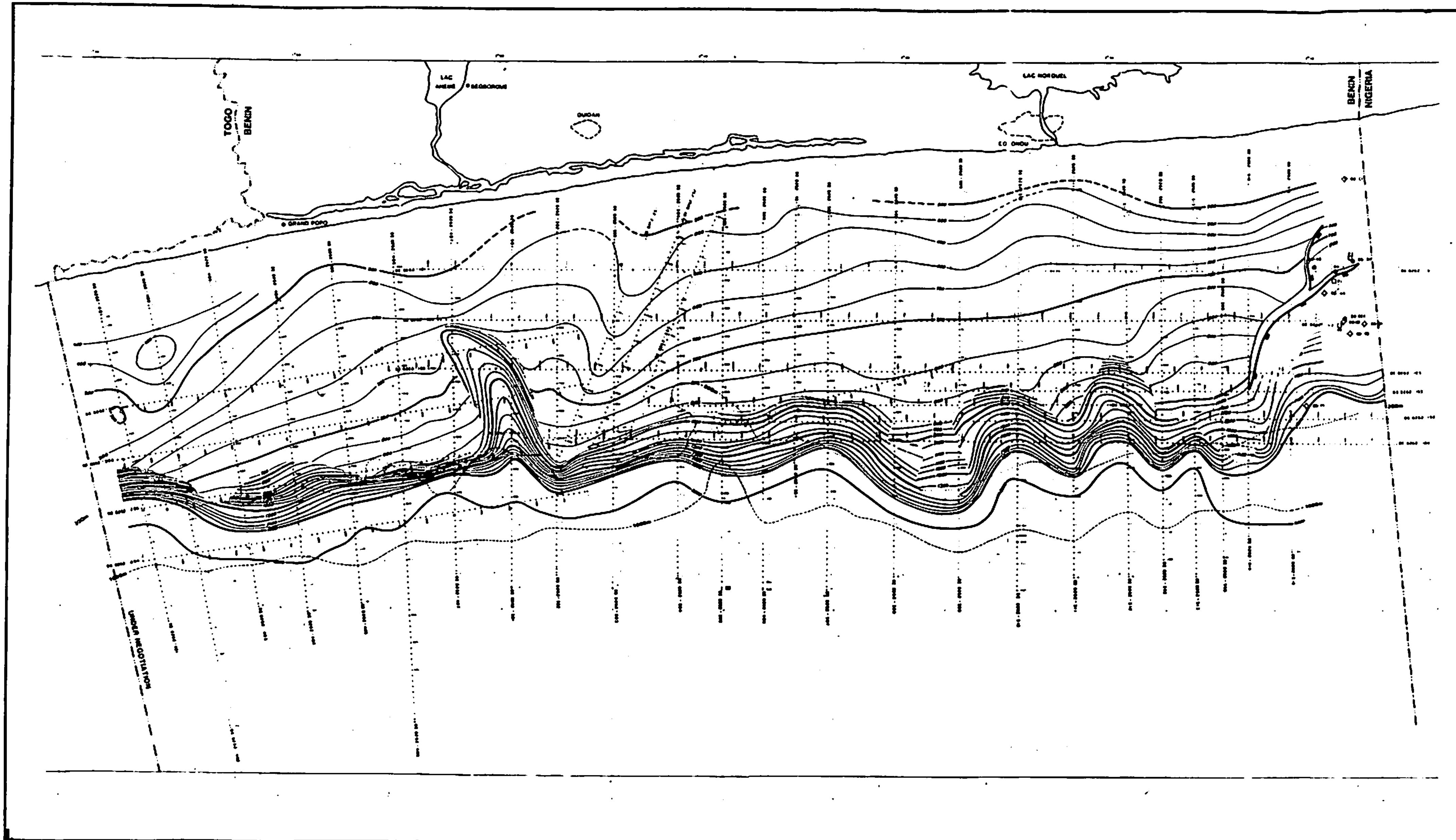

Fig. 5.15: Composite structural depth map horizons 2 and 3 showing Base Afowo Formation.

CHAPTER 6 22.6.84

SEISMIC STRATIGRAPHY

6.1 General

The seismic stratigraphic approach was undertaken to interpret the seismic facies and to help interpret the sedimentary history of the basin. The method used for the analysis is described in detail in AAPG Memoir 26 (Vail et al 1977, 11 sections).

Well data from the Sèmè Oil Field was used in calibrating the environmental interpretation and the age of the unconformities. The sequences discussed here are named numerically from youngest to oldest by H1 to H8 respectively. Fig. 6.1a attempts a stratigraphic summary of the interpreted sequences.

6.2 Interpretation

6.2.1 Seismic Facies Maps

The seismic facies maps were prepared for eleven sequences in the Benin offshore basin. The seismic facies were described for each sequence, and was transferred to the maps. Thereby an appreciation for the areal extent of these units was achieved.

An important observation of seismic facies maps is that the maps indicate the general depositional environment (fig. 6.1b). Within any sequence the environment may be highly mixed. Rarely do seismic facies represent a single depositional environment. This mixing is indicated by the stripping. The solid strips indicate areas with progradation.

CHAPTER 6 22.6.84

SEISMIC STRATIGRAPHY

6.1 General

6.2 Interpretation

6.2.1 Seismic Facies Maps

6.2.2 Seismic Sequences

6.3 Geologic Development of the Benin Offshore Basin

STF

DEPOSITIONAL ENVIRONMENT
* DELTAIC
* PRODELTA-SLOPE
DIFFICULT TO VERIFY ON SEISMIC DATA
* SMALL DELTAS
* DELTAIC
DELTAIC DEEP WATER SHALES AND SUBMARINE FANS
SUBMARINE EROSION
* DELTAIC SHELF
* FAN DELTAS
* FAN DELTAS * CARBONATE BUILDUPS
* FAN DELTAS
* FLUVIODELTAIC, * SUBLACUSTRINE FANS, TURBIDITES * FAN DELTAS

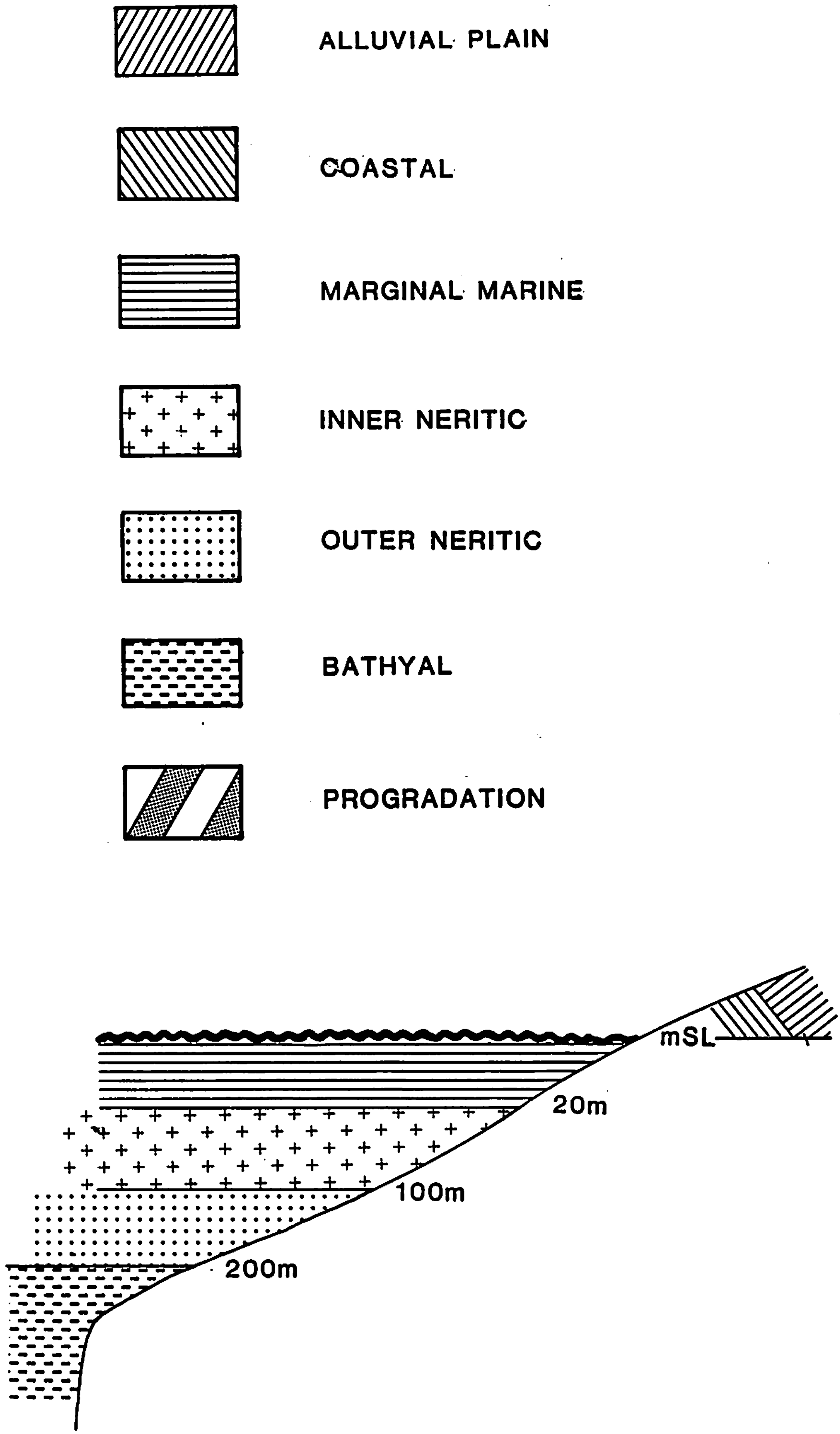

Fig. 6.1b: Stratigraphic information.

6.2.2 Seismic Sequences

In the following text, each sequence is given a general description as to its age, the reflection terminations at the sequence boundaries and the internal reflection character. The depositional environment for each sequence is also discussed here.

Top Ise Formation, H8

The sequence fills the "basement" half grabens (ref. chapter 5.2.1).

Age:
This sequence has been interpreted as being of Neocomian age (ref. chapter 5.2.1).

Boundaries (fig. 6.2):
The upper boundary is generally defined by erosional toplap, but there are some areas of concordance. The lower boundary termination varies between concordant and onlap, with the latter being prevalent.

Reflection Character (fig. 6.2):
The reflections are generally divergent, rarely being subparallel. The amplitude and frequency vary between high and low, while the continuity ranges from high to discontinuous.

Depositional Environment (fig. 6.3):
The sediments of this sequence were probably deposited by fan deltas in a lacustrine environment as the half grabens were

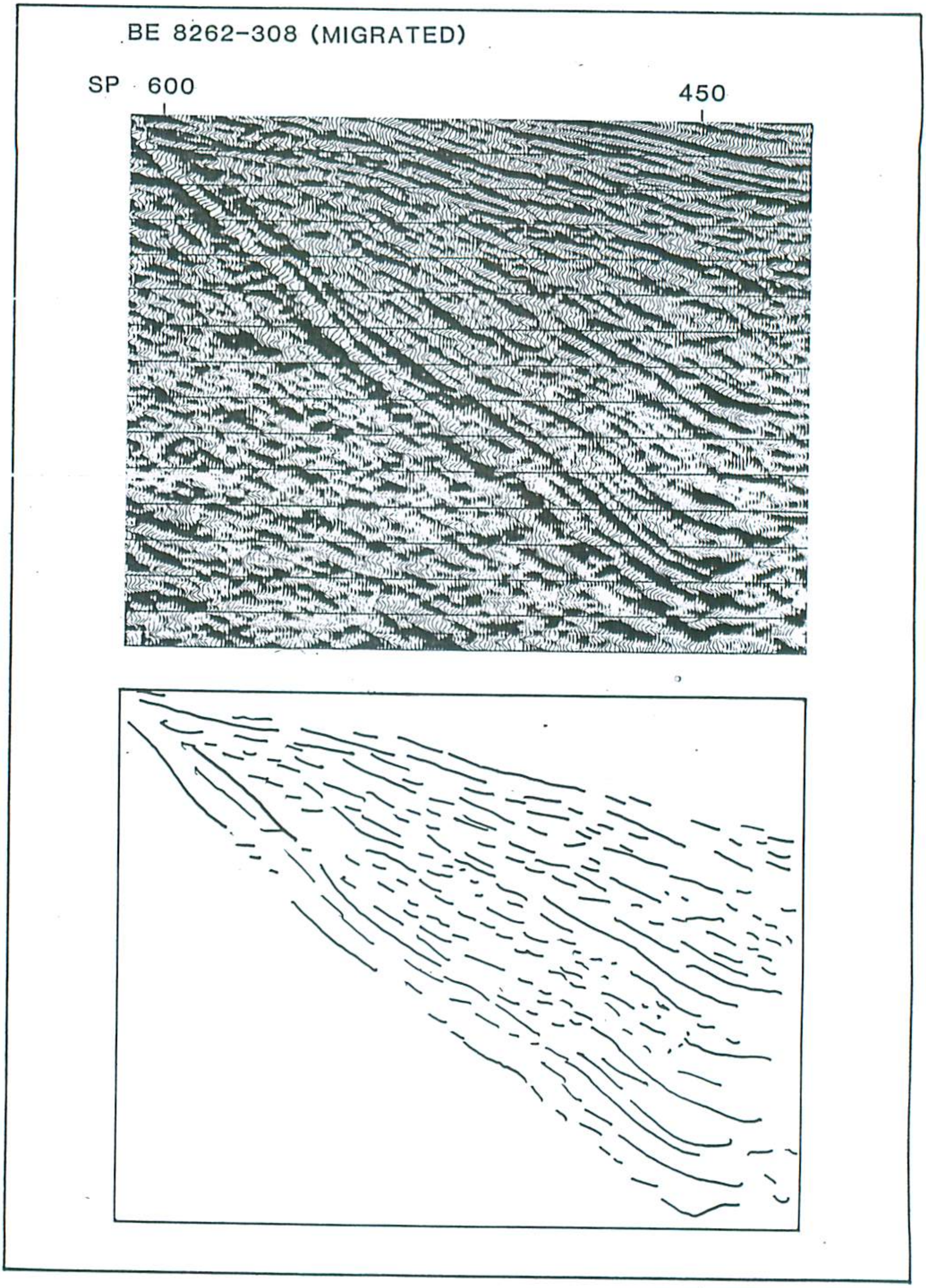

Fig. 6.2: Migrated line BE8262-308 shows the Ise Formation, H8. Note the slight divergence within the sequence, the onlap and the toplap. This sequence has been interpreted as lacustrine fill.

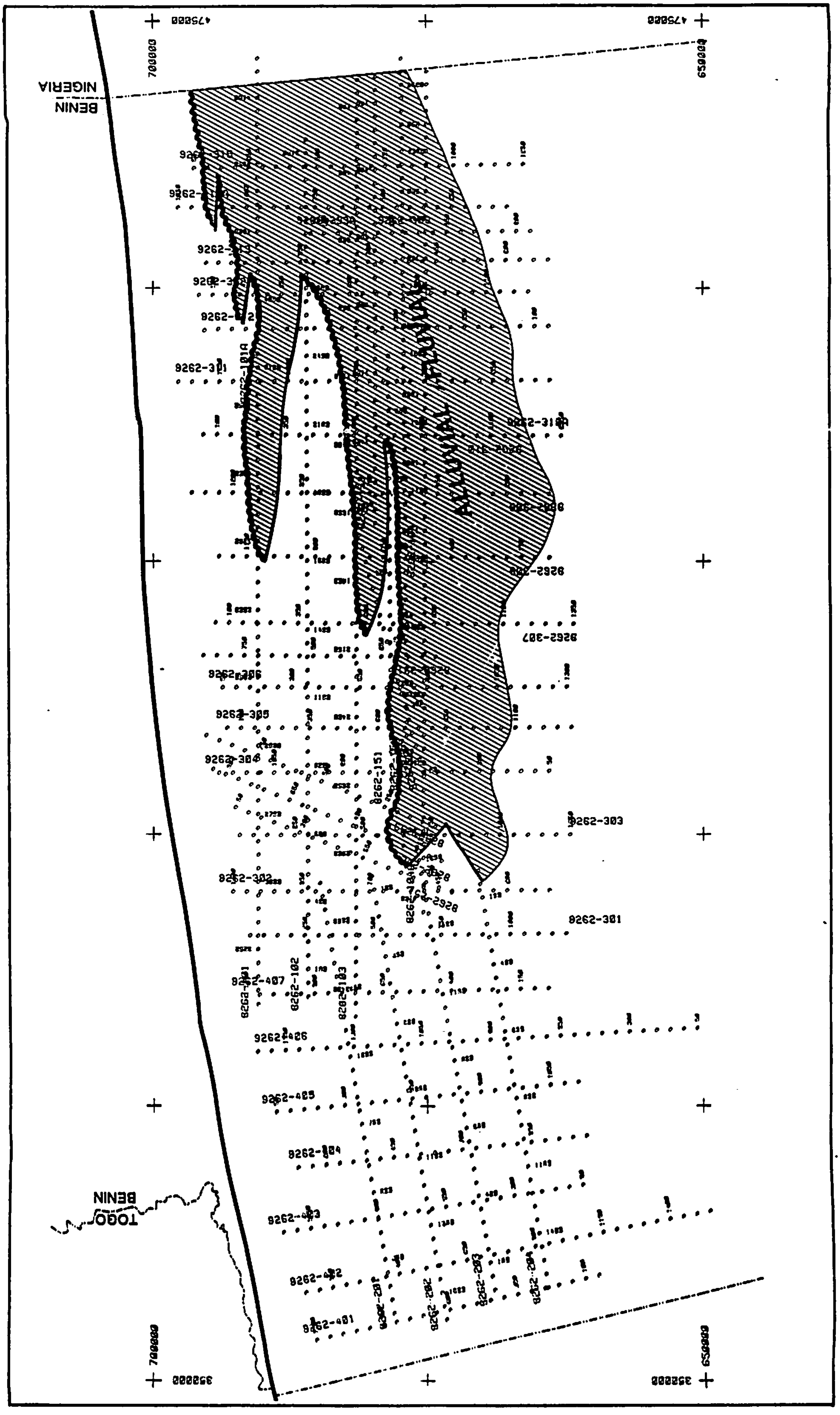

Fig. 6.3: Ise Formation, H8, environmental interpretation.

being formed. Deep water turbidites or mass flows may also be present.

Comments:
The divergent reflections indicate sedimentation during subsidence.

Top "Albian Sandstone", H7.0

This sequence is only present over the eastern half of the area with the overall same distribution as the Ise Formation.

Age:
Well information indicates the upper portion of the sequence is Albian in age. The lower most portion of the sequence may be (Late) Aptian.

Boundaries (fig. 6.4):
The upper boundary is generally concordant with little erosional truncation (toplap) observable. The lower boundary reflection termination of the sequence changes from onlap near the paleocoast to concordant, and then to downlap to the southeast.

Reflection Character (fig. 6.4):
The reflection configuration varies from subparallel - divergent to being hummocky or mounded. In general, the reflections are subparallel. Within the sequence the reflections generally have a high amplitude with medium to low frequency. The continuity ranges from high to discontinuous with high continuity seaward.

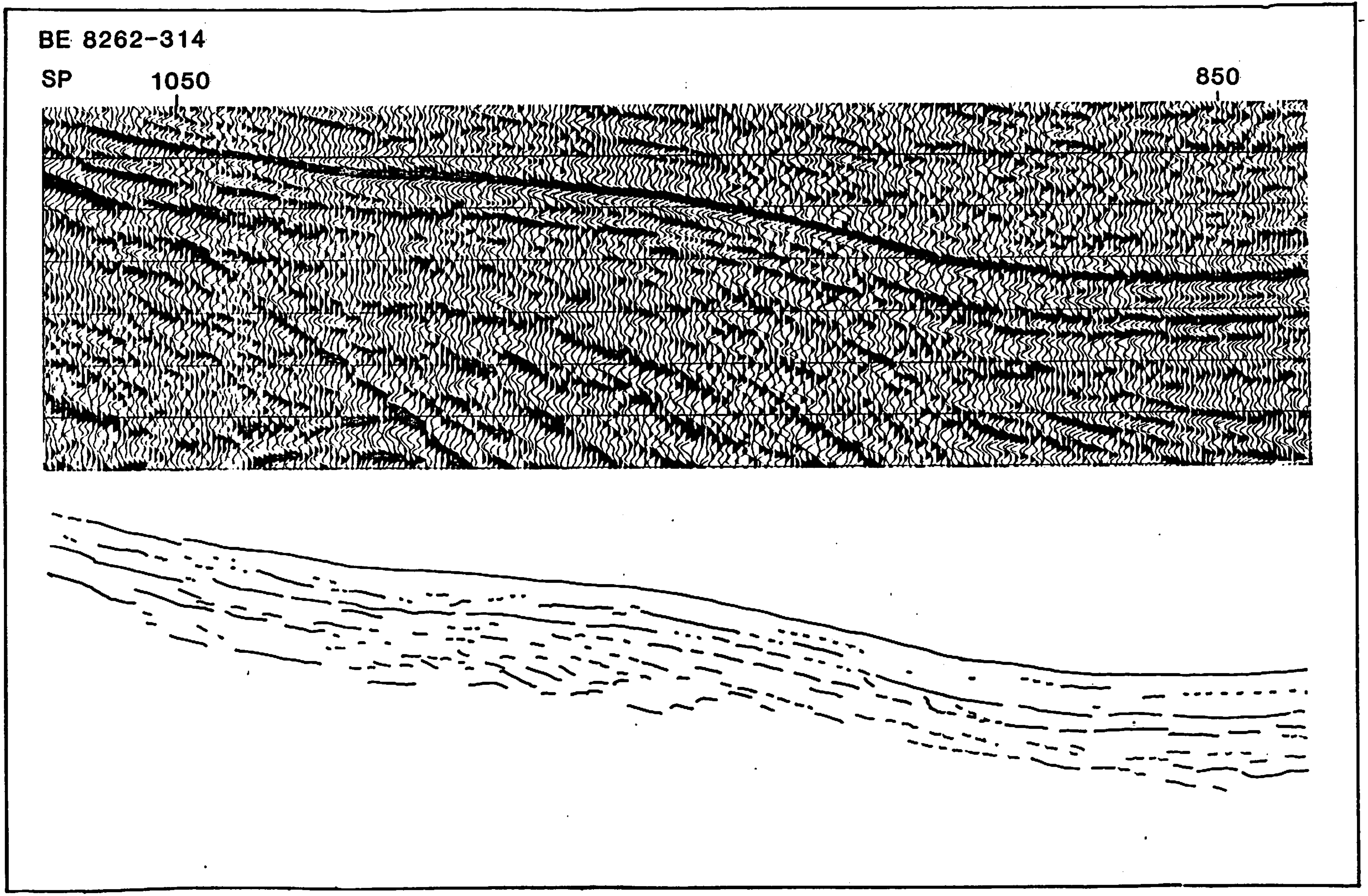

Fig. 6.4: "Albian Sandstone", H7. High amplitude reflection in the middle of the sequence may represent an additional sequence boundary.

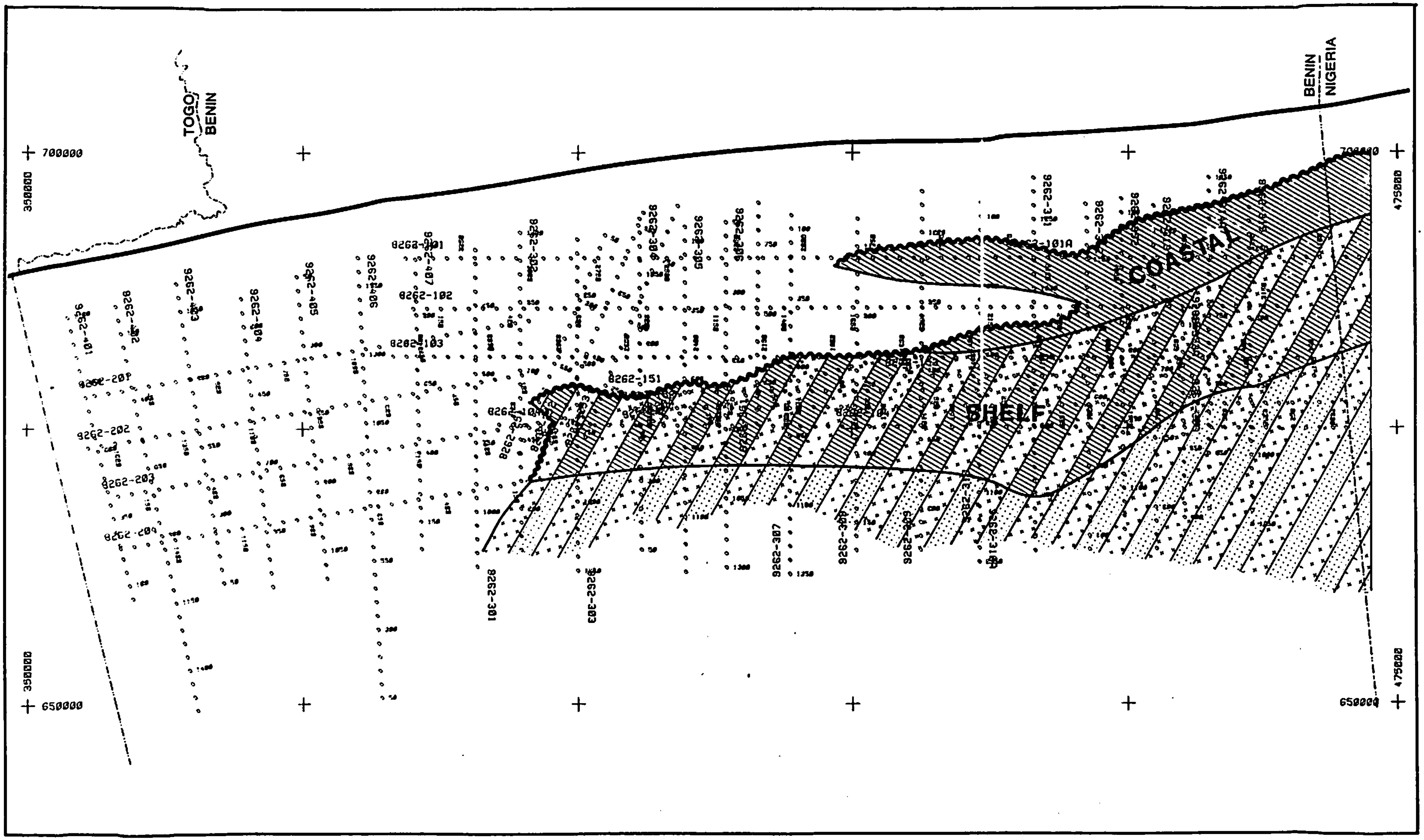

Fig. 6.5: "Albian Sandstone", H7, environmental interpretation.

Depositional Environment (fig. 6.5):
The depositional environment ranges from non marine to neritic. In the lower portion of the sequence the sediments were probably deposited by a fluviatial fan delta into a lacustrine environment. By middle of the sequence brakish water shallow marine shelf carbonates were deposited. The sediments of the upper part of the sequence were probably deposited by fan delta shelf system.

Comments:
This sequence may contain some bioclastic reefal build ups (fig. 6.6) identified by a loss of reflections and a mounded character. Possible pinnacle and fringing reefs have been identified. This sequence has been tentatively divided into two sequences of which the lower sequence H7.1 is interpreted as a Late Aptian(?) lacustrine sequence.

Lower "Turonian Sandstone", H6.1

The sequence is truncated to the north and west, thereby not being present in the western area.

Age:
The sequence ranges in age from 97 ma to 92 ma (Cenomanian).

Boundaries (fig. 6.7):
Where present the upper boundary of the sequence ranges from concordant to toplap and erosional toplap. The lower boundary varies between concordant to onlap and downlap. Downlap is the primary reflection termination for the sequence. Onlap and concordance are located south of the area with downlap.

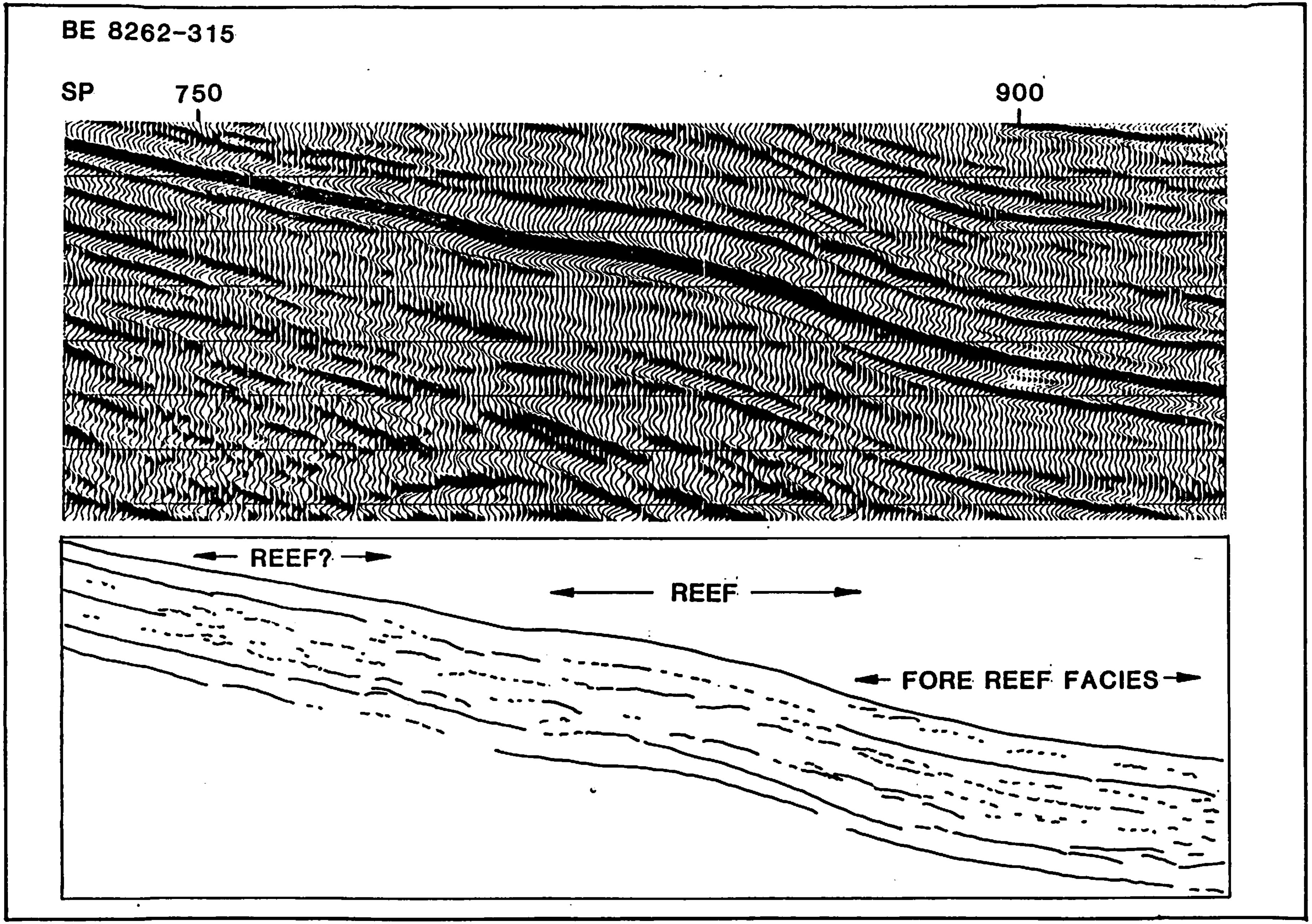

Fig. 6.6: Line BE8262-315 shows a couple of the possible carbonates within the "Albian Sandstone, H7, sequence. The possible carbonates are located where the mounding and loss of reflection amplitude are observed.

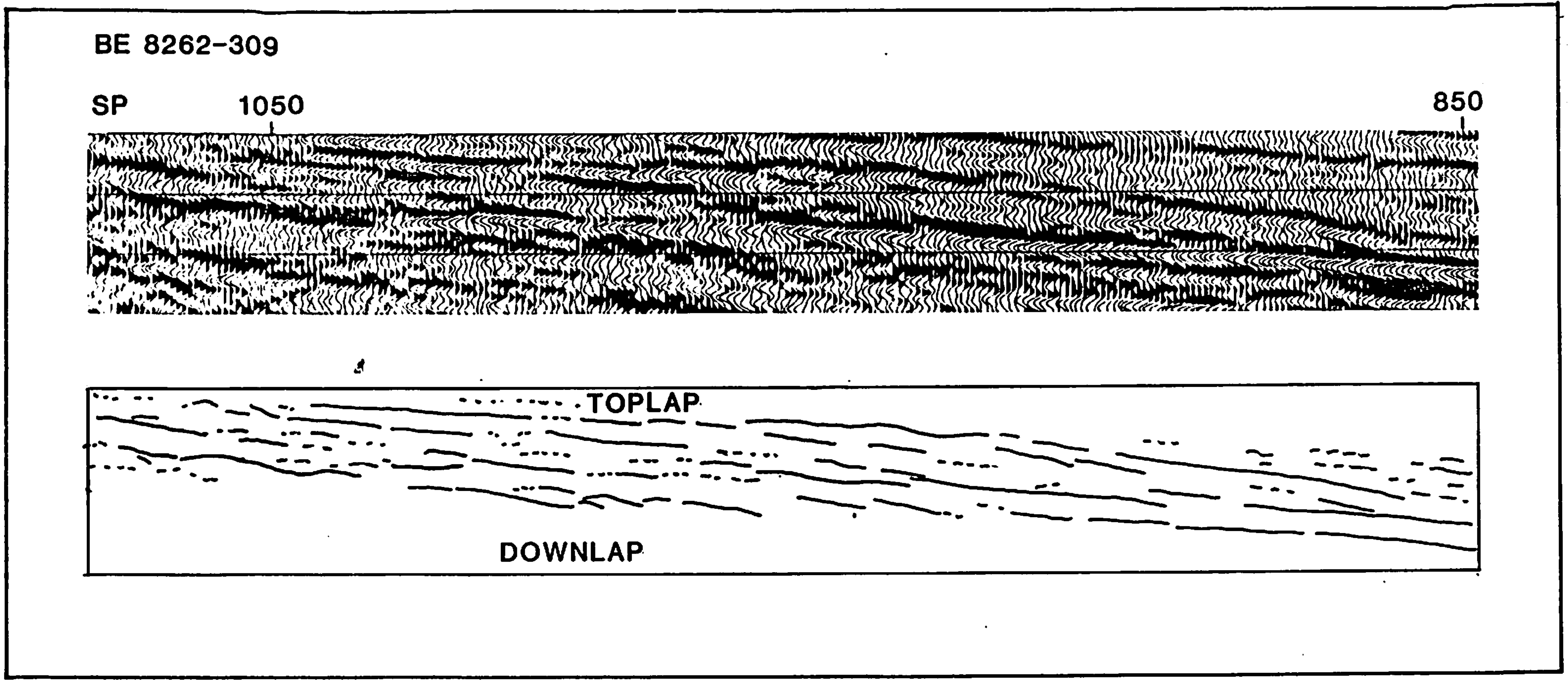

Fig. 6.7: Line BE8262-309 shows the progradational portion of Lower "Turonian Sandstone", H6.1, sequence. In this example the oblique character of the progradational system is displayed.

Reflection Character (fig. 6.7):
The <u>reflection configuration</u> varies from subparallel - divergent to progradational. The primary progradational feature is oblique tangential with a minor amount of sigmoidal patterns. The oblique pattern is nearest to the shore with sigmodal patterns next, followed by parallel and divergent.

Depositional Environment (fig. 6.8):
The depositional environment ranges from marginal marine to neritic. Most of the sediments were deposited by a fan deltaic system with three potential deltaic lobes. The marine waters will probably have had restricted circulation yielding potentially good source rock. This sequence was probably deposited by a relatively high energy source. The distal portions of the sequence may contain thin shale beds.

Top "Turonian Sandstone", H6.0

Over the western half of the area the sequence is very thin with the sequence being truncated to the south.

Age:
The sequence ranges in age from 92 ma to 87 ma (Turonian).

Boundaries (fig. 6.9):
The <u>upper boundary</u> varies between concordant to toplap with some erosional truncation. In the eastern half of the area, concordance is the predominant boundary configuration. Toplap is observed over the center of the area along with erosional toplap. Both concordance and erosional toplap is found in the western portion of the area. The <u>lower boundary</u> ranges between concordant, onlap and downlap. Downlap is observed over the

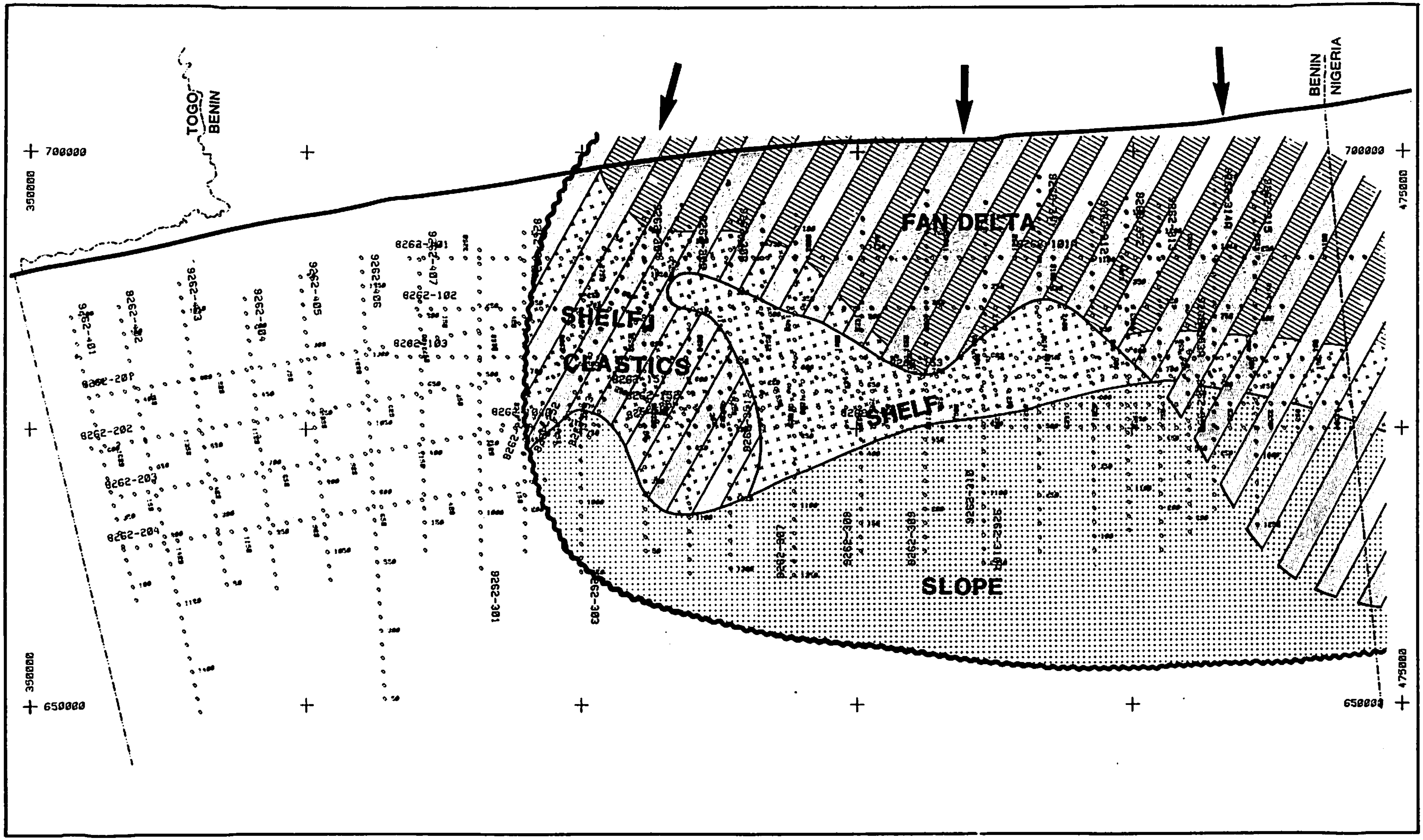

Fig. 6.8: Lower "Turonian Sandstone", H6.1, environmental interpretation.

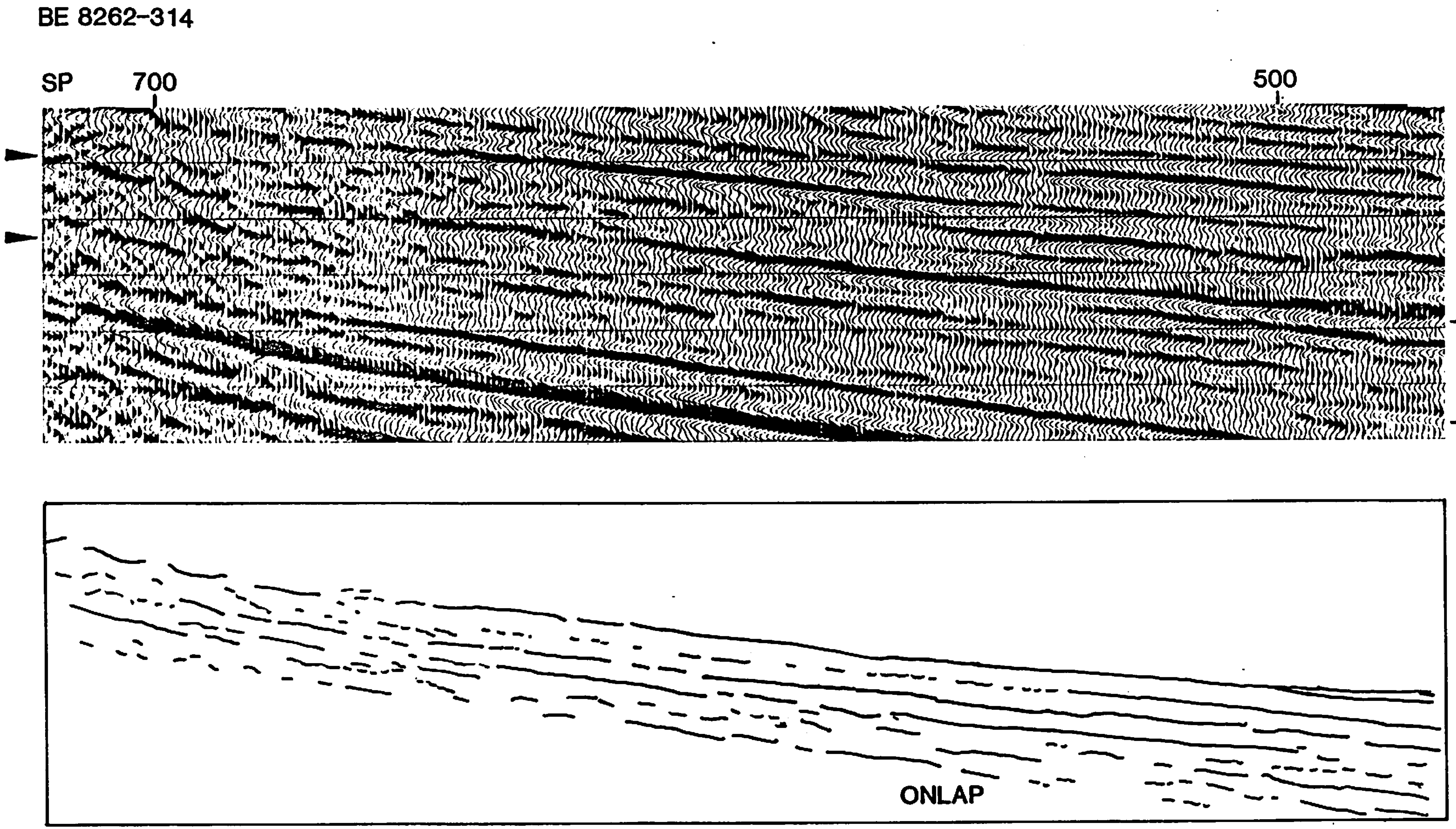

Fig. 6.9: Line BE8262-314 illustrates the concordance of the upper boundary and onlap at the base of the Upper "Turonian Sandstone", H6, sequence. The lack of continuity on the left side of the example is due to disturbances in the overlying section.

central portion of the area, with concordance and onlap located on either side of the downlap.

Reflection Character (fig. 6.9):
Over the central portion of the area of study, oblique and sigmoidal progradational patterns are observed with divergent subparallel reflections on either side. The continuity of the reflections varies from medium to low. The amplitude varies from high to low with the frequency generally being low.

Depositional Environment (fig. 6.10):
The sediments were deposited in a marginal marine to neritic environment by a fan delta shelf system (fig. 6.10). Over the rest of the shelf the sediments were probably distributed by wave action. The shape of the delta tends to indicate a wave dominated system.

Senonian Unconformity, H5

In the vicinity of the Sèmè Oil Field the sequence is strongly eroded by channels. Along the shelf edge the sequence is truncated by the Mid Miocene Unconformity.

Age:
Well data suggests that the sequence ranges in age from 87 ma to roughly 80 ma (Early Senonian - Coniacian).

Boundaries (fig. 6.11):
The upper boundary ranges from concordant to toplap with a fair amount of erosional toplap. The erosional toplap is observed all along the southern flank of the area. The toplap is

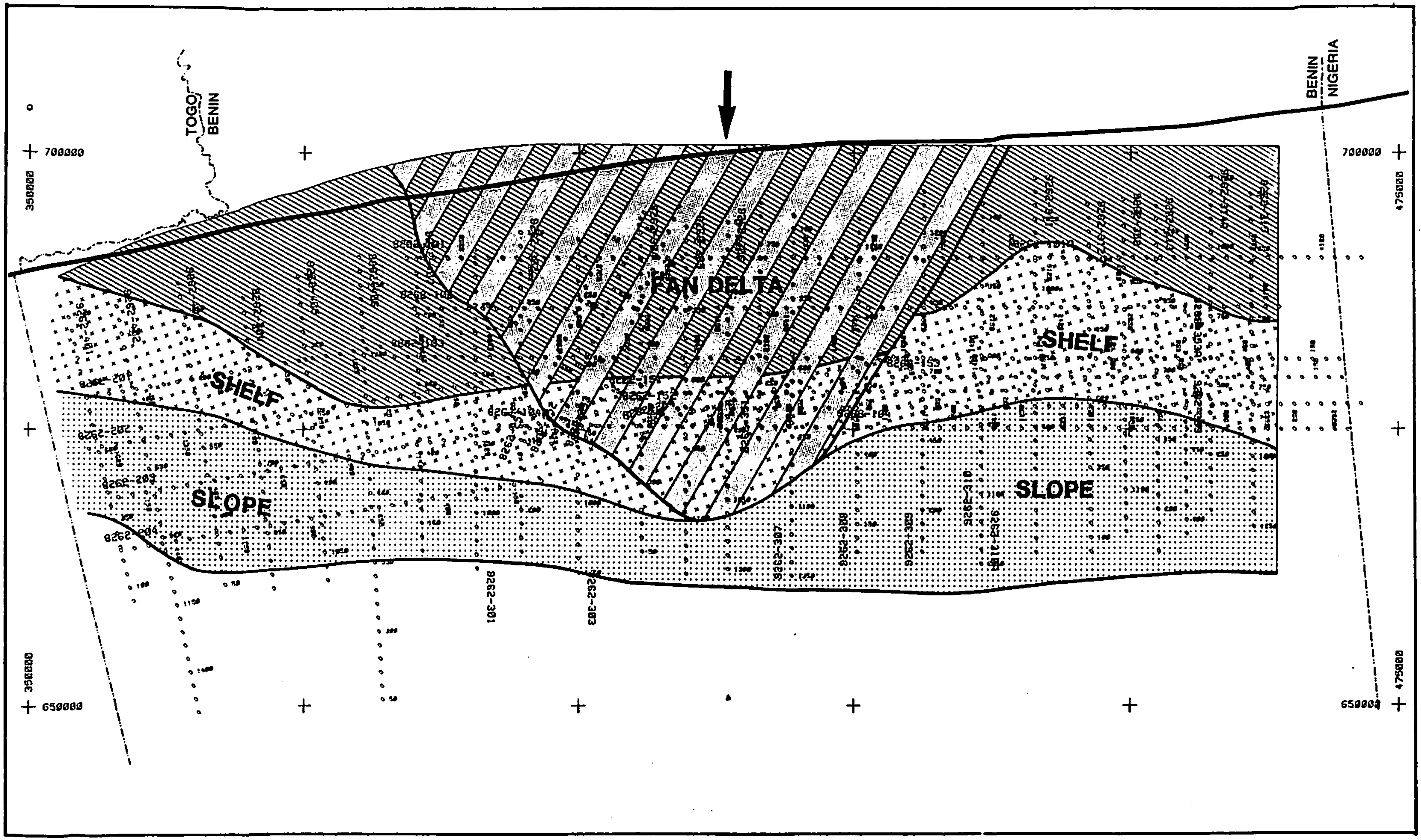

Fig. 6.10: Upper "Turonian Sandstone", H6, environmental interpretation.

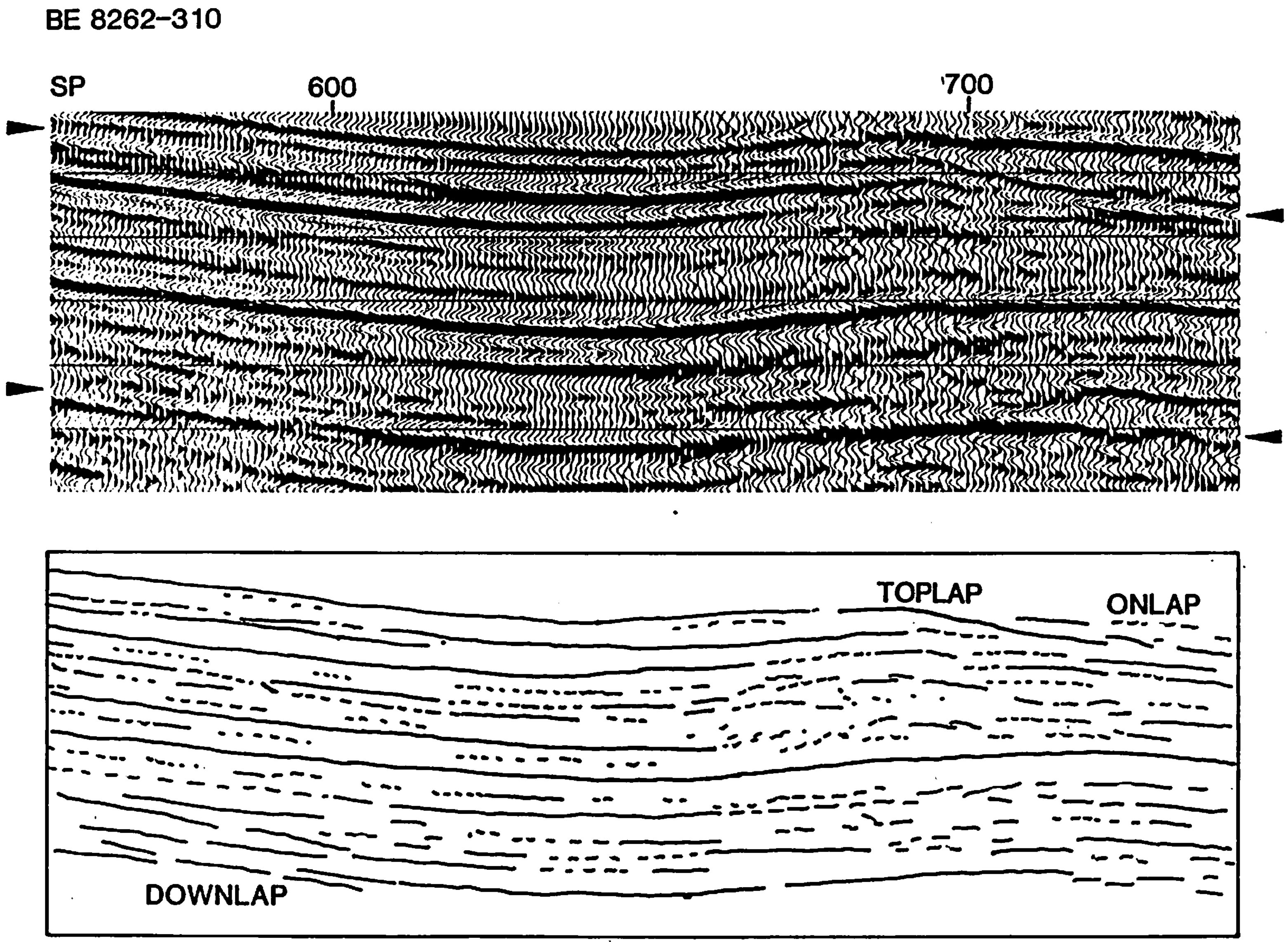

Fig. 6.11: Line BE8262-310 illustrates the Senonian Unconformity, H5, sequence (Awgu Formation). Note the minor onlap at the base and the erosion of the sequence upper right.

observed in the north central portion of the area. Concordance is over the remainder. The lower boundary reflection terminations range from concordant to onlap and downlap. The concordance is primarily located to the west of line 302. Downlap is located in the central northern portion of the study area and on the southern end of line 315. Onlap is located over the rest of the area.

Reflection Character (fig. 6.11):

The predominant reflection configuration is subparallel, with some progradational (sigmoid and oblique) character. A minor amount of hummocky reflections are also noted, generally on the distal portion of the seismic lines. The progradation features are located in the central northern portion of the area and on line 315. The subparallel reflections are observed over the rest of the block. The continuity of the reflections is generally medium with some being low or discontinuous. The amplitude ranges from medium to high and the frequency from low to medium.

Depositional Environment (fig. 6.12):

The depositional environment ranges from non marine to marine. There appears to be two minor deltas located in the northern central portion of the area.

Upper Araromi Shale, H4.0

This sequence is truncated in a seaward direction by the Mid Miocene Unconformity. The sequence is thin to the west (ref. chapter 5.3.3) overall a less or equal to 100 m on the entire shelf except for three depocenters in the vicinity of the Sèmè Field.

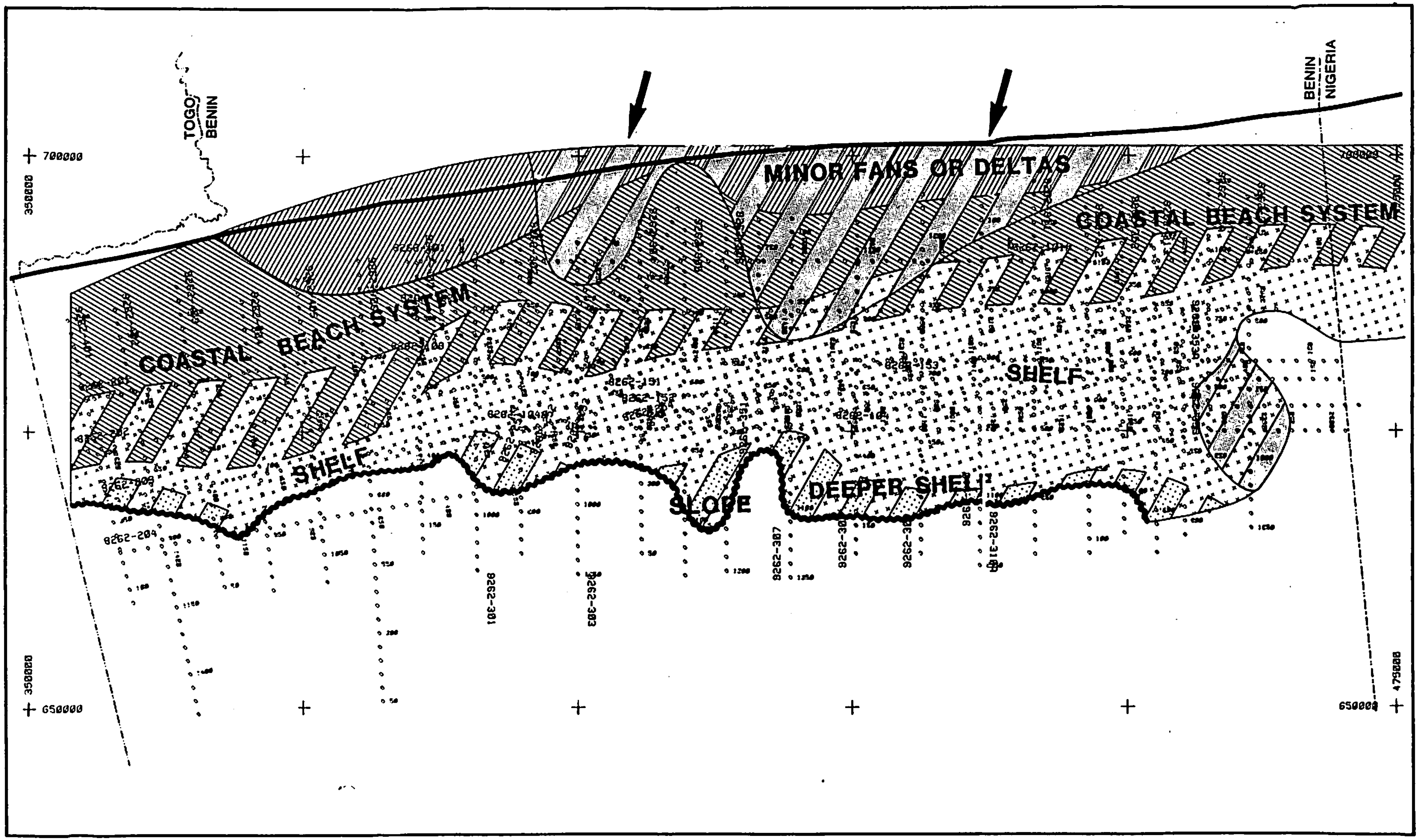

Fig. 6.12: Senonian Unconformity, H5, environmental interpretation.

Age:
This sequence ranges in age from 70 ma to 60 ma (Maastrichtian).

Boundaries (fig. 6.13):
The upper boundary reflection termination ranges from concordance to toplap with some erosional toplap. Concordance is observed over the western half of the studied area while toplap and erosional truncation (toplap) is predominant termination over the eastern half. The lower boundary has onlap and downlap. The onlap is the predominant reflection termination over the western half of the area. Most of the eastern half of the area is characterized by downlap. There is an area of concordance on the northern part of lines 309, 310 and 311.

Reflection Character (fig. 6.13):
The interval reflection configuration ranges from subparallel to progradational. The progradational features observed are sigmoidal and oblique. Some hummocky and mounded reflections are observed in the vicinity of the Sèmè Oil Field also to the south of the progradational feature. The progradational feature to the east is primarily a fill. The progradational feature in the center of the studied area is probably associated with an old source. Over the western half of the area there are generally subparallel to divergent with some hummocky features near the truncation zone.

The area has a wide range of continuity, ranging from discontinuous to having a high continuity. The amplitude ranges between high and medium with the frequency being generally low with some medium frequencies.

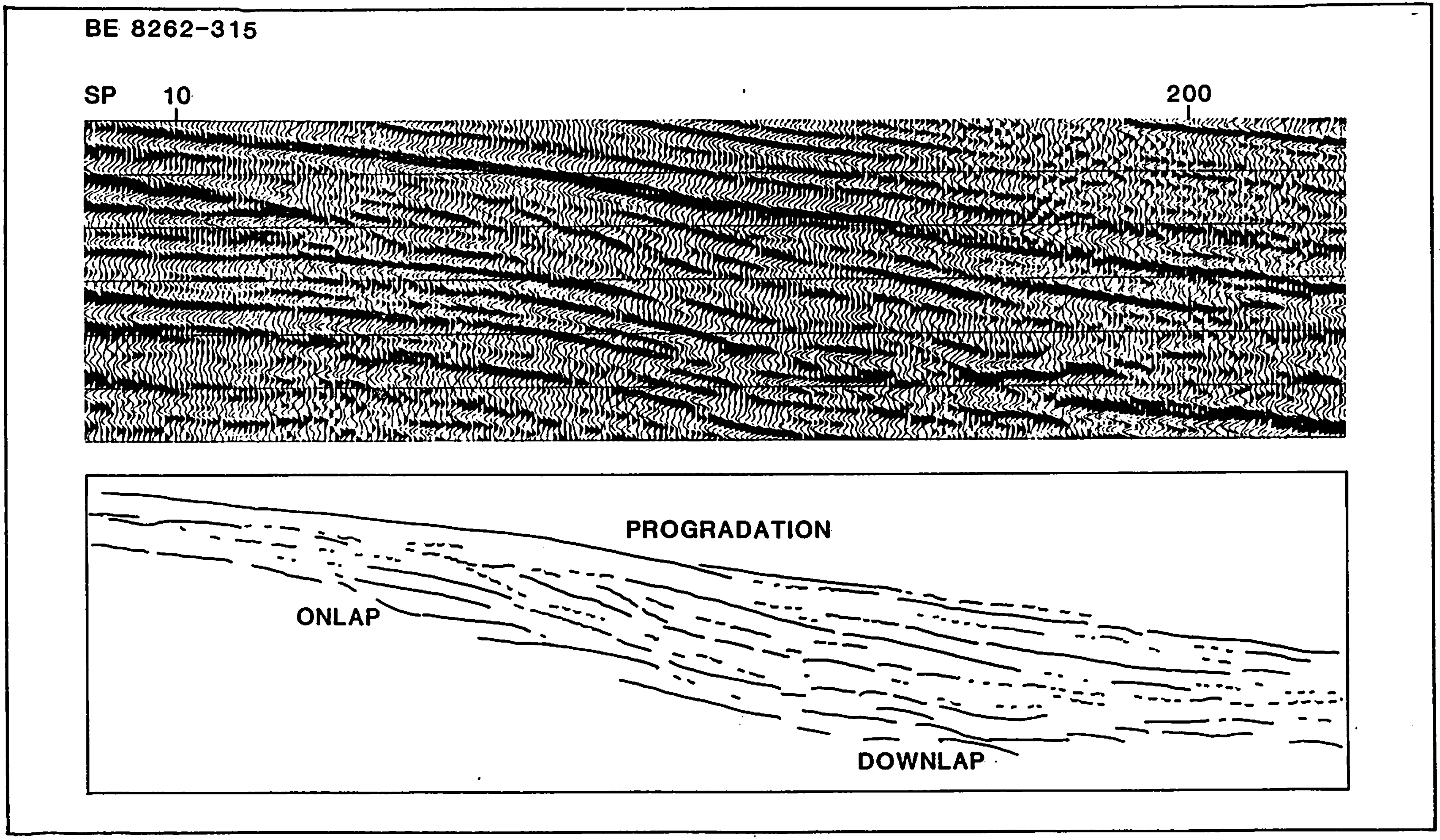

Fig. 6.13: An example of the Upper Araromi Shale, H4, progradational fill. Note the minor amount of toplap and the low angle of downlap.

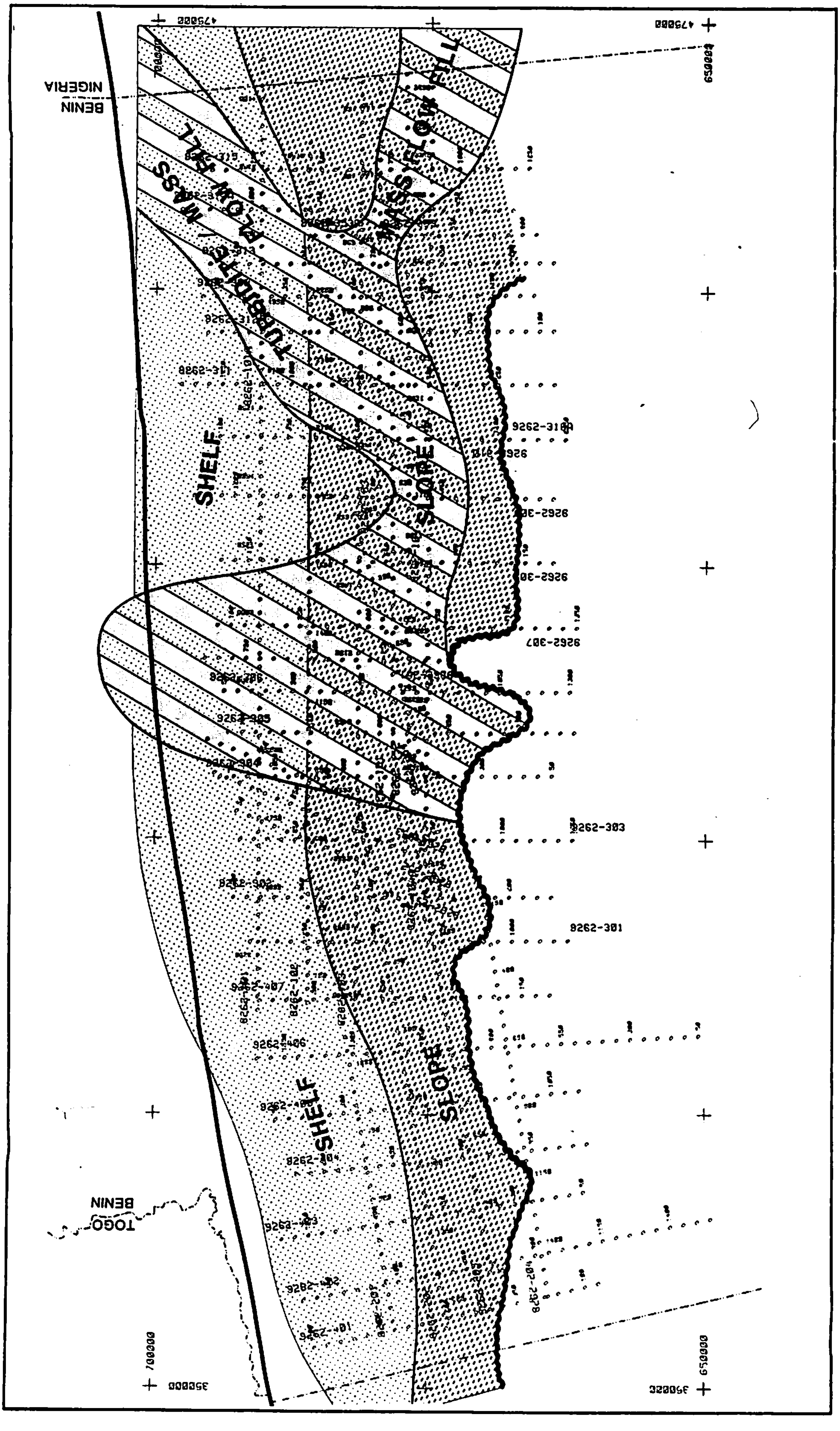

Fig. 6.14: Upper Araromi Shale, H4.0 environmental interpretation

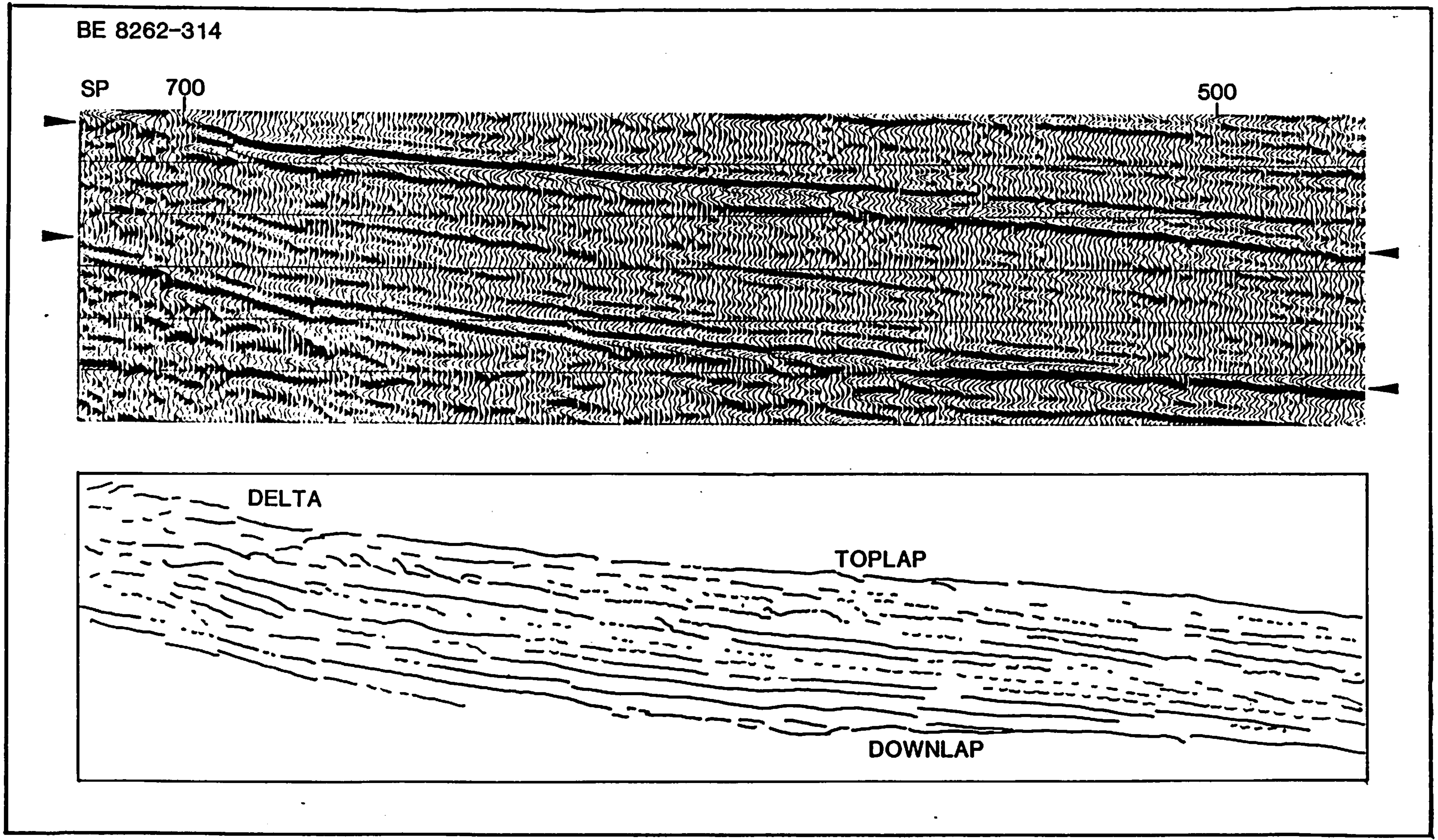

Fig. 6.15: An example of the low angle progradation of the Lower Imo Shale, H3.1, sequence on line BE8262-314. Note the possible toplap near the upper boundary.

to line 310. From 311-313 a sigmoidal pattern is observed. Subparallel to divergent reflections are observed seawards of the progradational unit and further seawards the hummocky reflections are observed. The continuity over the area is generally medium with some areas with high continuity. The amplitudes are generally medium with some areas with low amplitude, and the frequency is variable but generally medium.

Depositional Environment (fig. 6.16):
In the vicinity of the Sèmè Oil Field the environment for the sequence is predominantly bathyal. Over the majority of the area the environment is probably neritic. The progradation is that of a seaward building shelf generally low energy with a moderate sediment influx from a mixture of many smaller deltas. Mass flows are associated with the bathyal environment.

Upper Imo Shale, H3.1

In the vicinity of seismic line 8262-407 the sequence has been eroded away along with the seaward edge.

Age:
The sequence ranges in age from 56 ma to 50 ma (Late Paleocene to Early Eocene).

Boundaries (fig. 6.17):

The upper boundary ranges from concordant to toplap with erosional truncations. Most of the truncations are near the seaward truncation line.

The lower boundary ranges between concordance and downlap. The

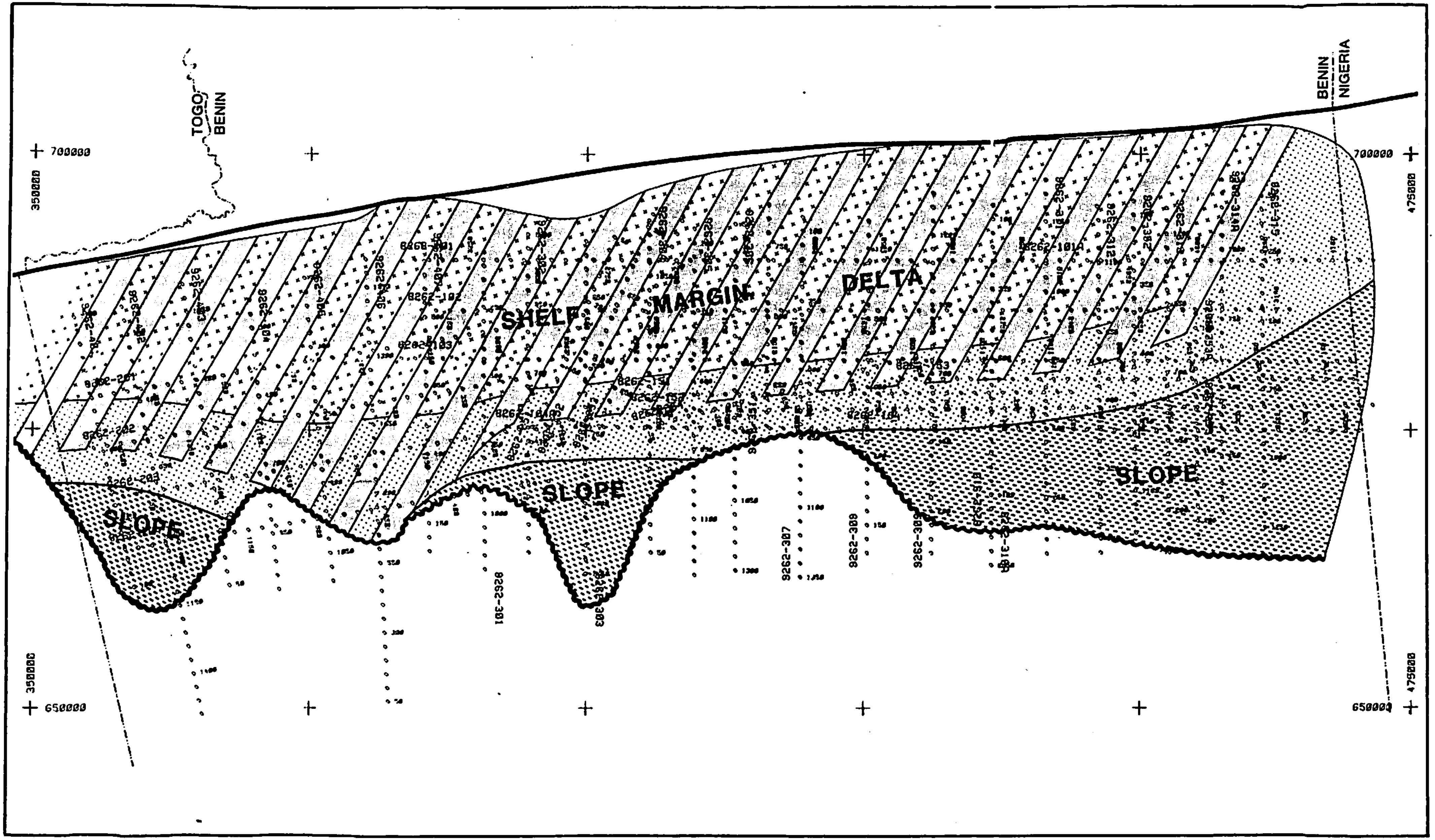

Fig. 6.16: Lower Imo Shale, H3.2, environmental interpretation.

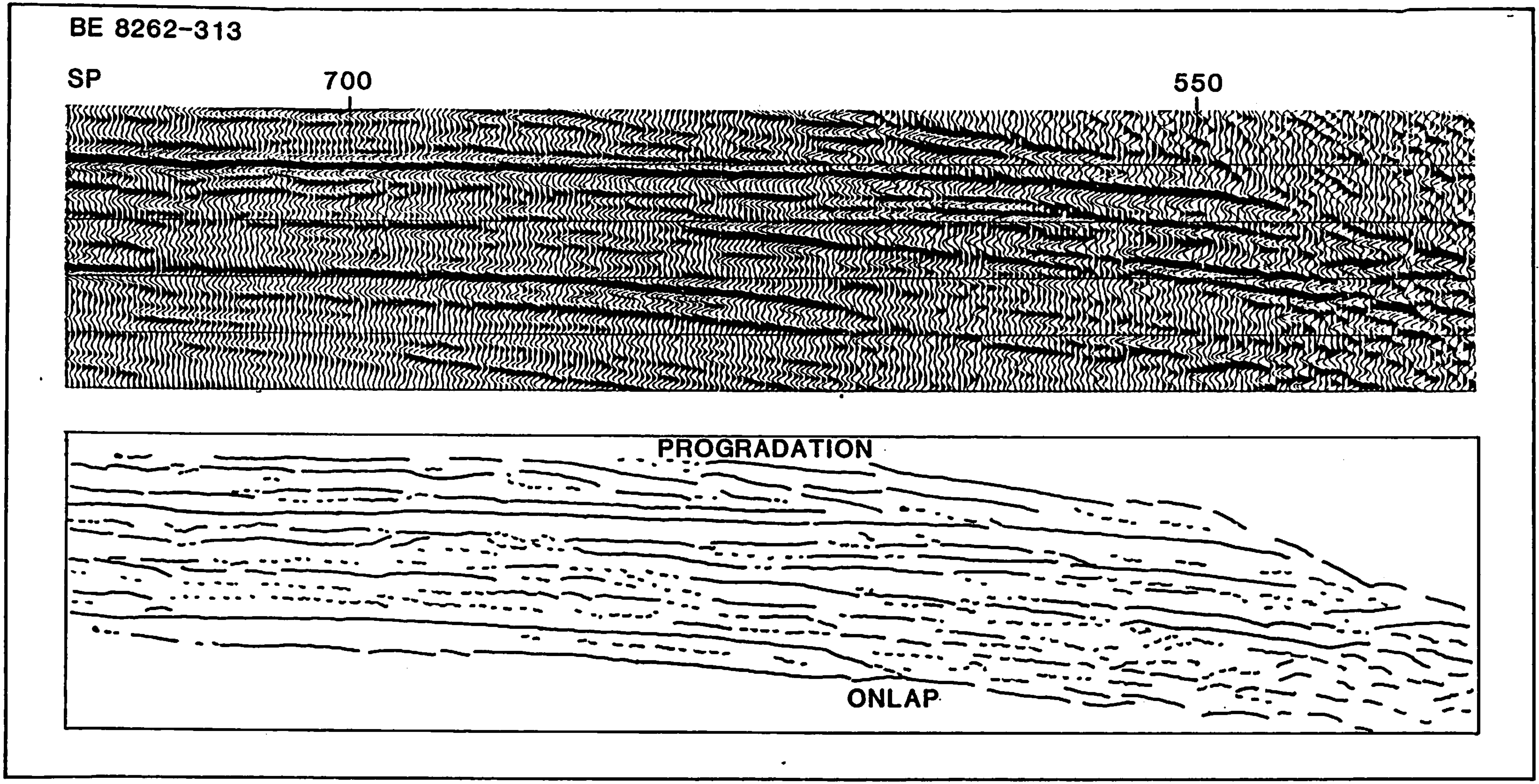

Fig. 6.17: Upper Imo Shale, H3.1, sequence on line BE8262-313. In this example it should be noted that the sequence can be divided into several sequences. Note the progradation in the upper portion of the sequence and onlap and toplap in the lower portion of the sequence.

downlap pattern has an areal shape of a wedge. No downlap has been observed to the west of the erosional channel.

Reflection Character (fig. 6.17):
The internal reflections range from subparallel to progradational. The most prominant progradational pattern is sigmoidal. In some areas a hummocky pattern is observable. This pattern is usually associated with the progradational features. No progradational patterns are observed to the west of the erosional channel. In general the continuity is medium to low with an occasional zone of high continuity. Both the amplitude and frequency are generally medium to low in character.

Depositional Environment (fig. 6.18):
Based on the Sèmè wells the sediments were deposited in bathyal to outer neritic conditions. The sediments were deposited on the shelf by several deltas. A long shore current from the west appears to have been present during the deposition of the sequence because the progradational systems trend to build to the SE.

Oshoshun Formation, H3

In the western part of the area this sequence has been eroded away in the form of a channel. The sequence is very thin to the west of the channel.

Age:
According to well information this sequence ranges in age from around 50 ma to 19 ma (Middle Eocene) with a hiatus between 40 ma and 22.5 ma.

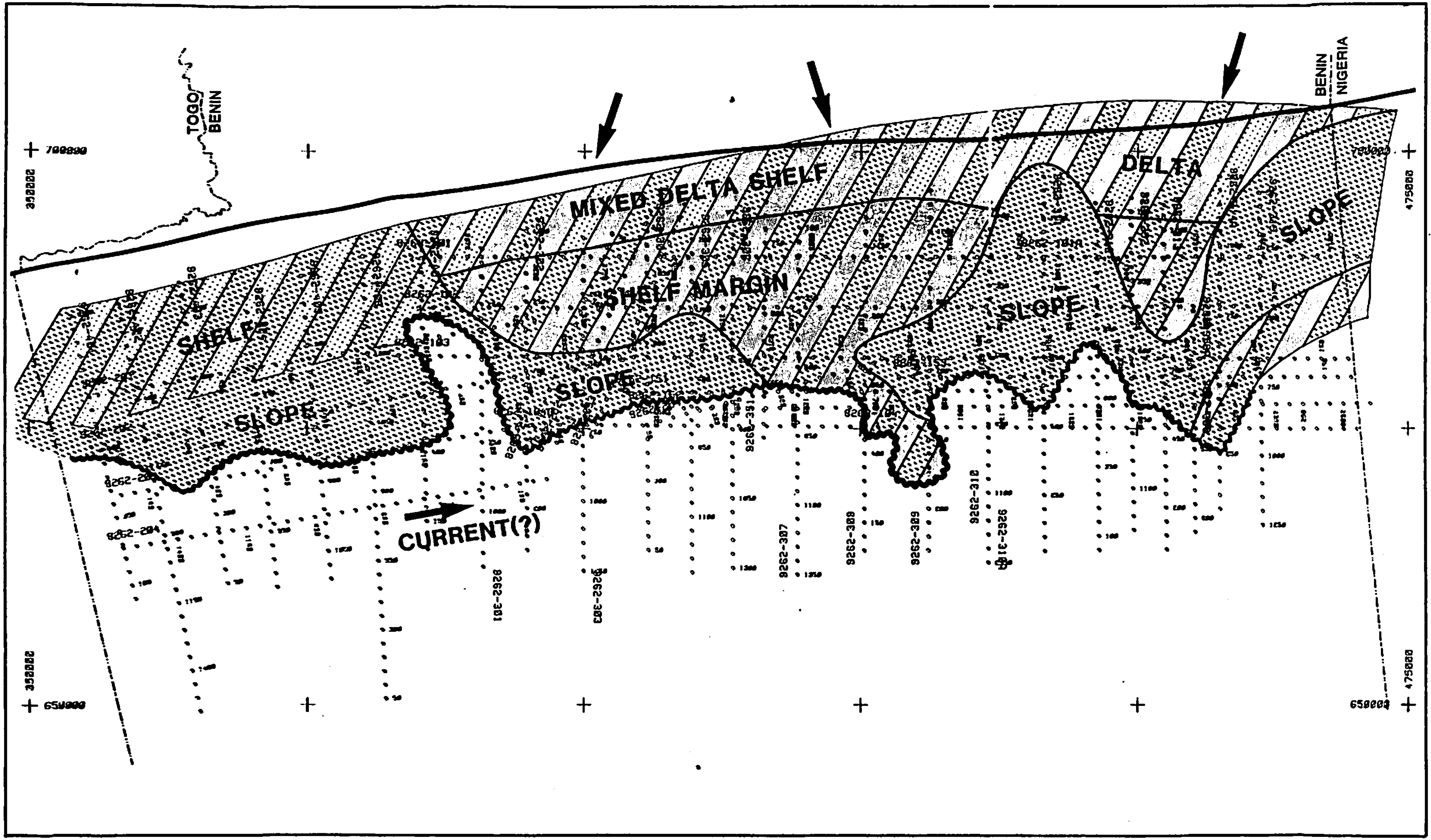

Fig. 6.18: Upper Imo Shale, H3.1, environmental interpretation.

Boundaries (fig. 6.19):
The upper boundary terminations vary from concordance to erosional toplap with some toplap.

The erosional truncation is predominantly located in the southern fringes and near the Sèmè Oil Field. Over the western portion of the area in the vicinity of the 400 series seismic line the upper boundary is concordant.

Over most of the Beninian shelf the lower boundary has downlap reflection terminations. The area in the vicinity of the 400 series seismic lines is concordant with some onlap.

Reflection Character (fig. 6.19):
Over half of the shelf the sequence has sigmoidal reflection character with the character changing to oblique tangential in the western part. To the west of the eroded zone the reflections are subparallel to parallel. The reflections generally have medium continuity with medium to low amplitudes and quite variable frequency. In some areas the reflections have low continuity to discontinuity, but this is due to the overlying section.

Depositional Environment (fig. 6.20):
The depositional environment ranges from outer neritic to bathyal with sediments having been deposited by a shelf margin delta or a mixture of several deltas. A long shore current from the west may have been present since the shelf margin delta does not appear to be present to the west of the erosional channel.

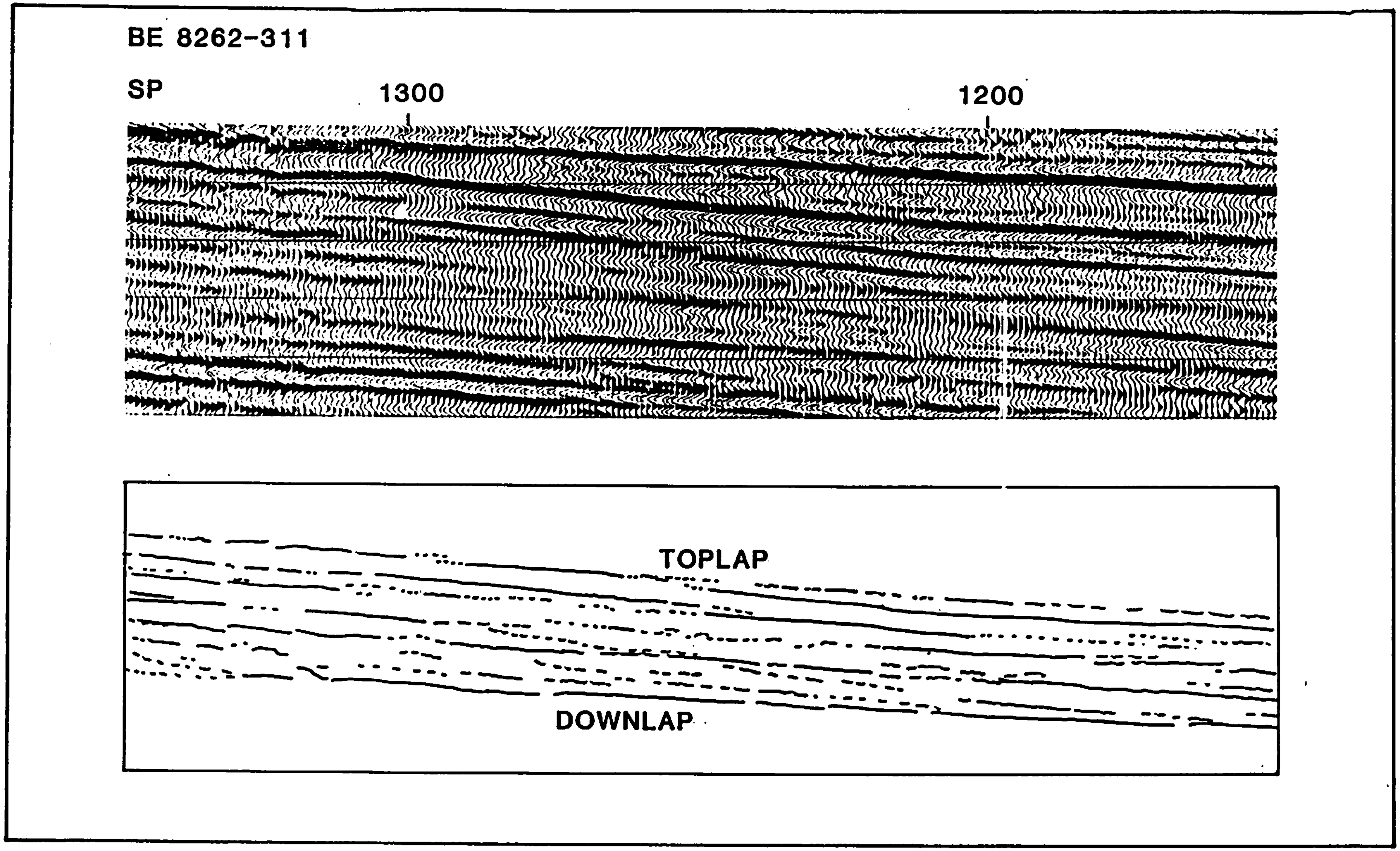

Fig. 6.19: Progradation of the Oshoshun Formation on line BE8262-311. Note the low angle downlap and minor amounts of toplap.

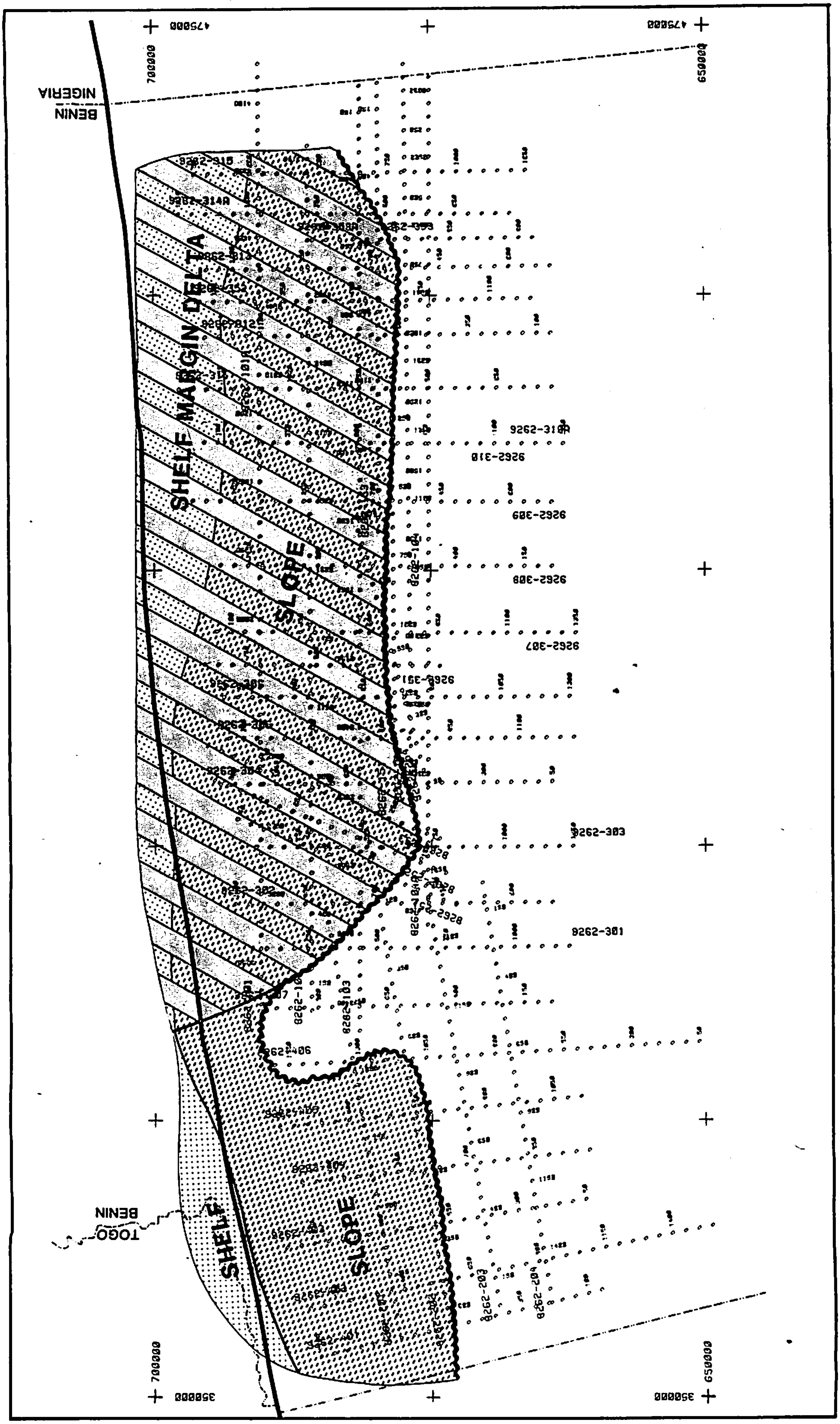

Fig. 6.20: Oshoshun Formation, H3, environmental interpretation.

Lower Afowo Formation, H2

In the western area an erosional channel has eroded the section.

Age:
This sequence ranges in age from approximately 22.5 ma to 16.5 ma (Early Miocene).

Boundaries (fig. 6.21):
The lower boundary termination ranges from onlap to downlap with some concordance. The onlap is primarily in the eastern part of the shelf with downlap and concordance over the rest of the shelf. The downlap gives the impression of two progradational lobes with concordance between and to the west. The upper boundary is generally concordant with some erosional toplap associated with a paleo shelf edge.

Reflection Character (fig. 6.21):
The sequence intended configuration ranges from subparallel to sigmoidal oblique tangential. Beyond the paleo shelf edge the section has a hummocky pattern with a slight progradational character.

The progradation patterns are separated into two main areas near shore, these are associated with two sources for the sedimentation. Over the area the continuity is relatively good.

Erosional truncation is observed over the southern portion of the seismic lines.

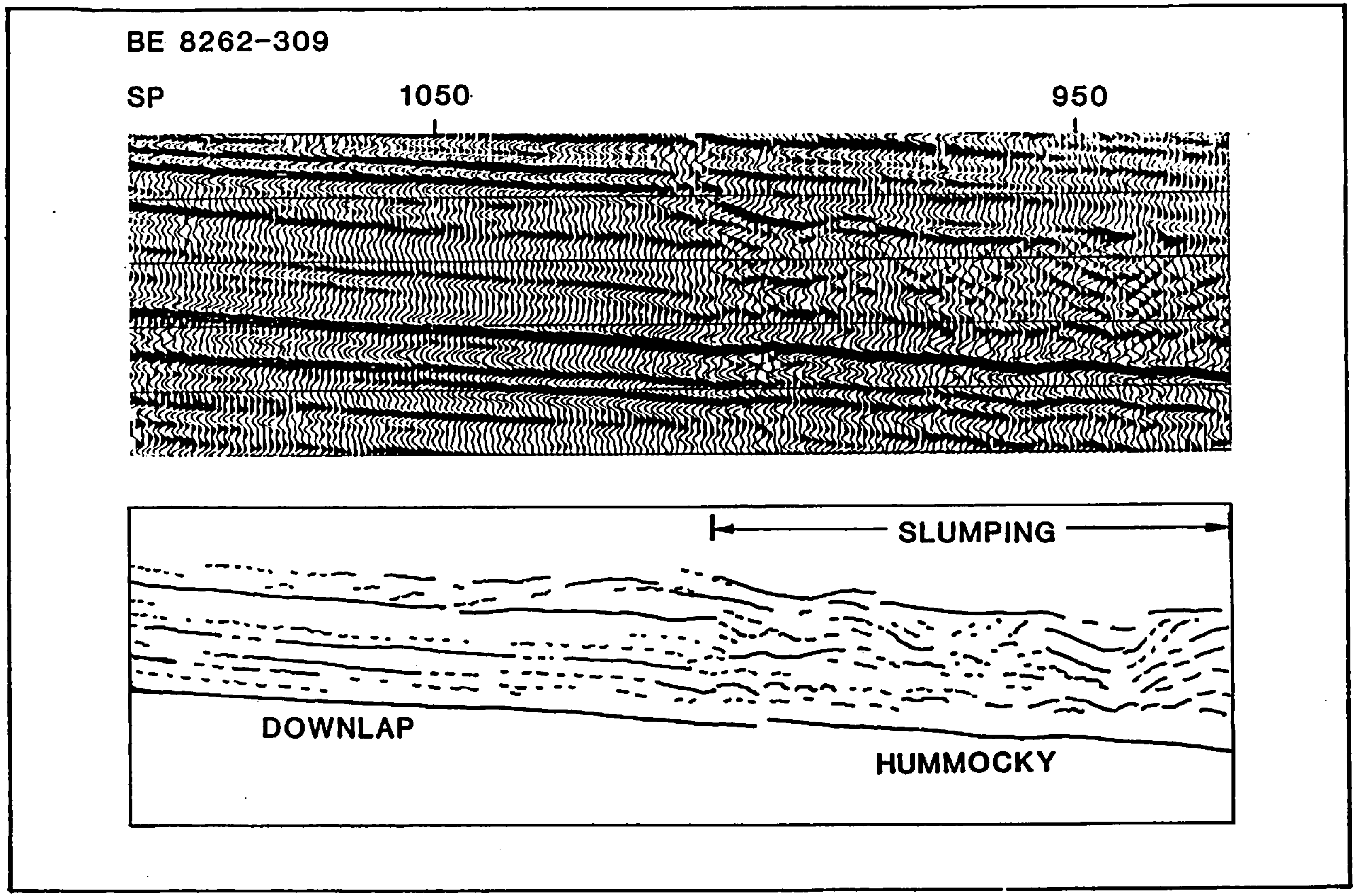

Fig. 6.21: Lower Afowo Formation, H2. This example here shows the progradation of the sequence with a mounded hummocky pattern indicating slumping. Note the relatively low angle of the progradation.

Depositional Environment (fig. 6.22):
The depositional environment for this sequence ranges from neritic to bathyal. The bathyal zone is associated with hummocky and slightly prograding reflections. The sediments for the sequence were deposited by delta and shelf progradation.

Water Bottom Sequence, H0

The water bottom sequence contains many individual sequences younger than 17 ma. The composite sequence has distinct areas of deposition associated with the Middle Miocene paleo shelf edge.

Age:
The sequence ranges in age from Recent to Middle Miocene (<16.5 ma).

Boundaries (fig. 6.23):
The boundary at the base of the sequence has both onlap and downlap. The downlap is associated with the sudden change in water depth in the vicinity of the paleo shelf edge.

Shoreward of the paleo shelf edge the basal boundary is onlapped. Onlap is also observed seaward of the zone of progradation.

Reflection Character (fig. 6.23):
The internal reflection configuration varies seaward from parallel subparallel to a complex progradation of pattern changing to divergent. In places the divergent section is overlain by the progradation. The sediments deposited under

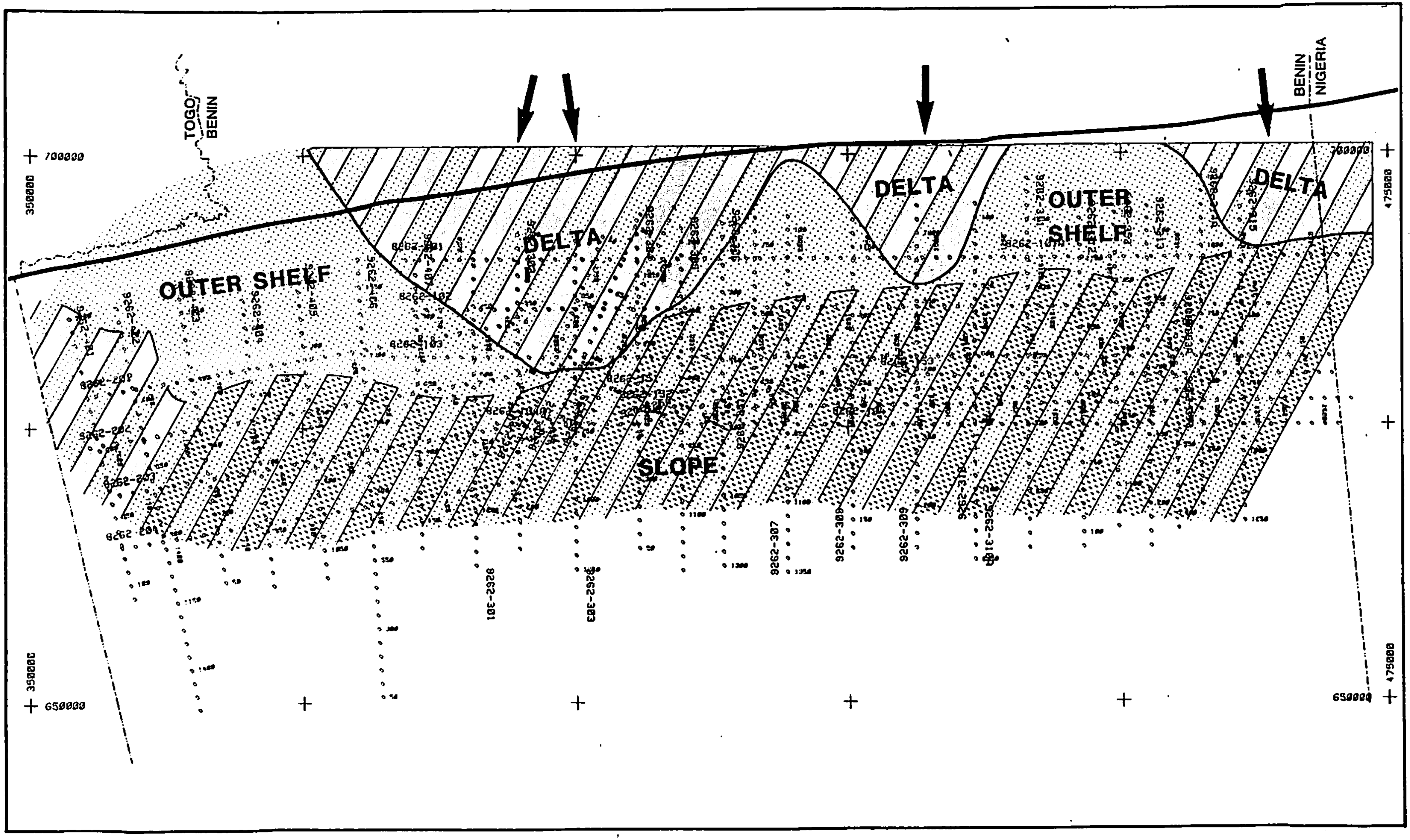

Fig. 6.22: Lower Afowo Formation, H2, environmental interpretation.

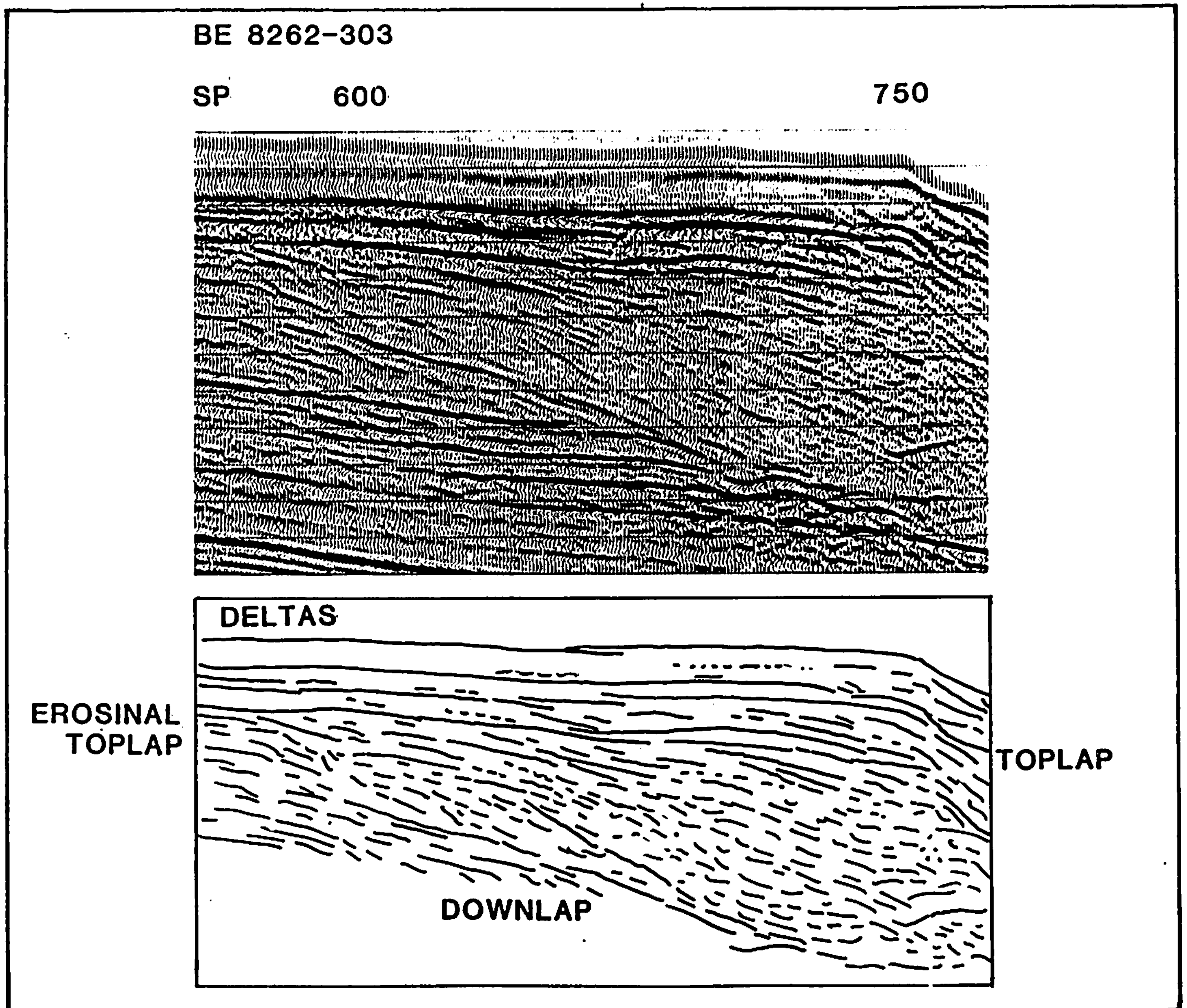

Fig. 6.23: Line 303, SP 550-740 illustrates the progradational nature of the younger sequence. In general the progradation is complex, with oblique tangential and sigmoidal characteristics. Truncation of the older sequences is also evident. A slight hummocky character is also observed within the sequence around 1 sec (SP 650-750). Above the high amplitude event at 1.2 sec (SP 640) low angle sigmoidal progradation is present.

and seaward of the progradation are interpreted as being associated with various types of mass flows. The continuity ranges from discontinuous to high continuity with the amplitude and frequency ranging from low to high. The discontinuous reflection are associated with hummocky to chaotic reflections possibly indicating rapid changes laterally in the lithology and higher energy deposition, whether due to rapid deposition or marine forces.

Depositional Environment (fig. 6.24):
The depositional environment ranges from neritic to bathyal with sediments having been deposited by a series of shelf margin deltas. A majority of the progradation is associated with a paleo shelf endge where the paleo topography steepens dramatically. At the seaward edge of each of the deltas mass flows are observed on the seismic sections.

Comments (fig. 6.25):
The channel in the figure is associated with a river which has been in its present position for roughly 50 ma.

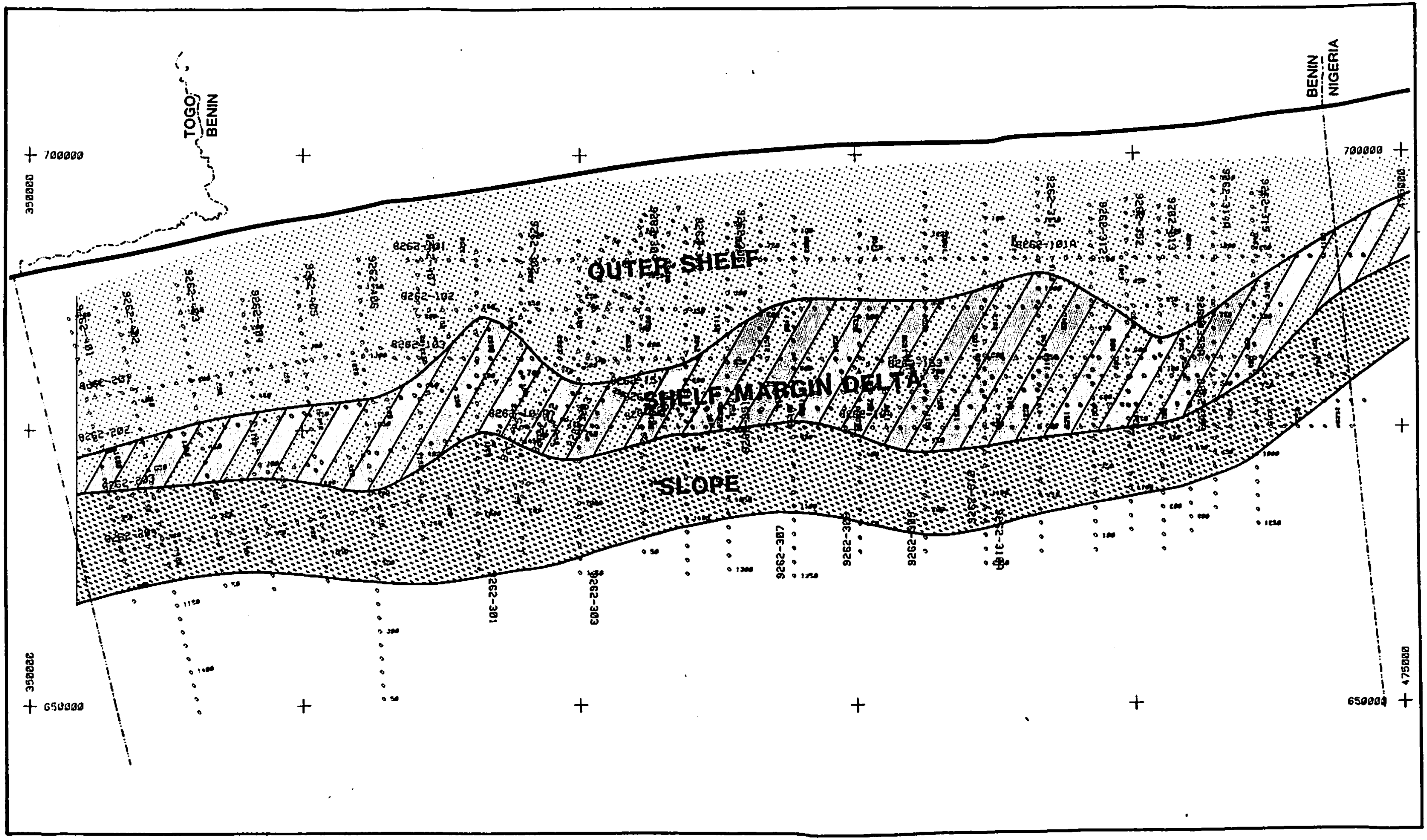

Fig. 6.24: Water Bottom Sequence, H0, environmental interpretation.

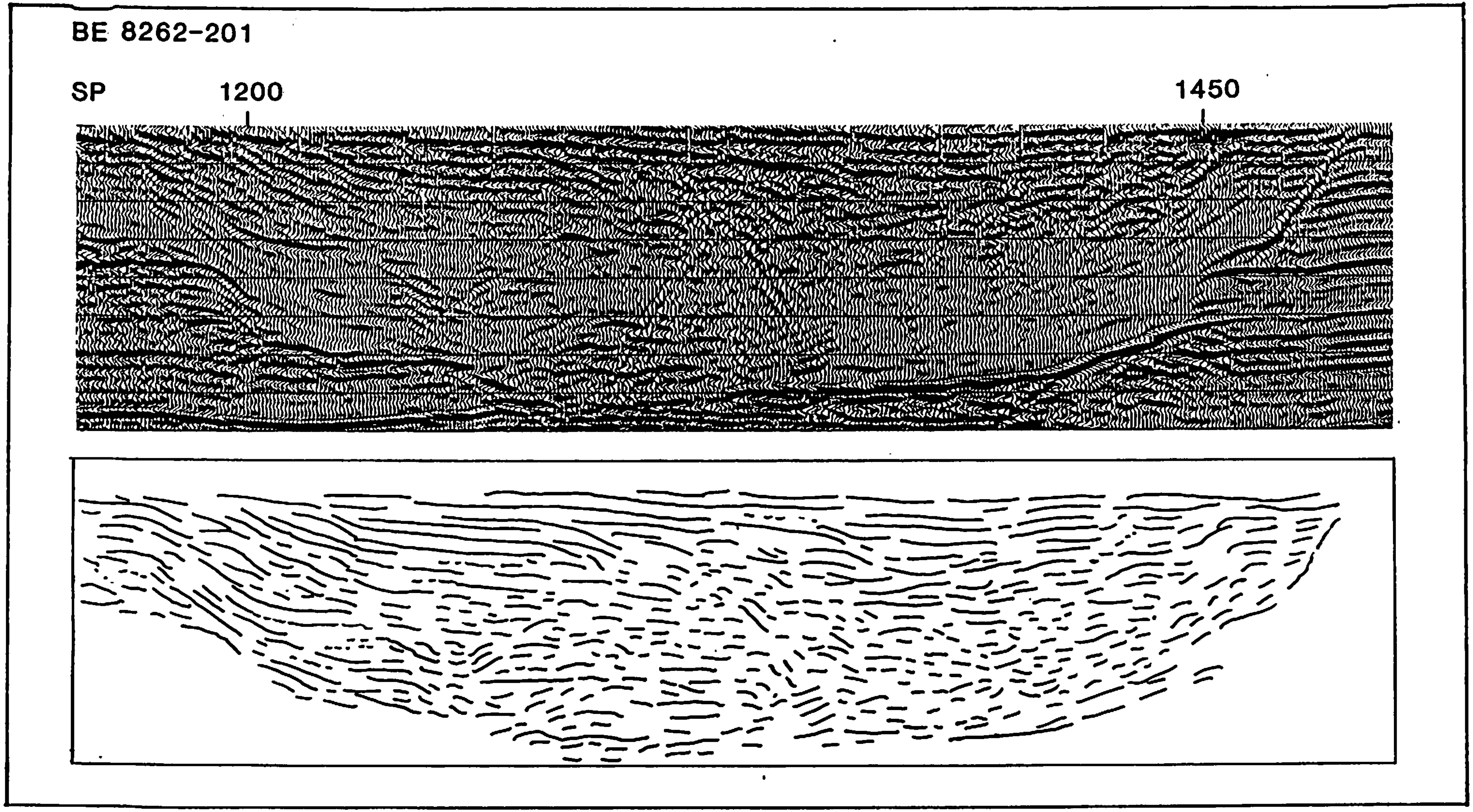

Fig. 6.25: Large channel in the western part of the Benin basin (line BE8262-201). Several different types of reflection characteristics are seen here. The channel fill is complex, having some progradation, some onlapping and hummocky characteristics etc. The progradation is primarily from the east and onlapping the western edge of the channel. The velocities of the sediments within the channel are quite high yielding the velocity pullup effect of the underlying beds. It should also be noted that the underlying parallel reflections are typical of a linear coast.

6.3 Geologic Development of the Benin Offshore Basin

During the formation of half grabens (Late Jurassic - Early Cretaceous) lacustrine sands/shales were deposited. These sediments were deposited as divergent fills as the half grabens were being formed.

Within the half grabens turbidites and/or types of mass flows probably occurred. The restrictive nature of the half grabens probably produced a fairly anoxic environment. By Early Aptian the half grabens had been filled and a larger lacustrine basin was being filled by fan deltas and braided streams. Around 112 ma massive erosion took place truncating many of the dipping half graben fill units. During the deposition of this unit the sequence was restricted to the eastern half of the Beninian shelf. During this period of time most of what is now the Beninian shelf was very stable having very little sudsidence, but the eastern half towards Nigeria was experiencing continued sudsidence.

As the basin continued to subside, the lacustrine environment prevailed for most of the Aptian. By latest Aptian the basin was beginning to be influenced by shallow marine conditions with the development of minor shelfal reefs and carbonate banks.

Around 97 ma a eustatic lowering in sealevel occurred causing the carbonate buildup to be subaerially exposed. Between 97 ma and 92 ma continued subsidence and/or eustatic rise in sealevel caused the carbonate sequence to be onlapped by siliaclastics probably deposited by a fan delta complex. There were probably several fan deltas filling the basin. The basins circulation may have been somewhat restricted yielding an anoxic environment.

An apparent fall in sealevel may have occurred around 92 ma.

At this time the depositional center initially became regressive.

Between 92 ma and 87 ma a single dominant source developed instead of the multiple source observed between 97 ma and 92 ma. The sediments of this sequence were deposited by a large fan delta. The apparent shape of the fan delta (fig. 6.10) tends to indicate a wave dominated environment in which we would expect offshore and barrier bars developing with possibly thin shales being deposited seward of the shore face.

At approximately 87 ma transgression occurred shifting the depositional center shoreward. During this time the subsidence of the shelf was relatively constant and low, making the shelf fairly stable.

Between 87 ma and 77 ma two minor deltaic lobes developed towards the center of the shelf with coastal strand system also developing. In the deeper water areas, possible turbidites were also forming.

Between 77 ma and 70 ma a depositional hiatus occurred over the shelf. During this time the shelf may have been under quite deep water. Sealevel probably began falling around 70 ma. It was probably this eustatic change in sealevel which caused the submarine erosion of the previous sequence.

Between 70 ma and 60 ma the sediments were being deposited in an outer shelf environment by shelfal processes. The deeper areas were filled by turbidites or other mass flows. These are observed as progradational fills. The most striking example of this is in the vicinity of the Sèmè Oil Field.

A regressive sequence developed between 60 ma and 56 ma. This sequence may have been initiated by the recognized global fall in sealevel. The shelf edge migrated seaward probably by a large number of minor deltas giving the apperance of a prograding shelf.

At about 56 ma, a transgressive sequence began developing with the depositional center initially shifting shoreward. Sedimentation was both by deltaic and shelfal processes in outer neritic to bathyal conditions.

Between 56 ma and 50 ma the mixed deltaic/shelfal system continued building seaward. Around 50 ma the shelf was transgressed, and the number of appearent sources increase yielding a shelfal progradation and seaward migration of the shelf edge. This shelfal progradation may have been caused by many small deltas and shelfal processes.

From 50 ma to 40 ma the shelf edge slowly built seaward.

From around 40 ma to 22.5 ma a major hiatus occurred on the Beninian shelf, and from 22.5 ma to 19 ma the shelf continued building.

Around 19 ma, a regressive phase in the shelf development was beginning to occur. Several shelf deltas were developing building out over the shelf. The water was still relatively deep.

Around 17 ma, a major fall in sealevel occurred subjecting the shelf to massive submarine erosion. From around 17 ma to the present the shelf has been building seaward by a large number of smaller deltas. A large number of mass flows are associated with this progradational regime.

CHAPTER 7 14.12.83

GEOLOGICAL EVALUATION

7.1 Hydrocarbon Source Rocks

7.1.1 General

Contained in this section is an organic geochemical interpretation of the sediment section offshore Benin. Items to be discussed include characterisation of oil samples from the Sèmè Field with respect to source rock origin, maturity and suspected degradation, source rock identification and maturity evaluation.

The organic geochemical data base is at present both areally and stratigraphically restricted. Oil analyses have been carried out on samples from the Sèmè 2, 3 and 4 wells (Booth 1983 a, b, Harriman 1983, Sauer 1983). The data base of relevance for source rock identification and maturity evaluation is restricted to a single comprehensive report from one well, Sèmè 1 (Sauer 1983), and a limited amount of data from the Sèmè 1, 2, 3 and 4 wells (Augedal et al. 1983, Throndsen and Klaveness 1983, Throndsen 1983) altogether covering the section from the top of the "Turonian Sandstone" to the Miocene Lower Afowo Formation. More analytical data are needed to fully evaluate the source rock potential, particularly with respect to the "Albian Sandstone" and the Ise Formation.

7.1.2 Organic Geochemistry of Oil Samples

Four oil samples from the Sèmè Field have been analysed in detail by means of organic geochemistry in order to estimate source rock origin, maturity and suspected degradation. Three of the samples are from the oil producing "Turonian Sandstone" reservoir whereas the fourth is from the deeper "Albian Sandstone" approximately 500 m below the main producing zone.

All the oils show very similar properties indicating that they have a common source origin. For convenience only one sample from the producing reservoir and the one from the "Albian Sandstone" will be discussed here. They are hereinafter called "Turonian oil" and "Albian oil". Detailed analytical results are contained in Sauer (1983) and Harriman (1983) respectively.

Bulk properties

The physical properties of the two oil samples (table 7.1) demonstrate them to be of moderate to heavy gravity with an API gravity of 22° in both. The trace metal vanadium is present in quantities less than 1 ppm which is very low, while the nickel contents are moderate to high, 43 ppm and 62 ppm respectively in the "Turonian oil" and "Albian oil". Sulphur is low in both oils, only 0.35%.

Oil samples	"Turonian oil"	"Albian oil"
API gravity	22	22
Vanadium	<1 ppm	<1 ppm
Nickel	43 ppm	62 ppm
Sulphur	0.35%	0.35%
Saturates	41.5%	49.3%
Aromatics	34.0%	32.6%
Asphaltenes	11.4%	10.4%
NSO-compounds	12.2%	7.7%
Carbon isotopes of saturates	-25.8 °/oo (PDB)	-25.5 °/oo (PDB)
Carbon isotopes of aromatics	-24.9 °/oo (PDB)	-24.7 °/oo (PDB)

Table 7.1: Bulk properties of Sèmè oils.

Gaseous hydrocarbons

The samples being analysed for organic geochemistry are very low in gaseous components due to the sampling techniques being used. The gaseous components have nevertheless been analysed for carbon isotope ratios (table 7.2). The results indicate that the methane is of biogenic origin, whereas the ethane and propane are associated gases released during the early phase of main oil generation at a maturity level of LOM 9-10 corresponding to a vitrinite reflectance of Ro = 0.7 to 0.8.

Methane	-62.6 $^{o}/oo$ (PDB)
Ethane	-33.9 $^{o}/oo$ (PDB)
Propane	-30.2 $^{o}/oo$ (PDB)

Table 7.2: Carbon isotope ratios in gaseous hydrocarbons from the "Turonian oil".

Gasoline range hydrocarbons (C_4-C_7)

A full complement of gasoline range hydrocarbons (C_4-C_7) are contained in the oils. Isobutane to n-butane ratios of 0.39 and 0.50 respectively indicate that the oils are mature, whilst the relative high 3-methylpentane to benzene ratios of 14.28 and 3.59 for the "Turonian oil" and "Albian oil" suggest that the oils may have been subject to some degree of water washing resulting in preferential removal of water soluble aromatics.

C_{15+} fraction

The C_{15+} fractions contain 41.5 and 49.3% saturates, and 34.0 and 32.6% aromatics respectively for the two oils (table 7.1). The balance consists of asphaltenes 11.4 and 10.4%, and NSO-compounds 12.2 and 7.7% respectively for the "Turonian oil" and "Albian oil".

Chromatograms of the C_{15+} saturate fraction (fig. 7.1) are nearly identical for the two samples and exhibit a full range of long chain normal alkanes. A maxima is achieved at nC_{17}, but the alkanes extend out beyond nC_{35} indicating that the oils are waxy. This suggests that the oils have been sourced from kerogens of algal origin with additional significant terrestrial input, whilst the abundant pristane and phytane indicate that the oils are not highly mature. Slight odd over even preferences are evident from nC_{25} to nC_{29}.

The aromatic chromatograms are also very similar for the two oil samples (fig. 7.1). They show a high background envelope coupled with a depletion of aromatic peaks. These features lend support to the removal of the more water soluble aromatic compounds.

The oil samples were also analysed by GC-MS by selected ion monitoring of triterpanes (m/e 191), steranes (m/e 217) and aromatised steranes (m/e 239, 253) primarily for correlation purposes. The two oils produce nearly identical fragmentograms at m/e 191 (fig. 7.2) peaking with the C_{29} and C_{30} hopanes. They show, in addition, rich abundances of tricyclic diterpanes. Series of C_{31+} higher hopanes are also present, although these appear to be rather depleted. The two oils produce also near identical fragmentograms at m/e 217, and a series of steranes have been identified (fig. 7.2). The ratio of the 20R and 20S isomers of the C_{29} steranes together with the abundance of the $C_{29}BB$ steranes suggest that the oil is

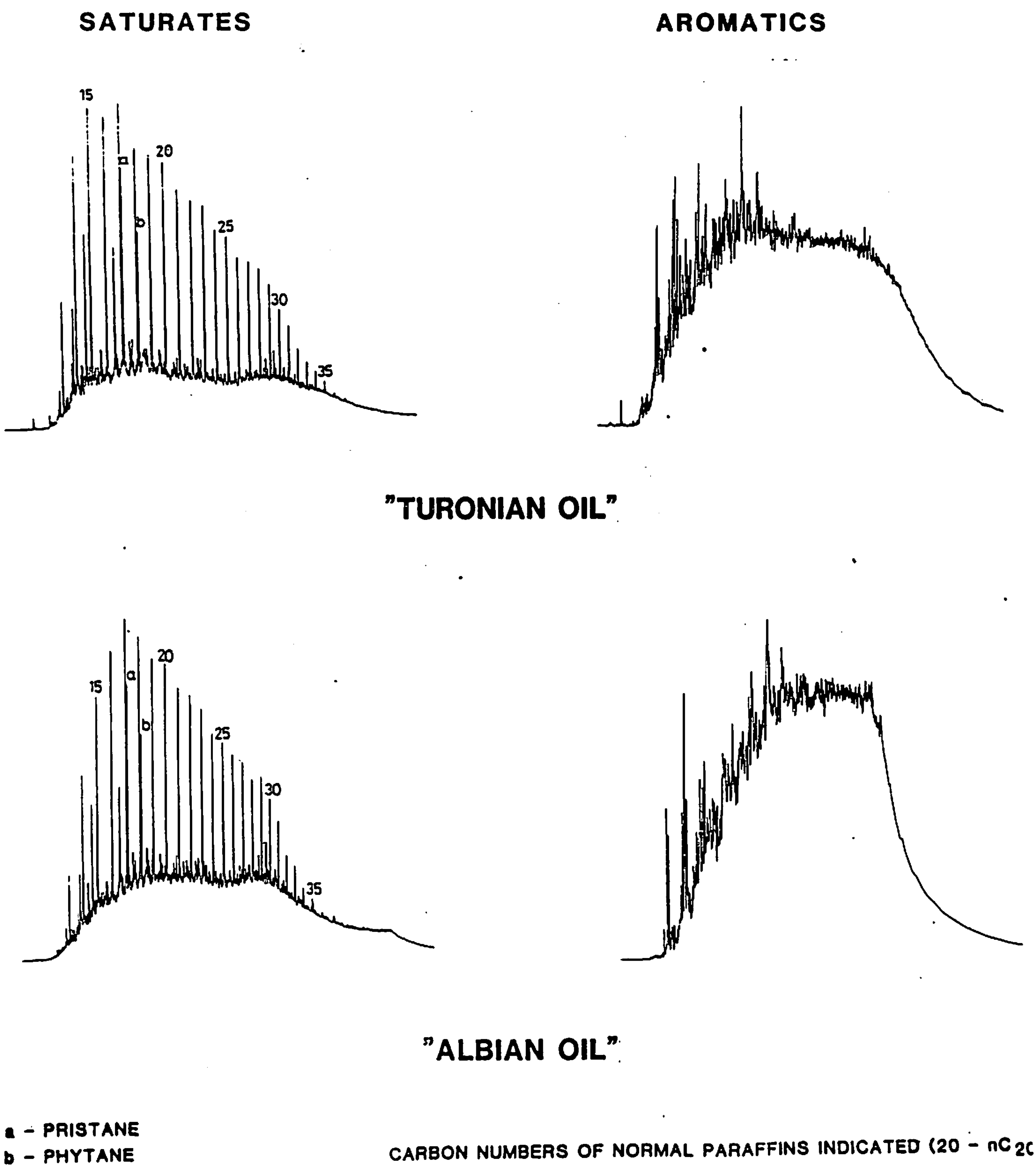

Fig. 7.1: Gas chromatograms of the C_{15+} saturate and aromatic fraction of "Turonian oil" and "Albian oil".

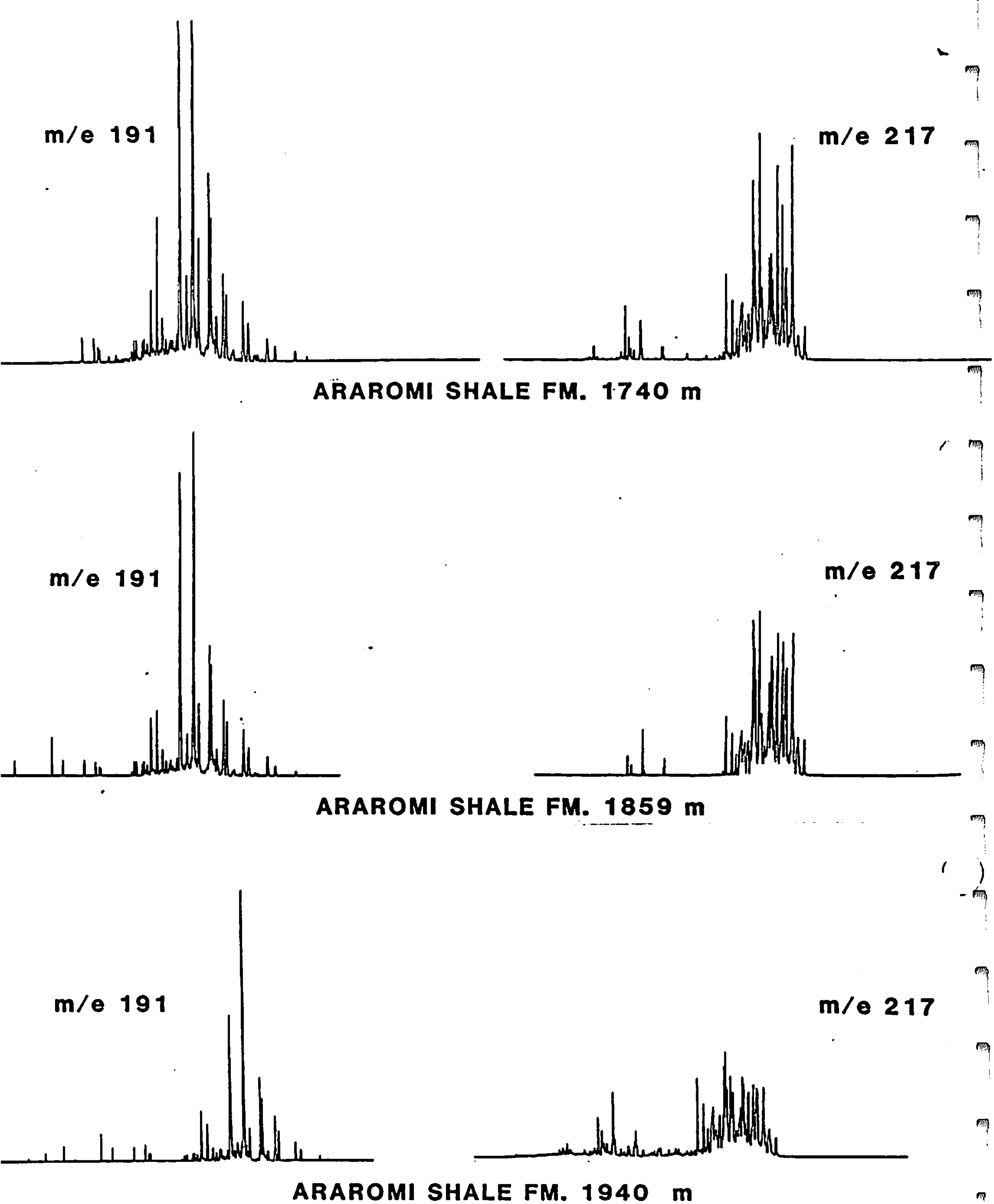

Fig. 7.2: Mass fragmentograms of shale extracts from the Sèmè 1 well, and from "Turonian oil" and "Albian oil".

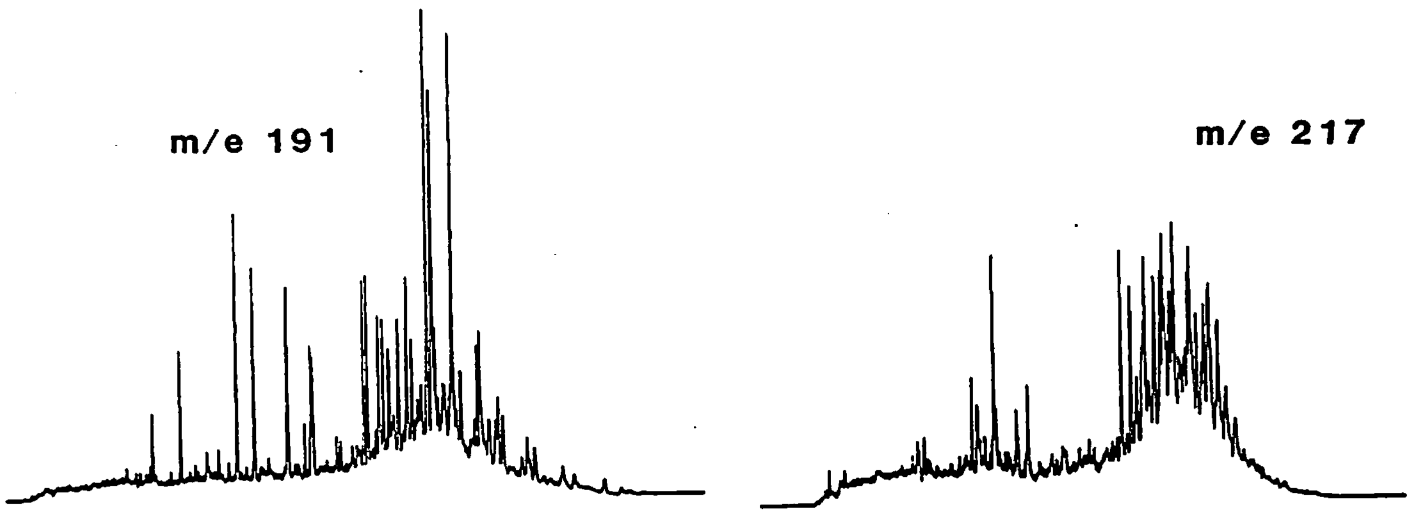

"TURONIAN OIL"

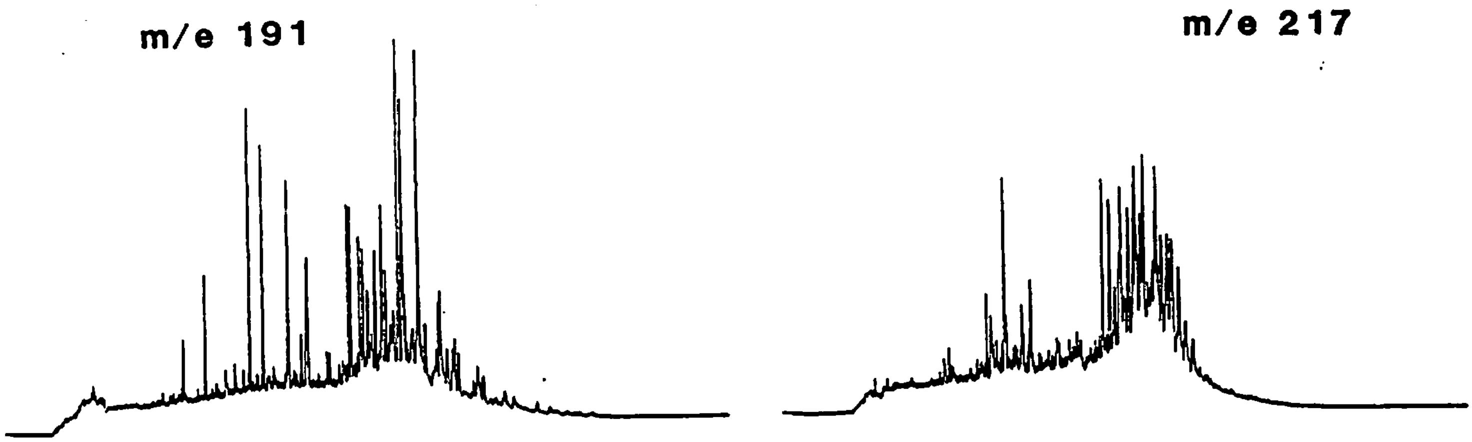

"ALBIAN OIL"

MASS FRAGMENTOGRAMS

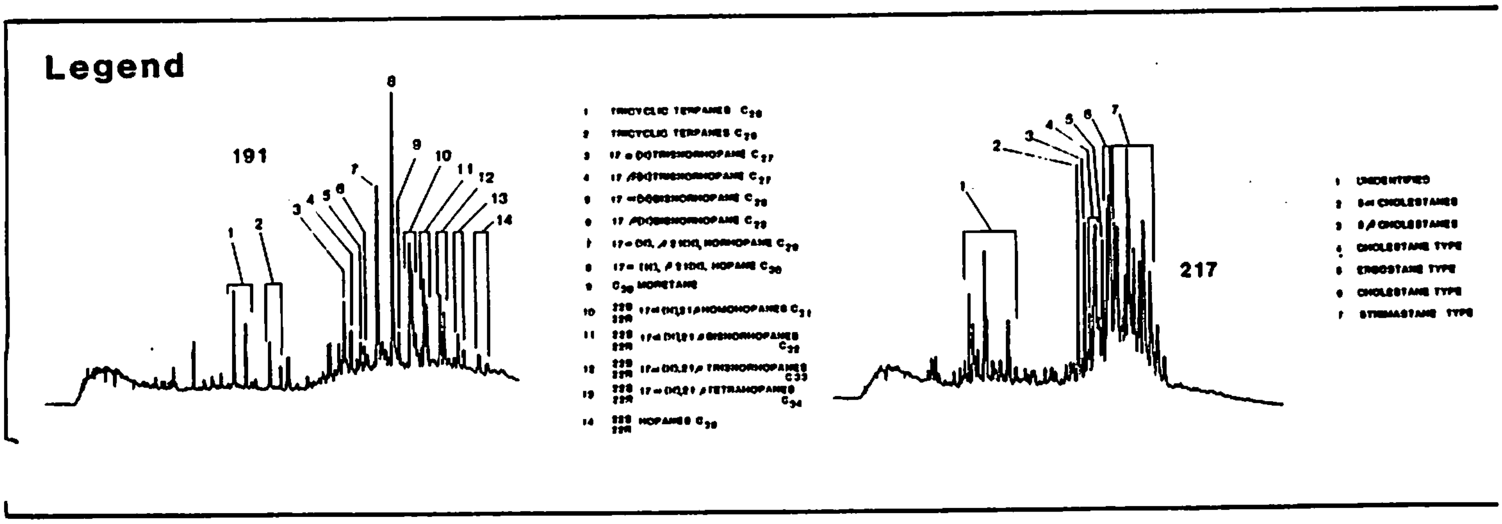

relatively mature.

Determinations of the stable carbon isotope ratios were undertaken upon the C_{15+} hydrocarbon fractions of the oils (table 7.1). Values of -25.8 $^{o}/oo$ and -24.9 $^{o}/oo$ were obtained for the saturate and aromatic fractions respectively in the "Turonian oil". The corresponding values for the "Albian oil" are -25.5 $^{o}/oo$ and -24.7 $^{o}/oo$. The values are nearly identical for the two oils and are suggestive of predominantly algal organic matter in the parent source rock.

Summary

Oils from the "Turonian Sandstone" and "Albian Sandstone" reservoirs within the Sèmè Field are virtually identical, and have a common source origin. They are fairly heavy (API 22^{o}), low sulphur (0.35%) crude oils. The oils are relatively mature and waxy, but appears to have experienced some water washing within the reservoir. Carbon isotope data suggest that the oils are derived predominantly from algal organic matter.

7.1.3 Source Rocks

The fact that accumulations and shows of oil have been encountered from various levels in the Sèmè Field proves that mature source rocks exist in the area and that migration has taken place. There is reason to believe that they are contained in one or more of the stratigraphic units recognized offshore Benin. They will be discussed separately below.

Ise Formation

The formation consists of interbedded sandstones and shales deposited under non-marine conditions in Early Cretaceous rift grabens. Shaly beds in deep lacustrine settings may have excellent oil source capabilities (Demaison and Moore 1980) and sufficient cumulative thickness to create a significant source rock.

The presence of Lower Cretaceous shales has been proven offshore Togo where abundant shaly layers are interbedded with sandstones frequently having oil and gas shows. However, no details are disclosed as to the organic quality and capacity of these shales, and it should be kept in mind that the shows could have been sourced from the Devonian Takoradi Shale present in the Togo sub-basins of the Dahomey Embayment or from younger Cretaceous rocks. It is not believed that the Devonian shales extend into the offshore Benin area.

As much as 248 m of the Ise Formation was penetrated in the DO-D2A well, and 229 m in DO-1 in the Sèmè Field area. In both wells the section was associated with hydrocarbon shows.

The areal distribution of the unit is outlined on fig. 7.3, showing that it is not present on the entire shelf and not at all onshore. It attains great thicknesses in downfaulted blocks beyond the shelf break (ref. fig. 5.16).

"Albian Sandstone"

The lithology of this unit is predominantly sandstone associated with frequent shaly and dolomitic stringers. A relatively thick shale sequence is present at the base of the unit. The depositional environment ranges from essentially non-marine to marine (ref. fig. 6.5) in a seaward direction

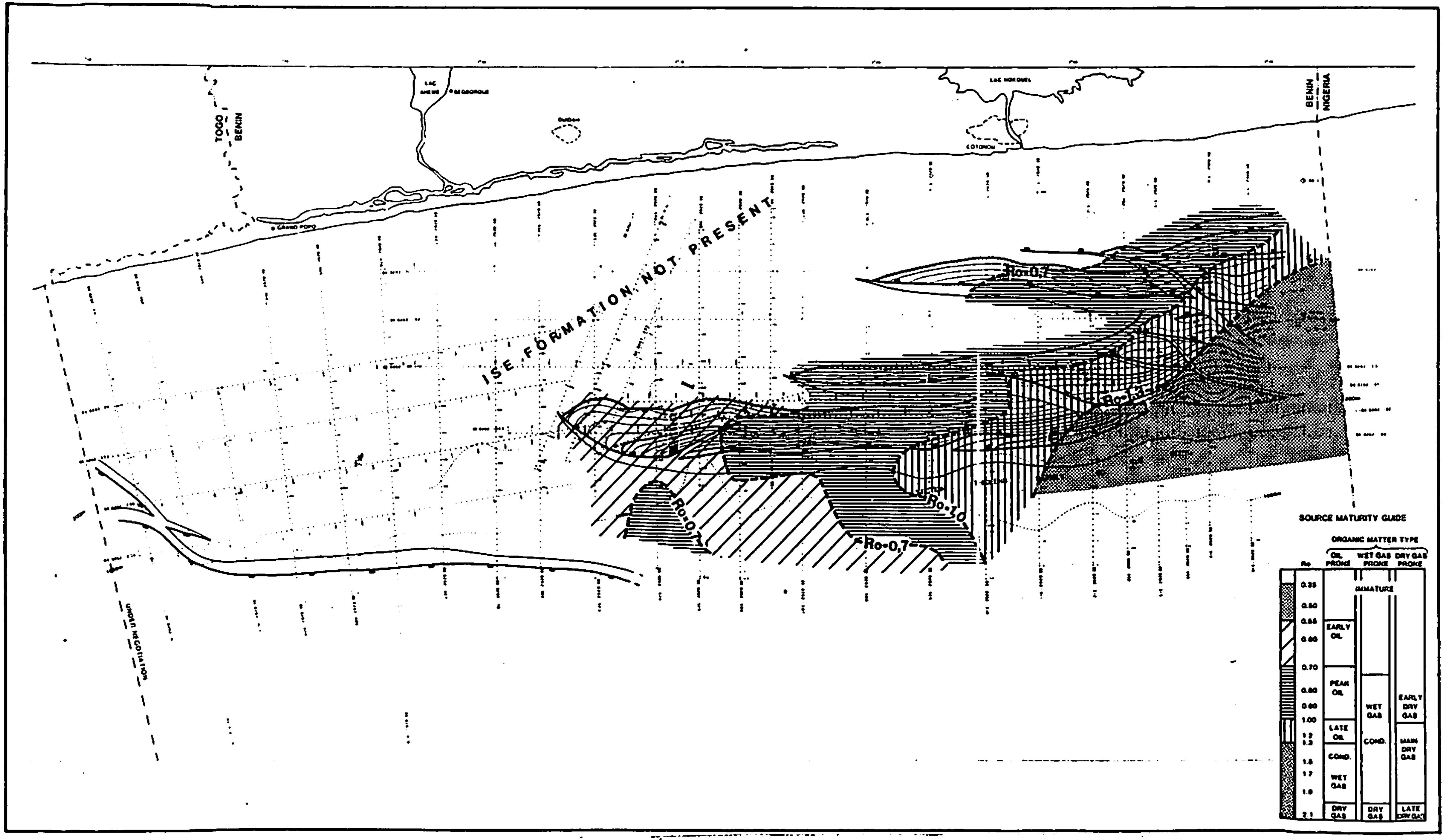

Fig. 7.3: Ise Formation. Maturity map (maturity at top of unit).

with a likely transition to predominantly shales beyond the shelf break. Oil and gas have been encountered from this unit within the Sèmè Field area, and this oil ("Albian oil") is identical to the oil from the producing "Turonian Sandstone" reservoirs indicating a common source origin (ref. chapter 7.1.2).

This unit is a possible source rock because it coincides in time with the anoxic conditions and black shale deposition that took place in southern Atlantic basins during mid-Cretaceous time (Tissot et al 1980). Shales in such settings tend to be organic rich and oil prone (Demaison and Moore 1980).

In addition Late Aptian to Early Albian transitional lacustrine/marine shales in a late rift to early marine setting are thought by many to have contributed significantly to the hydrocarbon source potential in the southern Atlantic region.

A maximum thickness of the unit of 455 m was penetrated in well DO-D2A whereas 405 m was encountered in DO1 and 234 m in C1, in all wells predominantly sandstone. The unit is not present on the entire shelf (fig. 7.4). The total thickness increases seawards, and accompanied with the possible transition to predominantly shales, it suggests that the unit may contribute to the source rock potential.

"Turonian Sandstone"

The litology of this unit is predominantly sandstone interbedded with shaly stringers. The depositional environment is interpreted as marginal marine to inner shelf (ref. figs. 6.8 and 6.10). Indications of restricted circulation (Augedal et al 1983), a possible seaward transition to predominantly shales, combined with the Mid Cretaceous anoxic conditions and black shale deposition in the southern Atlantic are the reasons

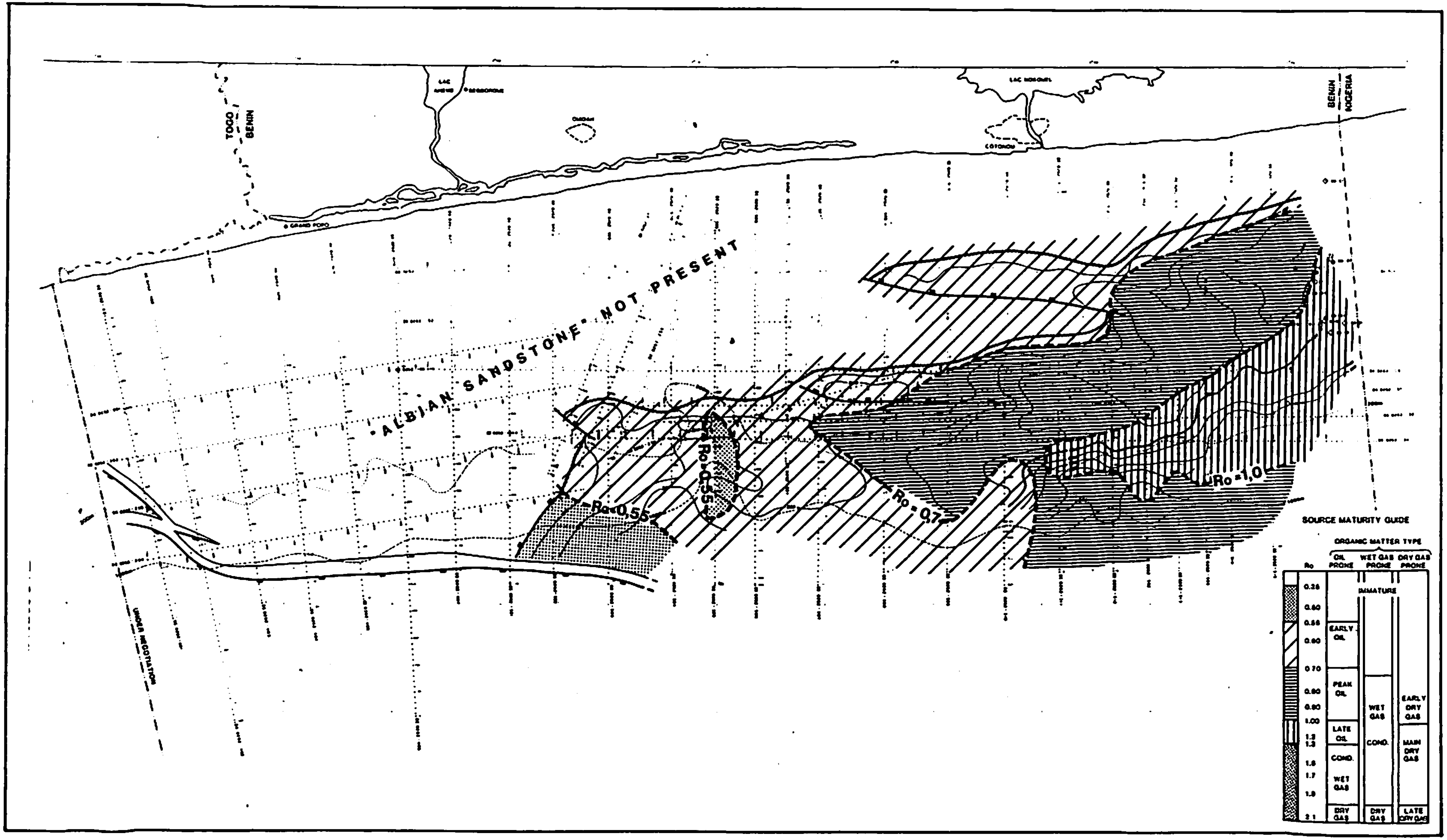

Fig. 7.4: "Albian Sandstone". Maturity map (maturity at top of unit).

why this unit, like the underlying "Albian Sandstone", is considered as a possible source rock.

The cored section in the Sèmè 2 well contained a few dark grey claystone beds interpreted as calm offshore marine deposition in an anoxic basin (Augedal et al 1983, Throndsen and Klaveness 1983). Two representative samples have been subjected to organic geochemical analysis (table 7.3). The contents of organic carbon are 4.2 and 7.1 weight percent which is very high. The pyrolysate yields (S2) are 13.4 and 37.8 mg/g sediment with corresponding hydrogen-index values of 315 and 531. These are all good values and indicate hydrogen rich, oil prone, type II kerogens.

Sample depth m	Organic carbon % wt	Pyrolysis* S2 mg/g	 HI
2283.0 core	4.24	13.36	315
2294.9 core	7.11	37.77	531

Table 7.3: "Turonian Sandstone", source rock data on dark grey shales (Sèmè 2). From Augedal et al (1983).

* : rock-eval pyrolysis
S2: pyrolysate yield, mg/g rock
HI: hydrogen-index

Microscopically the kerogen consists predominantly of herbaceous and amorphous material with a secondary input of woody and inertinitic material. The amorphous component shows granulous yellowish fluorescence when subjected to incident blue light illumination indicating an oil prone character. In reflected light microscopy the two samples consist of dark brown shales with abundant pyrite, and in blue light illumination they show yellowish fluorescent lipoide groundmasses (Teichmüller and Ottenjann 1977) and abundant small yellowish fluorescent exinite clasts further supporting the oil prone character.

Supposing the above characteristics are typical for the shales that prevail seawards and that the cumulative thickness attains significant values, it is clear that the "Turonian Sandstone" could constitute a significant contribution to the source rock potential in the area. The areal distribution is shown in fig. 7.5.

Awgu Formation

The formation consists of dark grey shales interbedded with siltstone and fine grained sandstone. The unit is probably deposited under anaerobic conditions suggesting that the shales could be organic rich and oil prone. Only a few geochemical data are available from the very thin section penetrated in Sèmè 1 (Augedal et al 1983). They are considered not representative for the formation as a whole. The formation has areal thicknesses in the size order of 300 m except for the Sèmè Field where it is significantly thinner.

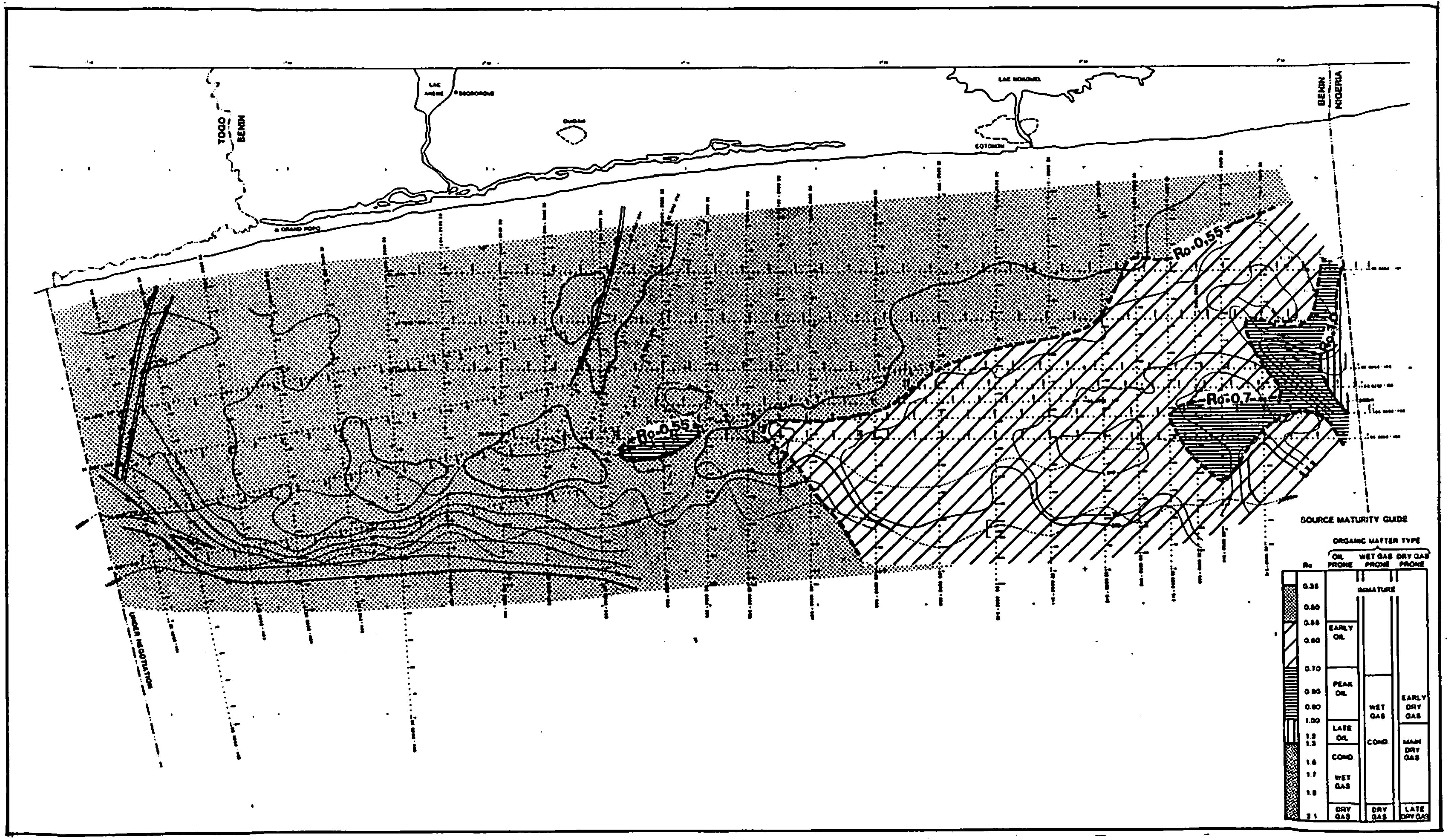

Fig. 7.5: "Turonian Sandstone". Maturity map (maturity at base of unit).

Araromi Shale

A representative section of the Araromi Shale Formation was penetrated in the Sèmè 1 well and analysed in detail by organic geochemical methods (Augedal et al 1983, Sauer 1983, table 7.4, enclosure 43). The lithology consists of dark grey claystones with abundant pyrite laid down under anaerobic conditions (Augedal et al 1983).

Organic carbon. The content of organic carbon ranges from 2.9 to 6.6 weight percent averaging at 4.9 weight percent which is very good.

Pyrolysis. The pyrolysate yield (S2) ranges from 7.0 to 29.2 mg/g sediment with corresponding hydrogen-index values ranging from 216 to 468 giving average values of 17.6 mg/g sediment and 351 respectively which are good and indicate a hydrogen rich, oil prone, type II kerogen.

Pyrolysis-GC. Several ditch cuttings samples have been analysed by means of pyrolysis gas chromatography (Sauer 1983). The pyrograms show methane and a succession of alkene-alkane doublets extending to nC_{25}-nC_{30} indicating a potential primary for oil. The strength of these peaks suggest a source potential for rather waxy oils. A representative pyrogram is shown in fig. 7.6.

Microscopy. The kerogen consists predominantly of amorphous material with a minor input of inertinitic, woody and herbaceous components. The amorphous component shows granulous yellowish fluorescence when subjected to incident blue light illumination indicating an oil prone character.

Table 7.4: Araromi Shale Formation, source rock data (Sèmè 1).
Data from Augedal et al (1983) and Sauer (1983).

Sample depth m	Organic carbon % wt	Pyrolysis** S2 mg/g	Pyrolysis** HI	Solvent extraction EOM ppm	Solvent extraction HC ppm	Solvent extraction EOM/ OC %	Solvent extraction HC/ OC %	Solvent extraction Pr/ Ph
1640	2.89							
60	3.56							
80	3.43							
1700.0 swc*	5.39	27.77	468					
00	6.46	15.37	238	5673	2620	10.9	5.0	1.68
18.2 swc*	4.24	15.99	377					
20	6.41							
40	6.28	16.73	266	7802	2992	14.1	5.4	1.49
50.0 swc*	4.03	12.29	305					
60	5.76							
71.0 swc*	3.00	7.02	236					
80	3.49	15.06	431	4217	1928	8.9	4.1	1.56
1800	3.80	15.75	414	4507	1775	10.2	4.0	1.52
20	4.97							
40	4.60	16.90	367	5668	2556	13.2	6.0	1.64
59	4.90	12.87	262	7072	3604	15.9	8.1	1.64
60.0 swc*	6.57	27.32	416					
73.0 swc*	6.36	29.18	458					
77	5.62	20.08	357	8349	4933	14.9	8.8	1.28
90.0 swc*	6.64	27.61	415					
96.0 swc*	3.98	15.08	378					
1901.2 swc*	4.10	16.72	407					
04	6.40	13.86	217	3021	1808	4.6	2.8	1.15
10.0 swc*	4.27	12.96	304					
15.0 core*	5.08	27.39	460					
15.9 core*	5.38	23.22	431					
20.8 core*	5.19	22.85	440					

Continued next page.

Continuation of table 7.4.

Sample depth m	Organic carbon % wt	Pyrolysis** S2 mg/g	HI	Solvent extraction EOM ppm	HC ppm	EOM/ OC %	HC/ OC %	Pr/ Ph
1922	5.66	17.87	316	10510	6049	20.5	11.8	1.43
33.0 swc*	4.15	15.38	370					
40	4.98	10.77	216	8752	5000	19.6	11.2	1.36
45.0 swc	3.72	11.28	303					
58	4.51	10.90	242	5367	3201	13.4	8.0	1.33
63.0 swc*	4.27	15.81	370					
AVERAGE	4.85	17.59	351					

* : sample data from Augedal et al (1983). Remaining sample data are from Sauer (1983).

** : sample data from Augedal et al (1983) are obtained from rock-eval pyrolysis, whereas Sauer's (1983) are from Geochem's in-house equipment.

S2 : pyrolysate yield, mg/g rock

HI : hydrogen-index

EOM: extractable organic matter yield.

HC : hydrocarbon yield.

OC : organic carbon

Pr : pristane

Ph : phytane

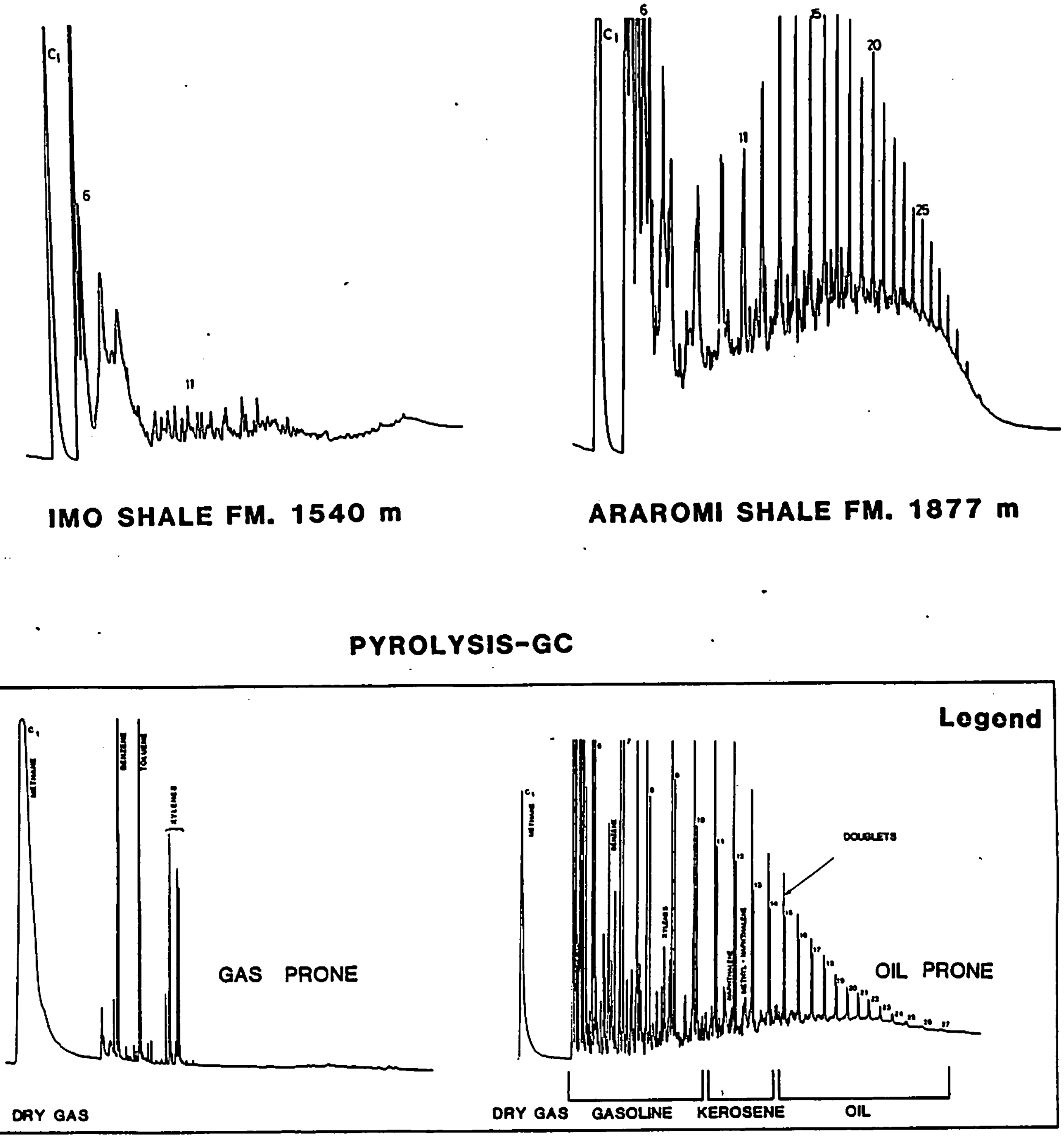

Fig. 7.6: Representative pyrograms from the Sèmè 1 well.

Examined in reflected light microscopy, the Araromi Shale lithologies consist of dark brown shales with abundant pyrite, and when subjected to blue light illumination, they show yellowish fluorescent lipoide groundmasses embedding small yellowish fluorescent exinite clasts further supporting the oil prone character.

Solvent extraction. The abundance of extractable organic matter is excellent ranging from 4217 to 10510 ppm, and indicates if indigenous to the formation, a very good source potential.

Hydrocarbon potential. The above considerations can be summarized with respect to hydrocarbon potential as follows (table 7.5):

Age	Thickness m	Total potential* mg/g rock	Expected hydrocarbons
E. Paleocene - Maastricht.	330	17.40	oil

Table 7.5: Araromi Shale Formation, hydrocarbon potential (Sèmè 1).

*Total potential: equal to pyrolysate yield (S2) for immature samples.

The Araromi Shale Formation has a rich potential for oil and gas. It is marginally mature in well Sèmè 1.

In Sèmè 1 a section of 330 m of this unit was penetrated. The areal distribution offshore Benin is shown in fig. 7.7.

Imo Shale Formation

A representative section of the Imo Shale Formation was penetrated in the Sèmè 1 well (1360 - 1635 m) and analysed in detail by organic geochemistry (Augedal et al 1983, Sauer 1983, table 7.6, enclosure 43). The lithology consists predominantly of dark grey claystone deposited in a marine oxygenated environment.

Organic carbon. The content of organic carbon ranges from 0.3 to 3.0 weight percent averaging 1.6 weight percent which is moderate.

Pyrolysis. The pyrolysate yield (S2) ranges from 0.7 to 7.9 mg/g sediment with corresponding hydrogen-index values ranging from 51 to 300. These give average values of 4.4 mg/g sediment and 196 respectively and indicate a moderately hydrogen rich, wet gas prone type III kerogen.

Pyrolysis-GC. Three cuttings samples have been analysed in more detail by means of pyrolysis gas chromatography. The pyrograms are very similar. They show methane and a limited distribution of heavier hydrocarbons indicating a potential primarily for gas. A representative pyrogram is shown in fig. 7.6.

Miscroscopy. The kerogen composition consists chiefly of inertinitic material mixed with significant amounts of woody, amorphous and herbaceous components.

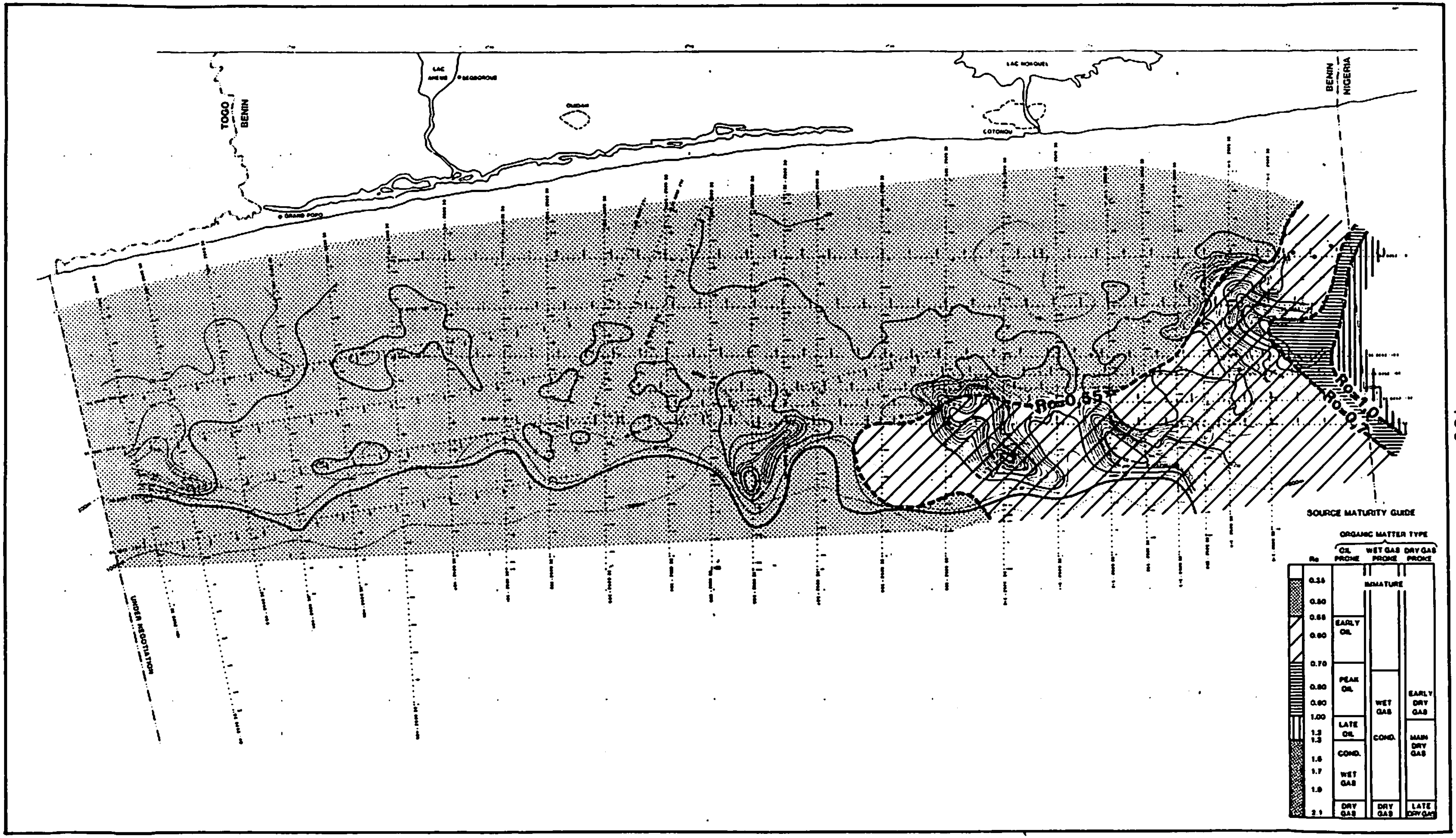

Fig. 7.7: Araromi Shale. Maturity map (maturity at base of unit).

Sample depth m	Organic carbon % wt	Pyrolysis** S2 mg/g	HI	Solvent extraction EOM ppm	HC ppm	EOM/ OC %	HC/ OC %	Pr/ Ph
1380	1.67							
1400	1.61							
20	2.97	7.92	267					
40	2.59	6.70	259					
60	0.30							
80	1.02							
1500	1.43	4.32	300	1200	341	7.5	2.2	1.16
20	1.44							
40	1.45			445	134	3.1	1.0	0.67
60	1.50							
80	2.10	2.03	97					
89.5 swc*	1.28	0.66	51					
1600	1.88	4.57	243	746	281	5.4	2.0	1.46
20	1.40							
AVERAGE	1.62	4.37	203					

Table 7.6: Imo Shale Formation, source rock data (Sèmè 1). Data from Augedal et al (1983) and Sauer (1983).

Legend: see table 7.4.

Solvent extraction. The abundance of extractable organic matter is poor to fair ranging from 445 ppm to 1200 ppm averaging at 797 ppm, and suggests when normalised to organic carbon, a fair to good source potential. The C_{15+} saturate chromatograms have pronounced bimodal distributions, strong pristane and phytane peaks, odd over even predominances and strong sterane-triterpane humps indicating contribution predominantly from immature indigenous organic matter. Gas chromatograms are shown in fig. 7.8.

Hydrocarbon potential (table 7.7). The Imo Shale Formation has a fair to good potential primarily for gas with some liquid hydrocarbons. It is immature to marginally mature in the Sèmè 1 well.

Age	Thickness m	Total potential* mg/g rock	Expected hydrocarbons
E. Eocene - E. Paleocene	275	4.36	primarily gas with some condensate

Table 7.7: Imo Shale Formation, hydrocarbon potential (Sèmè 1).

*Total potential: equal to pyrolysate yield (S2) for immature samples.

IMO SHALE FM.

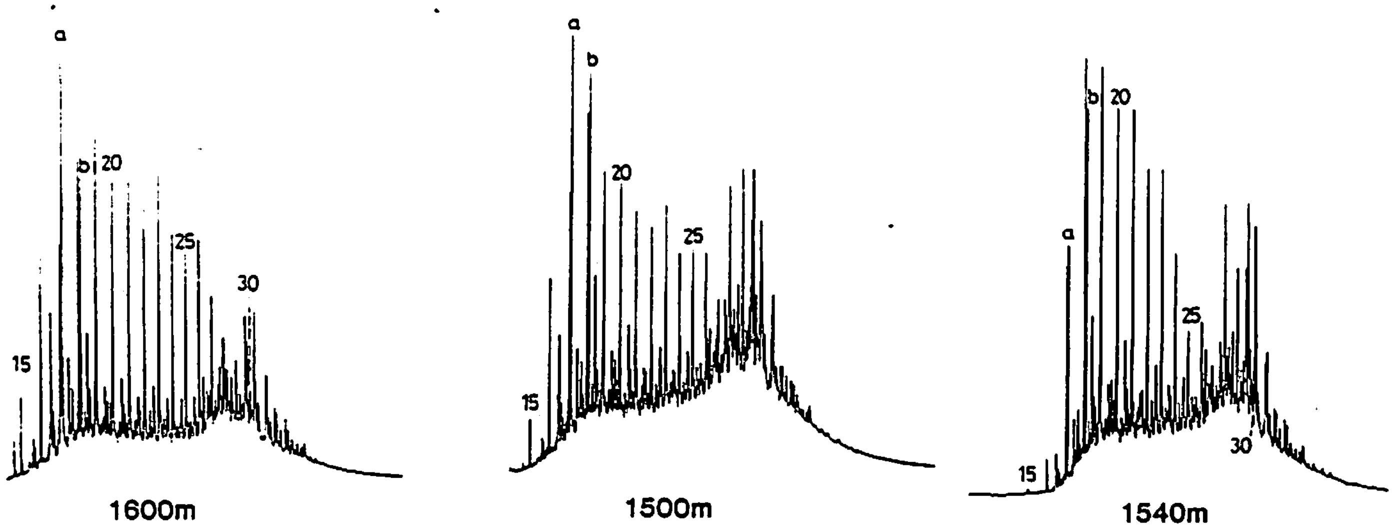

ARAROMI SHALE FM.

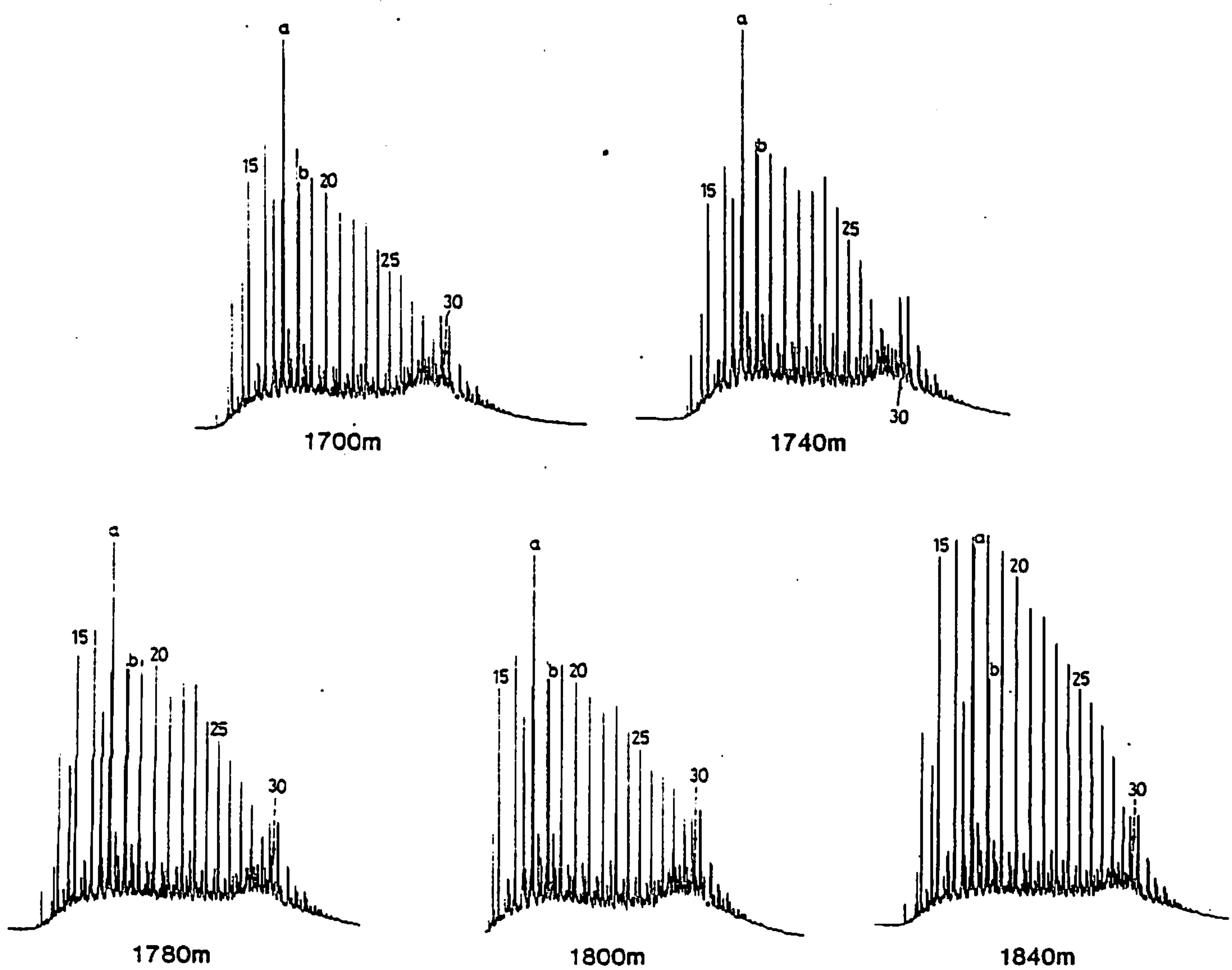

7.1.4 Correlation Oil - Source Rock

In part 7.1.2 of this section it was found that oils from the "Turonian Sandstone" and "Albian Sandstone" in the Sèmè Field had a common source origin. In order to identify the source rock for these oils, detailed organic geochemistry was carried out on the Araromi Shale Formation which is the only oil prone source rock analysed so far. For convenience here only the "Turonian oil" will be discussed in relation to the Araromi Shale Formation.

C_{15+} paraffin - naphtene distribution

The C_{15+} saturate fractions were examined for evidence of a correlation between the shales and the oil. Chromatograms of the paraffin - naphtene fractions display abundant isoprenoids including pristane and phytane but differ in the strength of the steranes and triterpanes at the nC_{27}-C_{31} position, due to enhanced contributions from indigenous species in the less mature shale extracts (fig. 7.8). Detailed isoparaffin finger-prints of the oil and shale extracts suggest only a tenous correlation.

Mass fragmentograms (fig. 7.2)

Hydrocarbons extracted from the shales produce nearly identical fragmentograms at m/e 191. The corresponding trace for the oil is rich in tricyclic diterpanes which overlap the C_{28}-C_{29} pentacyclic species. Their presence is sometimes associated with migration but may also indicate a change in source facies from the analysed shales (Sauer 1983).

At m/e 217 the cholestanes extracted from the shales become enhanced relative to the stigmastanes, as depth increases. An increasingly algal character is suggested from the shale at 1940 m which loosely correlate with those from the oil sample.

The mass fragmentograms suggest that a correlation although being a tentative one, does exist between the analysed shales and the produced oil.

Carbon isotope ratios of the C_{15+} fractions

Carbon isotope ratios of the C_{15+} hydrocarbons reflect the type of organic matter and environment in which the sediments were deposited. Maturation has a lesser effect. In the shale extracts at 1859 m and at 1940 m the saturated hydrocarbons yielded values of -28.5 $^{o}/oo$ and the aromatic fraction -27.3 to -27.1 $^{o}/oo$. Saturated and aromatic hydrocarbons extracted from the crude oil are isotopically heavier, -25.8 and -24.9 $^{o}/oo$.

This difference between the crude oil and shale extracts is too great for a correlation. 1 $^{o}/oo$ is an acceptable limit for a good correlation. The oil may as a result of suspected water washing be slightly heavier than the unaltered form. This effect is believed to be minor, and a change in source facies from those encountered in the analysed section is more probable.

Summary

The above results show that only a tenous correlation exists between the produced oil and the Araromi Shale Formation. The deviating points can, however, be explained in terms of facies changes downdip from the Sèmè Field to the mature hydrocarbon kitchen.

7.1.5 Maturity

Vertical maturity trend (Sèmè 1)

Vitrinite reflectance is, when properly used, probably the best maturity indicator available today. A relatively detailed vitrinite reflectance versus depth profile is established in the Sèmè 1 well. It forms the basis to which the maturity level will be referred. Secondary maturity indicators such as spore colour, pyrolysis T-max and solvent extraction are used primarily to confirm the vitrinite reflectance data (tables 7.8 and 7.9, fig. 7.9, enclosure 43).

In Sèmè 1 the vitrinite reflectance increases continuously with depth reaching Ro = 0.35 at 650 m and Ro = 0.55 at 1700 m. A vitrinite reflectance value of Ro = 0.70 is not reached in the well. It will be reached at approximately 2300 m based on extrapolation.

Spore colour estimations have been given over the interval 1500 m to 1958 m, with values ranging from 2- at 1500 m to 2-/2 at 1958 m indicating immaturity to marginal maturity.

Pyrolysis T-max. Rock-eval pyrolysis T-max values are recorded in numerous samples over the interval 1589.5 m to 1994.4 m. There is no obvious trend in the data, but they seem to range from around 439 °C at 1600 m to 444 °C at 2400 m indicating a marginally mature setting.

Solvent extraction. Numerous samples have been subjected to solvent extraction, chromatographic separation and gas chromatography over the interval 1500 m to 1958 m.

Table 7.8: Sèmè 1, maturity indicators.

Samples depth m	Vitrinite reflectance Ro	Spore colour TAI	T-max** °C	Solvent extraction S/A	HC/EOM	CPI	Pr/nC_{17}
Lower Afowo Fm							
1000	0.42						
1160	0.43						
1200	0.47						
1260	0.49						
Oshosun Fm							
1360	0.48						
Imo Shale Fm							
1420	0.46						
1500	1.09	2-		1.07	0.28	1.19	1.67
1510	0.59						
1540		2-		2.00	0.30	1.16	1.09
1589.5 swc*			439				
1600		2-		0.80	0.38	1.07	1.86
Araromi Shale Fm							
1640	0.48						
1700	0.46	2-		0.76	0.46	0.99	1.86
1700.0 swc*			435				
1718.2 swc*			439				
1740	0.49	2-?		0.75	0.38	1.01	2.01
1750.0 swc*			440				
1771.0 swc*			439				
1780		2-?		0.89	0.46	1.00	1.60
1800	0.48	2-/2- to 2?		1.00	0.39	1.02	1.58

Continued next page.

Continuation of table 7.8.

Samples depth m	Vitrinite reflectance Ro	Spore colour TAI	T-max** °C	Solvent extraction S/A	HC/EOM	CPI	Pr/nC_{17}
1840		2-		0.95	0.45	0.99	0.98
1859		2- to 2?		1.14	0.51	1.05	0.84
1860.0 swc*			441				
1873.0 swc*			443				
1877	0.55	2- to 2		1.26	0.59	1.01	1.02
1890.0 swc*			415				
1896.0 swc*			442				
1901.2 swc*			443				
1904		2- to 2		1.16	0.60	1.03	1.13
1910.0 swc*			440				
1915.0 core*			443				
1915.9 core*			441				
1920.8 core*			469				
1922		2- to 2?		1.25	0.58	1.01	1.13
1933.0 swc*			444				
1940	0.52	2- to 2		1.23	0.57	0.96	1.24
1945 swc*			443				
1958		2- to 2?				0.99	1.11
1963 swc*			444				
Awgu Fm							
1967.5 swc*			449				
1972.2 swc*			439				
Turonian Sandstone							
1976.0 core*			466				
1979.6 core*	0.60		444				
1986.8 core*			421				
1991.2 core*	0.56						
1994.4 core			440				

Legend: see next page.

* : sample data from Augedal et al (1983). Remaining sample data are from Sauer (1983).
** : rock-eval pyrolysis from Augedal et al (1983).
S : saturates.
A : aromatics.
EOM: extractable organic matter yield.
HC : hydrocarbon yield.
CPI: carbon preference index.
Pr : pristane

Sample depth m	Vitrinite reflectance Ro	T-max** °C
<u>Turonian Sandstone</u>		
2283.0		434
2292.1	0.64	440
2292.8		362
2292.4	0.64	
2294.9		434

Table 7.9: Sèmè 2, maturity indicators.

**see table 7.8.

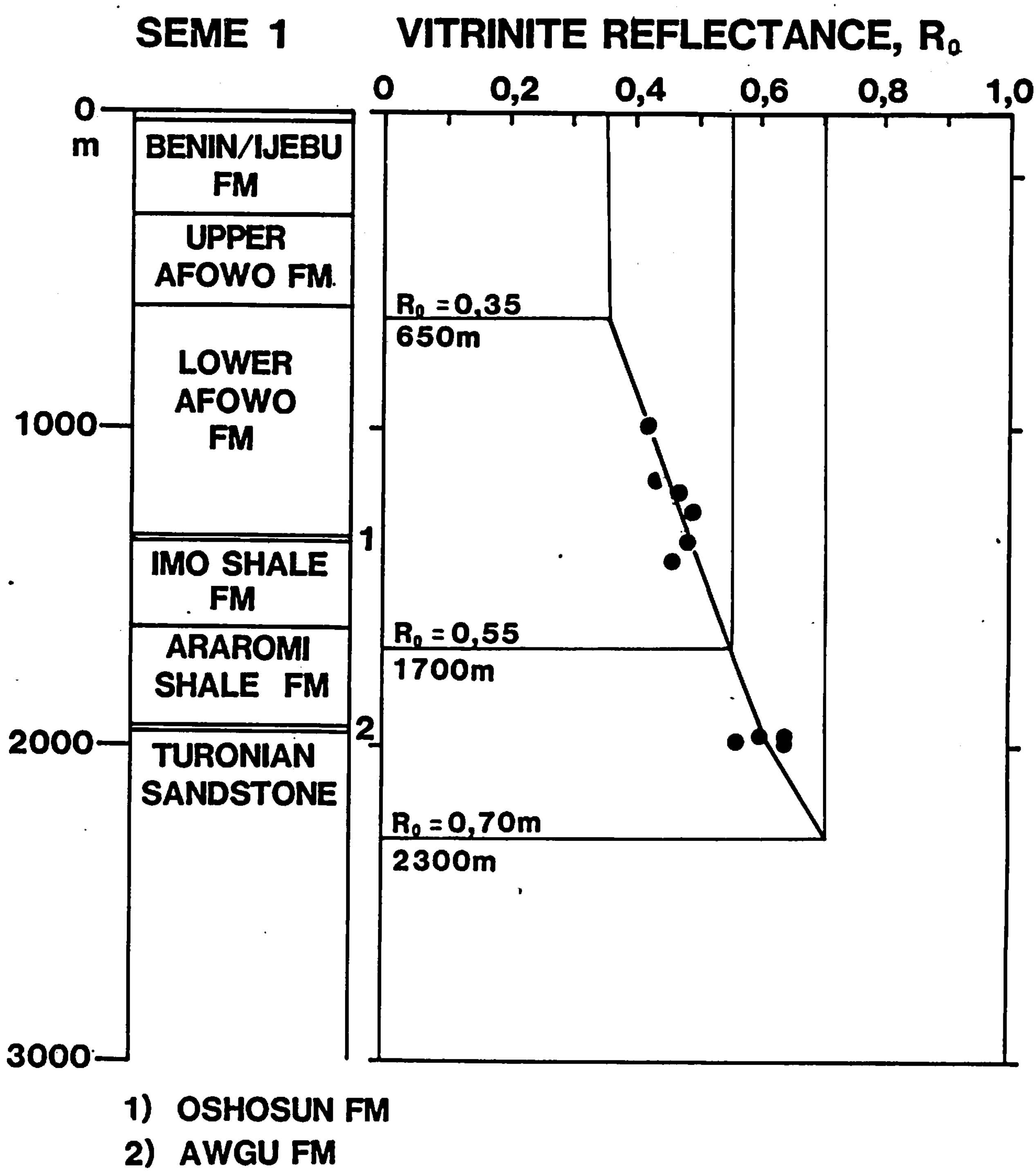

Fig. 7.9: Linear plot of vitrinite reflectance versus depth in the Sèmè 1 well.

Immaturity can be inferred for the Imo Shale Formation (table 7.8, fig. 7.8) based on odd over even predominances, hydrocarbon to total extract ratios below 0.5, pristane to nC_{17} ratios well above 1.0 and GC-chromatograms showing clearly immature features with typical bimodal distribution with a maximum for pristane, phytane and around nC_{29}. This is further supported by the proportion of biomarkers which is large, a feature which will diminish with increasing maturity.

Immaturity to marginal maturity can be inferred for the Araromi Shale Formation (table 7.8, fig. 7.8) down to 1800 m based on hydrocarbon to total extract ratios below 0.5 and pristane to nC_{17} ratio well above 1.0. The GC-chromatograms show a maximum for pristane and a moderately high proportion of biomarkers. Below 1800 m there is an increase in the hydrocarbon to total extract ratio to values above 0.5 accompanied by a decrease in pristane relative to nC_{17} to values close to 1.0. The proportion of biomarkers is, however, relatively high. These features could be indicative of the onset of oil generation.

<u>Vertical maturity trend</u>. Based on the above discussion it is reasonable to interpret the vitrinite reflectance profile as reliable, and the vertical maturity trend can be summarized as shown in fig. 7.9 and table 7.10.

Maturity level Ro	Depth m
0.35	650
0.55	1700
0.70	2300
1.00	-
1.30	-

Table 7.10: Tabulation of some maturity characteristics, well Sèmè 1.

Source rock maturity and timing

The vertical maturity profile established in the Sèmè 1 well forms a reliable basis for areal maturity mapping of the potential source rock intervals. We have used Gretener's (1981) method to calculate the maturity levels by calibrating his LOM_{PEG} scale (level of organic metamorphism) against the established maturity profile in the Sèmè 1 well. The maturity levels of various horizons are given in vitrinite reflectance in figs. 7.3, 7.4, 7.5 and 7.7.

The fact that accumulation and shows of oil have been encountered at various levels in the Sèmè Field proves that mature source rocks do exist and that migration has taken place. It is reason to believe that they are contained in one or several of the following stratigraphic units: the Imo Shale, Araromi Shale, "Turonian Sandstone", "Albian Sandstone" and Ise Formation. Overlying formations are immature and cannot generate hydrocarbons.

<u>The Imo Shale Formation</u> consists predominantly of dark grey claystone deposited under open marine conditions, having a fair to good potential primarily for gas with some liquid hydrocarbons. The formation is mostly immature. Marginal maturity is reached only in the very southeastern part of the shelf area, indicating that the Imo Shale Formation can only be rated as a very marginal or negligible source rock for the offshore Benin area. The formation has no <u>onshore</u> potential.

<u>The Araromi Shale Formation</u> consists of dark grey marine shales laid down under anaerobic conditions, having a rich potential for oil and gas. The unit is immature to fully mature. Fully maturity is obtained in the very eastern part of the offshore Benin area, where also the thickness of the formation is sufficient to give rise to a significant hydrocarbon generation. This active hydrocarbon kitchen is located close to the Sèmè Field and could be the actual source rock for the reservoired oil. This area first reached maturity in Middle to Late Miocene times. The <u>onshore</u> section will not be mature.

<u>The Awgu Formation, "Turonian Sandstone" and "Albian Sandstone"</u> contain significant amounts of shaly interbeds. Very few data, however, exist as to the organic quality and capacity of these shales. They are considered as possible source rocks because they coincide in time with the anoxic conditions and black shale deposition that took place in southern Atlantic basins during Mid Cretaceous time. They reach sufficient maturity to generate hydrocarbons in southeastern parts of the mapped area. They probably reached the mature stage in Miocene times. Their <u>onshore</u> potential is unfavourable due to both facies and lack of maturity.

The Ise Formation consists of interbedded sandstones and bright coloured grey to brown shales deposited under non-marine and lacustrine conditions possibly having source rock capabilities and sufficient thickness to constitute a significant source rock. The oils in the Sèmè Field can possibly have their origin in this unit. The unit has reached sufficient maturity to generate hydrocarbons, and beyond the shelf break it is even overmature at depths greater than approximately 3500 m, indicating that oil is not preserved in reservoirs below this depth. The deeply buried parts of this unit became mature very early, possibly as early as Albian and Turonian times.

7.2 Reservoir Evaluation

7.2.1 General

In the sedimentary sequence offshore Benin there are three formations with major sandstone development: The Lower Cretaceous Ise Formation and "Albian Sandstone", and the "Turonian Sandstone". In addition erosional channels and subsequent submarine fan infilling in the Maastrichtian - Danian may contain reservoir sandstones.

The bulk of the data available for the reservoir rock evaluation is from the exploratory wells drilled by Union Oil and above all the Sèmè Field wells, as wells as two exploratory wells offshore Togo.

Because the well data cover a limited area, the interpretation of lateral variations of the reservoir rocks are based mainly on a seismic stratigraphic approach.

The most important reservoir parameters as interpreted from log analyses, are listed in the tables 7.11, 7.12 and 7.13.

The parameters on the reservoir quality is based on CPI logs and the core analysis available (tables 7.11, 7.12, 7.13 and 7.14). Cut-off criterias used in defining net sand were porosity >10% and Vsh <40%, and pay sand has water saturation below 65%.

7.2.2 Ise Formation

Lithology

The Lower Cretaceous deposits of the Ise Formation has a lithology ranging from conglomerates to shales and carbonates (compare chapter 5.2.1). Because the deposition took place within fault controlled basins, the lithological changes are large both stratigraphically and laterally. The sandstones are medium to coarse, white or light grey with abundant kaolinite and some carbonate cement. The sandstones are immature with high content of feldspar, mica and chlorite. The shale and claystones have a variable colour: red, green-white and brown have been reported.

So far only thin beds of conglomerates have been penetrated, but the content is expected to increase towards the faults where the Ise Formation thickens.

Depositional environment

The Ise Formation was deposited in continental, rift half graben basins (fig. 7.10a and b). Fluvial and lacustrine processes are the main depositional mechanisms, but each basin has a different depositional history and must be evaluated separately. It has not been possible to map individual units within the formation, but rapid facies changes are common in this type of depositional system. It is likely that alluvial fans developed along the major faults with a transition to alluvial plain and lacustrine deposits more distal to the faults.

Because of the thin bedding of the units in the DO-1 and DO-D2A, it is more likely that the deposits here are fluvial sandstones with overbank and possibly silty lacustrine shales.

Diagenetic history

No results from mineralogical analyses are available from the

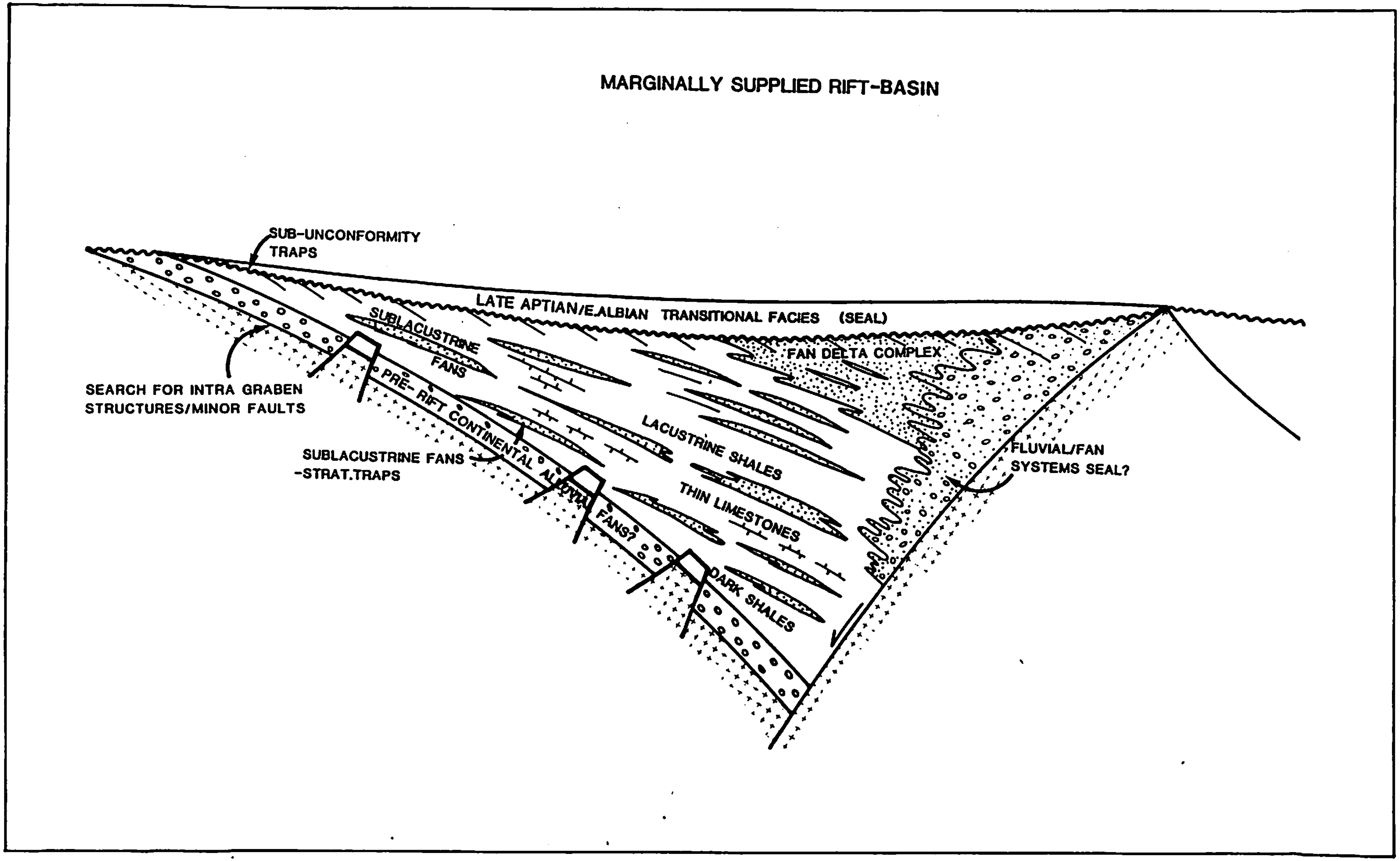

Fig. 7.10a: Depositional model of the Ise Formation based on a marginal supplied rift basin. Sketch by L. F. Brown.

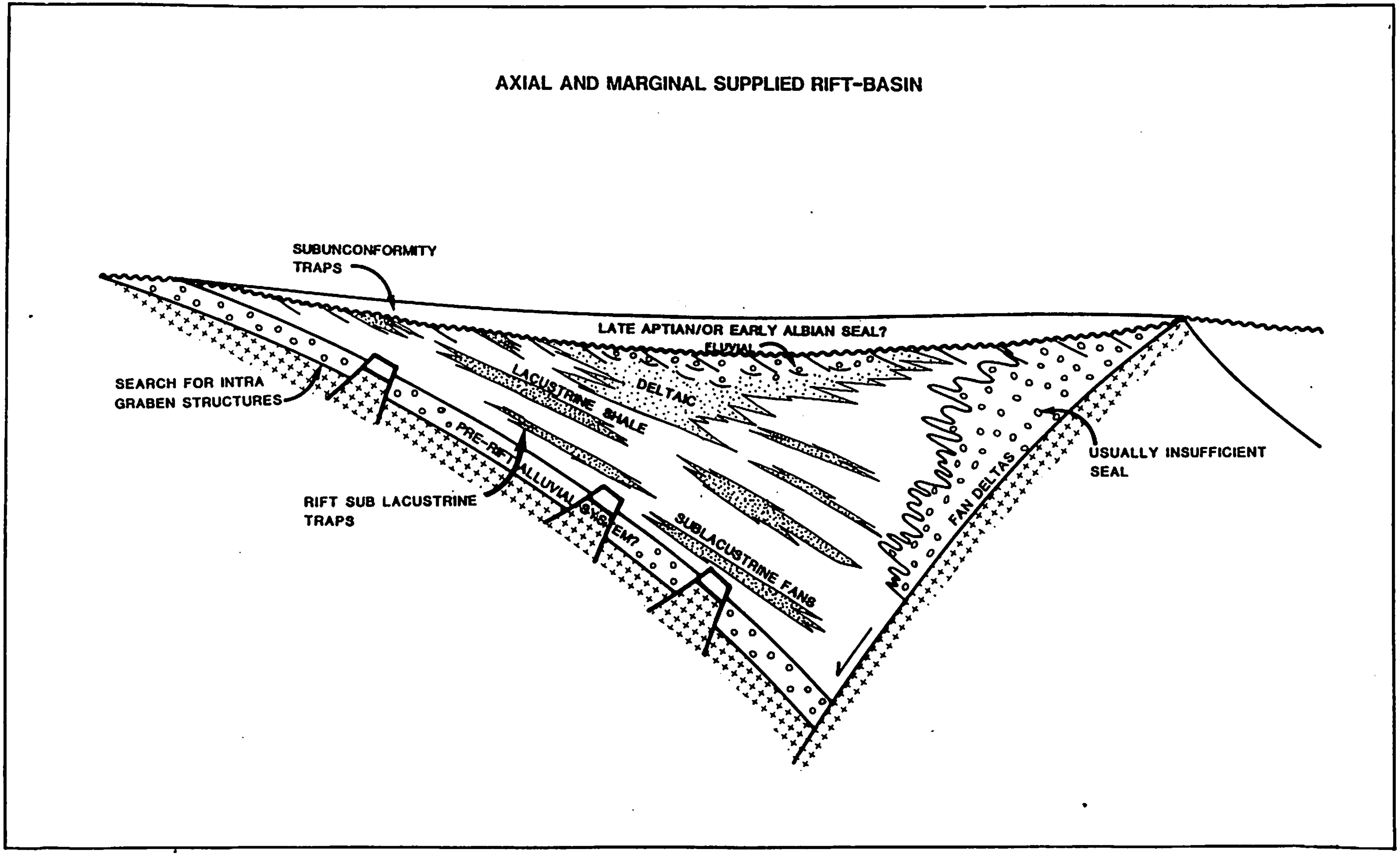

Fig. 7.10b: Depositional model of the Ise Formation based on an axial and marginal supplied rift basin. Sketch by L. F. Brown.

Ise Formation, but the net sandstone content from logs is low due to low porosity. Kaolinite is reported from cuttings description as a common mineral, and this is also typical for continental deposits in a warm humid climate. The fresh water introduced in the sandstones can rapidly change feldspars and other alumina and silica rich minerals to kaolinite. In addition a high primary clay content is common if the current energy of the fluvial system is rapidly changing. But it is expected that the sand content increases towards the major faults, and that the clay content is reduced because of higher current energies in the alluvial fan type deposits. Because of the immature mineralogy and general high primary clay content in the Ise Formation, it is expected that diagenesis could cause extensive poreblocking by changing the texture and increase the amount of clay minerals present.

Reservoir quality

The net sand content is low, ranging from 0.04 - 0.15 (table 7.11). The porosities are 11 - 13% in average down to 3000 m. But because of the expected large variations in the depositional environment, the values are not representative for the whole area. Closer to the faults the net sand content and the porosities and permeabilities are expected to improve because of clean sand being deposited in the high energy environment on the alluvial fans.

7.2.3 "Albian Sandstone"

Lithology

The lower part of the formation consists of shale and sandstone grading upwards into a shale, dolomite and sandstone sequence.

WELL	INTERVAL (m)	NET SAND (m)	NET PAY (m)	AVG. Ø (%)	AVG. V_{sh} (%)	AVG. S_w (%)	N/G
DO-1	2853 - 3066	8	0	11	30	100	0.04
DO-D2A	3020 - 3216	10	0	13	30	100	0.05
Sèmè 1							
Sèmè 2							
Sèmè 3							
Sèmè 4							

Table 7.11: Ise Formation.

* Water saturation in pay sand.

The uppermost part has a higher sandstone content and conglomerates do also occur (compare chapter 5.2.2).

The feldspathic sandstones and conglomerates of the "Albian Sandstone" are moderately to poorly sorted (figs. 7.11 and 7.12) and have similarities to the abovelying "Turonian Sandstone". The sandstones are dark brown to light grey, but the colour is strongly influenced by hydrocarbon staining. Low angle cross bedding and laminations are the most common structures, but also ripple marks and bioturbation occur (fig. 7.11).

The shales are medium to dark grey, in the uppermost part also greenish grey. Bioturbation is common in the shales.

The carbonates are tight and consist of calcite and dolomite. No analyses have so far been carried out to estimate the relative content of the two, but from descriptions of cuttings carried out well site, dolomite is the major constituent. The dolomite is brownish and grey with a blocky, microcrystalline or sucrosic texture. The limestone is grey to white, firm to hard with a dense microcrystalline texture. The carbonates and sandstones contain glauconite.

Depositional environment

The "Albian Sandstone" was deposited above eroded rift basins where the Ise Formation formed. A major transgression covered the area, and the sediment influx and downwarping of the area were kept in balance, and good lateral extent is expected of the different sandstone units (fig. 7.13). In the lower part of the formation, above the basal transgressive shales, fan delta sediments pinches out into calcilutites and dark shales.

The middle part, high in carbonate, probably represents shallow

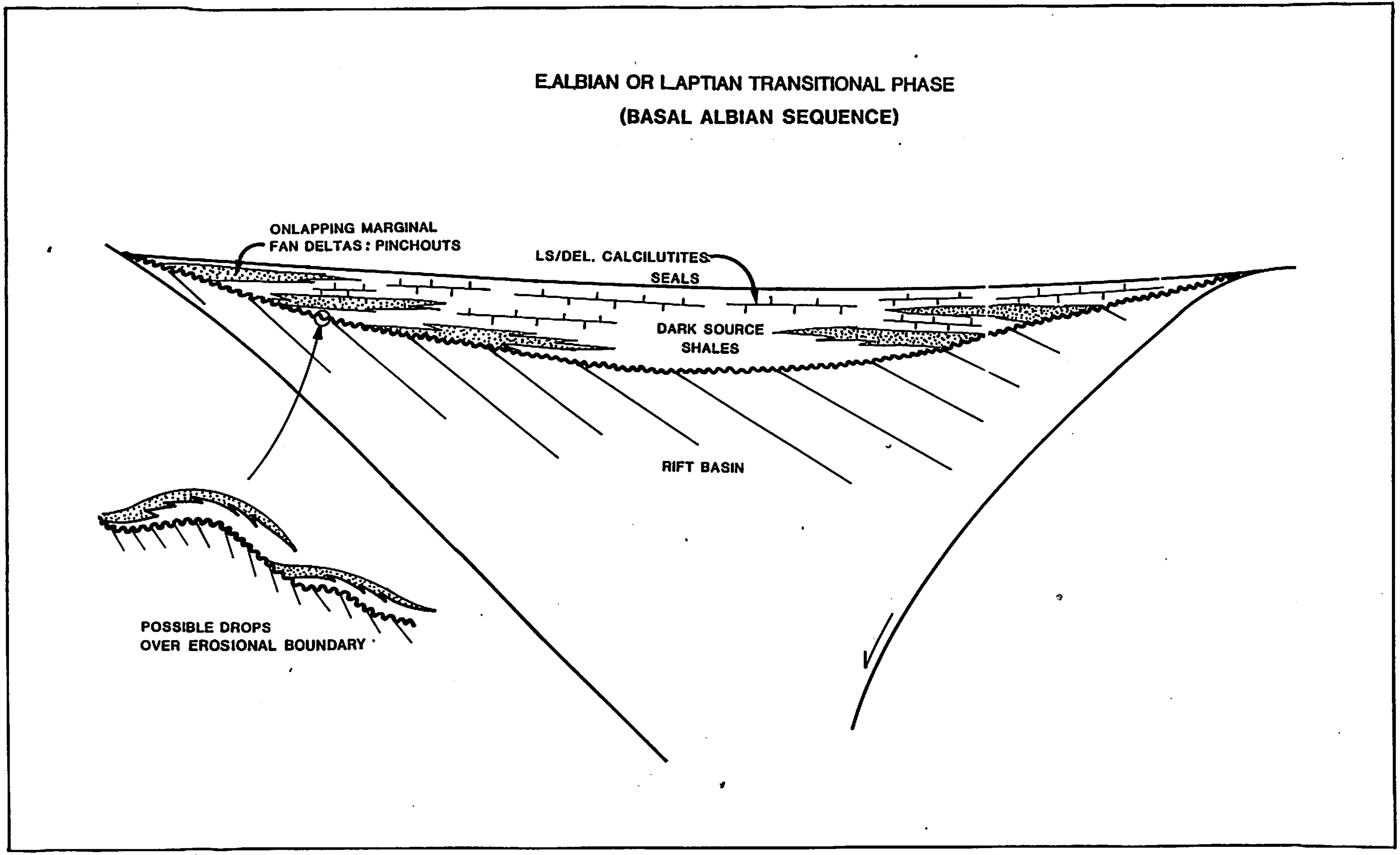

Fig. 7.13: Depositional model of the lower part of the "Albian Sandstone". Sketch by L. F. Brown.

marine deposits where tide and wave energy were the main transporting mechanisms. The higher sandstone content in the upper part is due to increased influx of clastic material and reworking by waves and possibly also tidal currents. The better sorting and the coarseness of the sediments have improved the reservoir quality of the sandstones in the upper part of the "Albian Sandstone".

The formation is truncated by a unconformity caused by an uplift and erosion down to different levels of the "Albian Sandstone".

Diagenetic history

Only a few mineralogical analyses are available from the "Albian Sandstone". From the textural descriptions and some x-ray and SEM-analyses, it seems that the diagenetic mineralogy has a lot of similarities to the better investigated "Turonian Sandstone" (7.2.3). There is one very important difference caused by the higher carbonate content of the "Albian Sandstone". This could easily create secondary porosity by dissolution or dolomitization and therefore preserve a higher porosity towards depth than expected from the porosity reduction gradient of 5-8% per km burial.

Diagenetic clay minerals as illite/smectite/chlorite and kaolinite are very common in addition to secondary quartz and albite (figs. 7.14 and 7.15). They are severely reducing the permeability.

It is expected that the forming of the abovelying unconformitity had a great impact on the diagenetic alteration with introduction of pore water with variable salinities. The quality of the uppermost sandstones is therefore dependant on the stratigraphic distance and setting towards the

Fig. 7.14:
DESCRIPTION: SEM - micrograph of a very coarse "Albian Sandstor from the Sèmè 4. Note the high content of clay minerals.
SCALE: White bar = 0.1 mm.

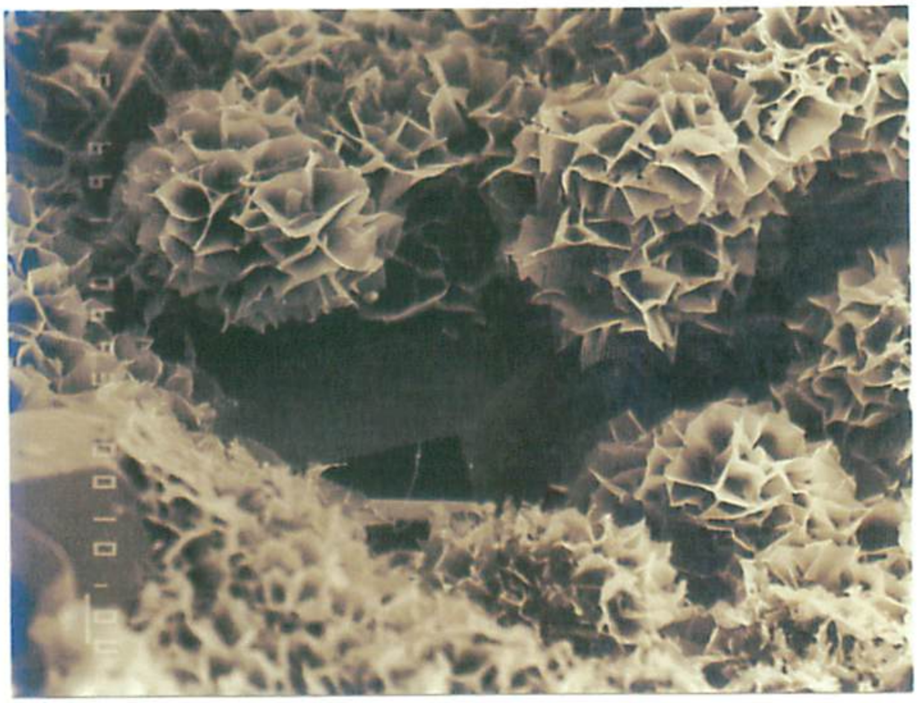

Fig. 7.15:
DESCRIPTION: Close up showing the complicated texture of the authigenic clay minerals which are mainly mixed layers between illite, chlorite and smectite.
SCALE: White bar = 0.01 mm.

unconformity. Particularly the content of kaolonite tends to increase if freshwater is penetrating into the sediment pores.

Reservoir quality

The net sand content is low, 0.11 and 0.20 in the two wells penetrating the whole formation (table 7.12). But it is expected good lateral continuity of the sandstones because of the marginal marine to shallow marine processes controlling the deposition. An increase of the shale content is expected southwards because of greater water depth during deposition (ref. fig. 6.7).

The best sorted sandstones has a maximum porosity of 15-20% and an average of 13-14% at approximately 2500 m in the Sèmè Field area. The porosity reduction by depth is expected to be similar to the "Turonian Sandstone", which is calculated to 5-8% per km burial.

The maximum permeabilities measured on core samples are 40-50 md with production test average from 27 md to no measurable permeability. The low permeabilities are largely due to the high content of authigenic clay minerals and partly quartz and albite overgrowth.

7.2.4 "Turonian Sandstone"

Lithology

The formation consists mainly (74-92%) of medium to coarse, feldspathic sandstones and conglomerates, interlayered with some black, grey or green shales (figs. 7.16 and 7.19).

WELL	INTERVAL (m)	NET SAND (m)	NET PAY (m)	AVG. Ø (%)	AVG. V_{sh} (%)	AVG. S_w (%)	N/G
DO-1	2450 - 2853	81	70	13	30	50*	0.20
DO-D2A	2565 - 3020	52	37	14	25	50*	0.11
Sèmè 1**							
Sèmè 2**							
Sèmè 3**							
Sèmè 4	2472 - 2714	106	13	16[1)]	9	58*	0.44

Table 7.12: "Albian Sandstone".

* Water saturation in pay sand.
**No "Albian Sandstone".

[1)]Core measurements in the upper part (2472 - 2490 m): Avg. helium porosity 14%, porosity by fluid summation 15%, horizontal permeability 15.5 md, vertical permeability 6 md.
In the upper part (2660 - 2666 m): Avg. helium porosity 14%, porosity by fluid summation 19%, horizontal permeability 3.5 md, vertical permeability 2 md.

The stratigraphic variation in lithology is not large in the Sèmè wells, but the changes are expected to increase towards south and west (compare chapter 5.3.1).

The sandstones are generally poorly sorted arkosic arenites (figs. 7.17, 7.18 and 7.20), and shale clasts of variable size are quite common. Sandstones, moderately to fair sorted, do occur in thin beds (figs. 7.16 and 7.21). The most frequent sedimentary structures in the medium to coarse sandstones and conglomerates are low angle (<20°) cross bedding and erosional cut and fill structures (fig. 7.16). Bioturbation, lamination ripple marks and flaser, lenticular bedding occur in the fine grained sandstones and siltstones.

The most fine grained rocks have a variable texture from green and light grey silty shales to black, organic rich massive claystones.

Depositional environment

The "Turonian Sandstone" is deposited by fan deltas prograding onto a stable continental shelf and reworked in a marginal marine to shallow marine environment (fig. 7.22).

The progradation is mainly from north towards south - southeast in the lower part of the formation (ref. fig. 6.8), while in the upper part a major lobe west of the Sèmè Field area causes more variation in the depositional pattern (ref. fig. 6.10). The eastern part of the shelf is therefore more reworked by shallow marine processes, while the area west of the Sèmè Field is marginal marine to continental. Because no data are available from the major lobe, it is not easy to interpret the transition from continental to marine sedimentary facies. Most of the "Turonian Sandstones" are immature with no distinct developed sedimentary cycles and have a high content of

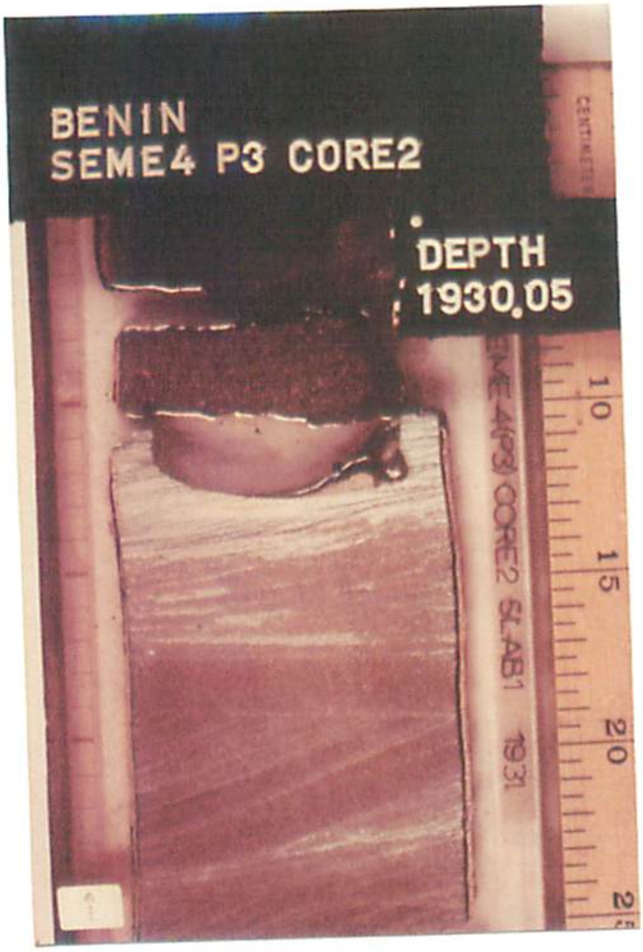

Fig. 7.16:

DESCRIPTION:

"Turonian Sandstone".
Finegrained, fair sorted sandstone with well developed cross bedding and truncation surfaces. Note the abrupt boundary to the abovelying medium sandstone.

Fig. 7.17:

DESCRIPTION:

"Turonian Sandstone".
Poorly sorted, conglomeratic sandstone with low angle cros bedding. This rock type is v common within the Turonian.

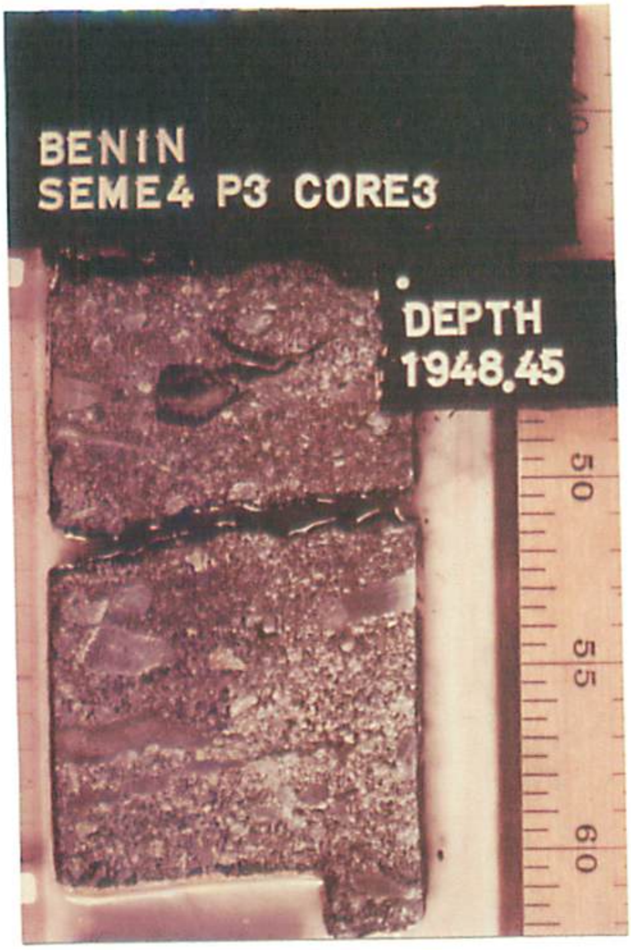

Fig. 7.18:

DESCRIPTION:

"Turonian Sandstone".
Conglomerate with a high cont
of shale clasts. Note the va
stratification.

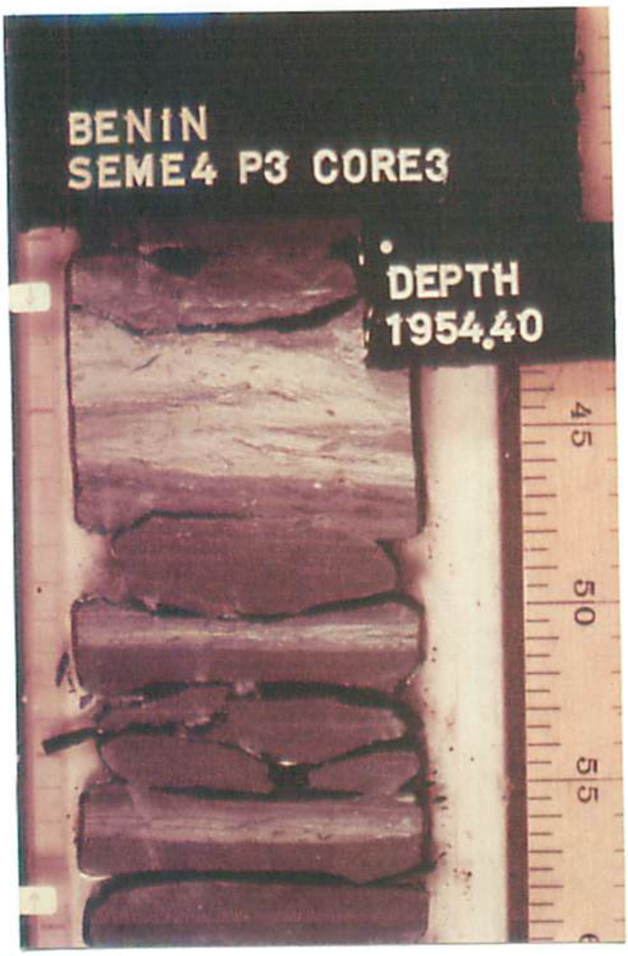

Fig. 7.19:

DESCRIPTION:

"Turonian Sandstone".
Dark grey shale interlayered
with very fine sand and coars
silt. Bioturbation, laminati
ripple marks and convolute
bedding is common.

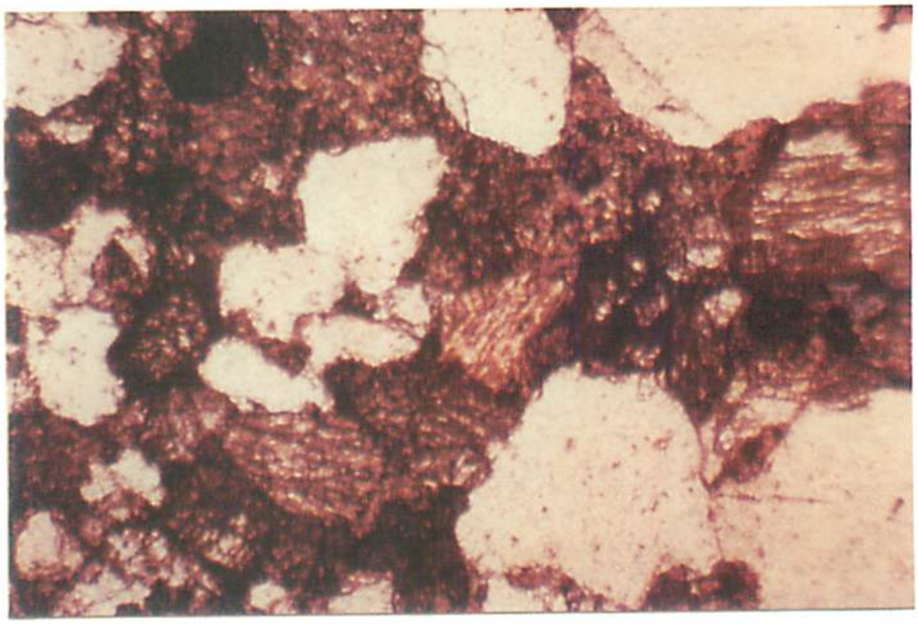

Fig. 7.20:
DESCRIPTION: Thin section micrograph of poorly sorted, coarse sandstone in the Sèmè 2 well. Note the high conte of phyllosilicates.
SCALE: Black bar = 1 mm.

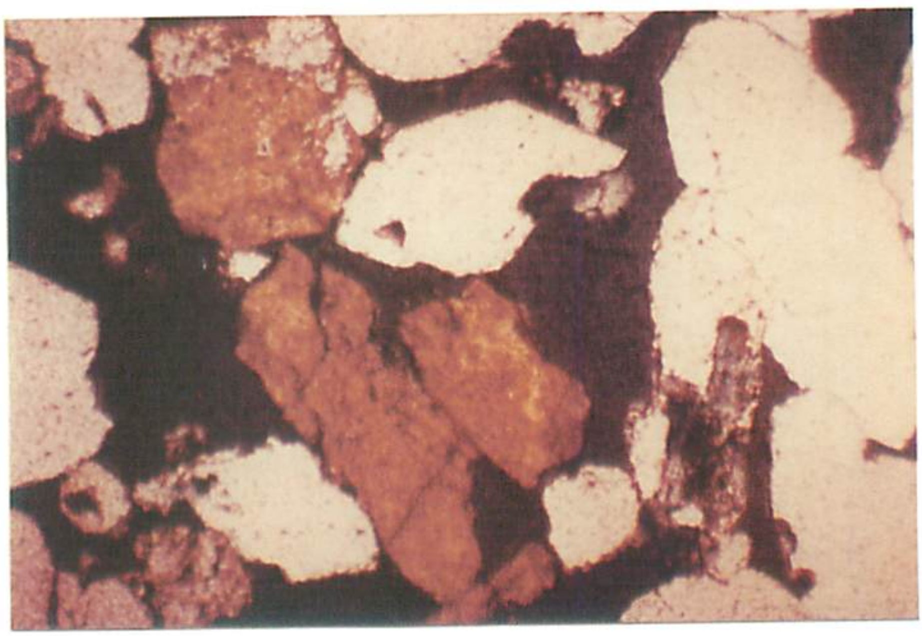

Fig. 7.21:
DESCRIPTION: Fair sorted, clean sandstone with high porosity an permeability. The blue color is blue resin impregnation in the pores. Note the clean pores compared to fig. 7.20. Samples from Sèmè 2.
SCALE: Black bar = 1 mm.

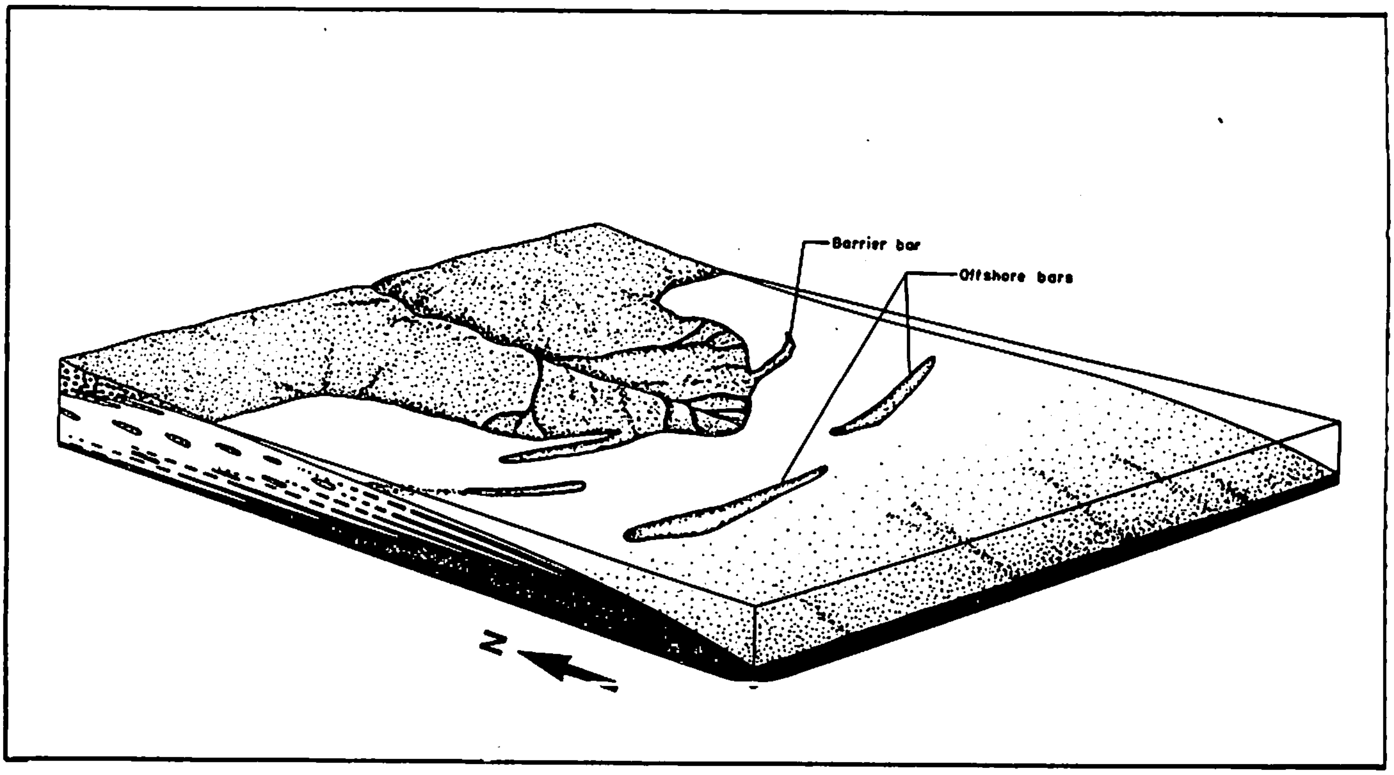

Fig. 7.22a: Depositional model of the "Turonian Sandstone". Fan delta prograding into a shallow sea and reworked by waves and longshore currents.

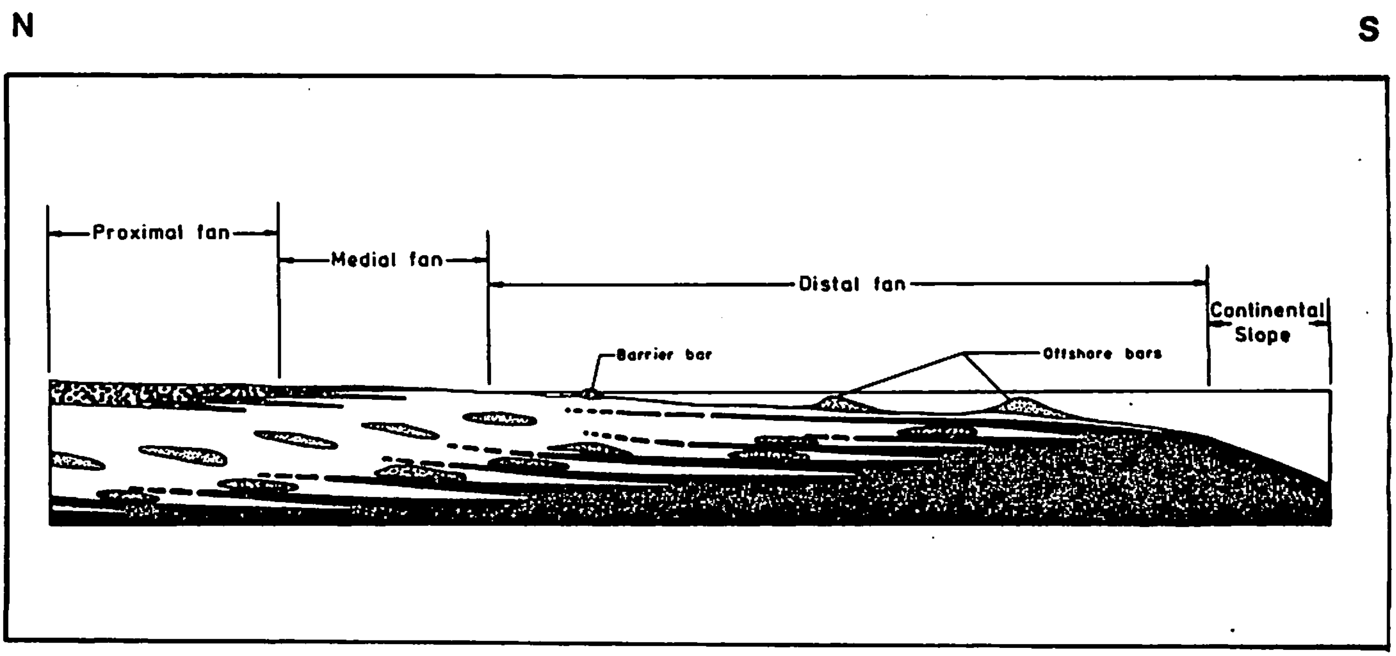

Fig. 7.22b: Simplified cross section through a "Turonian Sandstone" fan delta with bar development. Note the onlapping shales. The bars have the best reservoir quality.

feldspar and clay clast. The coarseness of the sediments also indicate short transport from the source to the final deposition. Marine fossils are detected in all the darker shales, and the most likely mechanism to carry the coarse clastics out in the sea are by fan deltas with braided streams as the major conduits. The large amounts of clastics were redeposited by wave generated currents, winnowing immature coarse clastics from shores exposed to an open sea. The poorly sorted sandstones were brought down to below average wave base during storm episodes, while the thin, fair sorted beds are due to reworking of sands during episodes of slow subsidence rate compared to the influx of sediments received to the shelf basin.

Towards the shelf break in the south, the water depth increased and the content of silt and claystones are expected to be higher. Particularly the anoxic environment registered in the Sèmè wells during deposition of the black, organic rich shales are expected to become more common towards the south.

Diagenetic history

During the deposition of the "Turonian Sandstone" pyrite started to form because of restricted water circulation. When the unconformity at the top of the formation developed, fresh water intruded the coarse clastics, forming kaolinite and transforming the clastic clay minerals. Also quartz growth (figs. 7.23 and 7.24) started at this stage and continued together with clay formation (figs. 7.25 and 7.26) until oil filled the reservoir, and up to present in the water zone. The clay formation changed character by deeper burial. The clastic smectite/illite and the early formed smectite recrystallized to a more well-defined illite, and the smectite content was reduced by the illitization and the formation of the chlorite group mineral corrensite. By deeper burial, potassium feldspar

Fig. 7.23:
DESCRIPTION: Well sorted, medium sandstone with clean quartz rimmed pore throats. Kaolinite is the main authigenic clay mineral. "Turonian Sandstone", Sèmè 2.
SCALE: White bar = 1 mm.

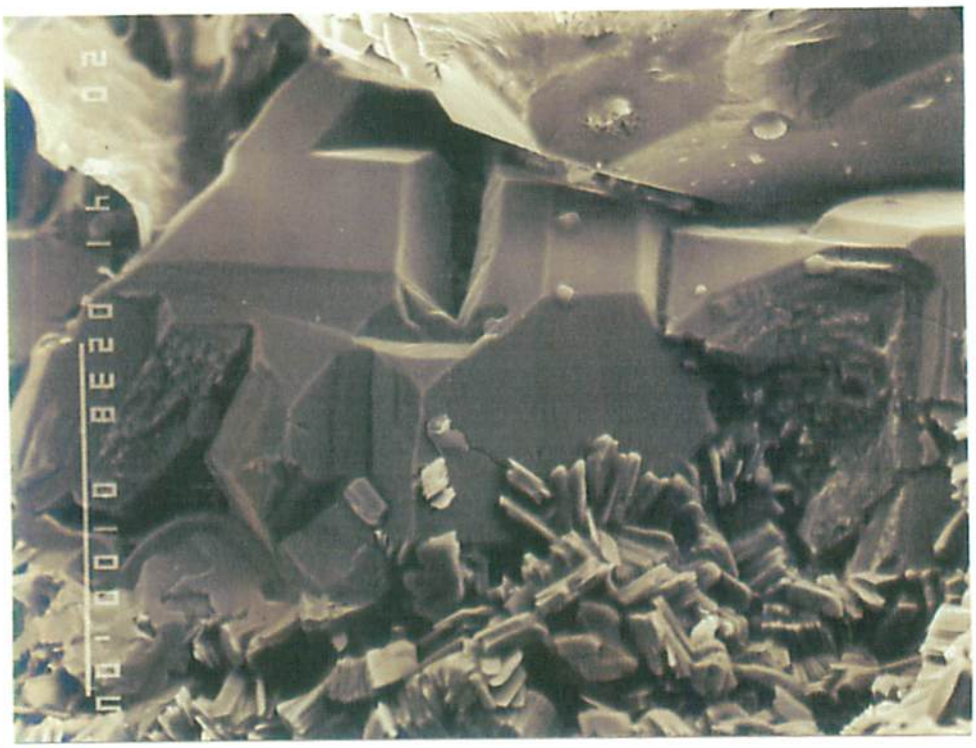

Fig. 7.24:
DESCRIPTION: Close up of quartz overgrowth covering earlier kaolinite. Same sample as fig. 7.23.
SCALE: White bar = 0.1 mm.

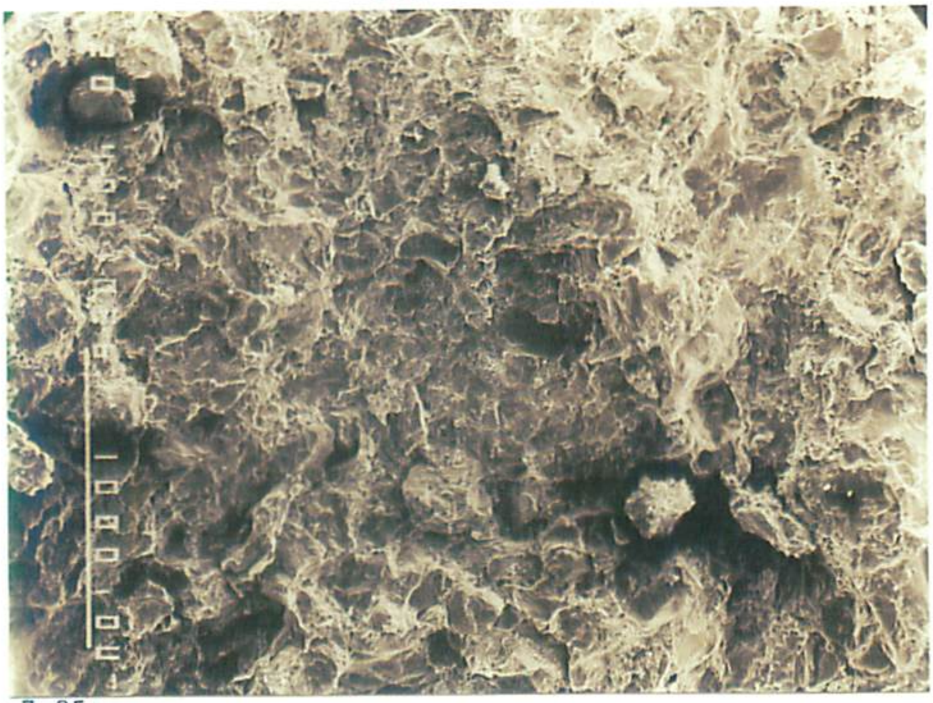

Fig. 7.25:
DESCRIPTION: Finegrained, poorly sorted sandstone with a high (
content. Note the lack of clean pore throats.
"Turonian Sandstone", well Sèmè 2.
SCALE: White bar = 1 mm.

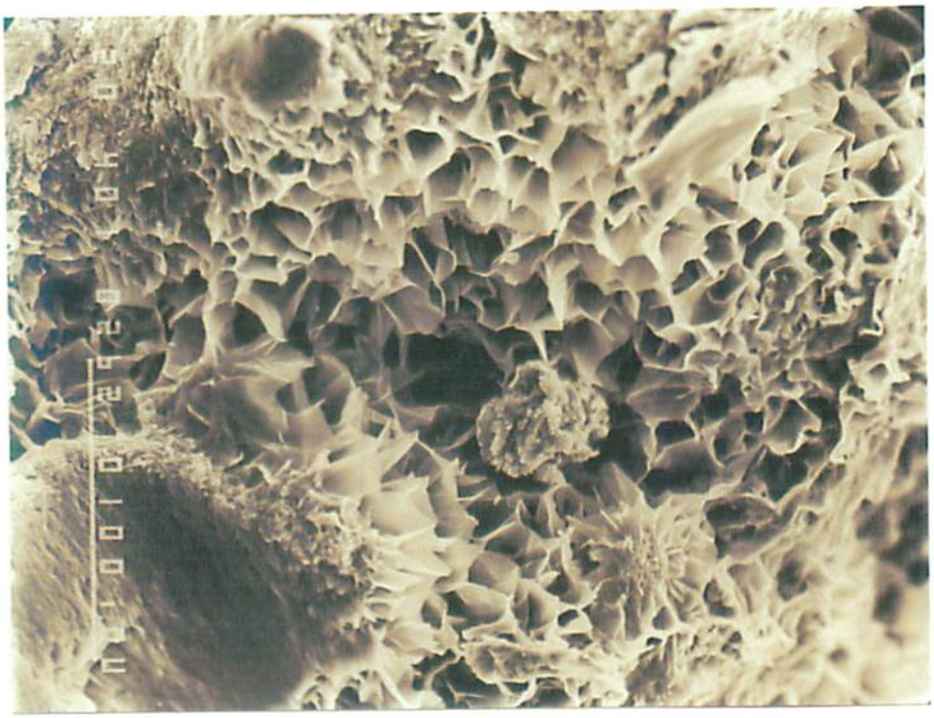

Fig. 7.26:
DESCRIPTION: Close up of the complicated network of the authige
illite smectite/chlorite aggregates. Same sample
fig. 7.25.
SCALE: White bar = 0.1 mm.

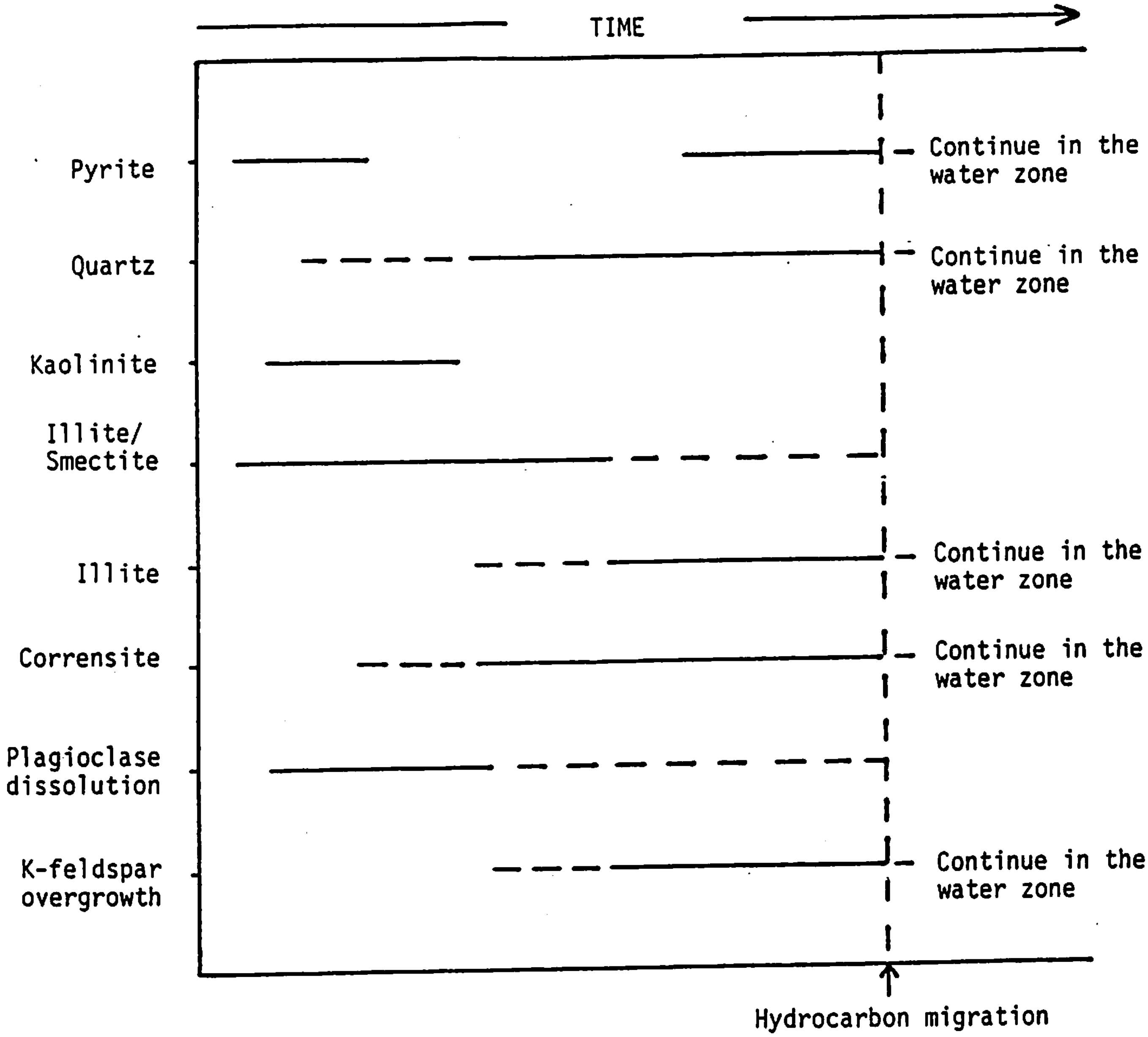

Fig. 7.27: Diagenetic sequence of the "Turonian Sandstone" reservoir in the Sèmè 1 and Sèmè 2.

overgrowth started and the pyrite formed nodules. The diagenetic sequence is shown in fig. 7.27.

The reduction in primary reservoir properties are mainly due to quartz growth and formation of illite, smectite/corrensite and kaolinite. The overgrowth of potassium feldspar and scattered carbonate nodules have minor effect on the reservoir properties. In some sections frequent pyrite nodules reduce porosity and permeability, while the more scattered occurence has little impact.

Reservoir quality

The net sand content for the whole "Turonian Sandstone" section is 74%, 86% and 92% in the three wells penetrating into the underlying "Albian Sandstone" (tables 7.13 and 7.14). It is expected on the basis of facies interpretation that the lateral continuity of the sandstone units are extensive. But a general increase in the shale content is expected towards the south.

The porosities are in the range of 15-23% at 2000 m depth in the Sèmè Field, while it is recorded an average of 27% at 1000 m in the Lome 2 well. Based on the knowledge of similar recent marginal marine and shallow marine deposits, the primary porosities are estimated to be 30-35% in the best sorted sandstones. From the diagenetic evaluation of the Sèmè wells, a 5-8% decrease per km burial is expected. It is not expected that secondary porosity has any major impact on the reservoir quality because quartz overgrowth and clay minerals are the most important diagenetic minerals.

The permeability is mainly controlled by the primary sorting of the sandstones and thereby the clay content. Because the rocks are generally poorly sorted with rapid textural variations, the permeabilities are strongly variable (fig. 7.28). According to

WELL	INTERVAL (m)	NET SAND (m)	NET PAY (m)	AVG. Ø (%)	AVG. V_{sh} (%)	AVG. S_w (%)	N/G
DO-1	1895 - 2450	511	15.5	16	25	45*	0.92
DO-D2A	1947 - 2565	529	14	24	15	30*	0.86
Sèmè 1	1974 - 2095	99	0	19	10	100	0.82
Sèmè 2	2256 - 2335	39	14	18	18	45*	0.65
Sèmè 3	2101 - 2195	74	23.5	20	10	29*	0.89
Sèmè 4	1922 - 2119	72	14	17.5	11	42*	0.74

Table 7.13: "Turonian Sandstone".

* Water saturation in pay sand.

WELL No.	LAYER No.	TOP TVD m MSL	GROSS m	NET/ GROSS RATIO	NET	$\bar{\emptyset}$ LOG	$\bar{\emptyset}$ CORE	$\bar{\emptyset}$ MODEL	$\bar{K}_{Geom}$ CORE	$\bar{K}_{Geom}$ MODEL	$\bar{S}_{wg}$ LOG
S2	1.1	1862.7	5.2	0.33	1.7	16.5	-	17.5	-	140	50.2
	1.2	1867.9	11.0	0.73	8.0	16.6	16.8	16.8	300	300	46.4
	1.3	T:1878.9 B:1885.7	6.8	0.59	4.0	20.7	22.3	22.3	1185	1185	40.4
S3	1.1	1868.1	5.3	0.53	2.8	19.5	-	19.5	-	360	45.9
	1.2	1873.4	14.2	0.92	13.1	19.6	-	19.6	-	370	27.2
	1.3	T:1887.6 B:1896.3	8.7	0.83	7.2	21.4	-	21.4	-	870	31.5
S4	1.1	1889.3	6.5	0.74	4.8	20.2	-	20.6	-	600	37.0
	1.2	1895.8	13.7	0.78	10.7	17.3	18.2	18.2	140	140	49.8
	1.3	T:1909.5 B:1922.8	13.3	0.70	9.3	18.9	18.8	18.8	270	270	82.8

LAYER No.	FIELD AVERAGE (weighed)	
	$\bar{\emptyset}$	$\bar{K}_G$
1.1	19.7	460
1.2	18.4	275
1.3	20.4	660

Table 7.14: Average values for the hydrocarbon bearing zone of the "Turonian Sandstone" in the Sèmè Field.

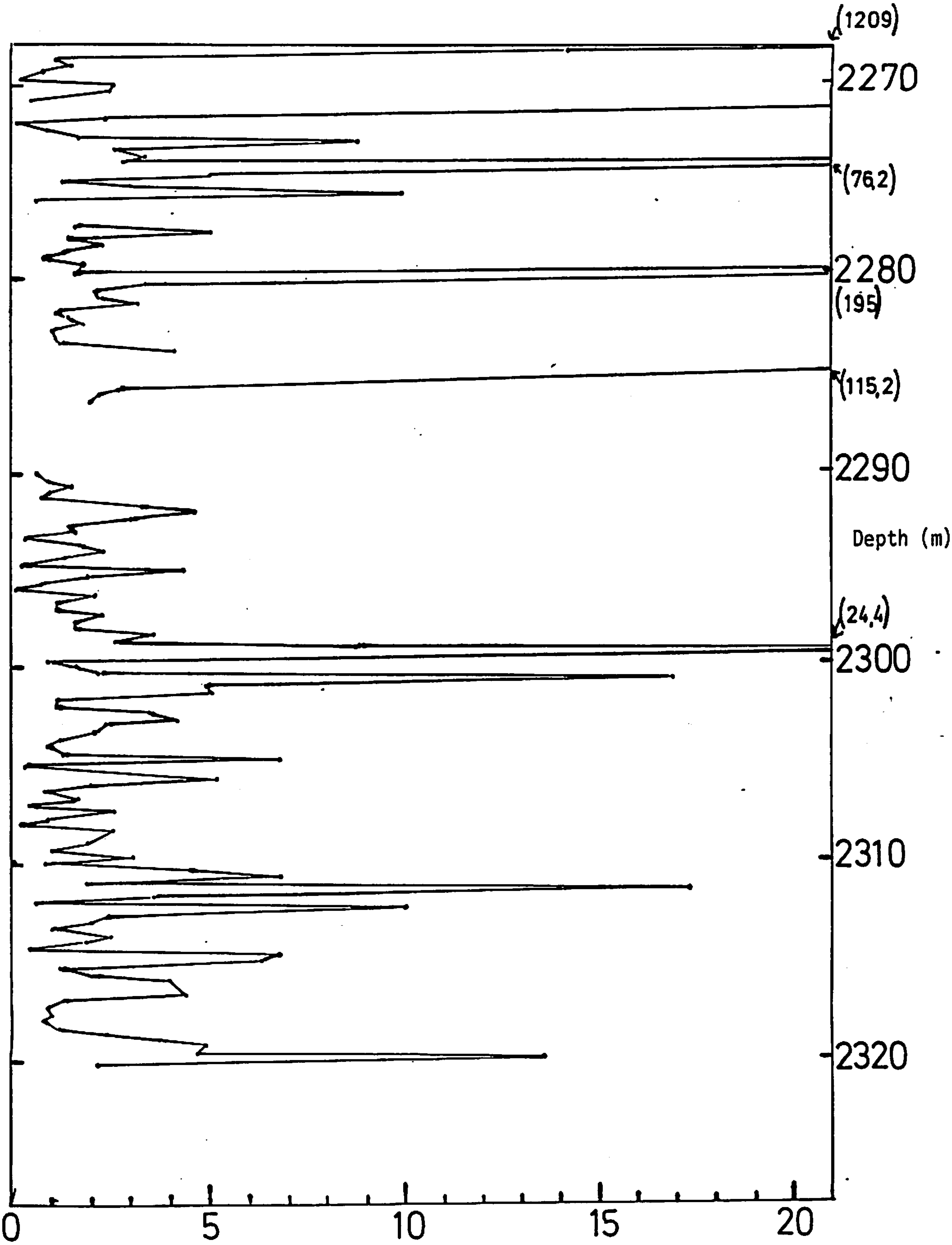

Fig. 7.28: $\frac{\text{Horizontal permeability}}{\text{Vertical permeability}}$ versus depth (m) in Sèmè 2 (Pl).

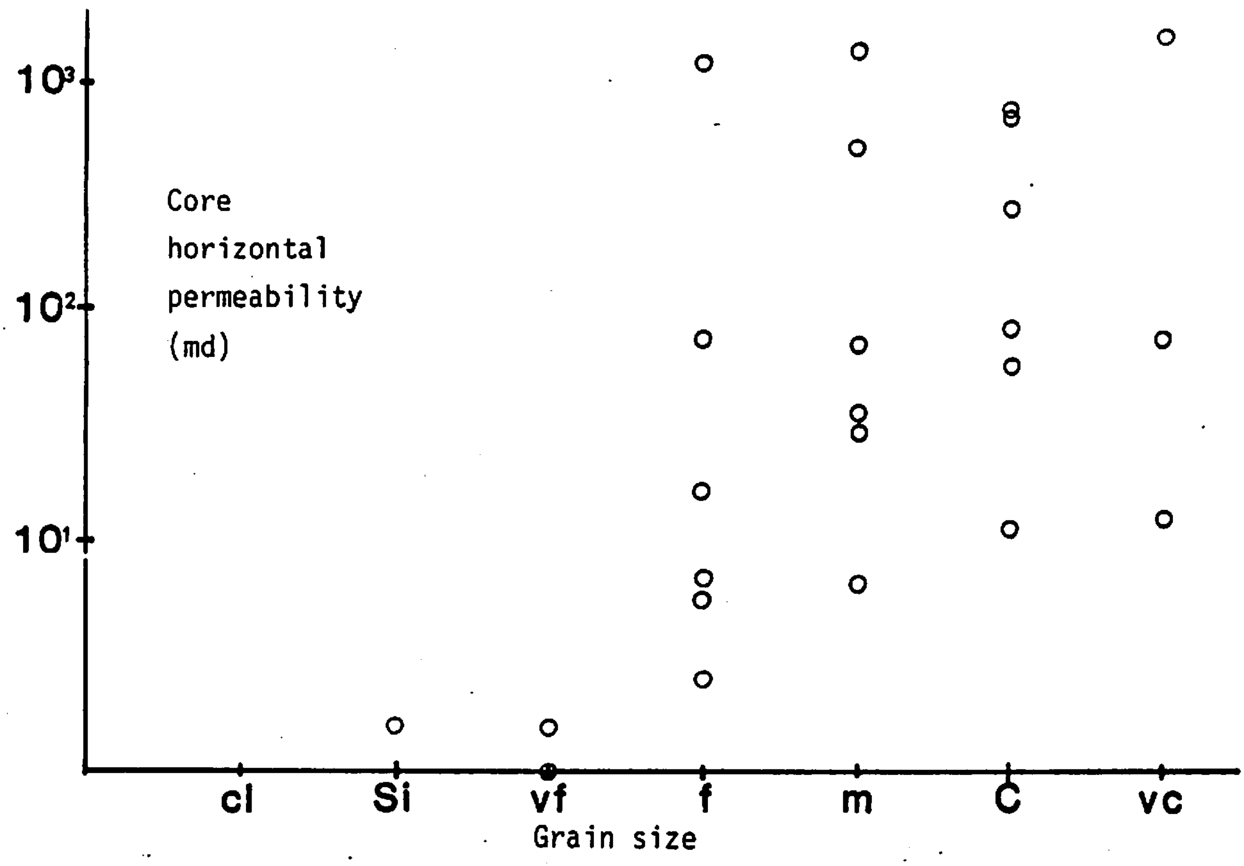

Fig. 7.29: Core horizontal permeability (md) versus average grain size from core descriptions, well Sèmè 2.

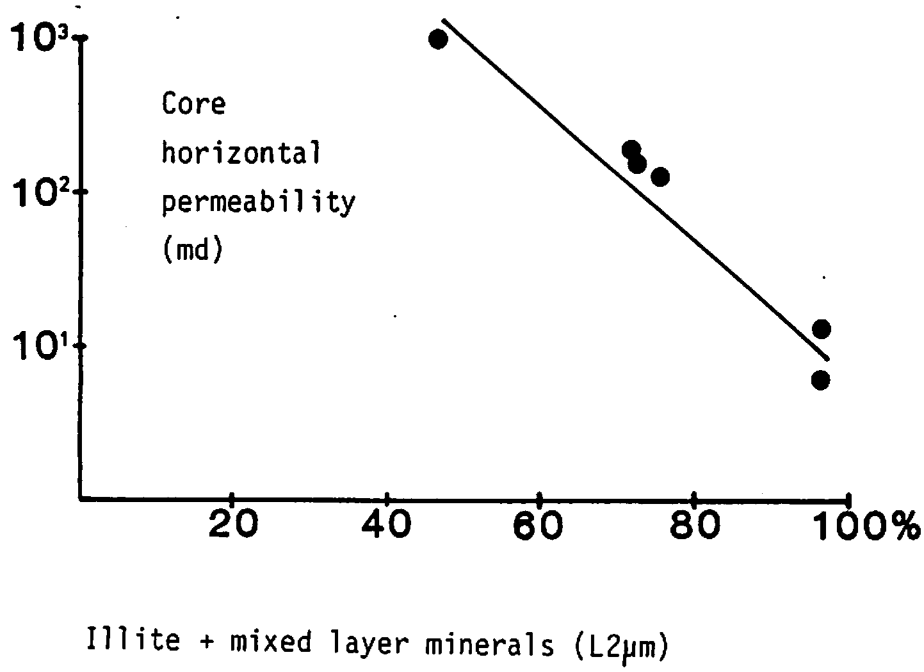

Fig. 7.30: Content of illite + mixed layer minerals in the clay fraction versus core horizontal permeability.

test data and core analysis the permeabilities range from a few darcy in the medium - coarse, fair sorted sandstones, to less than a millidarcy in the poorest sorted. In the poorly sorted rocks with high clay content the illite/smectite chlorite morphology strongly retards the liquid movements and creates microporosity with very low permeabilities (figs. 7.29 and 7.30). The cleaner rocks of the reworked sandstones have in contrast quartz rimmed pore throats which is smooth and preserve a high permeability (figs. 7.21 and 7.23).

7.2.5 Araromi Sandstones

Lithology

The lower part of the sediments deposited during Maastrichtian - Danian is thought to contain sandstones and conglomerates. As well data is not available, a sand ratio cannot be given. However, due to similarities with other turbidite fan systems, high sandstone content can be expected in the proximal parts. Also the sediment source is influencing the sand distribution considerably because of the different lithologies of the eroded underlying formations.

The upper part of the submarine canyon fills are comparable to the Araromi Shale penetrated in several of the Sèmè wells. It is not likely to contain sandstones, but only clay and siltstones.

The shales are carbonaceous, dark with a abundant pyrite. Limestone stringers are common in the upper part.

Depositional environment

The formation is deposited in submarine canyons cut into the underlying formations (fig. 7.31).

Even if no wells have penetrated the canyon fill sequence, the erosional truncations and consequent infill of sediments have been documented further west along the Ivory Coast and from Brazil (Brown and Fischer 1977).

As indicated from fig. 7.31 the first phase is the formation of major erosional channels cut back into the continental shelf. This is associated with deposition of eroded sediments further down the canyon.

The second phase in the canyon fill sequence is a clay, fine silt deposition during a later transgressive period. During this later stage the turbidite fan system was inactive and only suspension load sediments were deposited, causing clay deposition over the entire canyon fill.

Diagenesis

Because of the clay rich sediment source, it is likely that diagenesis is a very critical factor for the preservation of reservoir quality in the inferred Maastrichtian - Danian sandstones. However, potential reservoirs are shallow implying that the alterations are related only to early diagenetic transformations.

Reservoir quality

The lower part of the canyon fill contains proximal turbidite channel sandstones with good reservoir properties when sourced

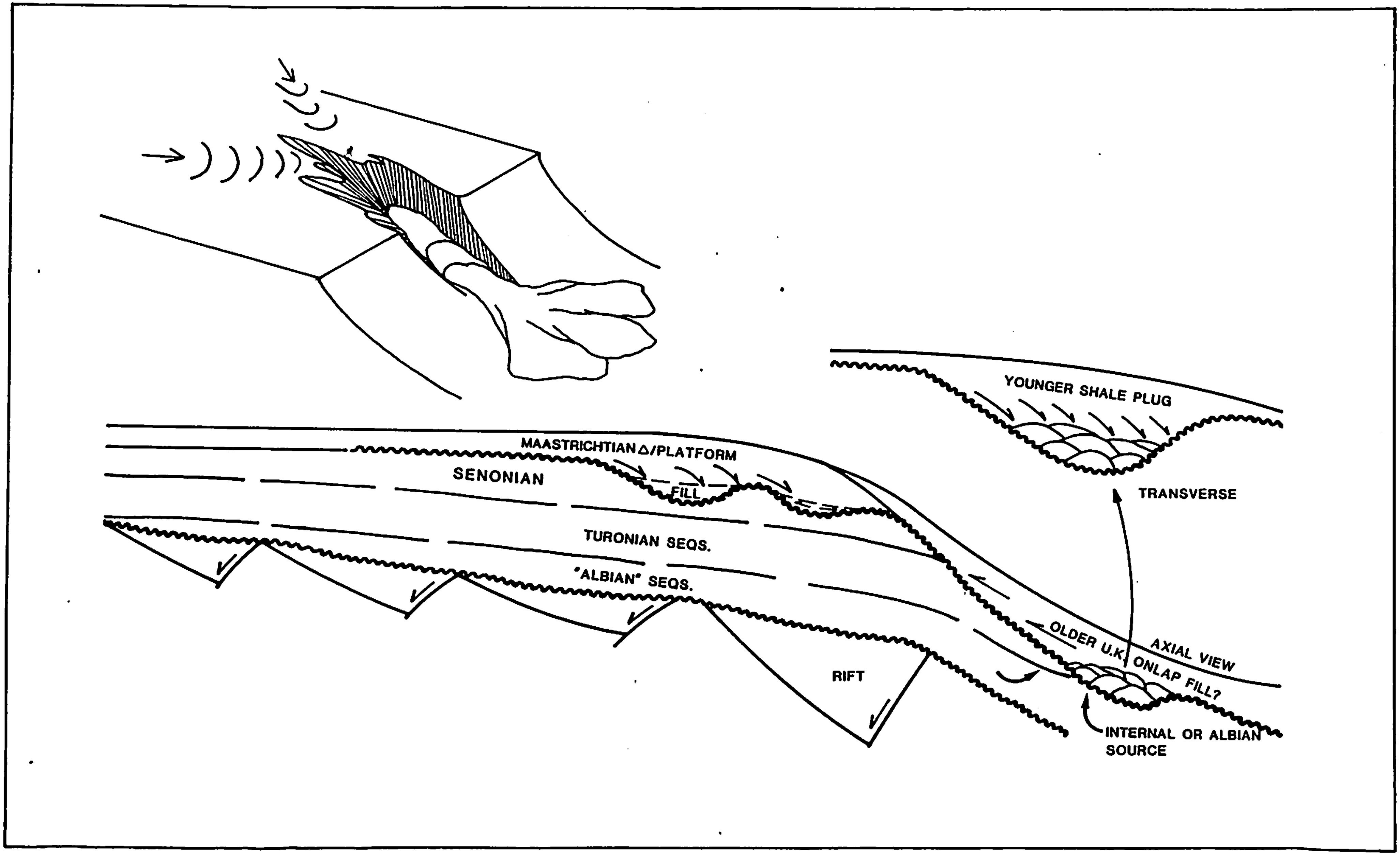

Fig. 7.31: Proposed Maastrichtian submarine canyon fill within erosional (Santonian to Campanian) canyon.

from an area with coarse grained clastics. The lateral extent of the sandstones are uncertain due to the coalescing nature of the turbidite system.

The later diagenetic reduction of the reservoir quality is primarily related to the sediment source and sorting. A high content of clay minerals and a poor sorting gives a rapid, early reduction of the porosity and permeability. Therefore, only the proximal parts of the fans deposited by high energy processes are expected to contain reservoir rocks with high porosity and permeability.

7.3 Cap Rocks

Opposed to for example reservoir rocks there is at present no way of quantifying a cap rock, i.e. to assess the quality by putting numerical units to it. The present account is therefore only qualitative. In this report a description of the lithologies acting as cap rocks are also described under chapter 5, "Lithostratigraphy".

7.3.1 Lower Cretaceous

Two potential reservoir formations are described that belongs to the Lower Cretaceous series, the Ise Formation and the "Albian Sandstone".

The Ise Formation, as known from Lome 1 and 2 in Togo, does have in part favourable reservoir characteristics at several stratigraphic levels. These sandstone beds are all encased by thick, massive shales that constitute cap rock. Our model of lacustrine shales enveloping fan deposits also includes excellent internal seals, thus preventing flushing during subaerial exposure. Also, the base of the "Albian Sandstone" is very shaly where the Late Aptian(?) subsequence is present thus providing a seal for the unconformity traps.

The cap rocks that are sealing the hydrocarbon zones within the "Albian Sandstone" have a much more subtle character. On top of Zone 3 lies a correlatable approximately 5 m thick shale that must act as a barrier. Zone 4 is capped by a thicker unit (40 - 50 m) of silty and sandy shale. The regional extent of these shales are not known, but due to the high content of shale in the "Albian Sandstone" sequence, the possibility of cap rocks present all over the Lower Cretaceous sub-basin should be rated as high.

7.3.2 Upper Cretaceous

In the Sèmè Field the "Turonian Sandstone" reservoir is capped by a thin shale at the base of the Awgu Formation and the thick and laterally extensive Araromi Shale. The Araromi Shale does only locally lie on top of the "Turonian Sandstone" on a regional scale. Sealing is therefore largely dependant on a shaly Awgu Formation in areas outside the Sèmè Field.

As discussed elsewhere the inferred Maastrichtian - Danian submarine fans are encased in shales that will serve as a proper seal.

7.4 Trapping

7.4.1 General

The following elaboration distinguishes between structural and subtle traps, of which subtle traps refer to stratigraphic, unconformity and paleogeomorphic traps as defined by (Halbouty 1972).

The discussion that follows is based on a structural as well as stratigraphic interpretation of the seismic data. Structure maps in depth and isopach maps have been constructed for all potential reservoir intervals and potential subtle traps are discussed with reference to both structure maps, the facies maps and the seismic lines.

As discussed in detail in chapter 4, the structural deformation of the Benin onshore and offshore basin is limited to an initial Lower Cretaceous rifting episode, Upper Cretaceous continental breakup and Turonian reactivation of rift faults. Although different types of structural traps are present in the area, subtle traps may be more frequent, and are anticipated to become more important in future exploration. A composite prospect map has been constructed (enclosure 1, fig. 7.32), in which the following features are outlined:

- structural highs
- potential unconformity traps
- Upper Cretaceous stratigraphic trapping potential
- Early Cretaceous rift grabens with potential stratigraphic traps.

A quite important observation made from this map is that the western half of the shelf is considered almost non-prospective in an immature exploration stage. This also applies to the onshore basin. This is due to the fact that this portion of the Benin basin only has a subtle trap potential with, at the present time, no mappable prospects. Following an initial exploration phase with increased lithologic information this situation may change.

7.4.2 Ise Formation Traps

The structure map in depth of the Ise Formation (fig. 7.33) shows a southeasterly dipping surface with increased dip in a seaward direction. Only within the Sèmè Field has structural closure been mapped. Outside this field closing contours are not readily appearent, but is indicated at some places and could thus possibly be located by a more detailed seismic grid. The structure map on basement level does neither indicate any closure within the rift sequence (Ise Formation).
Three potential unconformity prospects have been mapped (fig. 7.33). These are the most promising traps by virtue of their size. The traps are defined by H8 (Top Ise Formation) and H9 (Basement) (fig. 7.34). Critical elements of this prospect type are sealing properties of the overlying interval, rapid lateral changes in reservoir properties as well as the possibility of flushing prior to the deposition of a seal. Drilling in the Sèmè Field of two wells through the unconformity has proven shows of oil.

Stratigraphic traps can be inferred, but not accurately mapped. On the downthrown side of the rift faults onlap fill sands may have been deposited during active subsidence in deep rift lake centers, supplied by marginal deltas or fan deltas. The lenticular sands pinch out updip. Seals and source beds envelope the reservoirs, preventing any flushing and preserving their trapping potential during subsequent erosional episodes.

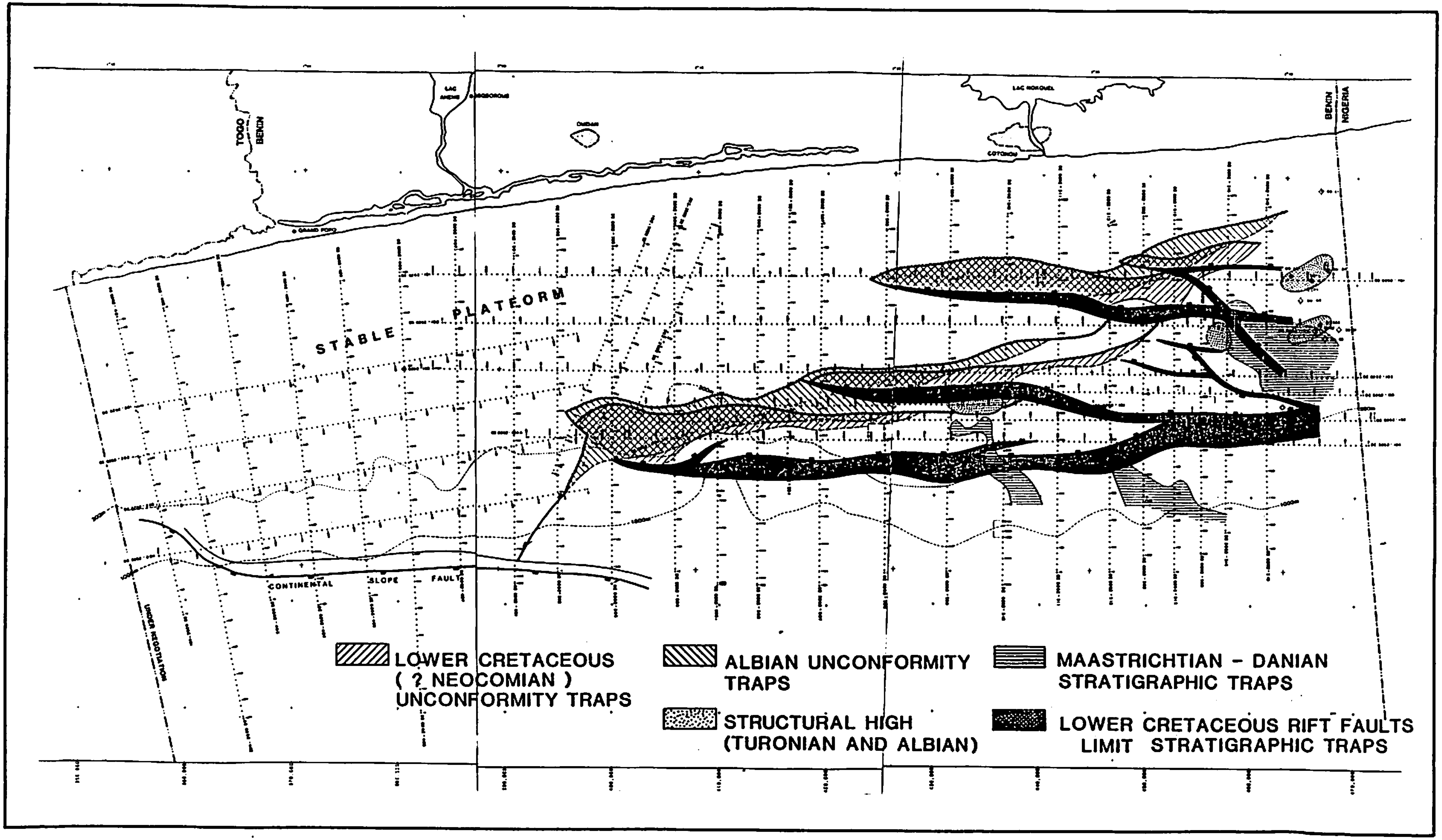

Fig. 7.32: Prospect map. See text for discussion.

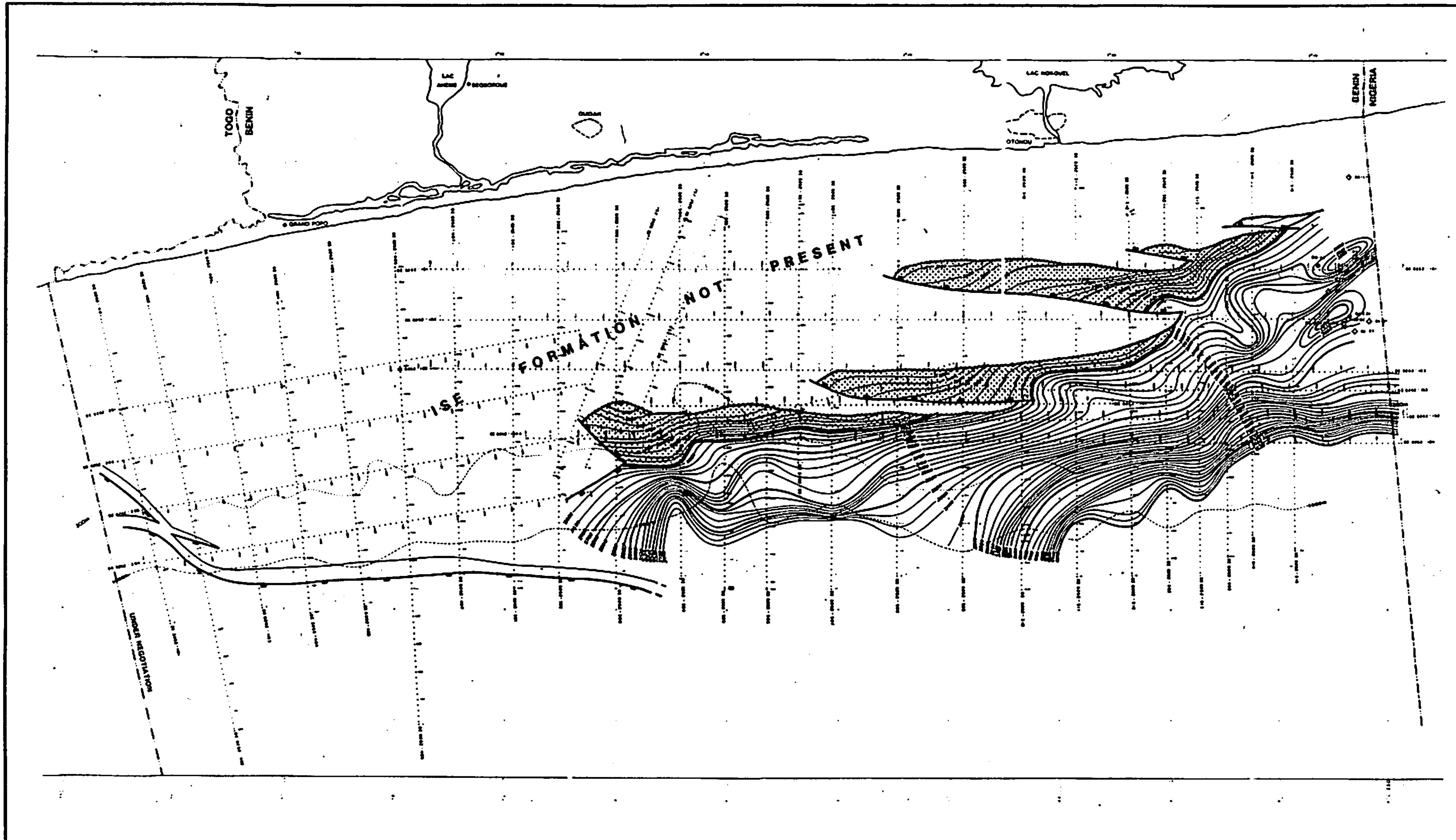

Fig. 7.33: Structural depth map Top Ise Formation with unconformity traps indicated.

Areas having a stratigraphic trap potential are indicated in fig. 7.32 where the E-W trending Fault System I is shown.

Principal trapping mechanisms of the Ise Formation are shown in fig. 7.35.

7.4.3 "Albian Sandstone" Traps

The structural depth map on top of the "Albian Sandstone" (fig. 7.36) shows a gently dipping surface on the continental shelf with an increased southeasterly dip beyond the shelf break. Closed contours are known from the Sèmè Field below both the northern and southern "Turonian Sandstone" accumulations. Possible closures have been mapped outside the Sèmè Field at two different locations. The areal extent is small for both, approximately 5 km^2, and the relief does not exceed 100 m for either of them. The eastern one is associated with a flat spot (ref. Appendix A.4) at approximately 2.25 s TWT (fig. 7.37) at a stratigraphic level known to contain gas in the Sèmè Field. Both structures are associated with basement highs, i.e. the upthrown side of the major east - west trending faults of Fault System I. Although the likelyhood of finding any major structure is considered small, there is a possibility of additional small structures that could be located by more detailed seismic and velocity models.

Two prospects of the unconformity type have been defined for the "Albian Sandstone" interval (fig. 7.36). Trapping is defined by the structure maps H7 (Top "Albian Sandstone") and H8 (Top Ise Formation) (fig. 7.38), and the isopach of this unit illustrates the seaward thickening (ref. fig. 5.5). The sealing capability of the overlying unit is again critical; in the Sèmè Field a seal does exist on top of the unconformity,

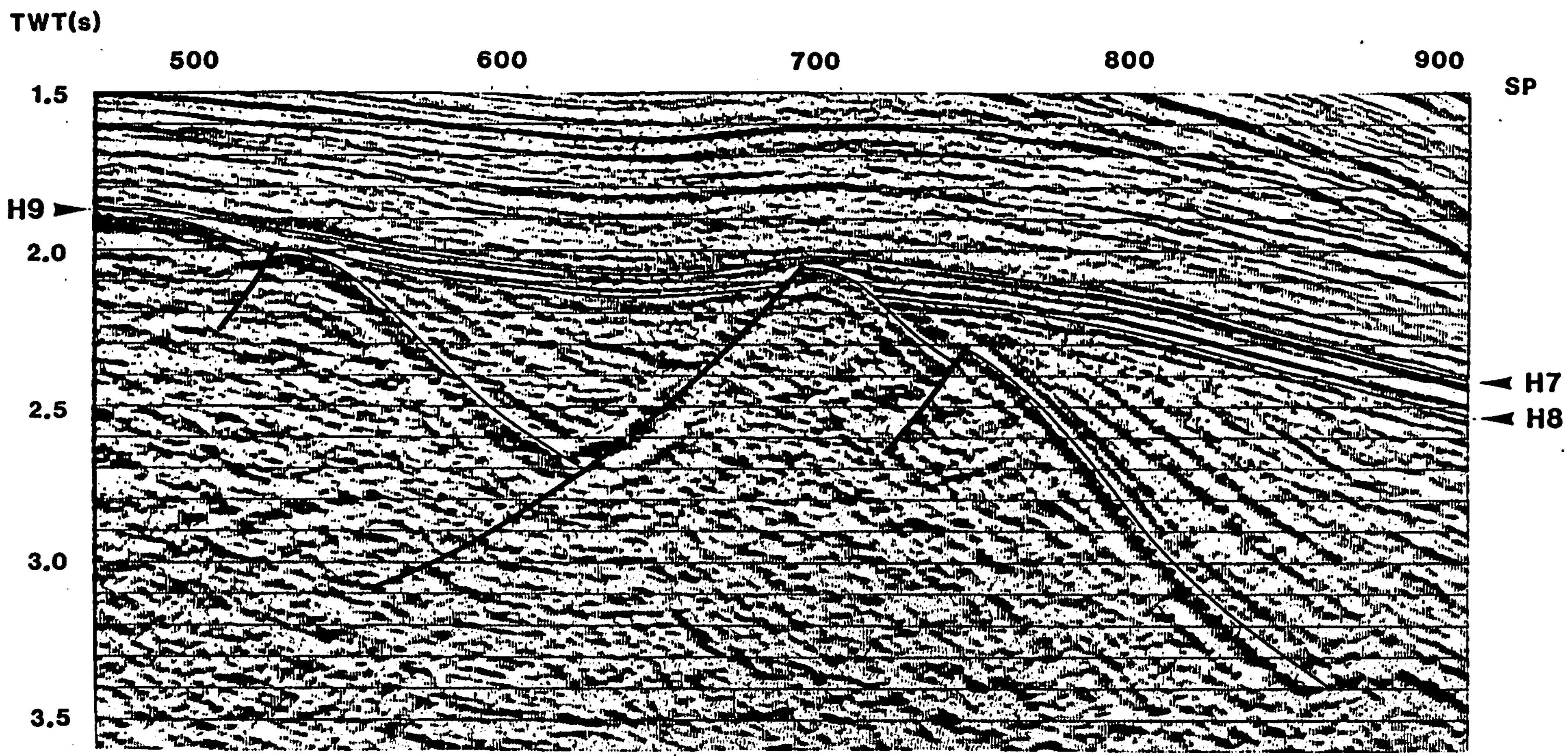

Fig. 7.34: Dip line (BE8262-310) illustrating Ise Formation and "Albian Sandstone" unconformity traps. Compare fig. 7.32.

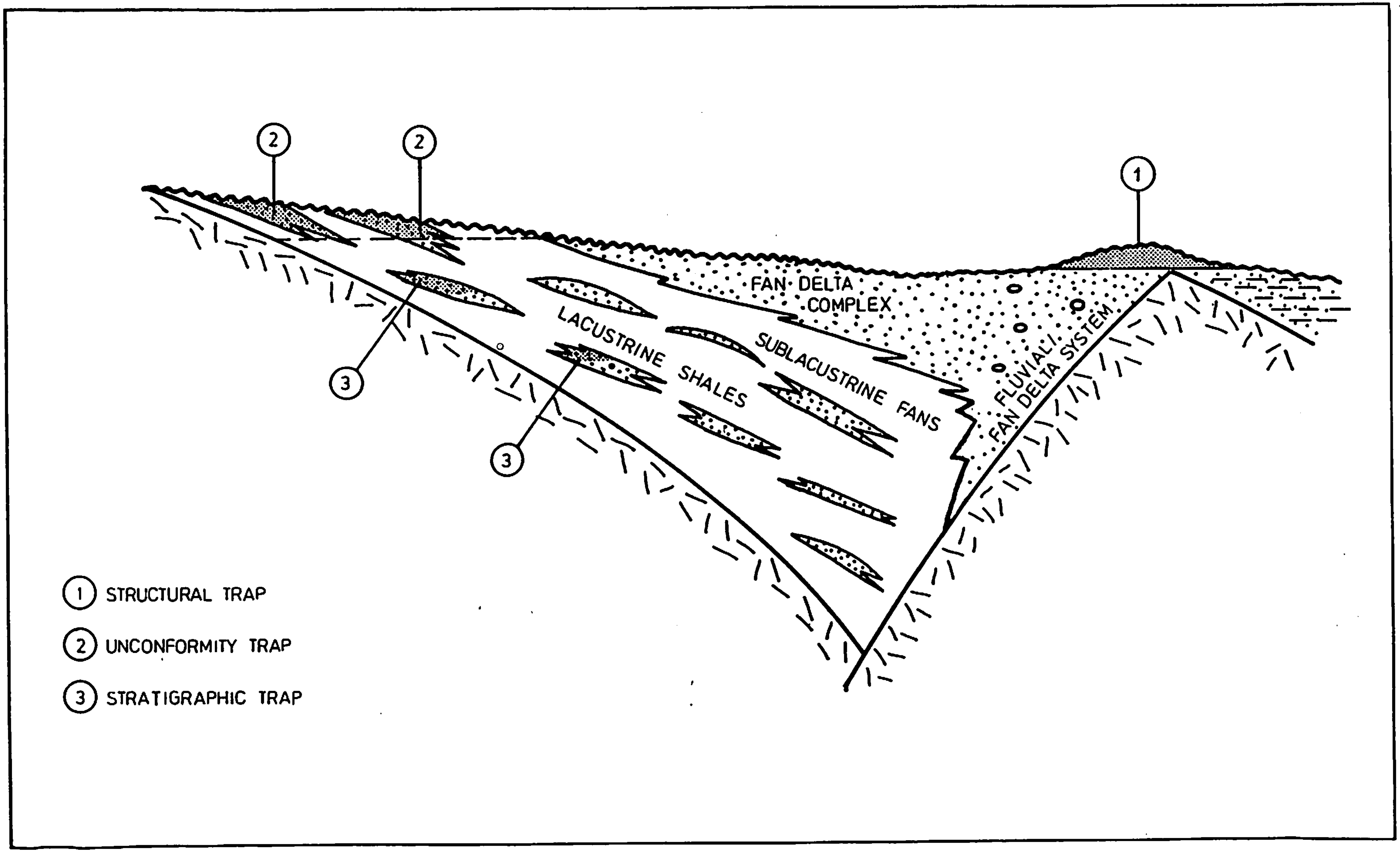

Fig. 7.35: Schematic illustration of principal trapping mechanism in the Ise Formation.

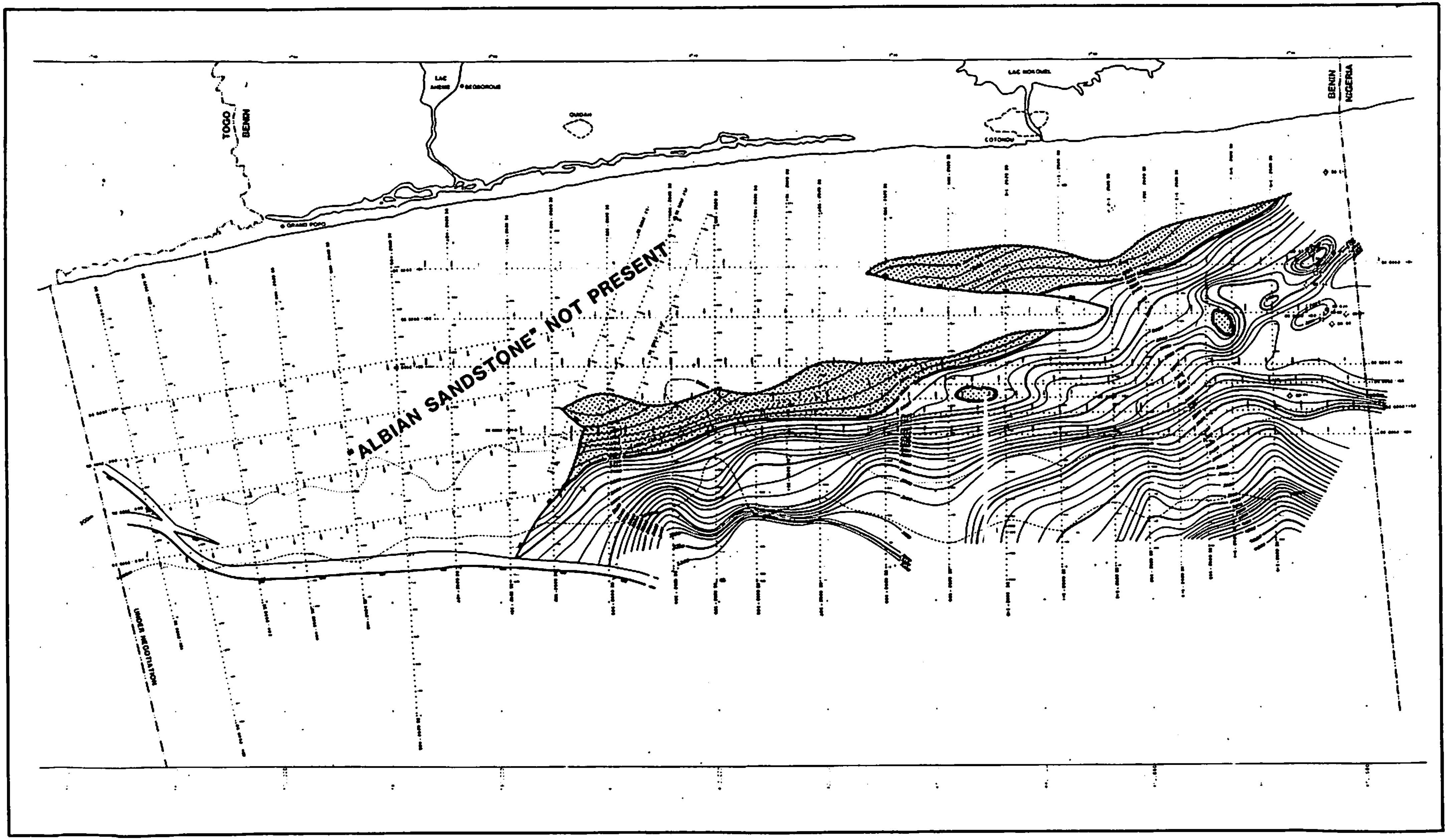

Fig. 7.36: Structural depth map Top "Albian Sandstone" with unconformity and structural traps indicated.

but the lateral extent of this is unknown. Water washing of any oil accumulation is likely to have occurred as is indicated for the "Albian" oil in the Sèmè Field, and this phenomenon may also have been responsible for the cementation discussed in chapter 7.2.

The southern prospect (I) has a maximum relief of approximately 400 m, while the northern (II) is somewhat smaller, both in areal extent (145 km^2 versus 105 km^2) and vertical relief (250 - 300 m). An optimistic model suggests closure along the 2350 m contour giving the possibility of combining I and II into a single gigantic prospect.

The northern prospect is associated with shallow amplitude anomalies that may be interpreted as being caused by minor gas accumulations below sea bed (fig. 7.39). No such anomalies are observed directly overlying the southern trap, although shallow amplitude anomalies further west may be associated with it assuming lateral migration through a Miocene channel (ref. Appendix A.4).

Stratigraphic and paleogeomorphic prospects can not be mapped within the "Albian Sandstone", only speculated upon based on a sedimentological model described in chapters 6.2 and 7.2.3. Two subsequences are recognized, a final Late Aptian(?) quiescent rift lacustrine sequence and an Albian early drift sequence (transitional).

The "unstructured" late rift sequence was possibly transgressed by the initial marine inundation when continental break-up occurred. Reefs or local carbonates on paleohighs may be found on distal margins of stable platforms overlying the rift system and facing the proto ocean. Onlap of fan delta facies against the post-rift unconformity provide a stratigraphic trap potential. Carbonate buildups may constitute paleogeomorphic traps that, however, necessitates more detailed seismic

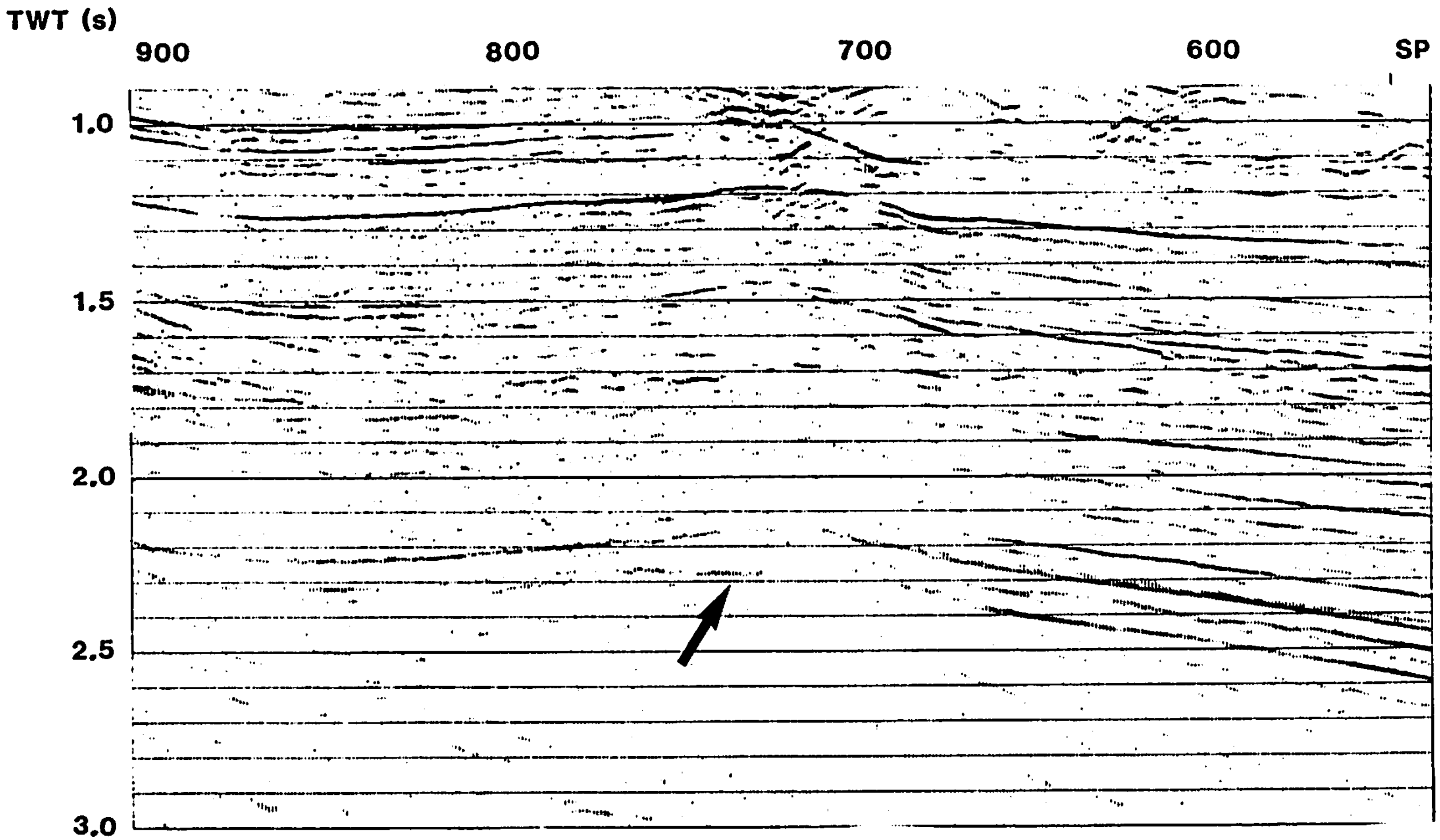

Fig. 7.37: Line BE8262-314, possible flat spot within the "Albian Sandstone" sequence.

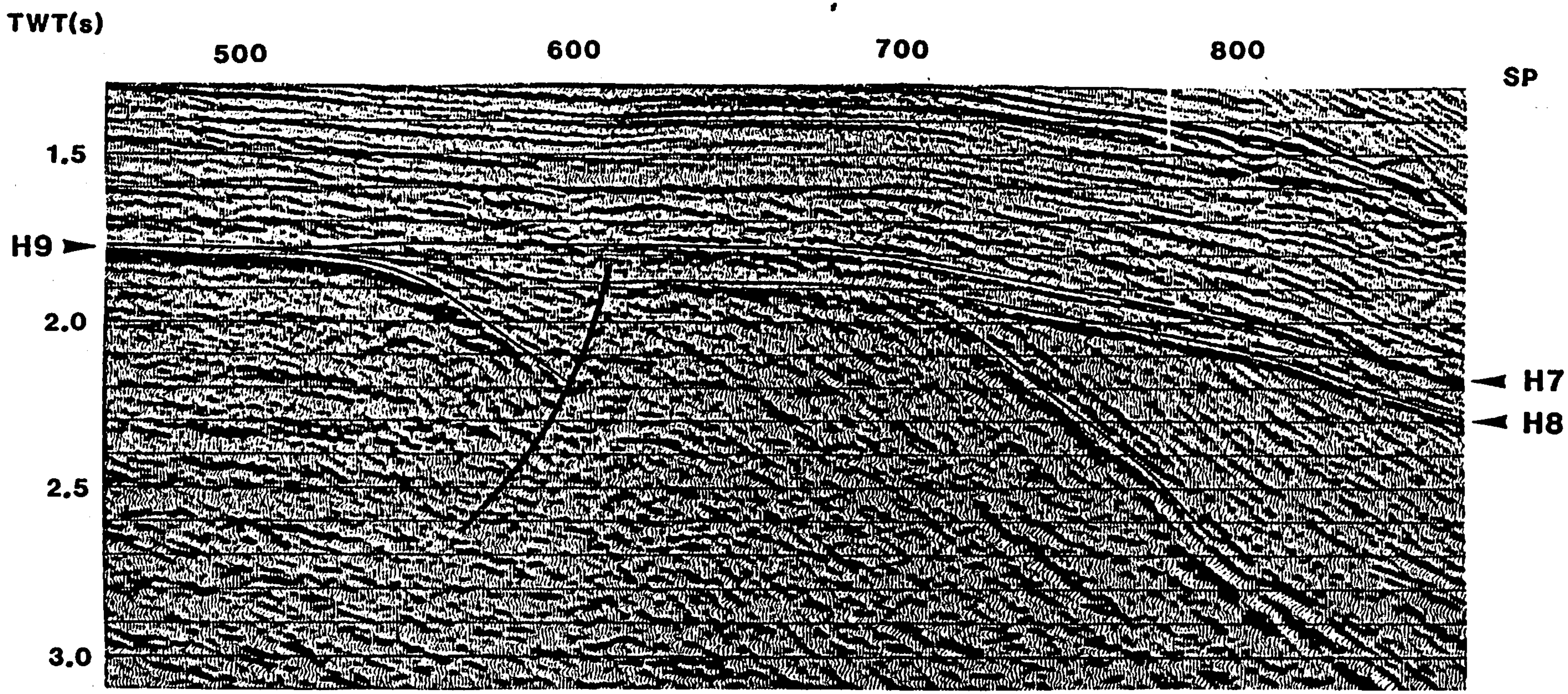

Fig. 7.38: Dip line (BE8262-307) illustrating Ise Formation and "Albian Sandstone" unconformity traps. Compare fig. 7.32.

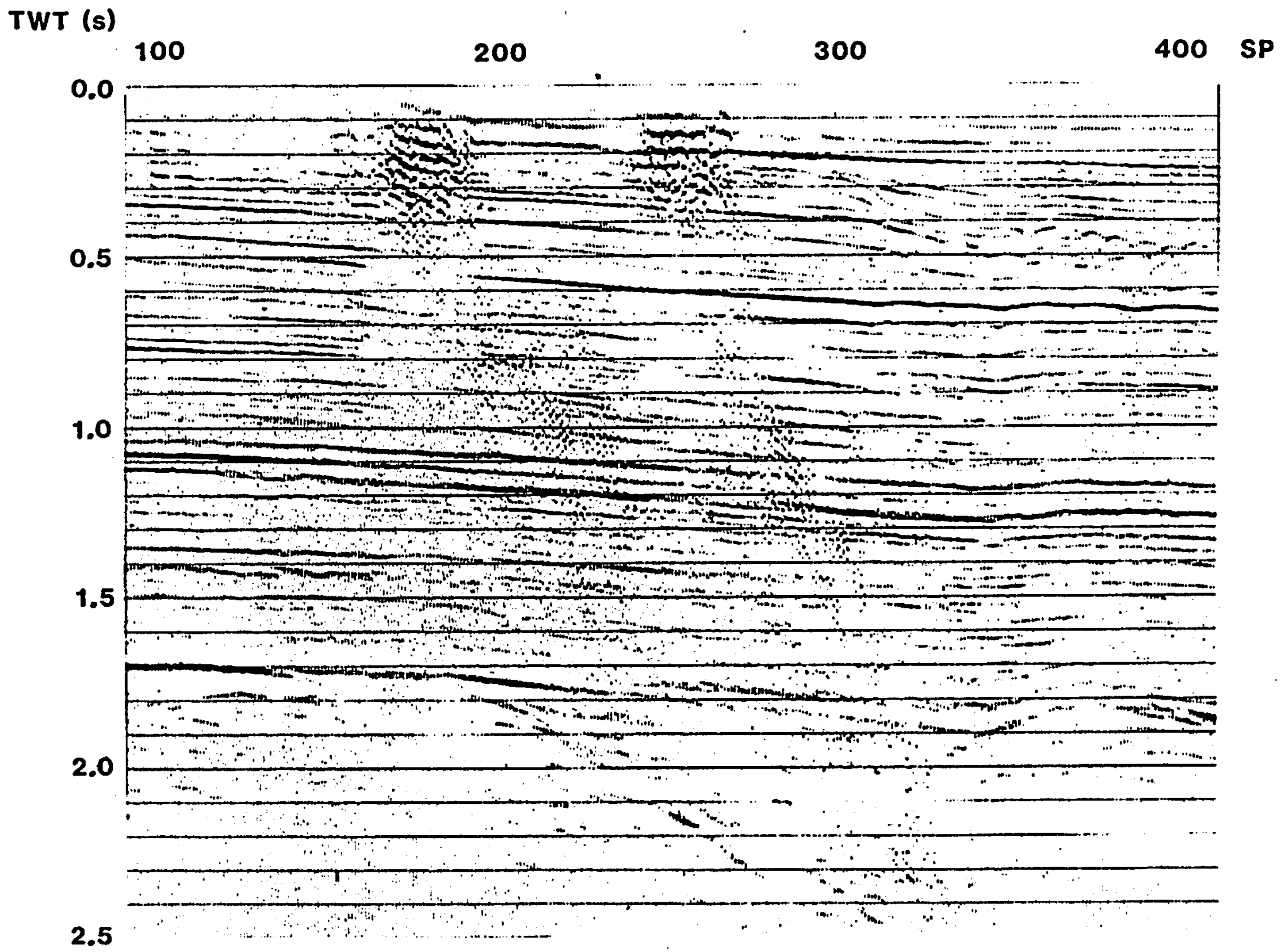

Fig. 7.39: Shallow amplitude anomalies directly overlying unconformity prospect of the "Albian Sandstone" and Ise Formation. Line BE8262-310.

interpretations to be properly defined.

In the "Albian" early drift sequence local reefs and fan delta reservoirs (ref. fig. 7.13) may constitute paleogeomorphic and stratigraphic plays in a mature exploration stage following detailed facies modelling.

7.4.4 "Turonian Sandstone" Traps

The structural depth map on top of the "Turonian Sandstone" (fig. 7.40) illustrates a southeasterly dipping surface with increased dip past the shelf break, with few irregularities that are significant in regards to trap definition. A NNE trending fault transects the horizon in the middle part of the shelf without causing structural closure. The Senonian Unconformity cuts deeply into the "Turonian Sandstone", mostly out on the continental slope, but also in the easternmost part of the shelf where it is partly responsible for the trap definition of the Sèmè Field (compare Appendix A.3). Nowhere else on the shelf, however, does this unconformity seem to be a trapping component. A possible closure may exist beyond the shelf break as indicated by line BE8262-315 (compare fig. 4.19).

The only closure mapped has a limited areal extent (8.5 km^2) and vertical closure (less than 40 m). Also, it is only seen on one seismic line (BE8262-151, fig. 7.41), although the surrounding contours indicate a structural anomaly.

It is concluded that additional structural traps may be present on the shelf for the good reservoir quality "Turonian Sandstone", but the present mapping does not outrule major closures. This is a result of very limited tectonic activity (except for basinward differential subsidence in response to

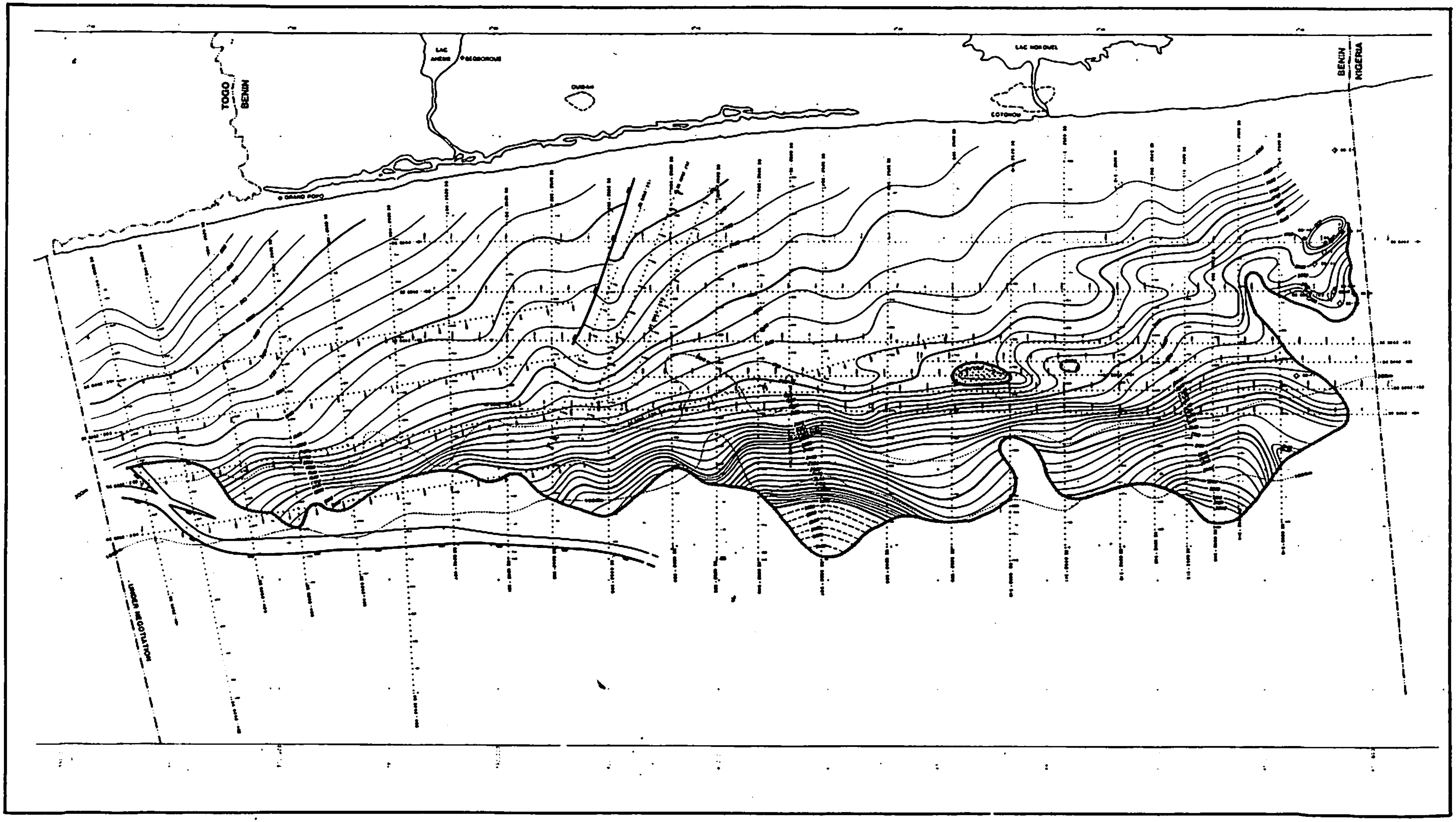

Fig. 7.40: Structural depth map H6. Possible closure cutlined.

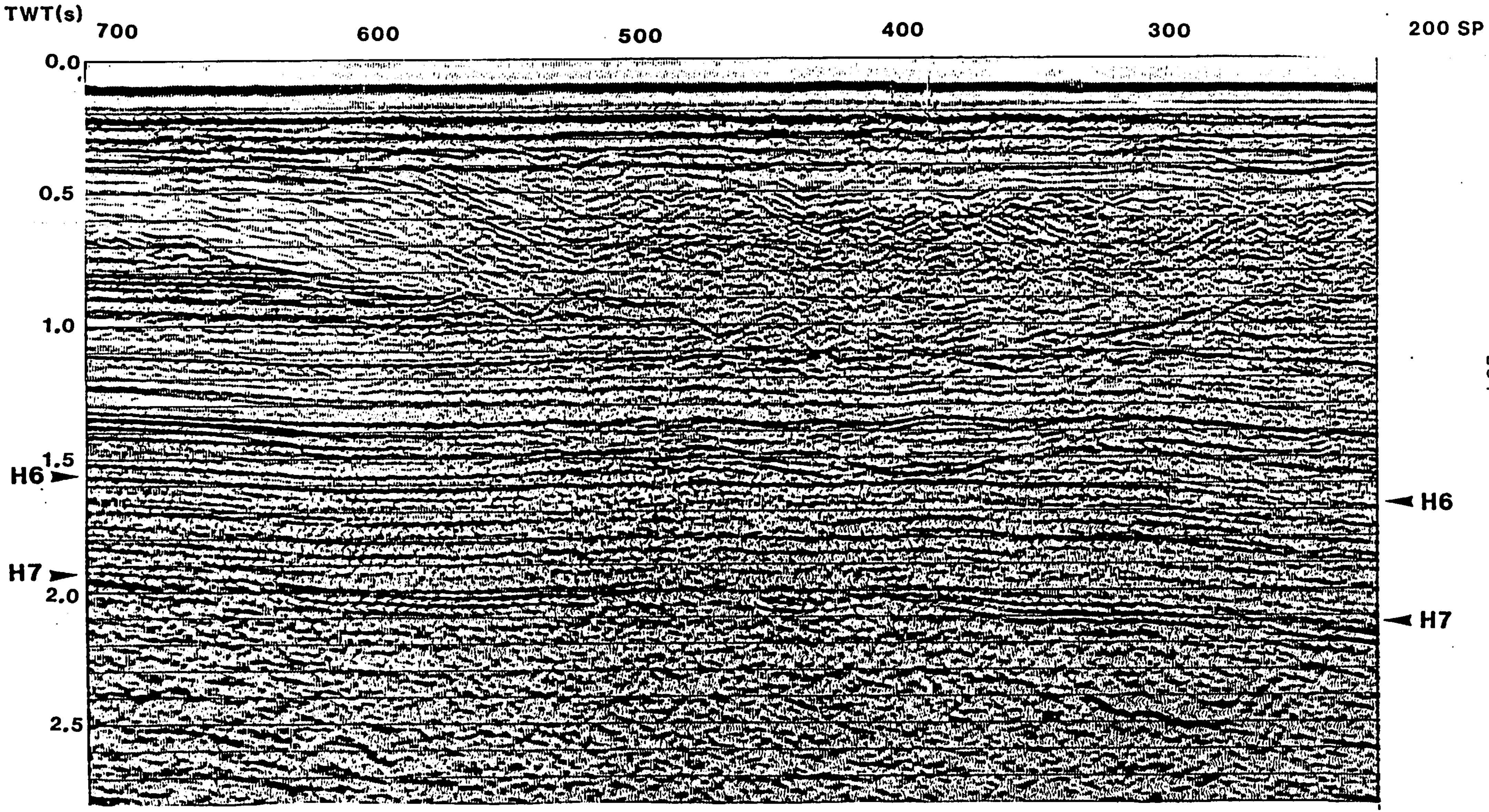

Fig. 7.41: Possible roll-over on the "Turonian Sandstone" (H6) and "Albian Sandstone" (H7) levels. Note Late Tertiary channel.

continental breakup) after the initial formation of the basin in Early Cretaceous time. Late Cretaceous reactivation of faults as suggested for the Sèmè Field (Appendix A.3) seems to be limited to the Sèmè area and a few other places. Detailed seismic coverage in selected areas (i.e. along the upthrown rift faults as indicated in fig. 7.32) is necessary to locate additional closures.

The "Turonian Sandstone" does have a stratigraphic prospect potential associated with offshore bars and pinchouts of fan-delta sequences (compare fig. 7.22) in conjunction with regional dip, compactional closures and minor structures beyond current seismic resolution. However, facies modelling and thus prospect definition necessitates additional well control. Exploring the stratigraphic potential of this sequence therefore belongs to a mature exploration stage. The same statement will be true for any unconformity and paleogeomorphic traps!

7.4.5 Araromi Sand Trap

The Araromi isopach map (fig. 7.42) shows a uniformly thick Araromi sequence of about 100 m over the larger part of the Benin offshore basin. Exceptions occur in the eastern area, due southwest of the Sèmè Field and at the outher part of the shelf and on the slope further to the southwest. These localized depocenters, characterized seismically as onlap fill sequences (fig. 7.43), form promising stratigraphic prospects. A period of submarine erosion (Santonian to Campanian), in which shallow channels were cut landwardly from the shelf with resulting sediment transport into deep water, preceeded the deposition of sandy submarine mounds consisting of sediments eroded from Turonian - Early Senonian fan delta systems on the shelf (fig. 7.31). The submarine fans will be enveloped in

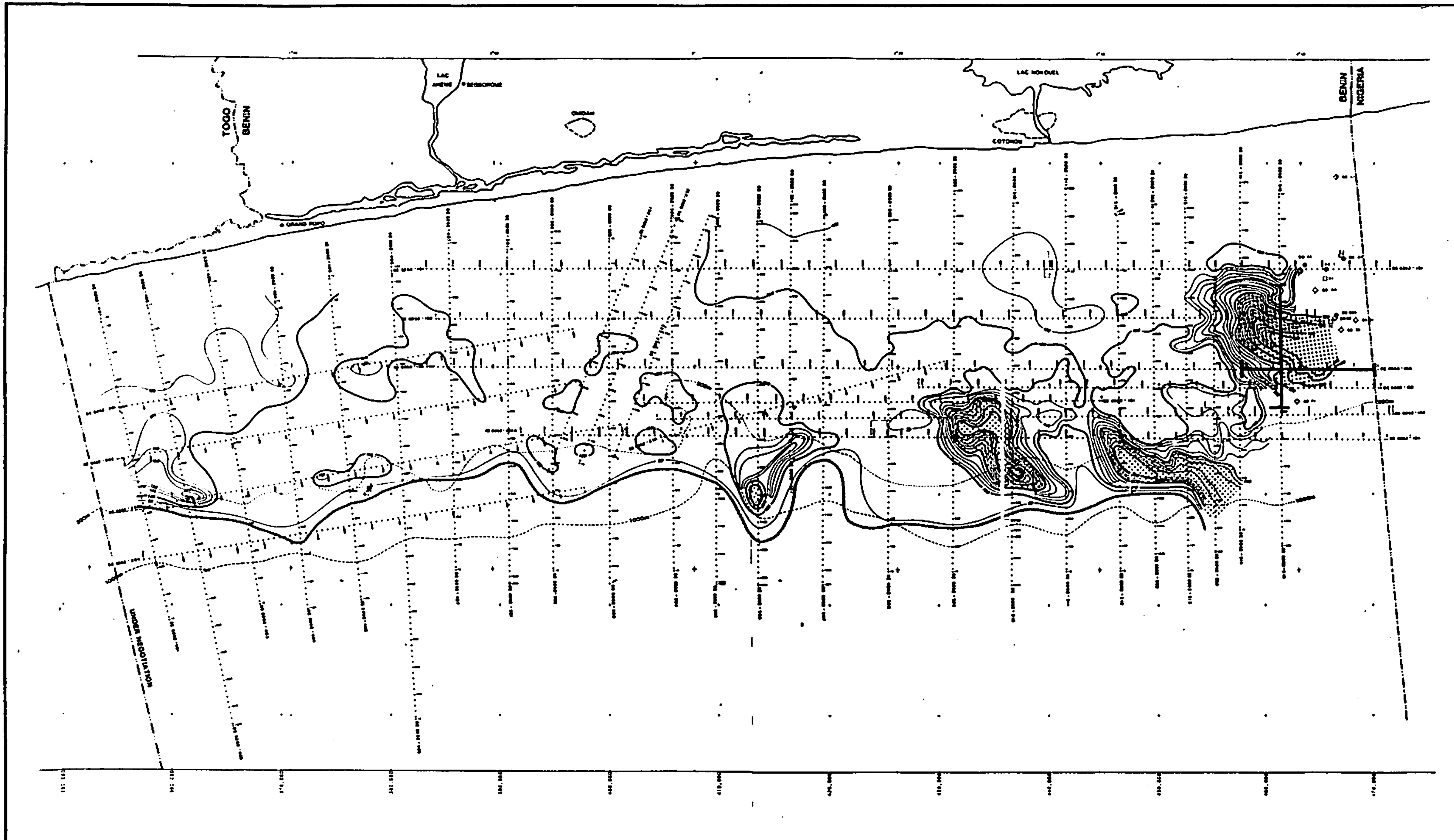

Fig. 7.42: Isopach map Araromi Shale (H4-H5) with possible stratigraphic traps outlined. Location of fig. 7.43 indicated by heavy line.

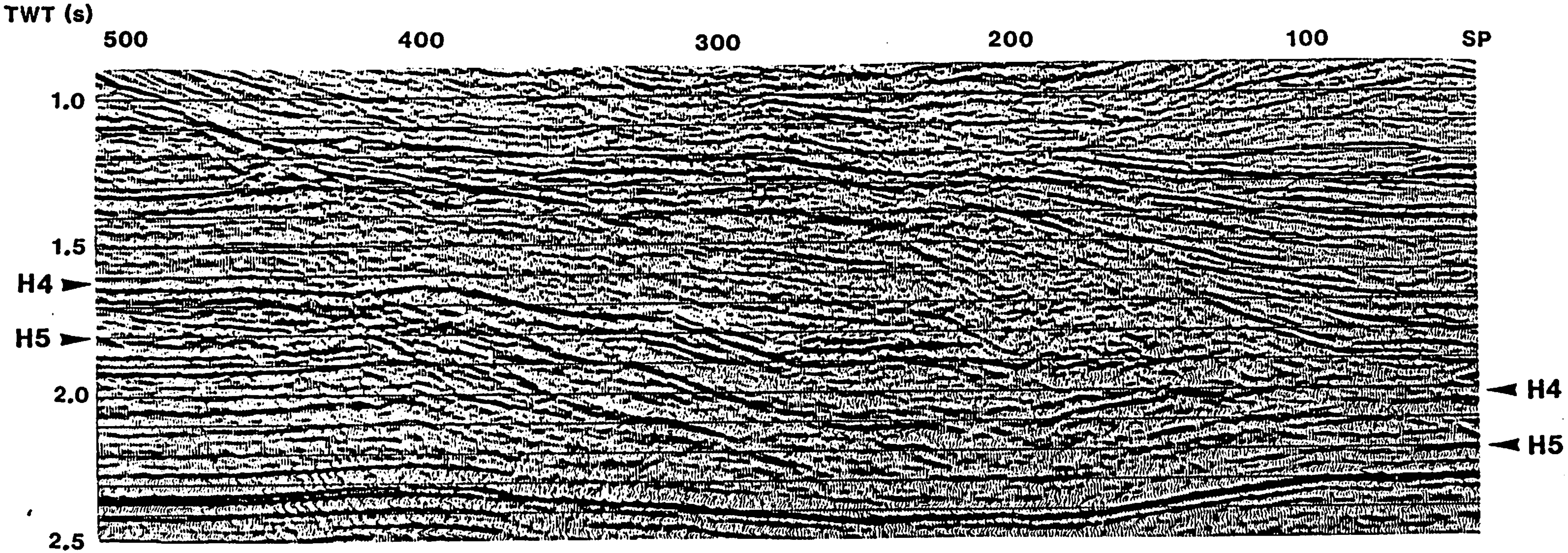

Fig. 7.43a: Onlap fill of the Araromi sequence defining possible stratigraphic trap. Line BE8262-103. See fig. 7.42 for location.

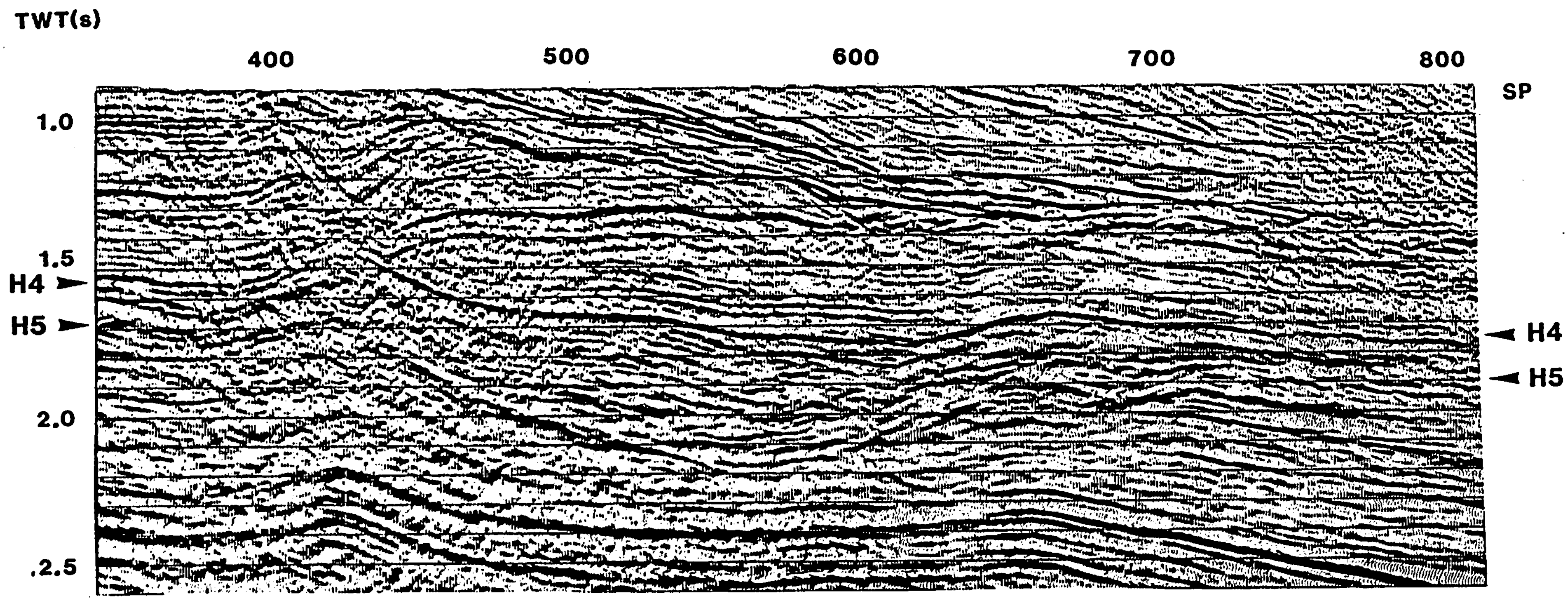

Fig. 7.43b: Onlap fill of the Araromi sequence defining possible stratigraphic trap. Line BE8262-315. See fig. 7.42 for location.

shales constituing both seal and mature source rock (ref. chapter 7.1.5). Additional source beds are located beneath the prospect (Lower Cretaceous shales). The submarine fans are likely to be sand rich as erosion is from the sandy Awgu Formation and "Turonian Sandstone".

7.5 Timing

7.5.1 General

By timing is meant a sequence of events that leads to the entrapment of petroleum. Included here are basically hydrocarbon generation, migration and trap formation, but other factors such as diagenesis, time of sealing, erosion and late structuring may be of importance.

It is already known that timing may be favourable in the Benin basin as demonstrated by the Sèmè accumulation(s). The trap is thought to have been formed in Late Cretaceous time, while hydrocarbon migration must have occurred at a later time. This is in agreement with the Araromi Shale being the source rock, but also with older inferred source horizons.

7.5.2 Timing of Structural Entrapment

Few structural traps are located as a result of this study presently mapped, and any additional traps will all (including the Sèmè Field) have the same structural history, i.e. they came into existence following the Turonian reactivation of rift faults (ref. chapter 4.4.2). The only potential source rock that could have expelled hydrocarbons generated prior to this is the Ise Formation lacustrine shales. The other source rocks (proven and speculative) reached the oil window in Late Tertiary time (ref. chapter 7.1.5). Favourable timing is therefore easily explained for any structural traps offshore Benin (fig. 7.44).

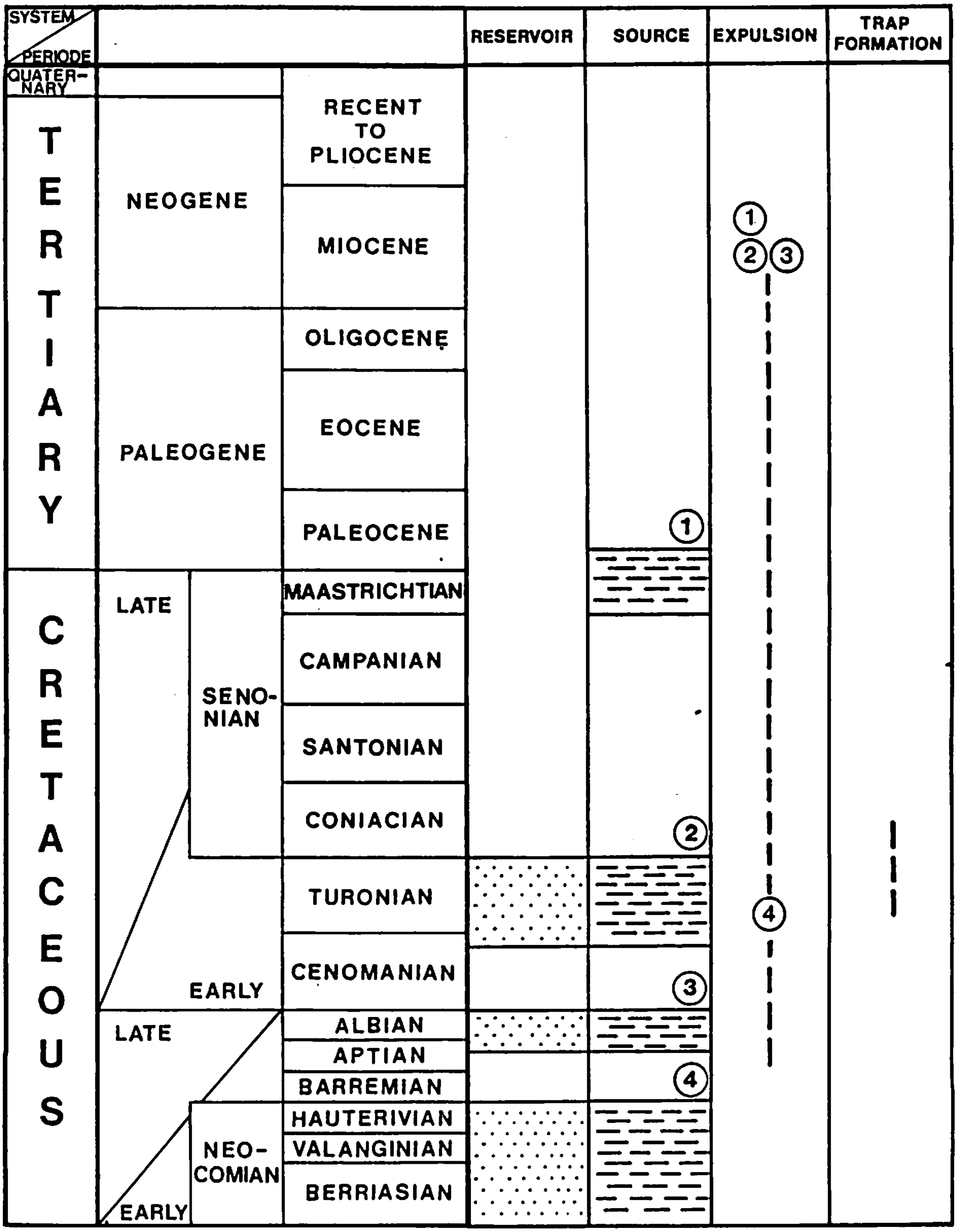

Fig. 7.44: Timing of structural entrapment, see text for discussion.

7.5.3 Timing of Subtle Entrapment

All subtle traps (stratigraphic, unconformity, paleogeomorphic) inferred and mapped in the Benin basin belong to the Lower and Upper Cretaceous series. Consequently, they were all formed before the end of the Cretaceous, although trap adjustment occurred as a result of basinward tilting in both Late Cretaceous and Tertiary times following continental breakup.

The Lower Cretaceous Ise Formation traps may have been sourced from lacustrine shales of the same formation that reached the mature stage at the end of or even after the deposition of this sequence. Its thickness leaves the possibility of a long interval with oil and gas expulsion still persisting today for the uppermost part, thus making the question of timing a favourable factor for both unconformity and stratigraphic traps of the Ise Formation. However, early generated hydrocarbons may have been lost before the formation of a seal on top of the unconformity traps.

A variety of subtle traps are discussed for the overlying ?Aptian - Albian sequence, but they all have in common being formed by the end of Albian or the 97 ma unconformity. As discussed above, Ise Formation potential source rocks may be regarded as a proper source and the same holds true for the Albian Shales as these will not have reached the oil window before into Tertiary time. Timing is thus also favourable for any "Albian Sandstone" traps.

The stratigraphic traps envisaged for the Maastrichtian - Danian sequence are enveloped in shales that may provide seal as well as source. The Araromi Shale has reached the mature stage in Late Cenozoic time, and generation and migration will still take place as discussed in chapter 7.1.

Overall therefore, timing is thought to have been favourable for all subtle traps as the potential source rocks have reached the oil generation stage in Tertiary time while the traps are of Cretaceous age (fig. 7.45).

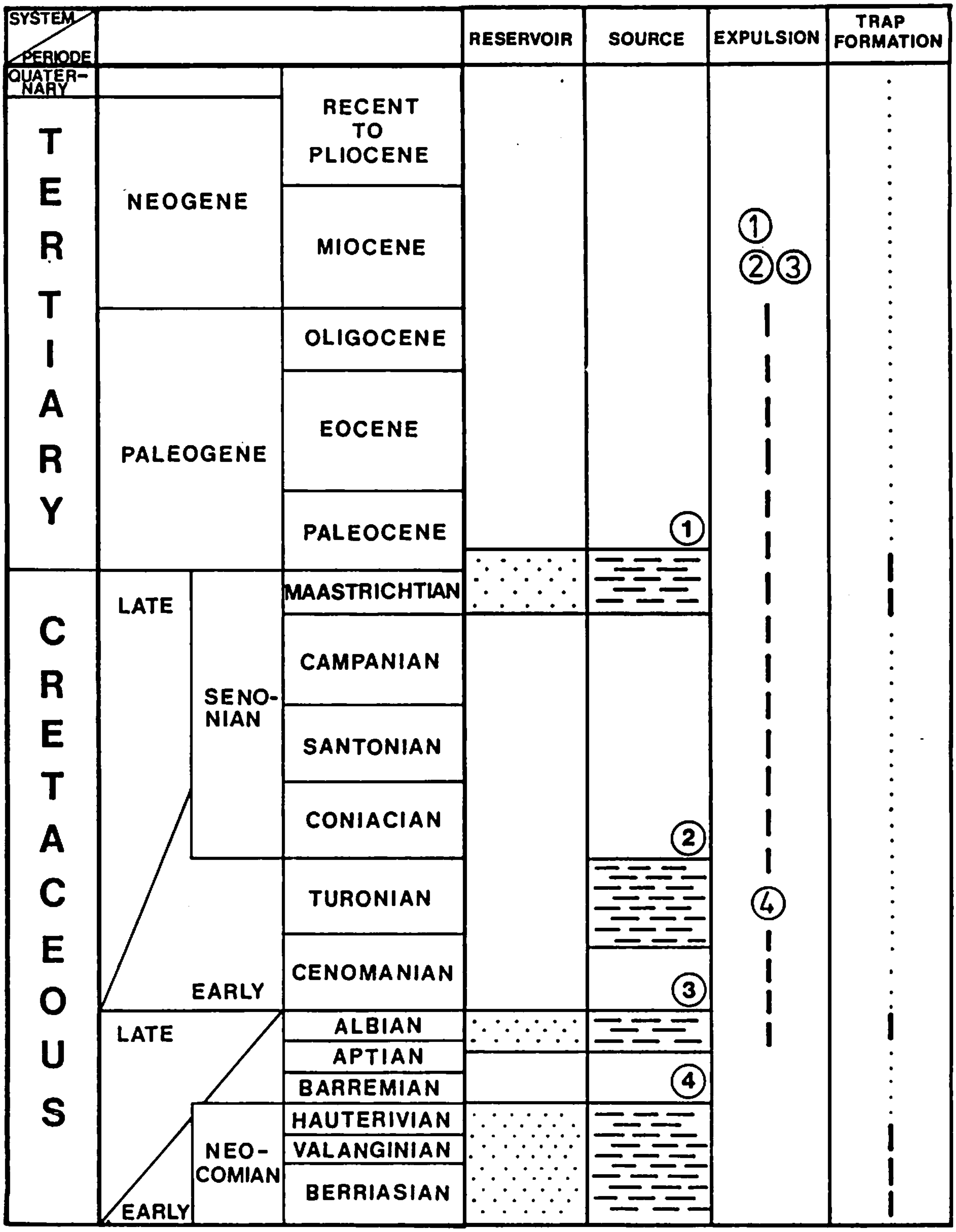

Fig. 7.45: Timing of subtle entrapment, see text for discussion.

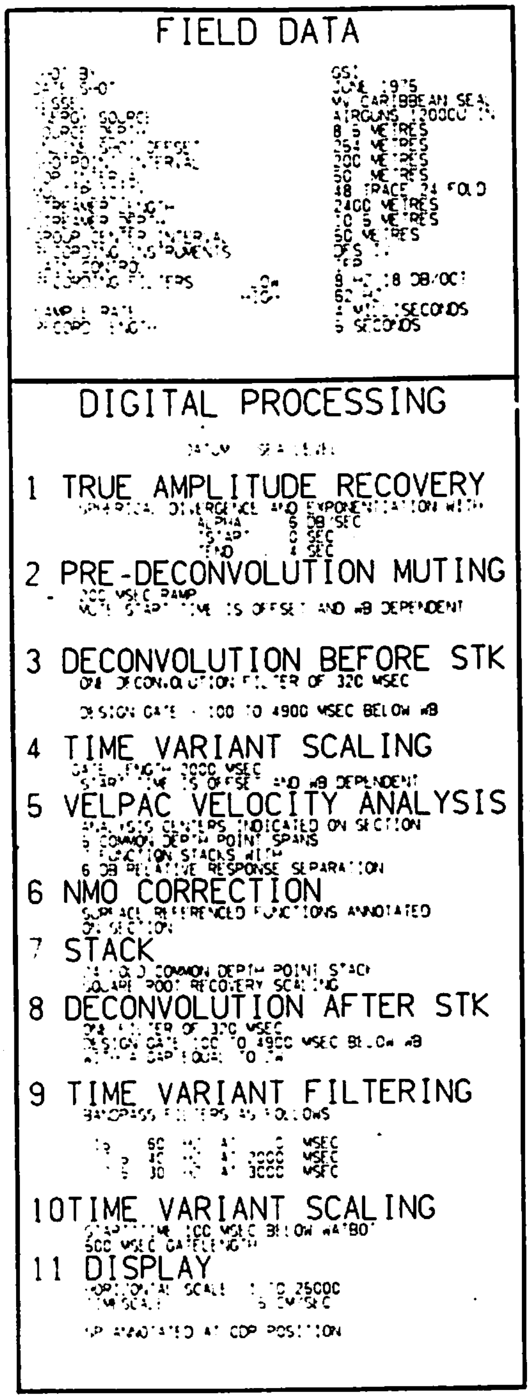

Fig. A.1.6: Recording data and processing parameters, GSI 1975.

APPENDIX A.1

SEISMIC DATA

A.1.1 Acquistion

A.1.1.1 Synopsis

A regional seismic survey comprising about 1450 km was recorded offshore Benin during August 1982.

Western Geophysical Company of America was chosen as contractor for the seismic data acquisition.

Exploration Consultants Ltd., U.K., was made responsible for the marine seismic quality control supervision. Their representative onboard the vessel was Mr. Keith L. Mackie. Project supervision was undertaken on location in Benin by Saga representatives Mr. Ø. Tønsberg and Mr. K. Berteussen.

To enhance accuracy of the seismic survey an advanced geodetic survey was undertaken by Western Geophysical in due time before starting the survey.

The final seismic programme was designed taking into account the quality and coverage of previously acquired data in Benin and optimized according to known geology, fault patterns etc.

A.1.1.2 Operational Summary

Client:	Government of Benin
Contractor (acquisition):	Western Geophysical Company of America
Contractor (supervision):	Exploration Consultants Ltd., U.K.
Vessel:	M/V "Western Ocean"
Prospect:	Offshore Benin
Line identification:	BE8262-XXX

Survey commenced:	August 9, 1982
Survey scompleted:	August 22, 1982
Duration of survey:	13.2 days
Working days:	10.15
Number of lines:	42 + 4 (Sèmè Field separate)
Total km:	1597.650
Benin Basin study:	1544.750
Sèmè Field:	52.900

\.1.1.3 Survey Details

A pre-survey geodetic calibration was carried out by Western in June 1983, using three-dimensional satellite positioning. The project was carried out as a translocation measurement using the Cotonou Lighthouse as translocation point. This project was initiated and supervised by Saga navigation project personnel.

The Saga supervisory personnel for the seismic survey arrived in Cotonou in the middle of July 1982 to start preparation for the seismic survey which at that stage was planned to start around August 1.

The Western Geophysical survey coordinator arrived in Cotonou late July to clear all navigation equipment out of customs and to start setting up the navigation stations. The three navigation engineers arrived early August, and all the navigation stations were in operation when the seismic vessel arrived.

Permission for, access to the navigation stations, setting up the navigation equipment and radio frequency transmission was applied for in the beginning of June. The licence was, however, not awarded before August 19, 1982. Still, this did not delay the survey in any way.

The seismic vessel M/V "Western Ocean" arrived in Cotonou harbour on August 8. After completion of the seismic instrument tests the vessel departed for the survey area on August 9. Onboard the vessel were the project quality control supervisor Mr. Keith L. Mackie from Exploration Consultants, London, the Saga representative Mr. Karl A. Berteussen and two representatives from the Ministry of Benin, Mr. Francois Chede and Mr. Gilbert Hueto.

The primary navigation system for the survey, Syledis, was installed at 5 locations onshore early August. All Syledis beacons were calibrated on August 5 under supervision of Mr. Mackie. Both Saga and Western Geophysical had representatives onshore during the seismic survey.

August 9 was spent mainly on scouting in the survey area, preparing all instruments for job start and cable-balancing work.

- 24.5 hours were used to record additional 4 lines over the Sèmè Oil Field, and this is a separate survey initiated by Ministry upon recommendation from Saga.

- No major problems were encountered during the survey, but at times strong currents were causing large feathering angles for the seismic cable. One line and part of another line were reshot due to this problem. Seismic production was achieved at 54% of the total survey time.

- The Quality Control Supervision Report was received from Exploration Consultants Ltd. on October 1, 1982, and copies were forwarded to the Ministry, Benin.

A.1.1.4 Shooting and Recording Parameters

Primary navigation:	Syledis (mobile + 5 beacons)
Secondary/backup:	Intergrated Satellite Navigation
Seismic recording system:	DFS V
Format:	SEG-B
Sampling interval:	2 ms
Filters, lo-cut:	5.3 Hz/18 dB per octave
hi-cut:	128 Hz/72 dB per octave
Cable length:	2400 m
No. of groups:	96
Group length:	25 m
Group spacing:	25 m
No. of geophones/group:	20
Sensitivity:	3.9 Volt/Bar
Offset (center source to center near group):	192 m
Energy source:	Western Geophysical High Pressure Airgun (4500 psi)
Source volume:	930 cu.in
No. of guns used:	15
Signature P/B ratio:	8:1

A.1.2 Processing

A.1.2.1 Introduction

Saga Petroleum a.s. acting as a consultant to the Beninian Government has operated the acquisition and processing of approximately 1450 km of marine seismic data offshore Benin. The data were acquired by Western Geophysical and processed in London by Sefel Geophysical (UK) Ltd.

This report describes the processing of the seismic data as experienced by the operator. The test sequence and the arguments for parameter selections are summarized.

Parallel to the testing by Sefel, Saga's internal VAX/DISCO processing system was used for extra testing on one of the test areas. This parallel testing is described.

As Western Geophysical was the acquisition contractor for this survey, whereas Sefel Geophysical was selected as the processing contractor, Western offered to show their capabilities by processing one line free of charge for the Beninian Government. Line BE8262-315 was chosen.

A short summary of their work is included in this report.

In 1981 line 7522, shot by GSI in 1975, was reprocessed by Horizon. The processing and results are compared.

A.1.2.2 Acquisition Parameters

The acquisition parameters for the 1982 seismic survey is shown in fig. A.1.1, taken from the side label on the final seismic section.

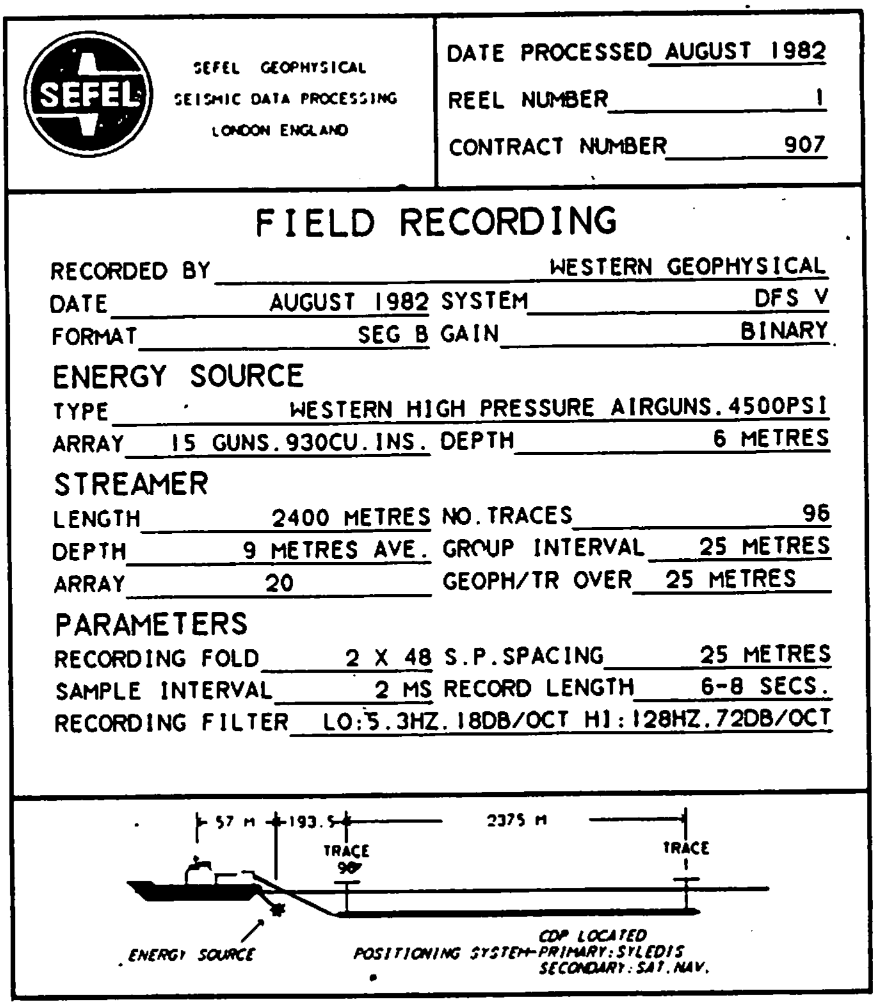

SEFEL GEOPHYSICAL
SEISMIC DATA PROCESSING
LONDON ENGLAND

DATE PROCESSED AUGUST 1982
REEL NUMBER 1
CONTRACT NUMBER 907

FIELD RECORDING

RECORDED BY WESTERN GEOPHYSICAL
DATE AUGUST 1982 SYSTEM DFS V
FORMAT SEG B GAIN BINARY

ENERGY SOURCE
TYPE WESTERN HIGH PRESSURE AIRGUNS.4500PSI
ARRAY 15 GUNS.930CU.INS. DEPTH 6 METRES

STREAMER
LENGTH 2400 METRES NO.TRACES 96
DEPTH 9 METRES AVE. GROUP INTERVAL 25 METRES
ARRAY 20 GEOPH/TR OVER 25 METRES

PARAMETERS
RECORDING FOLD 2 X 48 S.P.SPACING 25 METRES
SAMPLE INTERVAL 2 MS RECORD LENGTH 6-8 SECS.
RECORDING FILTER LO:5.3HZ.18DB/OCT HI:128HZ.72DB/OCT

Fig. A.1.1: Acquisition parameters for the 1982 seismic survey.

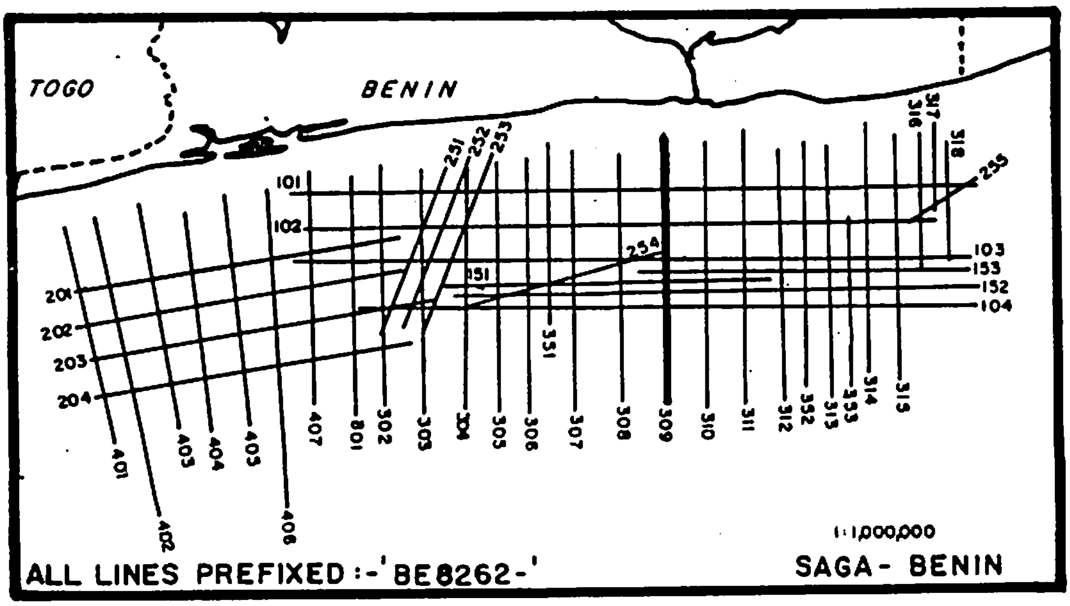

Fig. A.1.2: Seismic program relative to the Beninian coast line.

The seismic program relative to the Beninian coast line is shown in fig. A.1.2.

A.1.2.3 Test Sequence and Comments to Parameter Selections

Test areas

Near trace sections were requested for the following lines: BE8262-103, -202, -306, -315 and -404.

Line 315 was selected to represent the eastern complex geological area. Lines 101 and 306 defines the middle area with a thin nearly horizontal sedimentary sequence. Lines 202 and 404 lie in the western part of the Beninian Shelf, and line 404 goes into deep water.

Based on these near trace sections three test areas were chosen to cover the various geological provinces. They are:

Line	BE8262-315,	File	471-673
"	BE8262-103,	"	2820-3000
"	BE8262-404,	"	600-820

The testing started on line 315 as the field tapes for the two other test areas were included in a later shipment from Benin.

The following description of the processing tests corresponds to the flow chart in enclosure 29. All test panels are included in the processing report written by Sefel Geophysical.

Resampling and summation

Resampling and summation tests were run in parallel. The resampling to 4 ms did not reduce the detail quality in the test panel, and this version was chosen. Similarily the adjacent trace summed test panel showed the same detailed information as the unsummed panel whereas the noise content was reduced after summation. Hence adjacent trace summation was selected.

Designature

The seismic pulse for the 930 cu.ins airgun array was provided by Western Geophysical for the designature tests. This pulse was used to generate several signatures assumed to represent the pulse in the data. The frequency and phase content in the desired output pulse was also varied. The various operators are described in the flow chart. To be able to make the most relevant designature selection, a typical DBS operator with 24 ms prediction gap was applied in the test panel.

No obvious designature parameter decision could be made. The variations with different operators were minor. The filter based on the Western pulse with 6-60 Hz, zero phase desired output was chosen as a good compromise between the three test areas.

Decon before stack

Several standard short gapped decon operators were tried on the data as shown in the flow chart. A prediction gap shorter than 24 ms seemed to give an unstable DBS operator. Only minor differences were observed between the 24 and the 32 ms gap operator. The 24/200 ms operator using two derivation windows was selected.

Mute tests

The three test areas were stacked with four different mute functions. The optimum function at each depth level was selected.

Stack tests

Sefel has several stack programs. The following options were tried on the Benin data:

- Normal stack.

- PFL8. After normal moveout correction non horizontal dipping event in the CDP gathers are suppressed. This increases the amplitudes of the primary events relative to the multiples.

- VSTK. This program calculates the standard deviation of amplitudes along an event in the CDP gather. Extreme high and low amplitudes are neglected.

The PFL8 or VSTK process did not show any improvement, and the normal stack was selected.

F/K and mix filtering

As coherent noise was present in the seismic sections wave number/frequence filtering and mixing of data after stack were attempted. A special time varying mix program was written by Sefel enabling mixing in the noisy time window without disturbing the shallow section.

The F/K filter removed the noise without attacking the primaries and was selected for the production processing.

Decon after stack

Initially three short gap DAS operators were tried on all three test panels. After inspection of the resulting panels, three additional short gapped operators were run on line BE8262-103 as shown on the flow chart. Based on these tests no DAS was chosen for the TVF sections whereas a 24 ms gap 200 ms operator was selected for the broad band version.

After receiving the first few stacked sections some long periode multiple energy was observed on a couple of lines. An operator with long gap was tried on lines BE8262-201, -315 and -351, but was not selected as the primaries were disturbed.

Inverse sonogram test

Sefel has a posibility to construct a model section summing several traces along a dip direction after stack. The model section is summed together with the original section with a certain weight percentage. This process was attempted with various degrees of stack lift of the ordinary section, but was not selected for production processing.

Migration tests

The first migration tests were run on line BE8262-315. They consisted of a comparison of a finite difference algorithm with varying velocity field, F/K migration and no F/K filtering before migration.

The finite difference with 95% of stacking velocities applied was chosen. Sefel has the option to vary the Theta factor in the alogrithm. This factor defines the contribution of an explicite and implicite solution of the wave equation. Theta = 500 was selected. These parameters were applied in the migration of lines BE8262-303, -310 and -311.

As the migration of these lines resulted in noisy sections above the deep dipping reflector, it was decided to continue with further migration tests. These additional tests were run on line BE8262-310 which demonstrated the noise problem.

To reduce the noise content the F/K filter was applied after rather than before migration. One version was also plotted with a time varying mix after migration. The post migration mixing was selected to reduce the noise content.

Filter tests

An ordinary filter test was run to decide upon a TVF filter

The selected processing sequence is shown in fig. A.1.3.

A.1.2.4 Velocity Analysis

Prior to start of production processing, Sefel presented several options for velocity analysis.

Constant velocity analysis could be run every 3 km including 12 CDP's stacked with 35 velocities.

Alternatively semblance plots could be produced parallel to velocity function gathers and function stacks. The function

DIGITAL PROCESSING

SEQ	PROCESS	PARAMETERS
1	DEMULTIPLEX	TO 6 SECS AND 4MS WITH ANTI-ALIAS FILTER
2	TRACE SUM+CDP SORT	ADJACENT TRACE SUM AND 1X4800% CDP SORT
3	DESIGNATURE	USING WESTERN PULSE.ZERO PHASE 6-60HZ OUTPUT
4	GAIN	INVERSE AVERAGE AMPLITUDE DECAY APPLIED
5	DECONVOLUTION	TIME VARIANT FOLLOWING STRUCTURE. SEE BELOW
6	VELOCITY ANALYSIS	VVS. VVG AND SEMBLANCE EVERY 3KMS.
7	NMO.MUTE AND STACK	NMO REMOVAL. STRETCH MUTE AND 48 FOLD STACK
8	F/K FILTER	REJECTION VELOCITY: 1250 M/S
9	FILTER	BAND PASS. SEE BELOW
10	EQUALIZATION	500MS 50% OVERLAPPING WINDOWS. AVM TYPE
11	DATUM STATIC	10 MS GUN AND CABLE STATIC APPLIED
12	MIGRATION	FINITE DIFFERENCE. 95% VELOCITIES
13	T.V. MIX	SPACE VARIANT 1:4:1 MIX. UNCONFORMITY-EOD
14	T.V. FILTER	SEE BELOW
15	SCALING & DISPLAY	WHOLE TRACE EQUALIZATION. 0-4 SECS.

DECON.	• OPERATOR LENGTH	PREDICTIVE GAP	DERIVATION WINDOWS	APPLICATION WINDOWS
SEQ 5	200MS	24 MS	0MS-UNCONFORMITY	AS DERIVED
	200MS	24 MS	UNCONFORMITY-EOD	AS DERIVED

ADDITIONAL PARAMETERS

FILTER	CUT OFF POINT	100% PASS POINT	100% PASS POINT	CUT OFF POINT	APPLICATION TIMES FOR SHOTPOINTS SPECIFIED		
					ALL		
SEQ10 SEQ13	3	5	55	65	0-EOD		
	3	5	60	70	0-1500MS		
	3	5	55	65	1800-2500MS		
	3	5	50	60	2800-3500MS		
	3	5	40	50	3800-EOD		

APPLICATION TIMES

ALL TIMES IN MILLISECONDS ALL FREQUENCIES IN HERTZ
FILTERS INTERPOLATED LINEARLY BETWEEN APPLICATION TIMES
APPLICATION TIMES INTERPOLATED LINEARLY BETWEEN SHOTPOINTS
*OPERATOR LENGTH GIVEN IS ACTIVE LENGTH ADD GAP FOR TOTAL LENGTH

Fig. A.1.3: Selected processing sequence.

stacks would include 15 CDP's stacked with 7 velocity functions.

Following several parameter tests to optimize the semblance plots, these were selected for the production processing.

Semblance plots, velocity function gathers and function stacks were produced for all lines. The velocity analysis were interpreted by Sefel, and NMO corrected gathers were displayed every 1 km for quality control by Saga.

At this stage Saga representatives went through all velocity analysis for quality control.

To be able to incorporate velocity information from previous seismic surveys and well information, stacking velocity maps had been produced on Base Tertiary and Near Basement levels. Together with corresponding seismic time maps they were used as a guide in the velocity control.

1.2.5 Production Processing

The first shipment of tapes was delivered to Sefel in mid August 1982. Included in this shipment was line BE8262-315 which was used for the first test sequence. The remaining data was received by Sefel in mid September after a delay in Cotonou. Processing tests were then run in parallel on lines BE8262-315, -103 and -404.

All prestack parameters had been agreed upon within the 8th of October 1982. This enabled Sefel to continue with prestack production including velocity analysis. The first part of the velocity analysis was ready for quality control by Saga in the beginning of November, and all lines had been quality controlled by the 3rd of December.

Stacking of the data started as soon as the velocity analysis on the first line had been checked by Saga. Preliminary stacks were sent to Saga for checking before final plotting, and all lines had been stacked by the 20th of January 1983. The migration was completed by the beginning of February.

1.2.6 Parallel Testing on Saga's Internal Vax/Disco System

Internal testing by Saga was done at two stages in the processing sequence. Copies of the field tapes for line BE8262-315, SP 159 to 842 was requested for testing of a complete processing sequence.

At a later stage a raw stack tape for the same line was produced by Sefel for a parallel post stack and migration test.

A detailed velocity study was performed on line BE8262-315. Velocity spectra were run each kilometer and interpreted using the stacked section from Sefel. Based on the resulting stacking velocities and Dix formula an interval velocity model was generated for line 315. Velocities from the Sèmè wells were also used to finalize the velocity model. This model was used by Sefel in their interval velocity model migration test shown in the test flow chart (enclosure 29).

After a limited amount of testing the following sequence was applied to the field tapes:

1. Demuliplex.

2. Resample to 4 ms.

3. Spherical divergence correction.

4. CDP sort.

5. Mute

Offset:	200	230	1000	2570
Time:	100	300	1000	2200

6. Decon before stack
   Operator: 200 ms
   Gap: 24 ms
   Designate neartrace: 200:4000
   fartrace: 2500:5000

7. Automatic gain: 1000 ms window.

8. NMO and stack: 4800%.

9. Automatic gain control: 100 ms window.

10. Wave equation migration. Extrapolation step 20 ms.

11. 10 ms gun & cable static applied.

12. Running mix with weights 1 2 1

13. Bandpassfilter

Time	Filter	Low cut	High cut
0	10-60Hz	3 db/cy	3 db/cy
3000	8-40 Hz	3 db/cy	3 db/cy

The filtered and migrated sections are in enclosures 30 and 31.

As the migration process introduced noise in the seismic section, a raw stack tape was requested from Sefel for a parallel migration of line BE8262-315.

The filtered and migrated sections based on Sefel's stack tape can be found in enclosures 32 and 33. For comparison Sefel's final version is included in enclosure 34.

A.1.2.7 Processing by Western Geophysical

As Western Geophysical acquired the 1982 Benin data whereas Sefel Geophysical was selected for the processing, Western offered to process one line free of charge for the Beninian Government.

Line BE8262-315, SP 159 to 842 was chosen for this test. The processing tests were run by Western without any input from Saga.

Western's processing resulted in three different TVF versions and one migrated version.

The first TVF version involves a wavelet decon processing as follows:

1. Resample to 4 ms.
2. Multichannel filter pass zone = +/- 9 ms.
3. Signature deconvolution.
4. CDP sort.
5. NMO and 48 fold stack.
6. DAS: 32 ms gap, 232 ms operator.
7. TVF and TV scaling.

(See resulting section in enclosure 35.)

In addition to the sequence above the next TVF version had a trace sum applied between the TVF and the scaling (enclosure 36. For the third TVF section the signature deconvolution was replaced by a DBS operator with 24 ms gap and 224 ms operator length. No trace summation was applied on this section (enclosure 37).

The migrated section was based on filtered version with the DBS but without the trace summation. A finite difference algorithm was used in migration (enclosure 38).

A.1.2.8 Comparison with 1982 Reprocessing

As part of the Basin Evaluation study for the Beninian Government Horizon reprocessed one of the 1975 Shell lines shot by GSI. The reprocessing job is described in a Saga report "Reprocessing report for line 7522, shot by Shell in 1975 offshore Benin".

The reprocessed line is parallel to - and 1 km away from - line BE8262-309 recorded in 1982. The original GSI section, the reprocessed Horizon sections and line BE8262-309 are shown in enclosures 39, 40, 41 and 42.

A.1.2.9 Comparison of Processing Sequence and Data Quality in Seismic Survey in Benin

The following surveys are included in this comparison:

- 24 fold airgun data acquired and processed by GSI in 1971.

- 24 fold airgun data acquired and processed by Mandrel

Geophysical in 1972.

- 24 fold airgun data acquired and processed by GSI in 1975.

- 48 fold airgun data acquired by Western Geophysical and processed by Sefel Geophysical in 1982.

Details on acquisition and processing parameters are listed in figs. A.1.1, A.1.3, A.1.4a, A.1.4b, A.1.5 and A.1.6.

Comparing the 1971 GSI survey with the 1972 Mandrel survey the first data set seems to be of superior quality. Even in deep water areas good penetration is observed.

Relative to the 1971 and 1972 surveys the 1975 data acquired by GSI are generally of better quality. If stack tapes for these lines had been available, the interpretation could have been improved by replotting.

The 1982 survey acquired by Western Geophysical is considered to have the best quality regarding penetration and resolution.

A.1.2.10 Conclusion

The 1982 acquisition combined with a standard processing sequence have resulted in good quality seismic data for regional mapping. Within the test sequence most attention was paid to the migration process as the complex deep structures generated migration noise in the sections. Finally a running mix after migration was applied to reduce the noise content and a smooth section was achieved.

Recording Data.

Shot for Shell by G.S.I. Field Party 903, OCTOBER 1971.
Shooting Contractor: G.S.I. Boat M.V. Arctic Seal. Coverage: 24 Fold, 48Trace.
Recording Instruments: D.F.S. 4. Record Length: 6 seconds.
Recording Filters: Hi 62 Hz, 72 db/octave; Lo 8 Hz, 18 db/octave.
Energy Source: Airgun Array; Gun Depth: 8 metres; Gun Capacity: 900 cubic inches.
Gain Mode: A.G.C. Instantaneous Floating Point.
Type of Geophone: Pavie Crystals, 30 Geophones per group
Group Interval: 50 metres, all live.

Spread Diagram.

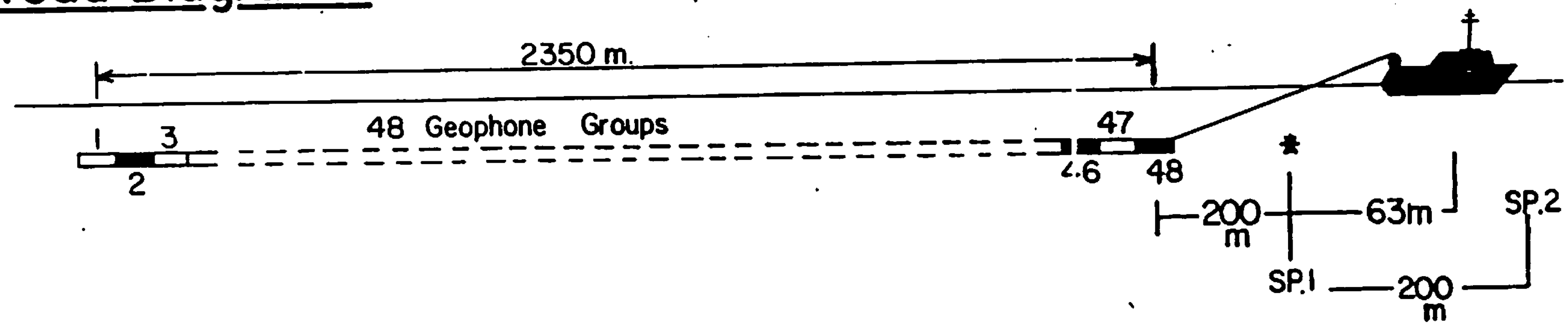

Fig. A.1.4a: Recording data, GSI 1971.

Order of Processing, and Parameters.

Input Digital Tape Type, and Format: T.I.A.C 1", 21 Track, DFS 4, 4ms Sample Rate, 712 B.P.I. Packing Density.

T.A.R. and Seismic Edit.

Time Variant Deconvolution.

3 Filters per Trace (filters overlap by 50%).

Filter Length: 196 ms., 50 points.

Design Gate : Varies with Water Depth.

Velocity Analysis : C.V.G.s, C.V.S.s, and MINI 700's With Dip Search.

24 Fold Dynamic Correction.

First Break Suppression (see taper-on record): Varies with Water Depth.

24 Fold C.D.P. Stack.

Time Variant Deconvolution

2 Filters per Trace Filter Length 228ms 58 points

Design Gate: Varies with Water Depth

Time Variant Digital Filtering

Fig. A.1.4b: Processing parameters, GSI 1971.

FIELD INFORMATION

RECORDED BY	MANDREL MARINE CREW 261
DATE RECORDED	13th DECEMBER 1972
METHOD	STAGARAY AT DEPTH OF 9-11 METRES
RECORDING SYSTEM	DFS III BINARY GAIN WITH FILTER OUT -62
RECORDING LENGTH	6 secs at 4ms S R (WITH TIME DELAY TO 200ms FROM WATER BOTTOM)
CABLE	2 4 KMS CABLE OF NEUTRAL BUOYANCY ·48 CHANNEL WITH 46 HYDROPHONES PER CHANNEL CHANNEL SPACING OF 50 M CABLE AT DEPTH OF 14 METRES
POP INTERVAL	50 M GIVING 24 FOLD COVERAGE OFFSET: 255 M TO NEAR TRACE (TRACE 48)

PROCESSING PROCEDURE

1) DEMULTIPLEX FIELD REELS TO MPX-1, WITH GAIN RECOVERY
2) DECONVOLUTION 40 point operator, 2000ms WINDOW (LAG OF 8 POINTS)
3) AVERAGE VELOCITY DETERMINATION - VELSTACK
4) STACK - 24 FOLD C D.P WITH GEOPHONE/GUN STATICS APPLIED (DATUM AT S L)
5) DECONVOLUTION 75 point operator (LAG OF 10 POINTS) ANALYSIS WINDOW 0·3 TO 2·3 SECONDS START ANALYSIS TIMES BELOW WATER BOTTOM VARYING WITH DEPTH
6) TIME VARYING FILTER (START TIMES VARYING WITH DEPTH OF WATER)
7) SPECIFIED GAIN CONTROL

TIME-VARYING BANDPASS FILTER

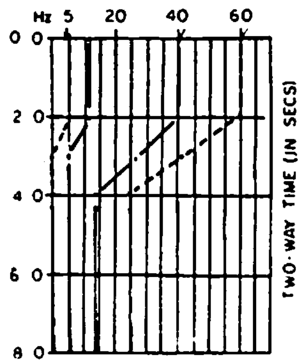

PRESENTATION

SHOT POINT NUMBER = ACTUAL DEPTH POINT POSITION.

SCALES

HORIZ 24 traces / inch

: 1 25,000

VERT 5 cm /sec

W/O NUMBER 3226

DATE PROCESSED MARCH 1973

Fig. A.1.5: Recording data and processing parameters, Mandrel 1972.

APPENDIX A.2 22.6.84

SEISMIC INTERPRETATION

A.2.1 Seismic Data Base

Approximately 1450 line kilometers of seismic data of the 1982 regional grid (ref. chapter 2.2) were interpreted and digitized for the purpose of map construction. The regional data acquired by Shell (ref. chapter 3.2) were used as infill for the construction of the fault pattern (fig. 4.12).

2.2 Data Quality

The 1982 data set was shot using a high pressure air gun source (930 cu.ins. at 4500 psi). A 96 channel cable was used to produce a 48 fold stack output. The data has been migrated using the finite difference method.

The survey shows good reflection characteristics all the way down to the basement reflector over the entire continental shelf. Seismic resolution is generally poorer beyond the shelf break. Compared to previous surveys in this basin the data quality is superior.

A.2.3 Horizon Identification

Identification of the reflectors has been made by tying BE8262-101 to well DO-1. This did not present any problems as the data quality is good. Additional ties were made with the 1977 detailed survey grid within the Sèmè Field thus giving extra credibility to the stratigraphic definition (table A.2.1, fig. A.2.1).

Horizon No.	Geological horizons	Colour code
H0:	Seabed	red 1
H2:	Middle Miocene Unconformity	green
H3:	Base Miocene Unconformity	orange 1
H4:	Top Araromi Shale	red 2
H5:	Senonian Unconformity	purple
H6:	Top "Turonian Sandstone"	yellow
H7:	Top "Albian Sandstone"	orange 2
H8:	Top Ise Formation	blue
H9:	Basement	brown

Table A.2.1: Colour code for the geologic horizons.

A.2.4 Depth Conversion

The method used for depth conversion is the layer cake method, where the interval velocities are functions of reflection time to the layer being converted.

Depth to layer i:

$$Z_i = \tfrac{1}{2}(t_i - t_{i-1}) \times V_i(t_i) + Z_{i-1}$$

where

Z_i = depth to layer i

t_i = two-way time to layer i

$V_i(t)$ = interval velocity for layer i at time t_i.

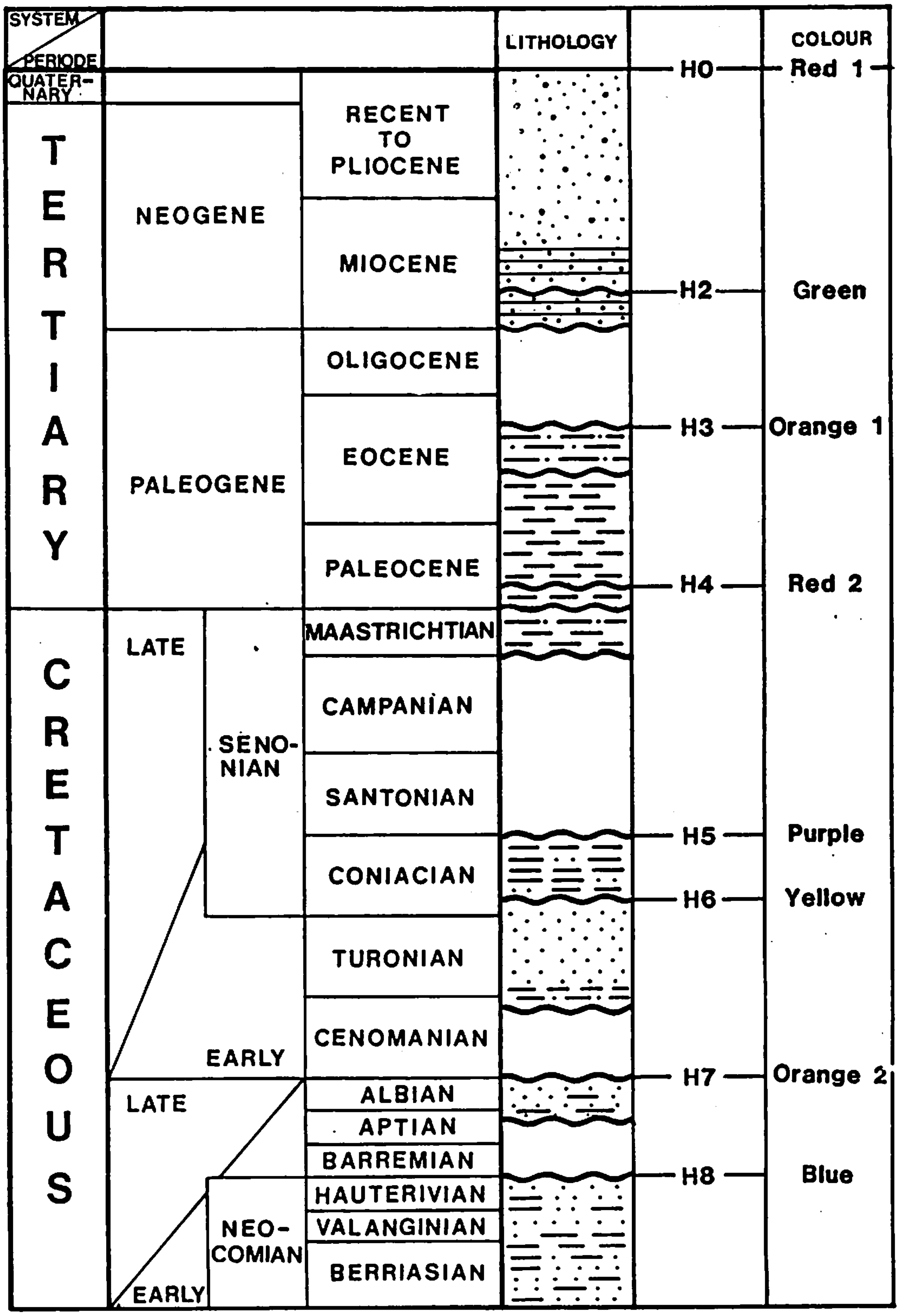

Fig. A.2.1: Colour code compared to chronostratigraphy.

Velocity functions have been defined for the following layers (fig. A.2.2) :

- water layer (V = 1500 m/s) (H0)
- seabed to Mid Miocene Unconformity (H2)
- Mid Miocene Unconformity to Base Miocene Unconformity (H2 - H3)
- Base Miocene Unconformity to Top Araromi Shale (H3 - H4)
- Top Araromi Shale to Senonian Unconformity (H4 - H5)
- Senonian Unconformity to "Turonian Sandstone" (H5 - H6)
- "Turonian Sandstone" to Top "Albian Sandstone" (H6 - H7)
- Top "Albian Sandstone" to Ise Formation (H7 - H8)
- Top "Albian Sandstone" to basement (H7 - H9)

The velocity functions derived are based upon stacking velocities from the following seismic lines, all with prefix BE8262-: 103, 203, 303, 306, 309, 315, 401 and 407.

After the interpretation new velocity picks were made on the horizons that were interpreted. The interval velocities were then calculated using Dix' Formula:

$$V_i(t_i) = ((\bar{V}_i^2(t_i) \times t_i - \bar{V}_{i-1}^2(t_i) \times t_{i-1})/(t_i - t_{i-1}))^{\frac{1}{2}}$$

where

$V_i(t_i)$ = interval velocity for layer i at time t_i

$\bar{V}_i(t_i)$ = average velocity from datum to the bottom of the layer i (stacking velocity)

t_i = two-way time to layer i

After calculations of interval velocities for all above layers on every CDP's where velocity analysis were run, we used all these data pairs ($V_i(t_i)$, t_i) to establish a linear function:

$$V_i(t_i) = a_i(t_i) + b_i$$

valid over the total basin out to a water depth of 200 m. We have also used this function in deep water causing a somewhat exagerated dip on the depth maps.

The following interval velocity functions have been derived (fig. A.2.2):

$$V_{0-1} = 1500$$
$$V_{1-2} = 0.4145 \times t_2 + 1589$$
$$V_{2-3} = 0.7260 \times t_3 + 1635$$
$$V_{3-4} = 0.2886 \times t_4 + 1958$$
$$V_{4-5} = 0.2992 \times t_5 + 2228$$
$$V_{5-6} = 0.3800 \times t_6 + 2098$$
$$V_{6-7} = 0.8874 \times t_7 + 1508$$
$$V_{7-8} = 0.5750 \times t_8 + 2547$$
$$V_{7-9} = 0.2340 \times t_9 + 3745$$

In the above functions the two-way travel time t_i (i = 1, 2, 3, 4, 5, 6, 7, 8 and 9) is given in milliseconds and the velocity V_{i-i+1} in m/s.

A.2.5 Description of Mapped Horizons

Seabed, H0 (fig. A.2.3, enclosure 4)

The seabed is mapped for the purpose of depth conversion. As parts of the 1982 survey were shot in shallow water less than 20 m, the echosounder readings had to be incorporated to obtain accurate values.

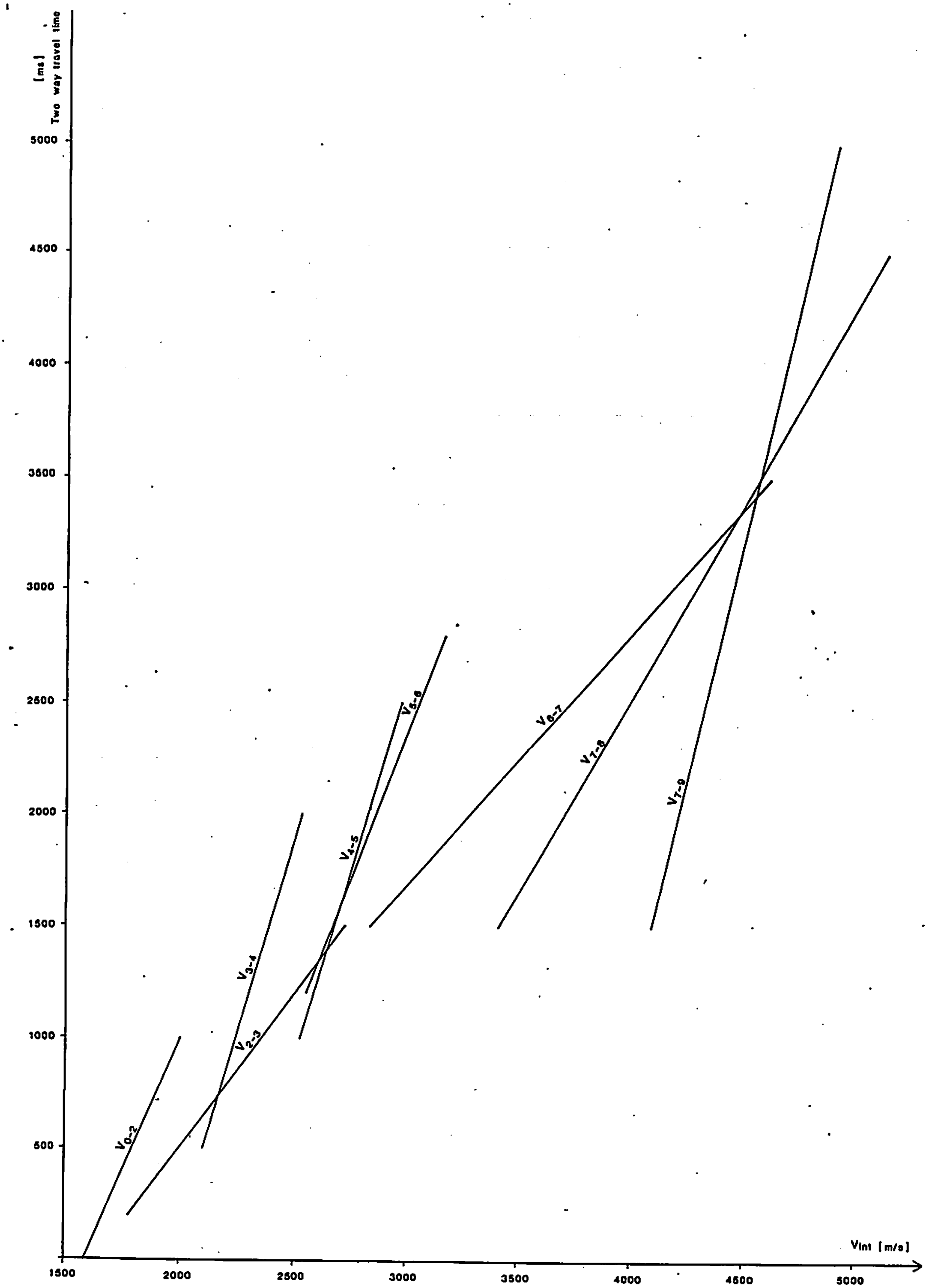

Fig. A.2.2: Velocity functions applied offshore Benin for depth conversion purposes.

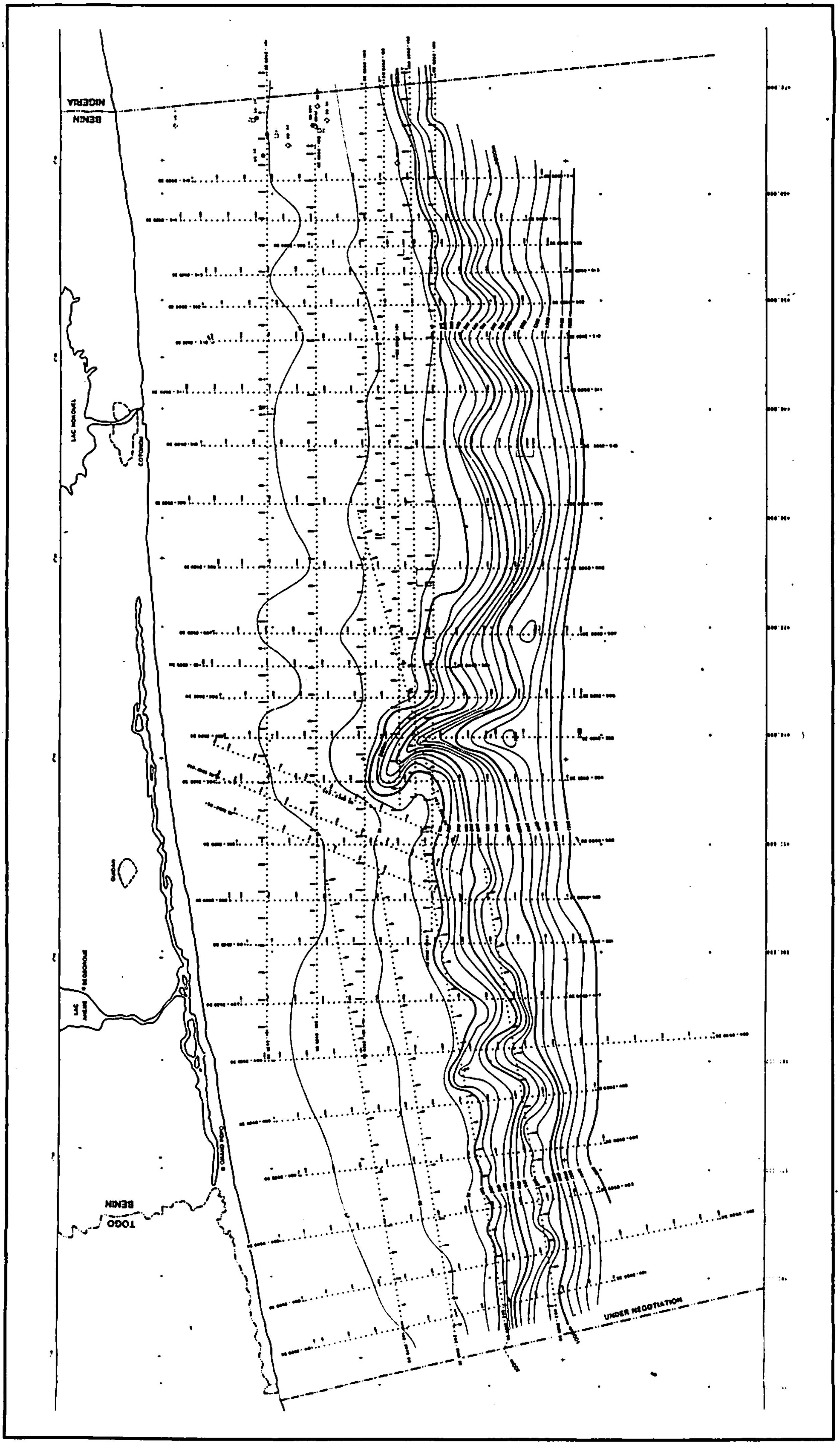

Fig. A.2.3: Seabed (H0), depth map.

Middle Miocene Unconformity, H2 (figs. A.2.4 and A.2.5, enclosures 5 and 17)

This reflector results from an increase in velocity across the Middle Miocene Unconformity. It is present on the entire shelf area and is also mapped on the continental slope. The character varies, and it may be hard to trace both in a landward direction (where it is shallow) and in a seaward direction, as it truncates stratigraphically deeper reflections.

Base Miocene Unconformity, H3 (figs. A.2.6 and A.2.7, enclosures 6 and 18)

The Base Miocene reflector is associated with an increase in velocity. The horizon is truncated inside of the shelf break and can be mapped with confidence where present. The reflector defines a surface gently dipping to the south.

Top Araromi Shale, H4 (figs. A.2.8 and A.2.9, enclosures 7 and 19)

This reflector is also an unconformity and is clearly associated with an increase in velocity from the overlying Imo Shale. Over the larger part of the shelf it is a continuous, high amplitude reflector defining a seaward dipping horizon that is truncated by the Middle Miocene Unconformity past the shelf break. In the easternmost part of the shelf the reflection character is somewhat changed as it represents top of onlap fill.

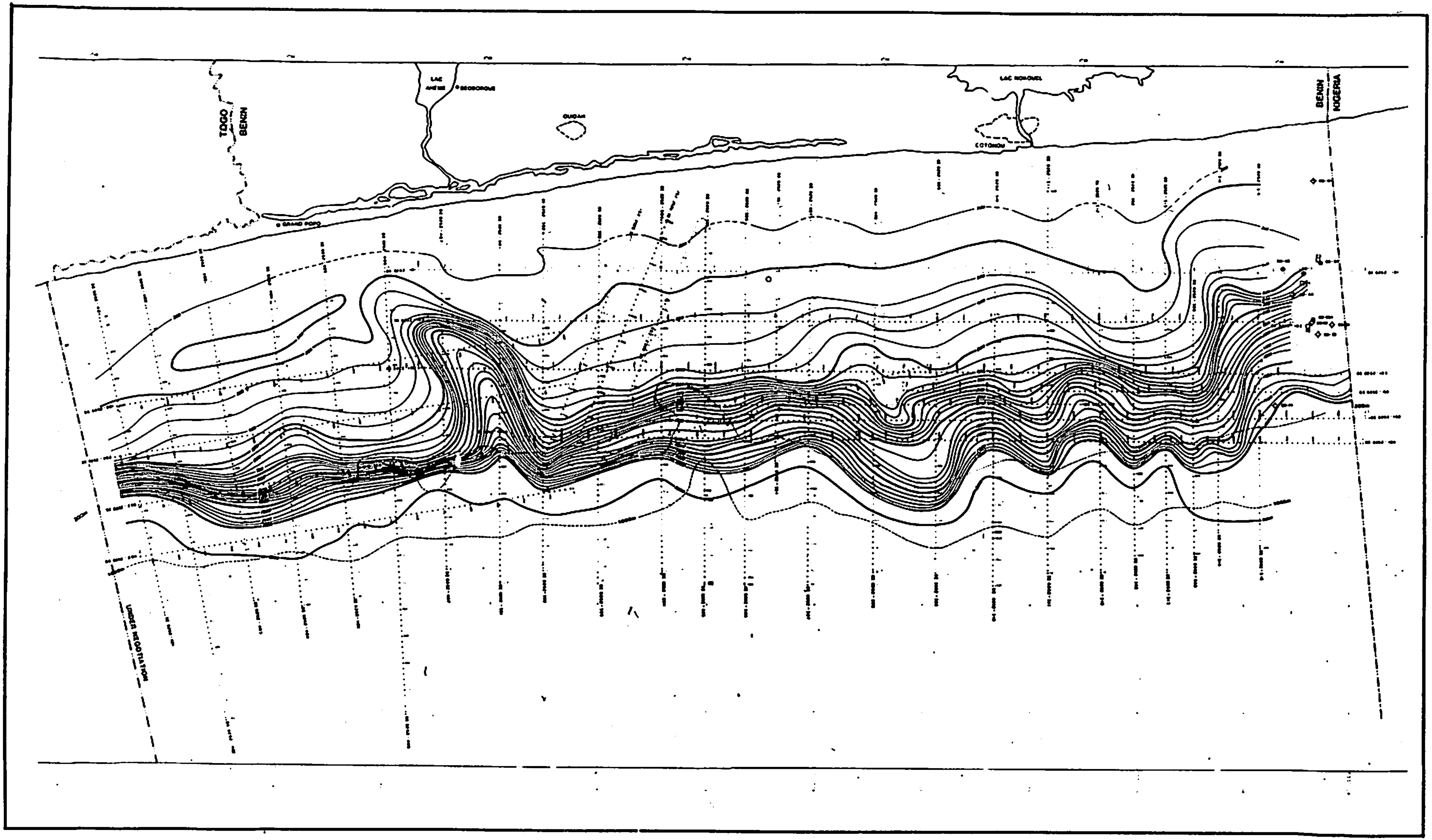

Fig. A.2.4: Mid Miocene Unconformity (H2), structural depth map.

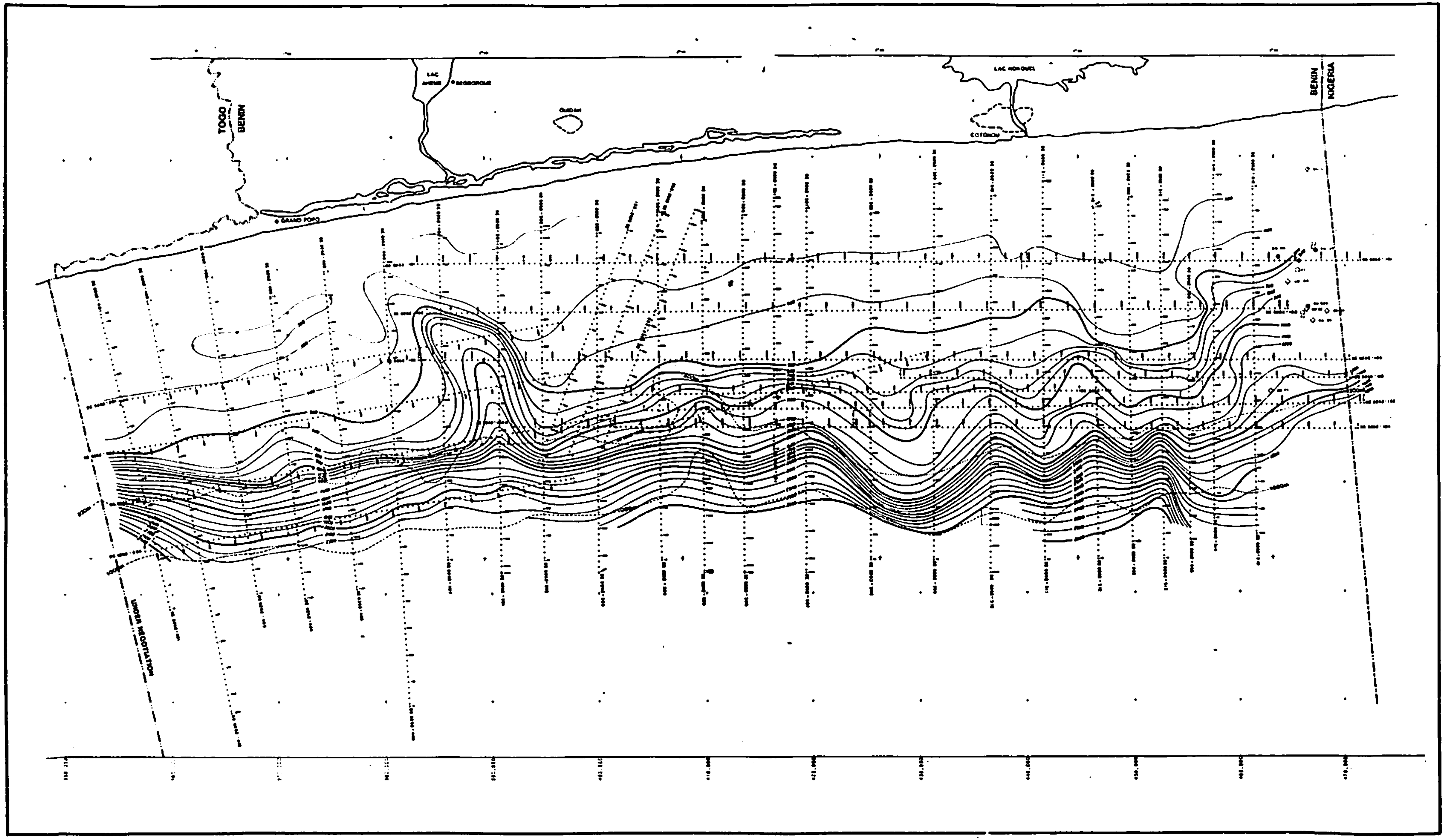

Fig. A.2.5: Mid Miocene Unconformity (H2), two-way time map.

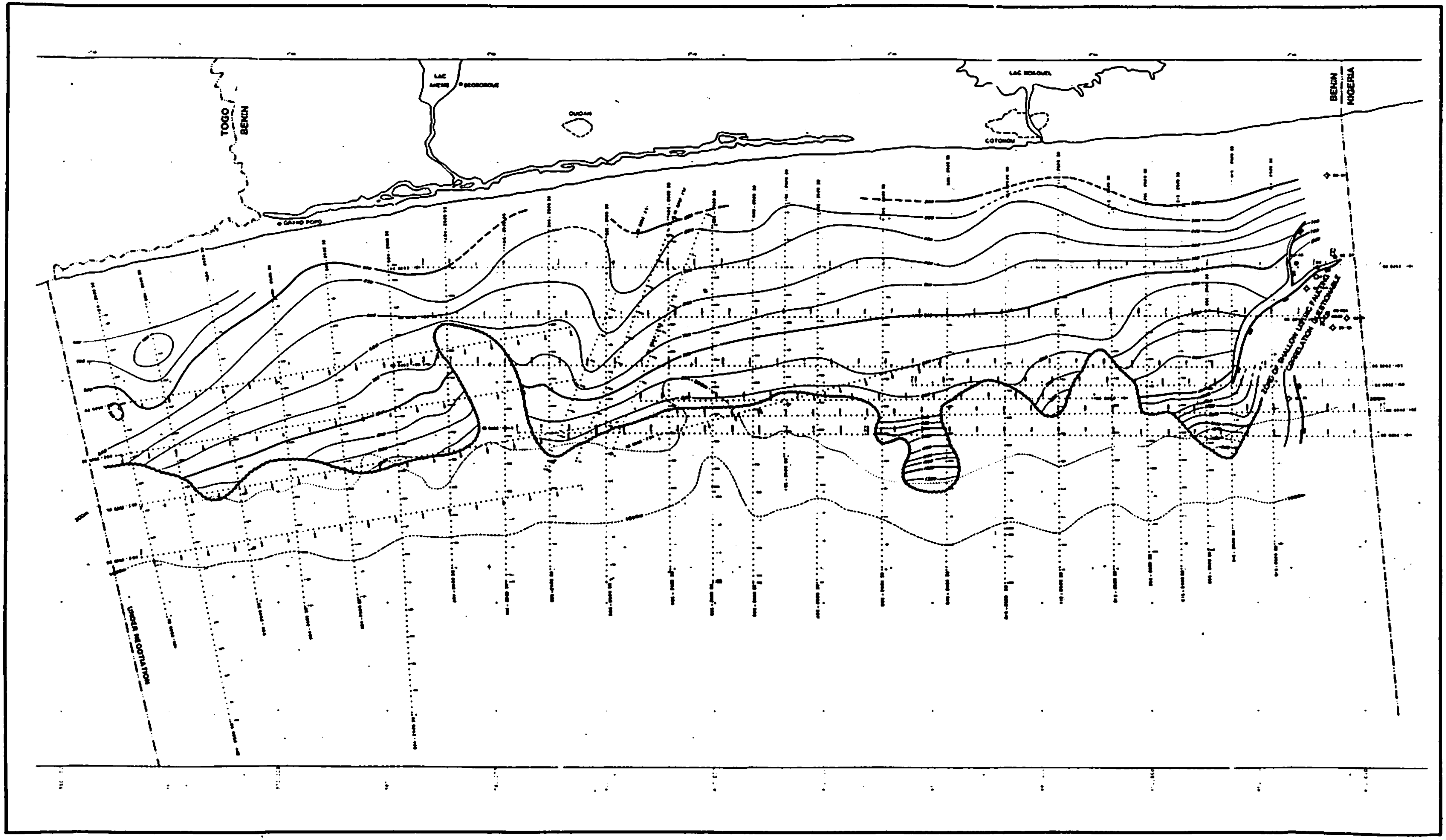

Fig. A.2.6: Base Miocene Unconformity (H3), structural depth map.

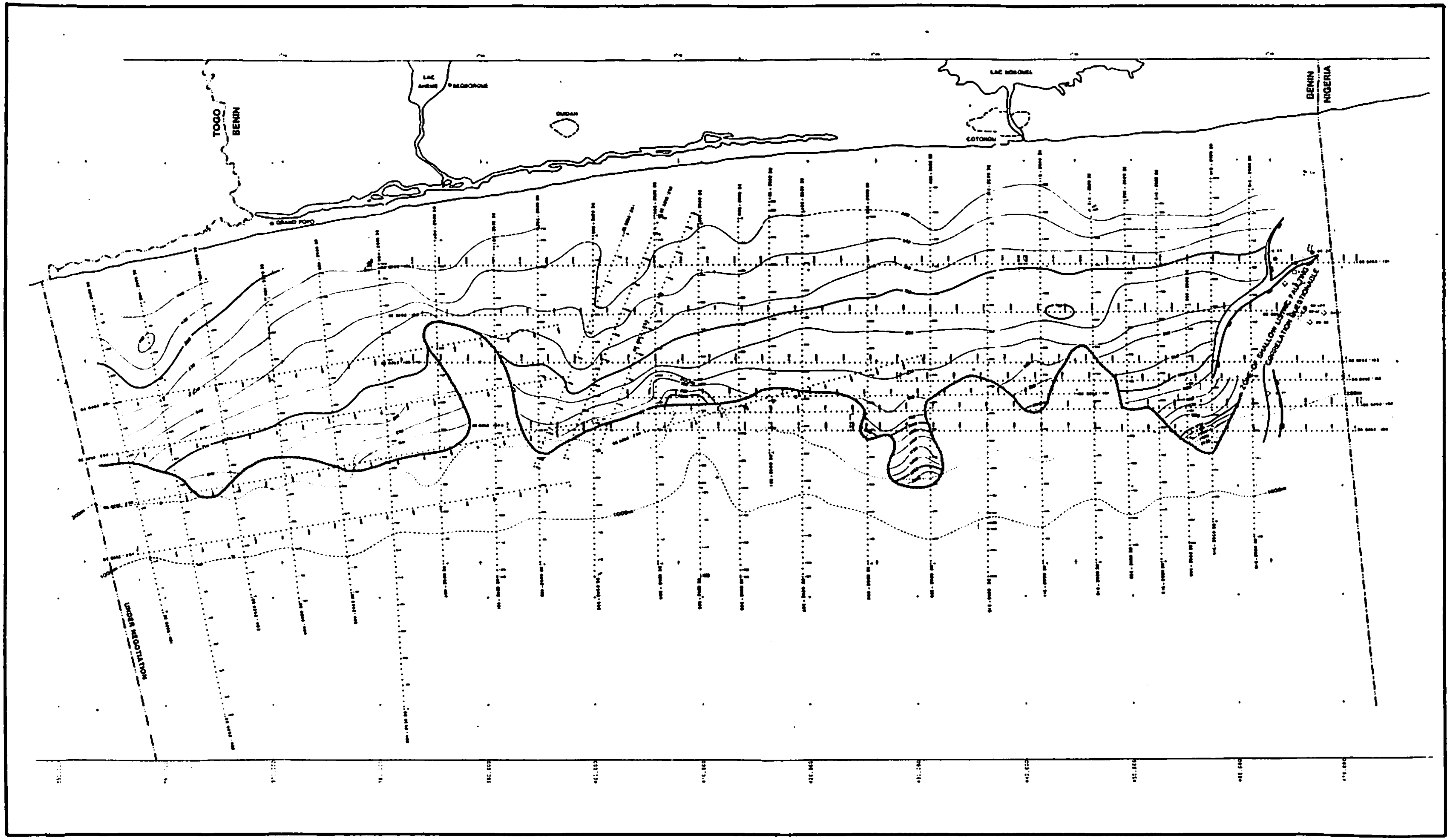

Fig. A.2.7: Base Miocene Unconformity (H3), two-way time map.

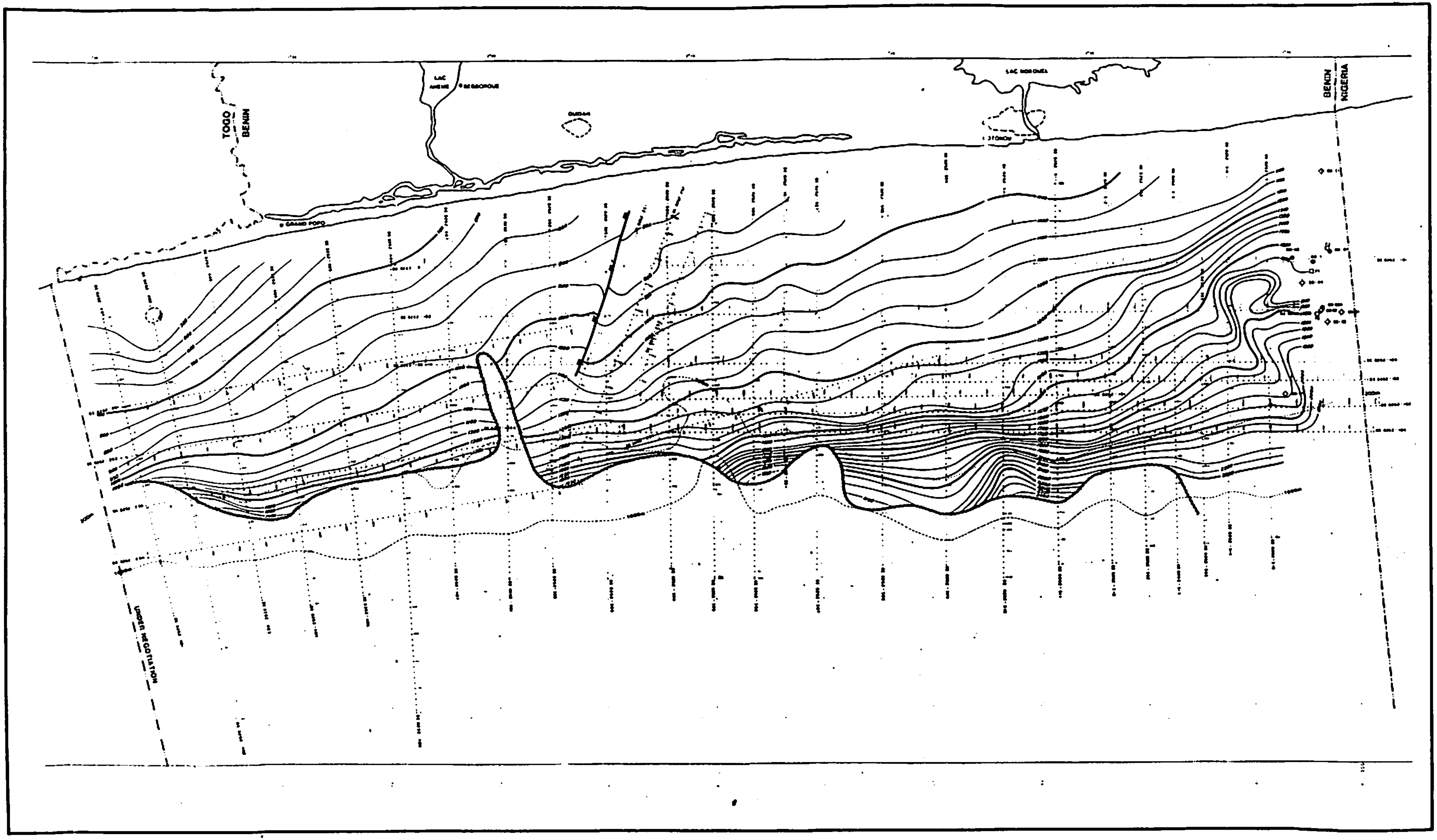

Fig. A.2.8: Top Araromi Shale (H4), structural depth map.

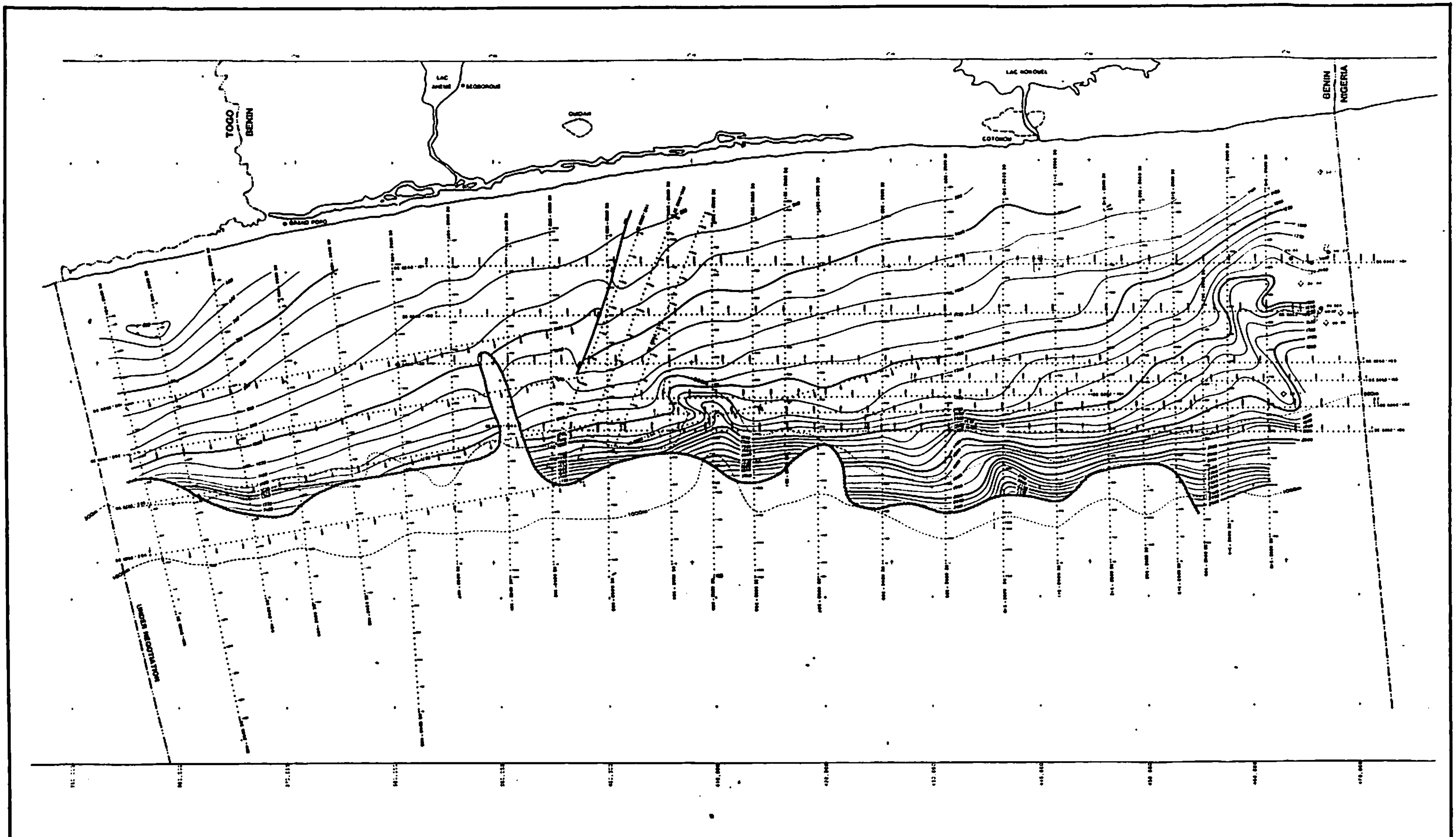

Fig. A.2.9: Top Araromi Shale (H4), two-way time map.

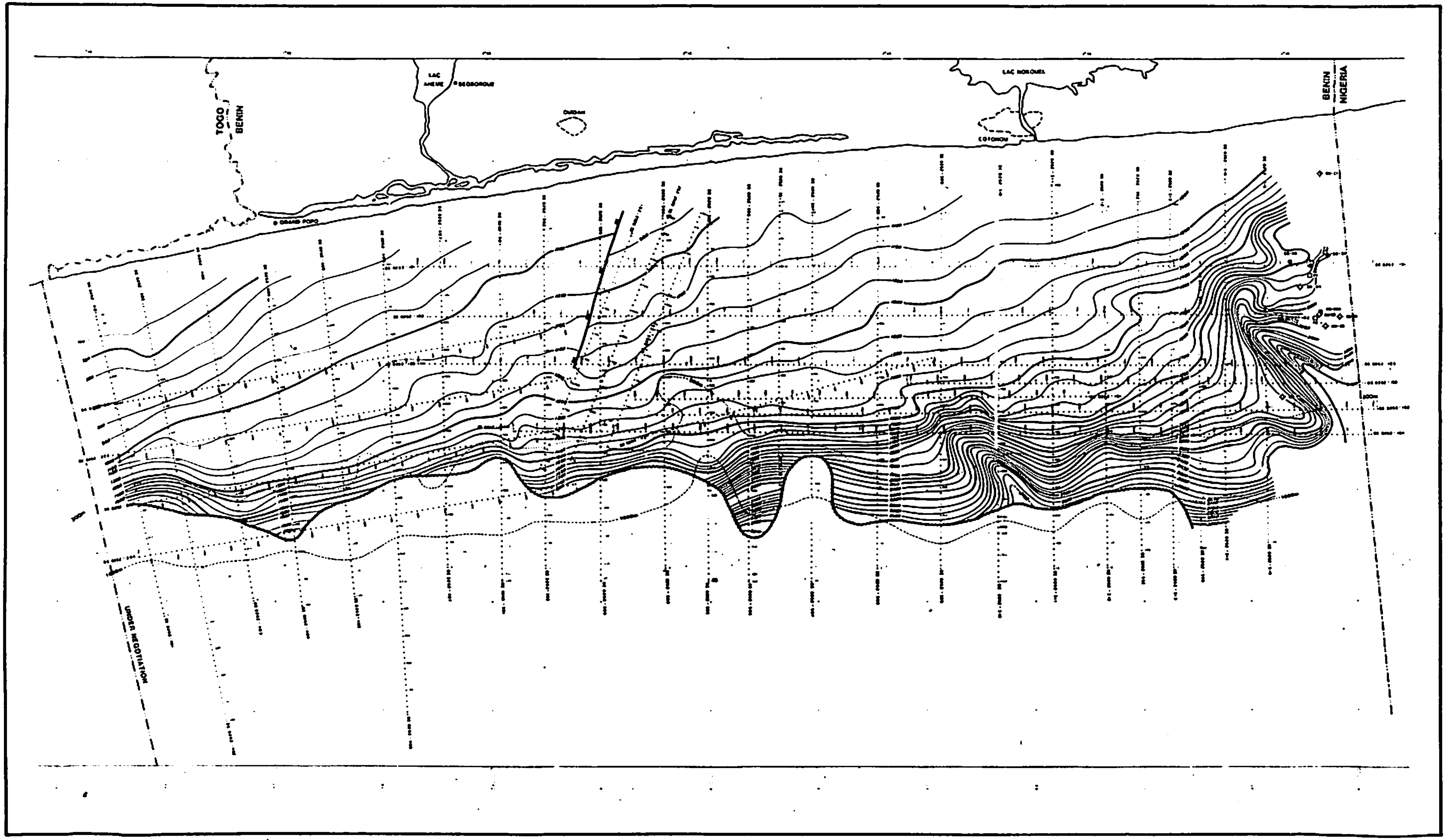

Fig. A.2.10: Senonian Unconformity (H5), structural depth map.

Senonian Unconformity, H5 (figs. A.2.10 and A.2.11, enclosures 8 and 20)

This is a very characteristic reflector within and in the vicinity of the Sèmè Field. There it represents the boundary between the higher velocity underlying sandy Awgu Formation and the Araromi Shale equivalent with submarine onlap fill. On the remaining and larger part of the shelf area it still represents a strong event almost conformable with the H4 reflector, and dipping uniformly to the south - southeast.

Top "Turonian Sandstone", H6 (figs. A.2.12 and A.2.13, enclosures 9 and 21)

The reflector named Top "Turonian Sandstone" is caused by a velocity increase and is identified as an unconformity on the entire shelf. It does, however, have a weak and variable reflection character and is not always mapped with confidence. This is in particular true in a westward direction. The constructed map shows a south - southeasterly gently dipping surface that is truncated on the slope by the Middle Miocene Unconformity and cut by a few faults in the western half of the basin.

Top "Albian Sandstone", H7 (figs. A.2.14 and A.2.15, enclosures 10 and 22)

The Top "Albian Sandstone" sequence boundary defines a characteristic, continuous, high amplitude event where present in the eastern half of the shelf basin. An increase in velocity is evident downwards from the overlying "Turonian Sandstone". The reflector onlaps basement at the edges of the Lower Cretaceous basin. Overall, it dips to the south - southeast with an increased dip beyond the shelf break and loss of

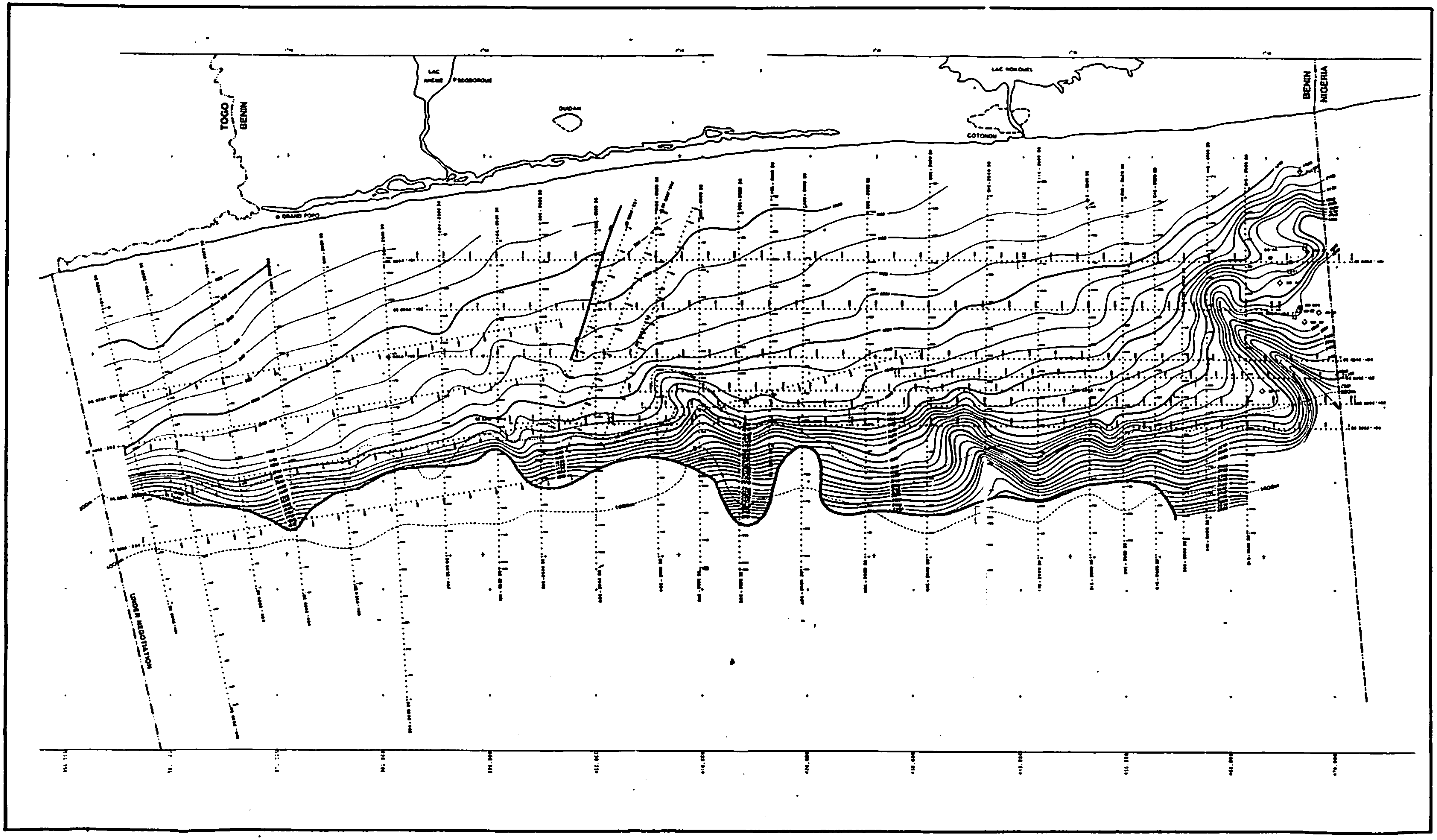

Fig. A.2.11: Senonian Unconformity (H5), two-way time map.

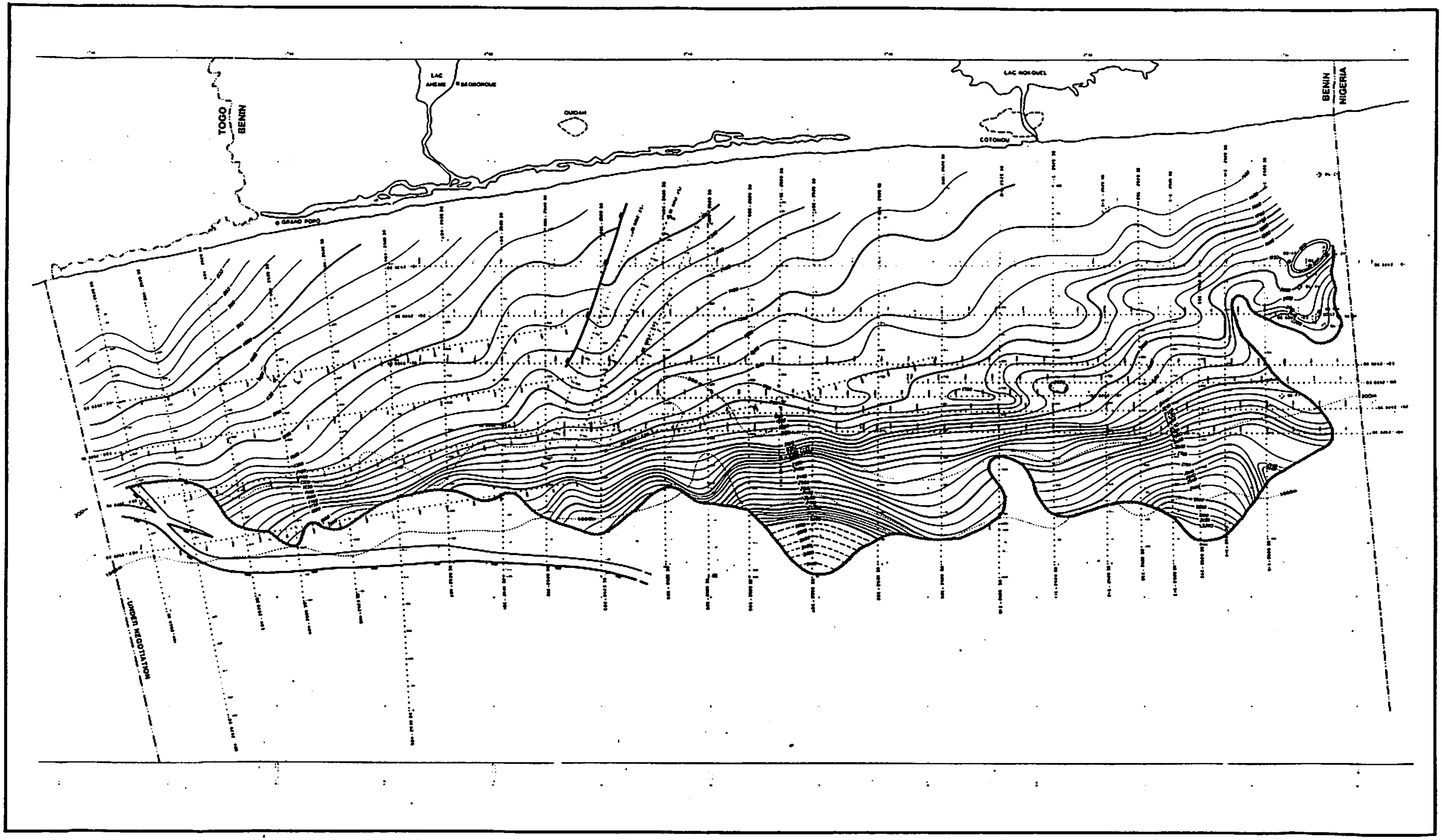

Fig. A.2.12: Top "Turonian Sandstone" (H6), structural depth map.

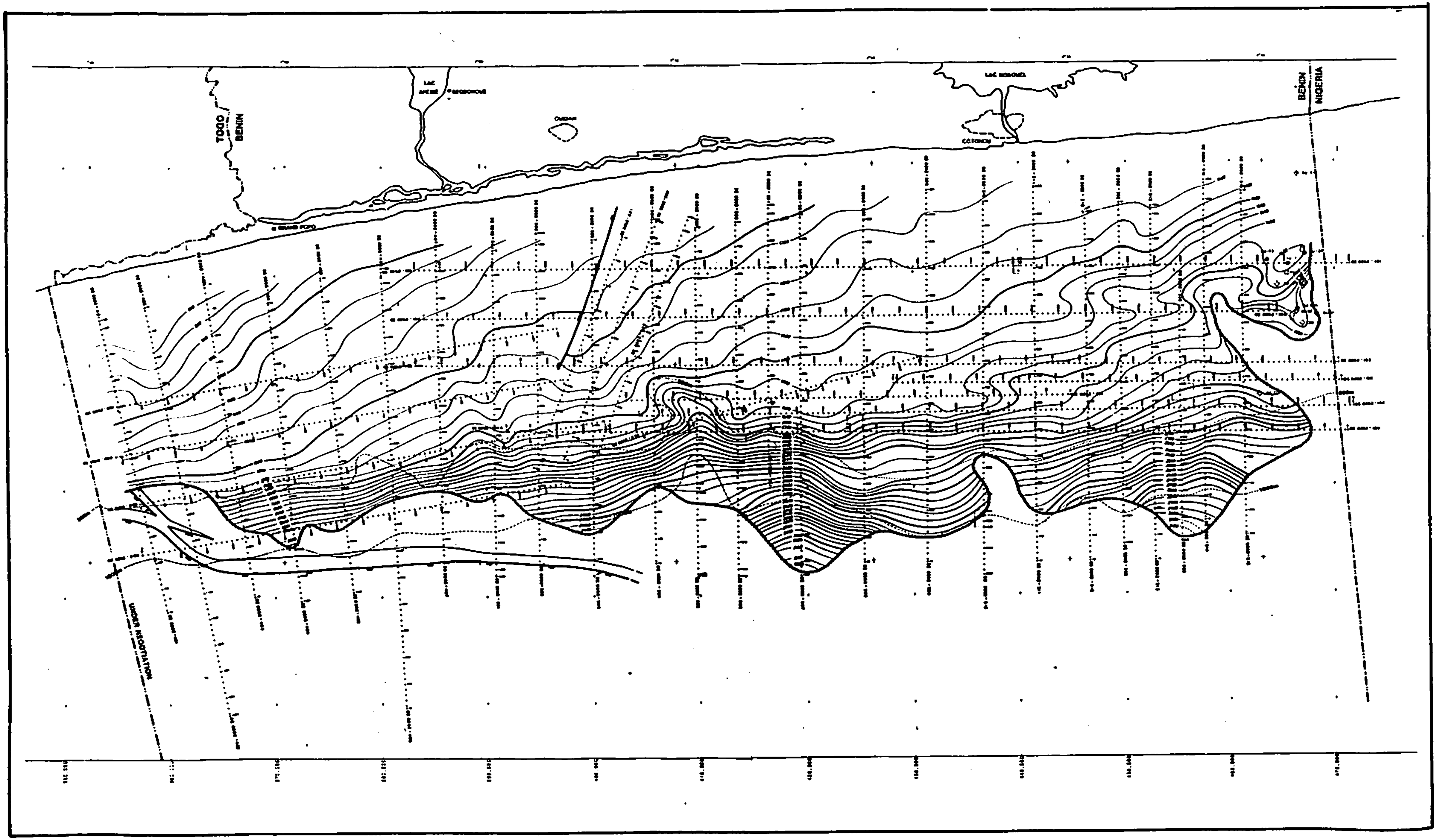

Fig. A.2.13: Top "Turonian Sandstone" (H6), two-way time map.

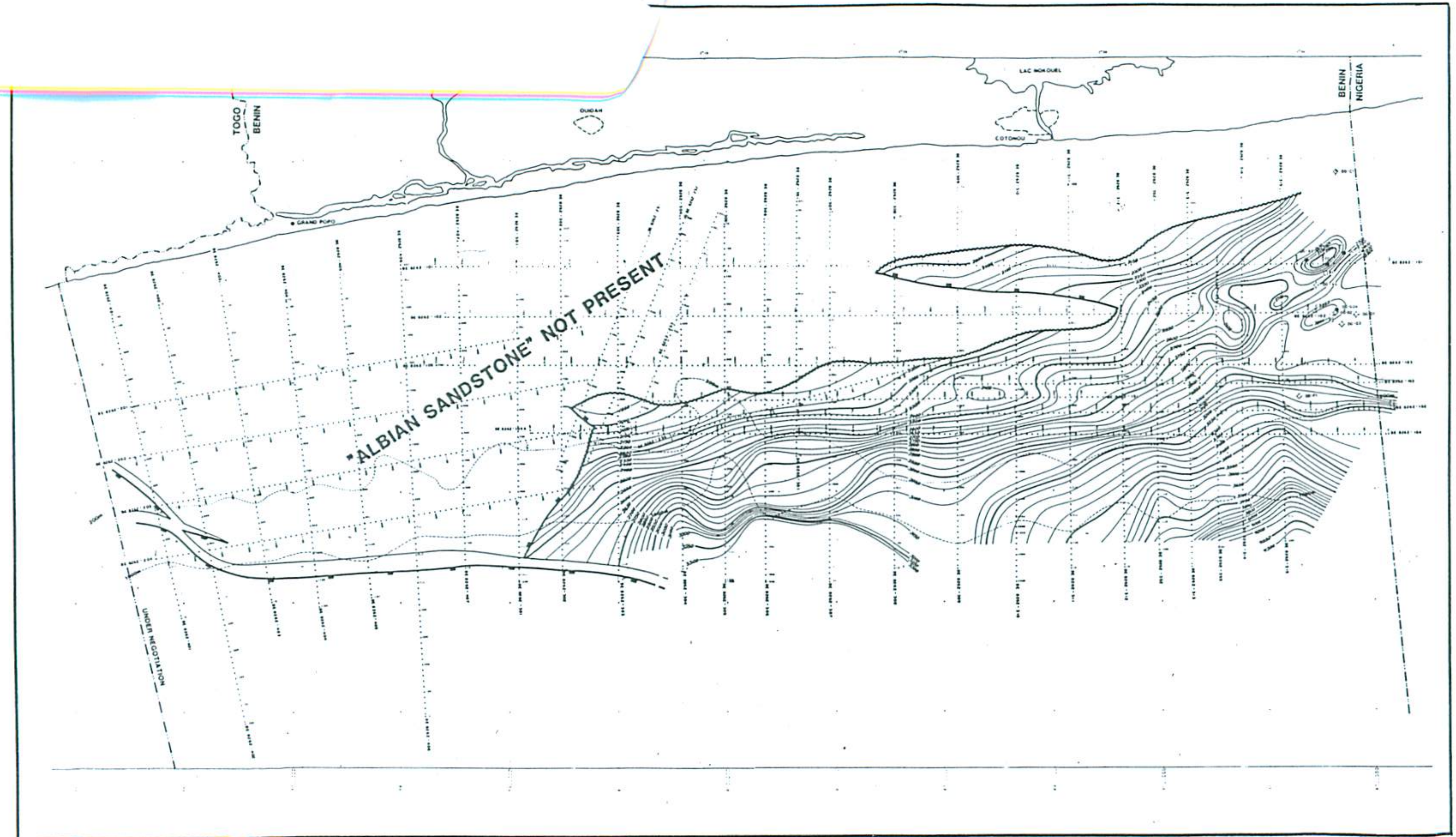

Fig. A.2.14: Top "Albian Sandstone" (H7), structural depth map.

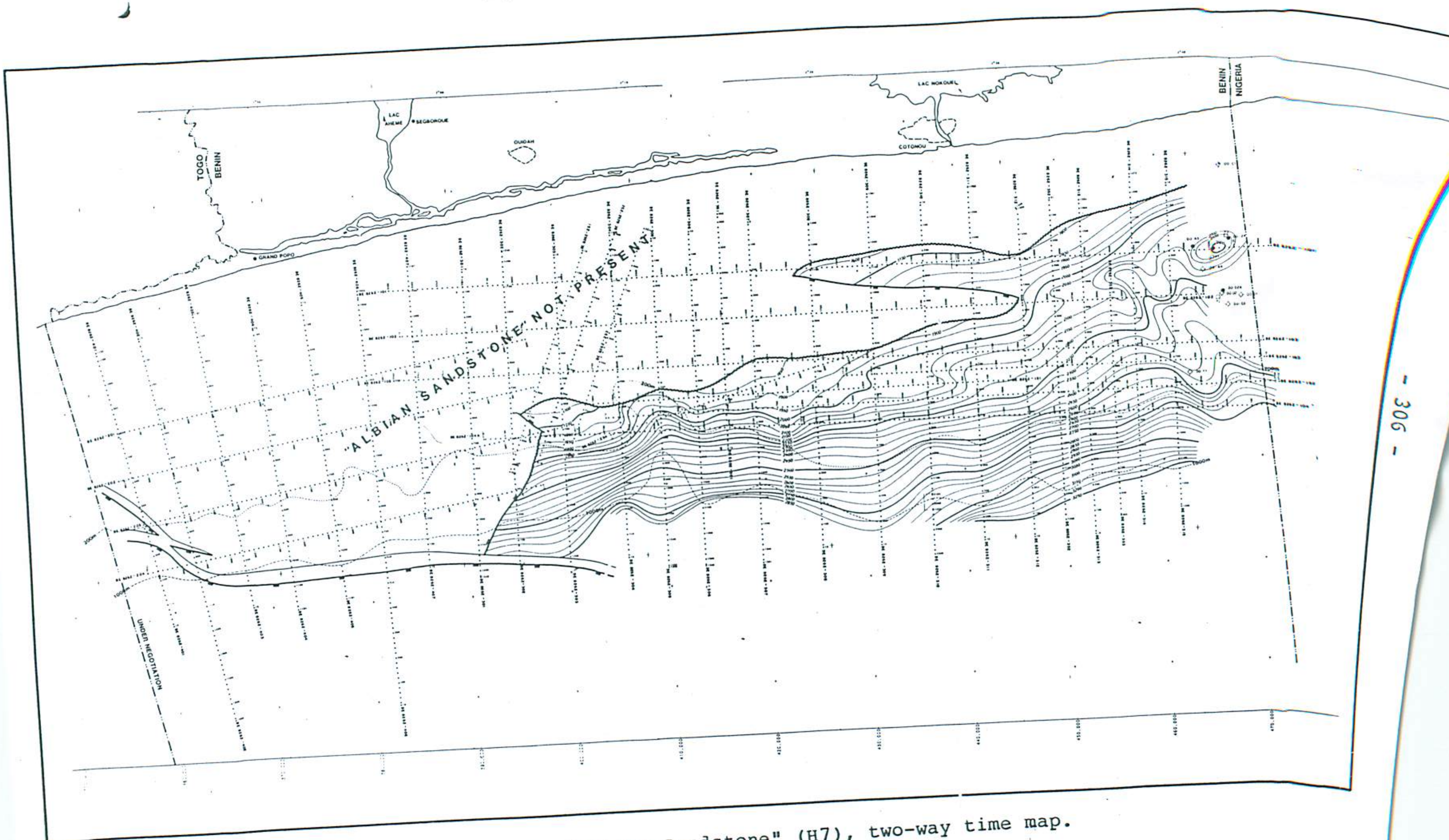

Fig. A.2.15: Top "Albian Sandstone" (H7), two-way time map.

resolution in deep water.

Top Ise Formation, H8 (figs. A.2.16 and A.2.17, enclosures 11 and 23)

There is a substantial increase in velocity across this rift unconformity. In spite of typical toplap terminations the reflector cannot always be mapped with confidence. The sequence itself has a truly different reflection character from overlying strata. The reflector is only present in the eastern part of the shelf where it defines a steeply seaward dipping horizon. An increased dip is observed on the slope.

Basement, H9 (figs. A.2.18 and A.2.19, enclosures 12 and 24)

The basement reflector is mapped all over the shelf area where it mostly defines a strong, continuous event. In the eastern half of the shelf, within the rift grabens with a thick sediment cover, some difficulties arise in identifying the fault pattern. Confidence may also be lost in deep water. Due to appreciable dip there is a marked difference between the filtered stack and migrated sections. The maps are all based on migrated lines.

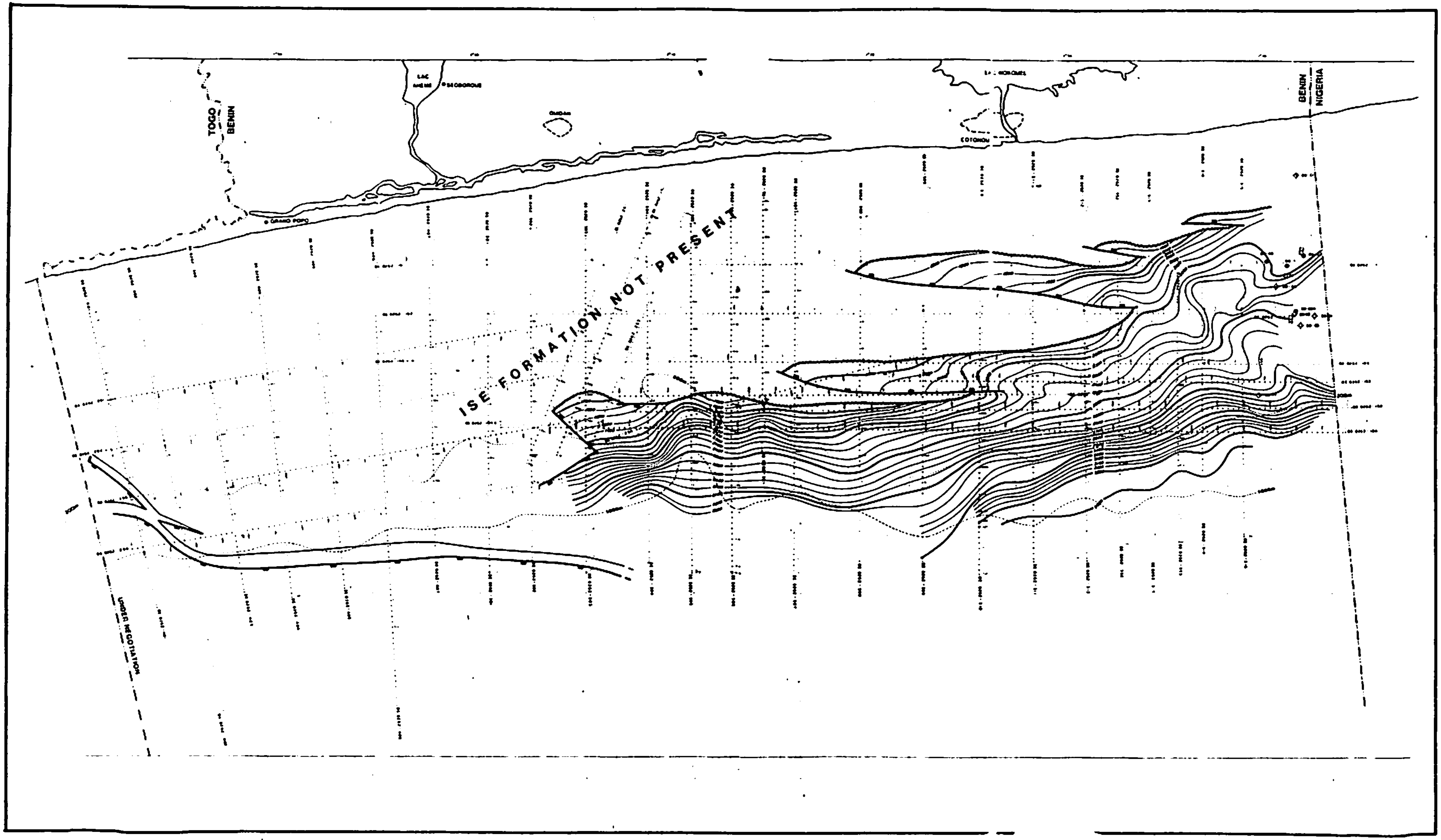

Fig. A.2.17: Top Ise Formation (H8), two-way time map.

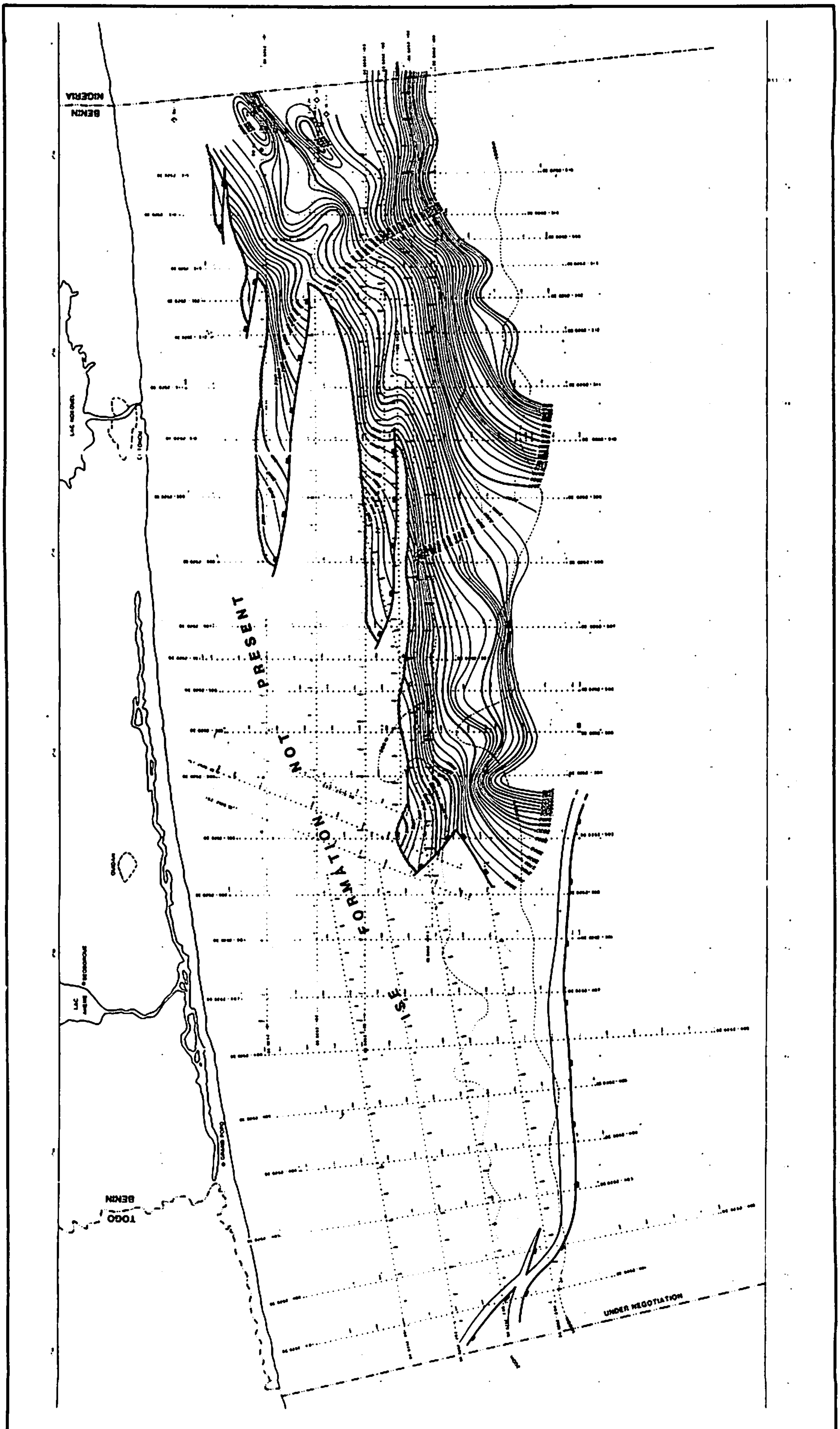

Fig. A.2.16: Top Ise Formation (H8), structural depth map.

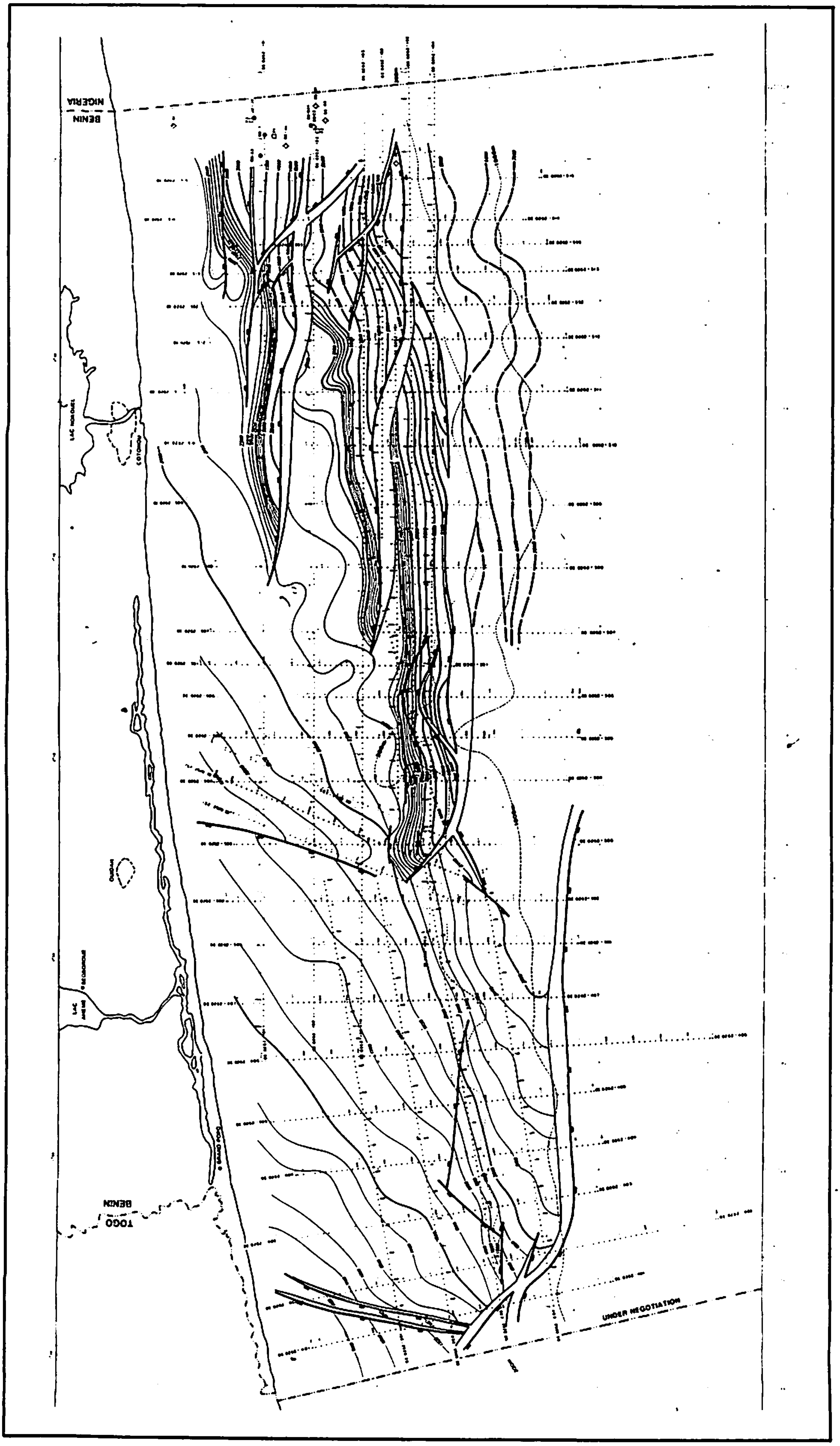

Fig. A.2.18: Basement (H9), structural depth map.

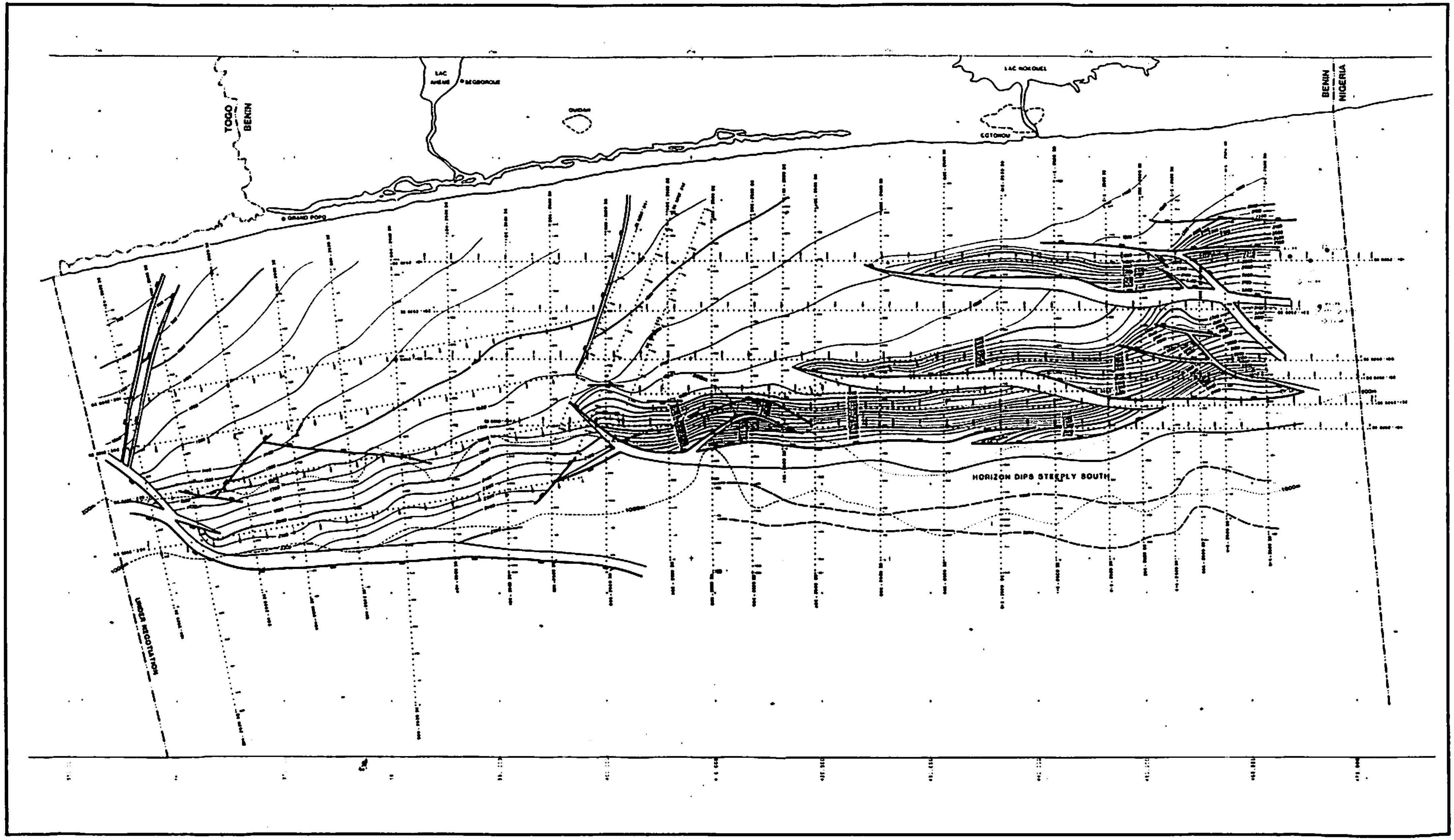

Fig. A.2.19: Basement (H9), two-way time map.

APPENDIX A.3 22.6.84

SEME OIL FIELD

A.3.1 Introduction

The Sèmè Oil Field is located on the eastern part of the Benin continental shelf close to the Nigerian border. The field was discovered in the late 1960's by Union Oil, but after drilling a total of 9 holes of which 4 were oil producers, Union gave up the concession. In 1980 the Government of the Republic of Benin decided to develop the oil field awarding a service contract to Saga Petroleum Benin a.s., but with the Republic of Benin retaining 100% ownership of the field. The field came on stream in October 1982, and has as of September 1983 produced roughly 1 000 000 barrels of oil currently from 3 wells in the northern Sèmè structure (fig. A.3.1). The southern structure has not yet been drilled in the development phase.

A.3.2 Structural Geology of the Sèmè Oil Field

In the Sèmè Oil Field the structural picture is thought to have arised from several episodes of deformation. The deepest structures are seen as NE-SW trending basement faults with a considerable NW-erly throw. The fault blocks have been rotated towards SE. The area is also influenced by N-S trending faults on basement level. The fault pattern on higher levels were regarded as secondary effects caused by reactivation of the deeper fault system. Ræstad et al (1983) concluded that the structural history might be divided into three events (figs. A.3.2, A.3.3 and A.3.4):

1. Early Cretaceous block faulting with SE-erly rotation of the fault blocks.

2. Early Late Cretaceous reactivation and rotation of fault blocks resulting in doming and fracturing of the Albian to Turonian sedimentary sequences.

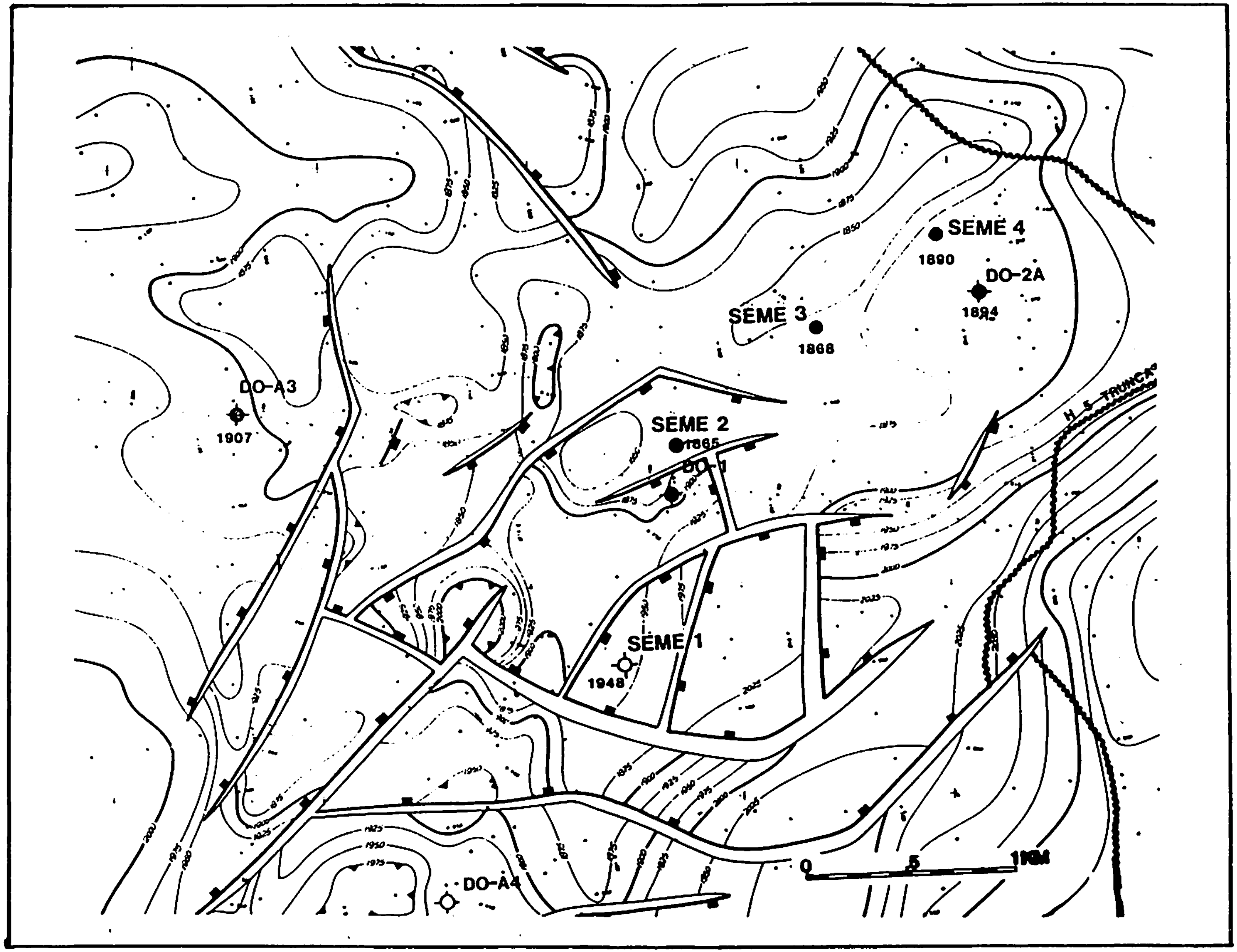

Fig. A.3.1: North Sèmè Oil Field, structural depth map top reservoir.

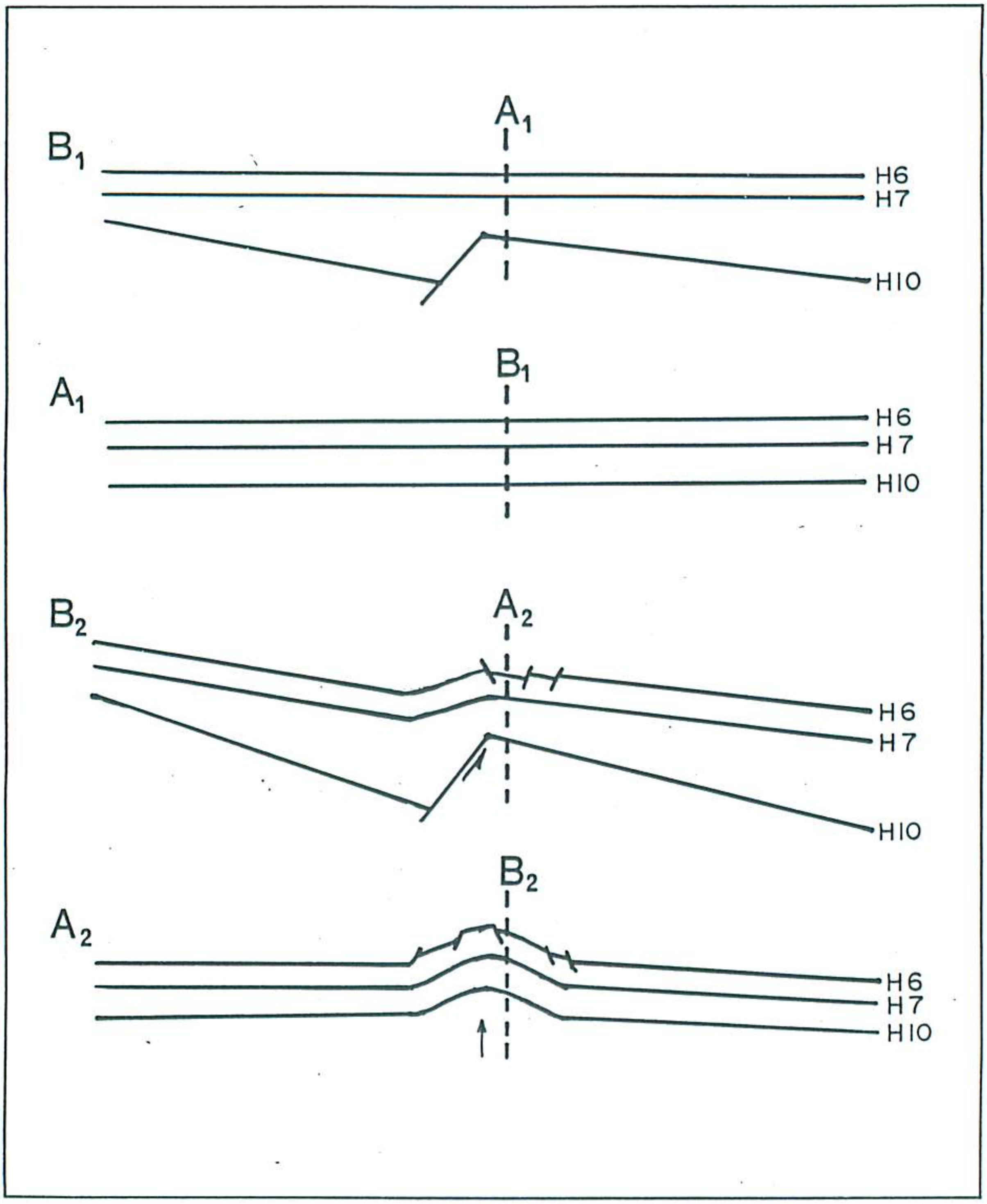

[illegible]2: Sketch showing development of fault system across A-structure Sèmè Oil Field. Line B runs N-S and line A E-W. H6 = Top Abeokuta Sandstone. H7 = Top "Albian Sandstone". H10 = Basement.

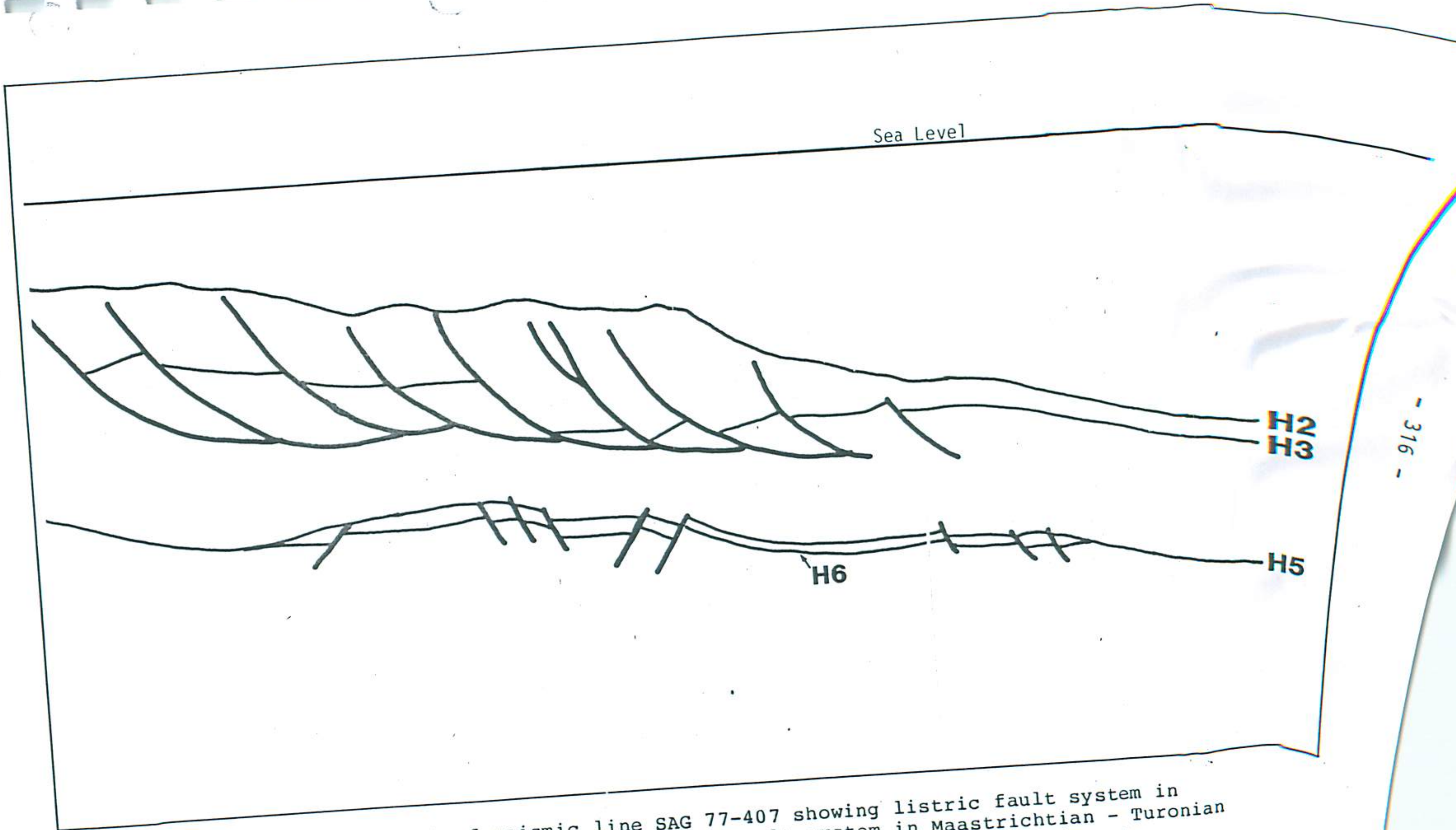

Fig. A.3.3: Sketch of seismic line SAG 77-407 showing listric fault system in Miocene sediments and normal fault system in Maastrichtian - Turonian sediments. H2 = Mid Miocene Unconformity. H3 = Base Miocene Unconformity. H5 = Senonian Unconformity. H6 = Top Abeokuta reservoir.

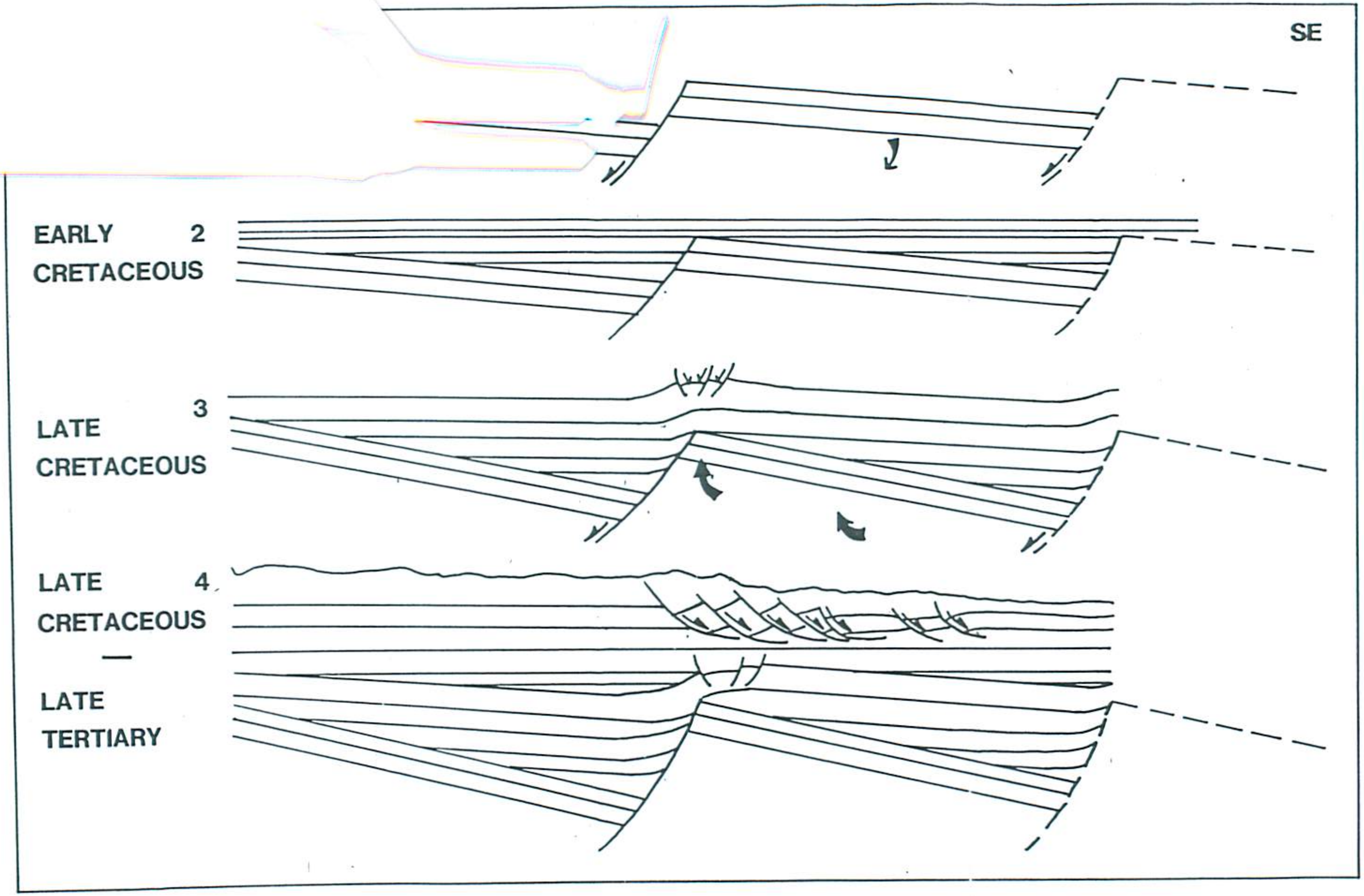

Fig. A.3.4: Structural development of the Sèmè area.

3. Tertiary oceanward gravity sliding (listric faulting).

Although the timing of the deformational episodes deviates slightly from what is seen on a regional scale in the present analysis, the sequence of events is strikingly similar.

Consequently more detailed investigations, as in the case of the Sèmè Oil Field, reveals a more complicated pattern, as would be expected due to local effects.

A.3.3 <u>Reservoir Geology</u>

Four separate hydrocarbon bearing zones have been tested in the wells on the north Sèmè structure, all in the Cretaceous sequence from Turonian to probably Albian in age.

Zone 1 of the "Turonian Sandstone" (Abeokuta Formation in the field terminology), at about 1900 m subsea, is the main oil zone which so far has been put on production.

Zone 2 is a localized oil zone at about 2250 m subsea in the middle part of the "Turonian Sandstone". While probably not containing significant reserves in north Sèmè, it emphasizes the possibility of hydrocarbon accumulations within a predominantly sandy sequence.

Zone 3 is an oil zone at the top of the "Albian Sandstone" sequence at about 2450 m. In the wells penetrating the Albian almost all permeable intervals have good oil shows. The oil in place figures appear to be substantial, but producability is debatable due to low permeability. Union tested 330 BOPD from Zone 3.

Zone 4 is a gas reservoir, and in the Sèmè 4 well 47 m of good

~uality gas sand was encountered at 2600 m. The gas appears to be underlain by a significant volume of tarry oil which with conventional techniques is not thought to be producable. Union estimated gas flow rates of up to 8 MMSCF/D from the gas zone, while Zone 4 has not yet been tested in the development phase. The Sèmè 4 well has been completed as a Zone 1 producer with the intention to recomplete in Zones 3 and 4 at a later stage.

The remaining part of the discussion will be focused on Zone 1. As shown on the structure map (fig. A.3.1), the main reservoir is an anticlinal feature limited to the north and southeast by structural closure, to the northeast by truncation of the Senonian Unconformity and to the southwest probably by faulting. Development drilling found the field to be structurally more complex than originially anticipated. Reservoir parameters have, however, proved to be better than expected (table A.3.1). Pressure maintenance indicates an effective natural water drive. The upper producing main oil zone is limited by an appearantly field wide permeability barrier, giving a good edge water drive.

Average porosity	19%
Average water saturation	30%
Net sand to gross formation	0.60
Oil FVF	1.1271
Average net pay	approx. 20 m

Table A.3.1: Reservoir parameters Zone 1 "Turonian Sandstone". Compare chapter 7.2.

Additional hydrocarbon potential has been identified to the west. An appraisal well that was drilled in August 1983 to test this, found oil in the western part of the structure.

A.3.4 Production Data

Fig. A.3.5 shows the cumulative oil production from Sèmè north field as of September 1983. In table A.3.2 are listed analyses from the initial completion tests on the three producing wells. Originally the wells were completed with downhole pumps, but due to mechanical failures of the pumps the production has so far been on natural flow. The oil is a 22.6^{o} API low sulphur crude which shows fairly strong naphtenic qualities (compare chapter 7.1.2).

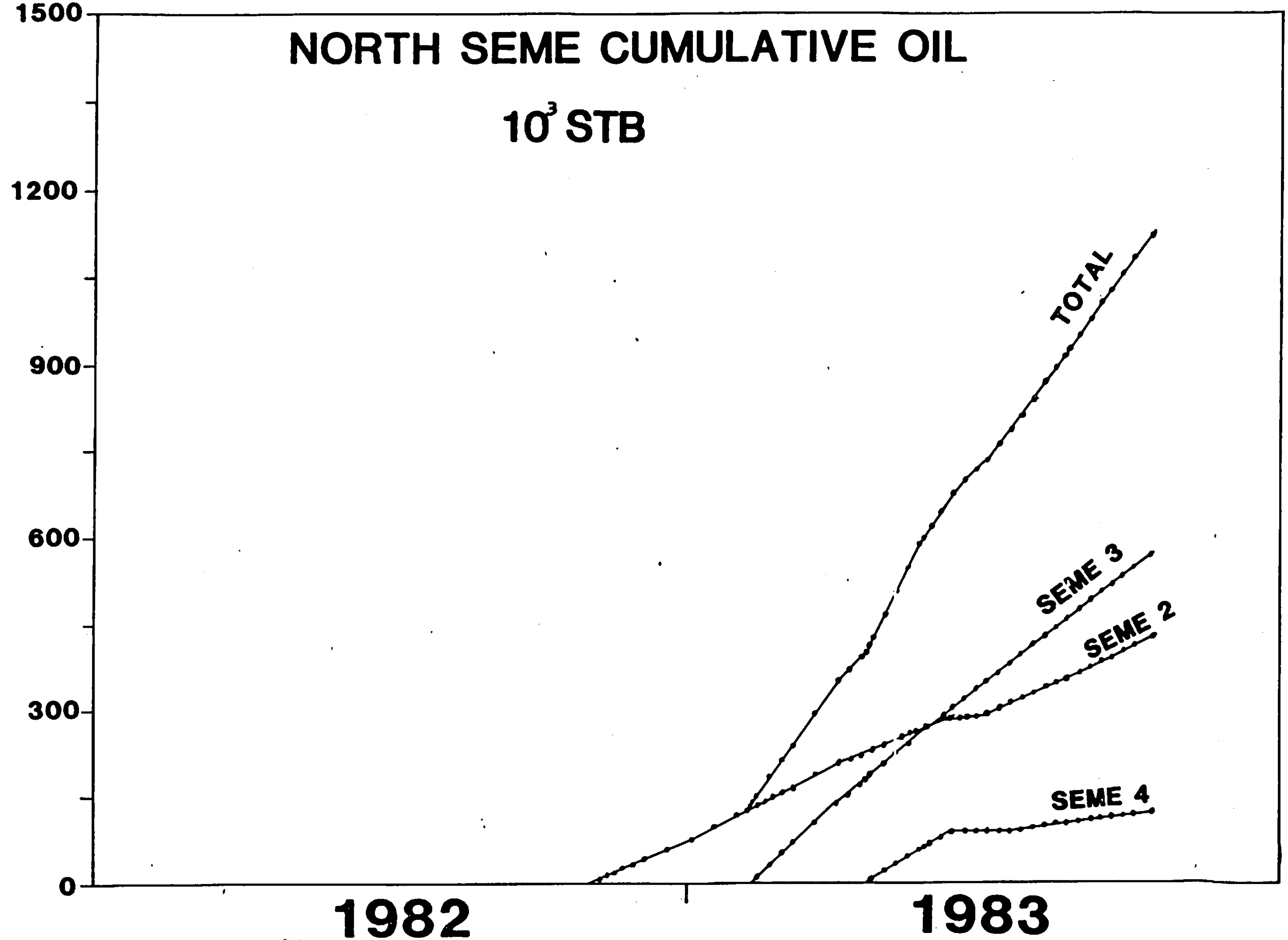

Fig. A.3.5: Cumulative oil production Sèmè north.

	Sèmè 2 Test No. 1	Sèmè 3 Test No. 1	Sèmè 4 Test No. 1
Dates	5-10.10.82	3-7.2.83	31.3-5.4.82
Reservoir pressure (p psia at 1880 m MSL)			
Inital (Oct. 82)	2 723	2 677	2 593
Workover (Oct. 83)		2 580 (preliminary)	
Perforated interval (TVD m)			
Initial (Oct. 82)	18.0	21.7	6.0
Workover (Oct. 83)		15.4	12.0
Stabilized flow rate STB/D with choke ½"			
Initial (Oct. 82)	900	1 437	456
Workover (Oct. 83) (on pump)		4 100	2 500
Well capacity (md.ft)	27 735	75 999	8 743
Permeability md	539	1 066	522
Skin	9.5	3.2	2.9
Real PI STB/PSI/D	2.48	12	1.5
Ideal PI (S=0)	6.23	17	2.1
BHT, °C	113	118	115

Table A.3.2: List of analysis results from initial completion tests performed on wells S-2, S-3 and S-4.

Since these initials tests, there is some evidence that the wells will clean up. A recent pressure built up in well S-2 (6.3.83) now indicates a skin of 1.2 and a real PI of 4.1.

APPENDIX A.4 22.6.84

HYDROCARBON INDICATORS

A number of shallow amplitude anomalies can be observed on the seismic sections. The most outstanding of these are marked on fig. A.4.1. Most of the anomalies can be observed only at the sea bottom or directly below it, while some of them may be observed down to more than 1 s two-way time. With the mute function applied, only the near trace is used down to approximately 0.3 s two-way time, then there is linear increase so that roughly one third of the cable is used at 0.8 s two-way time. Thus most of these anomalies are based on only very few traces in the stack.

All of the marked anomalies occur in shallow waters, mostly less than 30 m. With 30 m depth the sea bottom reflection recorded at the near trace will take place at an angle of close to 80 degrees, i.e..an extremely large angle of incidence and well beyond the critical angle for any reasonable set of geophysical sea bottom parameters. Any obstacles at or near the sea bottom or even small changes in sea depth may then result in large changes in amplitude for a number of reasons; the most prominent of these being: the extreme rapid variation the reflection coefficient may have at such angles, large focusing and defocusing effects at such near gracing angles and rapid variations in the response pattern of the live elements of the cable at such angles. Any utilization of these variations therefore should be done with extreme care.

Separate from the anomalies marked on fig. A.4.1 is the anomaly observed at close to 2.25 s two-way time around SP 740 on line BE8262-314 (ref. fig. 7.37). This is a very interesting feature and should be given some extra consideration as this anomaly might represent a gas liquide contact. In order to investigate this further a small part of this line should be reprocessed emphasizing the high frequency content of the signals. Also a small modelling study could give some additional information.

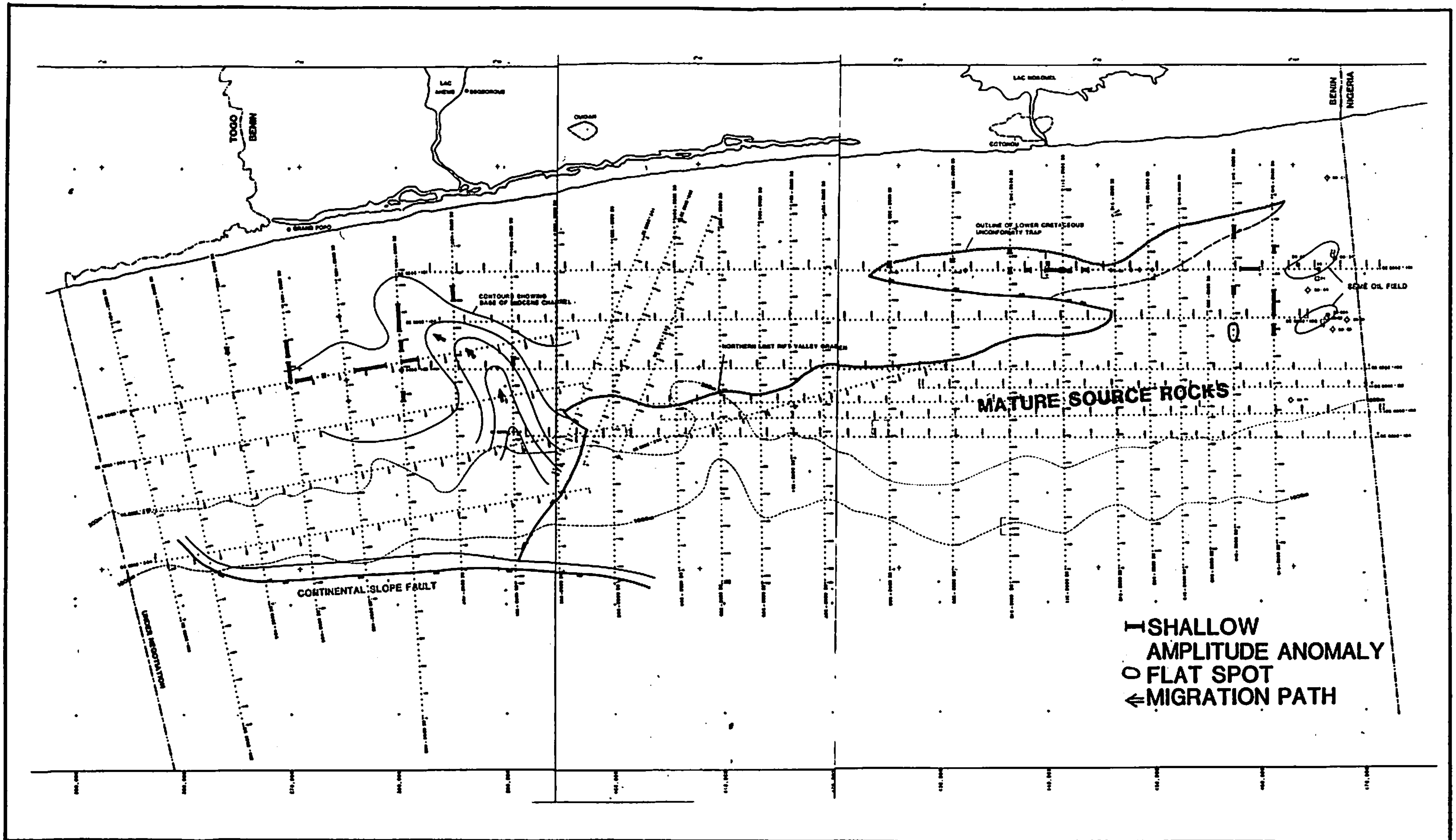

Fig. A.4.1: Hydrocarbon indicators.

APPENDIX A.5 22.6.84

TEST RESULTS OF UNION WELLS

DST results

The following summarizes the DST results for DO-1, DO-2A, DO-D2A, DO-A3 and Lome 1.

DO-1

Interval m RKB	Flow Rate bbl/d	PI bbl/d/psi	Permeability mD	Res. Press at depth psi at M RKB
2739-2734	Tight			
2730-2734	Tight			
2686-2698	741*	273**	0.5	3940 at 2670
2662-2667	Tight			
-2655	Unusable data			
2629-2640	Water/very little gas			
2454-2470	240	0.39	27	3340 at 2440
2257-2260	137	0.14	122	3158 at 2237
2257-2264	240	0.52	178	3162 at 2237
2106-2164	Water/ well died			
1923-1926	1509	4.4	1061	2678 at 1904
1897-1903	731	1.0	135	2616 at 1877

DO-2A

Interval m RKB	Flow Rate bbl/d	PI bbl/d/psi	Permeability mD	Res. Press at depth psi at M RKB
2661-2678	7-8 mm SCF/d			
1924-1928	Recovered some oil, no press results.			
1919-1922	Recovered some oil, no press results.			
1914-1922	488 BOPD, data not usable			
1896-1928	379 BOPD, 68% oil and 32% salt water.			

DO-D2A

Interval m RKB	Flow Rate bbl/d	PI, actual bbl/d/psi	Permeability mD	Res. Press at depth psi at M RKB
3073-3079	No recovery of oil/gas			
2798-2832	77	0.02	20	4224 at 2775 m
1947-1952	780	3.45	950	2738 at 1926 m

DO-A3

Interval m RKB	Flow Rate bbl/d	PI bbl/d/psi	Permeability mD	Res. Press at depth psi at M RKB
2723-2727	Tight			
2708-2727	Tight			
2696-2701	Water			
2689-2686	Oil/No pressure data			
2679-2692	Oil cut diesel			
-2656	Oil cut diesel			
2541-2587	Water			
2505-2513	Water			
2492-2499	Water			
1928-1932	912	2.3	1584	2691 at 1909 m

APPENDIX A.6 22.6.84

REFERENCES

Adegoke, O. S., 1969: Eocene stratigraphy of Southern Nigeria. Extrait de Memoires du B.R.G.M. - N° 69, 49 p.

Adegoke, O. S. & Ibe, R. C., 1982: The tar sand and heavy crude resources of Nigeria.
Second International Conference on Heavy Crude and Tar Sands, Caracas, Venezuela, February, 7.-17. 1982.

Akapati, B. N., 1978: Geologic structure and evolution of the Keta Basin, Ghana, West Africa.
Geol. Soc. Amer. Bull, v 89, No. 1, pp 124-132.

Asmus, H. E. & Ponte, F. C., 1973: The Brazilian marginal basins.
In: A. E. M. Nairn & F. G. Stehli (eds.): The ocean basins and margins, 1 The South Atlantic, Plenum, New York, pp 87-132.

Augedal, H. O., Elvsborg, A. & Throndsen, T. O., 1983: Stratigraphy and sedimentology of the Upper Cretaceous of the Sèmè 1 (Pl) and Sèmè 2 (Pl).
Saga Petroleum a.s. Exploration Report No. 64/83, 122 pp.

Billman, H. G., 1976: Offshore stratigraphy and paleontology of the Dahomey Embayment, West Africa.
Prepared for the 7th African Micropalentological Colloqium, Ile - Ife, Nigeria 1976.

Booth, B., 1983: The detailed geochemistry of a crude oil sample from well: Sèmè 2, Benin, West Africa.
Paleochem Ltd. Petroleum Geochemistry Report, 8 pp.

Booth, B., 1983: The detailed geochemistry of a crude oil sample from well: Sèmè 3, Benin, West Africa.
Paleochem Ltd. Petroleum Geochemistry Report, 12 pp.

Brown, Jr., L. F. & Fisher, W. L., 1977: Seismic-stratigraphic interpretation of depositional systems: Examples from Brazilian rift and pull-apart basins.
AAPG, Memoir 26.

Burke, K., 1969: Seismic areas of the Guinea Coast where Atlantic fracture zones reach Africa.
Nature v 222, No. 5194, pp 655-657.

Burke, K., 1976: Development of graben associated with the initial ruptures of the Atlantic Ocean.
Tectonophysics, v 36, pp 93-112.

Burke, K., Dessauvagie, T. F. J. & Whiteman, A. J., 1971: Opening of the Gulf of Guinea and geological history of the Benue depression and Niger Delta.
Nature Phys. Sci., v 233, No. 38, pp 51-55.

Burke, K., Dessauvagie, T. F. J. & Whiteman, A. J., 1972: Geological history of the Benue Valley and adjacent areas.
In: A. J. Whiteman & T. F. J. Dessauvagie: African Geology. Ibadan 1970, pp 187-206.

Carstens, H., 1982: The continental margin of the northern Gulf of Guinea: structural evolution and basin formation.
Saga Petroleum a.s. Exploration Report No. 52/82, 34 pp.

Crittenden, S., Tykoezinski, H., Meyerick, R. W. & Gueinn, K. J., 1983: Well Sèmè 2 (Pl) stratigraphical/paleontological final report.
Paleoservices Ltd. Report, project No. 1036.

Crowell, J. C., 1974: Origin of Late Cenozoic basins in southern California.
In: W. R. Dickinson (ed.): Tectonics and sedimentation. Spec. Publ. Soc. Econ. Paleont. Miner. Tulsa, 22, pp 190-204.

Delteil, J., Valey, P., Montadert, L., Fondeur, P., Patriat, P., & Mascle, J., 1974: Continental margin in the northern part of the Gulf of Guinea.
In: C. A. Burk & C. L. Drake (eds.): The geology of continental margins. Springer, Berlin, pp 297-311.

Demaison, G. J. & Moore, G. T., 1980: Anoxic environments and oil source bed genesis.
AAPG 64 (8), pp 1179-1209.

Emery, K. O. E., Phillips, U. J., Bowin, C. & Mascle, J., 1975: Continental margin off West Africa: Angola to Sierra Leone.
Am. Assoc. Petrol. Geol. Bull., 59, pp 2209-2265.

Francheteau, J. C., & Le Pichon, X., 1972: Marginal fracture zones as structural framework of continental margins in South Atlantic Ocean.
Am. Assoc. Petrol. Geol. Bull., 56, pp 991-1007.

Glenne, B., 1981: Development of Benin's first oil field under way.
Oil and Gas Journal, January 12, 1981.

Gretener, P. E., 1981: Geothermics: Using temperature in hydrocarbon exploration.
AAPG Education Course Note Series No. 17, 156 pp.

Halbouty, M., 1980: Methods used and experience gained in exploration for new oil and gas fields in highly expected (mature) areas.
AAPG Bull., v 64, pp 1210-1222.

Harding, T. P., 1974: Petroleum traps associated with wrench faults.
Am. Assoc. Petrol. Geol. Bull., 58, pp 1290-1304.

Harding, T.P., 1983: Graben hydrocarbon plays and structural styles. in: J.P.H. Kaasschieter & T.J.A. Reijers (eds.): Petroleum geology of the southeastern North Sea and the adjacent onshore areas. Geol. Mijnbouw, 62, 3-23.

Harland, W. B., 1969: Contribution of Spitsbergen to understanding of tectonic evolution of North Atlantic region.
Tulsa, Am. Assoc. Petroleum Geol. Mem., 12, pp 817-851.

Harriman, G. E., 1983: Geochemical evaluation of the oil from 2470 m in Saga's Sèmè 4 well offshore Benin, West Africa.
Geochem Laboratories (UK) Limited Geochemical Service Report, 4 pp.

Jones, H. A. & Hockey, R. D.: The Geology of part of south-western Nigeria.
Geol. Surv. Nigeria Bull. 31.

Klemme, H. D., 1980: Petroleum basins - classifications and characteristics.
Journal of Petroleum Geology, v 3, pp 187-207.

Kogbe, C. A., 1974: The Upper Cretaceous sediments of the south-western Nigeria.
Nigerian Field, v 39.

Kumar, N. & Ladd, J. W., 1974: Origin of compressional structures on the shelf off Brazil and Ghana formed during the opening of Equatorial Atlantic.
Geol. Soc. Am. Abstr. Progr, 6, p 835.

Larson, R. L. & Ladd, J. W., 1973: Evidence from magnetic lineations for the opening of the South Atlantic in the Early Cretaceous.
Nature, 246, pp 209-212.

Machens, E., 1964: Structural evolution of West Africa.
Z. Deut. Geol. Ges., v 116, pp 589-597.

Machens, E., 1973: The geologic history of the marginal basins along the north shore of the Gulf of Guinea.
Book: ISB Ø-306-37771-3, Plenum Press, New York, v 1, pp 351-390.

Murat, R. C., 1972: Stratigraphy and palaeogeography of the Cretaceous and Lower Tertiary in Southern Nigeria.
In: A. J. Whiteman & T. F. J. Dessauvagie: African Geology, Ibadan University, pp 251-266.

Rodgers, D. A., 1980: Analysis of pull-apart basin development produced by en echelon strike-slip faults.
In: P. F. Ballance & H. G. Reading (eds.): Sedimentation in oblique-slip mobile zones. Spec. Publ. Int. Ass. Sediment., 4, pp 27-41.

Ræstad, N., Battié, J. E., Gabrielsen, R. H. & Carstens, H., 1983: Reinterpretation of the Sèmè Oil Field, Republique Populaire de Benin.
Saga Petroleum a.s. Exploration Report No. 67/83, 53 pp.

Sauer, M. J., 1983: Geochemical evaluation of the 1000 - 2120 metre interval in Saga's Sèmè 1 well offshore Benin, West Africa.
Geochem Laboratories (UK) Limited Geochemical Service Report, 13 pp.

Slansky, M., 1962: Contribution a l'étude geologique du bassin sédimentaire côtier du Dahomey et du Togo.
Mem. Bur. Rech. Geol. Min.

Short, U. C., and Stäuble, A. J., 1967: Outline of geology of Niger Delta.
AAPG Bull., v 51, pp 761-779.

Tchalenko, J. S., 1970: Similarities between shear zones of different magnitudes.
Geol. Soc. Am. Bull., 81, pp 1625-1640.

Teichmüller, M. und Ottenjann, K., 1977: Liptinite und lipoide Stoffe in einem Erdölmuttergestein.
Erdöl u. Kohle, Erdgas, Petrochemie 30, pp 387-398.

Throndsen, T. O., 1983: Some vitrinite reflectance data from the "Turonian Sandstone" section in the Sèmè Field offshore Benin, West Africa.
Saga Petroleum a.s. Exploration Report, in prep.